Thesis submitted to obtain

the degree of Ph.D.

(Dental Materials)

2010

Study of photopolymerization reaction of dental resins:

Answers of fundamental research to clinical issues.

Julian Leprince

FNRS research fellow

School of Dental Medicine and Stomatology

Institute of Condensed Matter and Nanosciences - Bio & Soft Matter (IMCN/BSMA)

Center for Research and Engineering in Biomaterials (CRIBIO)

Université catholique de Louvain

«La science moderne est un admirable monument qui fait honneur à l'espèce humaine et qui compense (un peu) l'immensité de sa bêtise guerrière».

Hubert Reeves (L'Espace prend la forme de mon regard).

« En science comme ailleurs, l'inertie intellectuelle, la mode, le poids des institutions et l'autoritarisme sont toujours à craindre ».

Hubert Reeves (Patience dans l'azur).

. À ma famille.

Acknowledgments

«Un an et on verra»… voilà comment cette thèse a commencé… il y a maintenant 3 ans et demi. Je me suis donc pris au jeu, et ce manuscrit est le fruit d'une expérience qui a été pour moi une vraie révélation, d'une passion pour la recherche d'une part, et d'une envie de la faire partager d'autre part.

Pour mener à bien ce genre de travail à la frontière entre la dentisterie et la science des matériaux, j'ai eu besoin de deux promoteurs: une dentiste et un ingénieur, tous deux extrêmement efficaces et surtout complémentaires pour une équipe qui marche.

Je souhaite remercier en tout premier lieu la personne qui a été non seulement à l'origine de ce parcours, mais également présente de manière exceptionnelle à chaque étape de celui-ci: Mme le professeur Gaetane Leloup. Gaetane, tu n'as pas hésité à me donner ma chance très tôt lors d'une présentation chahutée à l'ADF. Ecrire tous les remerciements que tu mérites en si peu de lignes revient à écrire un abstract de 200 mots pour une thèse de doctorat… pas facile. Alors, comme souvent la solution est de prendre la tangente, et résumer par une image, celle d'un inoubliable «road trip» américain à Portland, qui représente bien je pense, notre collaboration: amicale, efficace et honnête. Merci pour tout.

En second lieu pour des raisons chronologiques mais certainement pas par son implication dans ce travail, je voudrais remercier Mr le professeur Jacques Devaux. Jacques, tu as été mon guide dans ce réseau polymère complexe, et tu m'as permis de m'en tirer, d'y garder une certaine mobilité, et de ne pas m'y engluer par gélification! Je n'oublierai jamais nos discussions incontrôlables (et incontrôlées) au cours desquelles tu as su si bien me transmettre ton enthousiasme, toujours avec beaucoup d'humilité et d'humour. Merci.

L'évaluation d'un travail à la frontière de différentes disciplines nécessite un jury polyvalent, dont j'aimerais remercier ici les différents membres.

Tout d'abord, merci au professeur Bernard Gallez, non seulement pour avoir accepté de faire partie de mon jury, mais aussi et surtout pour son aide précieuse tant au niveau logistique que scientifique. La partie RPE a été une partie essentielle de cette thèse. Bernard, merci pour tes idées, tes remarques toujours très pertinentes et souvent

originales. Je planche d'ailleurs toujours sur l'idée de la dent transparente et l'article devrait arriver sur ton bureau «hier»!

Then, let me switch to english to thank Dr William Palin. Will, what a good idea I had last year to send you that e-mail to propose a common work! The 6 wonderful and prolific weeks spent in Birmingham were a fantastic experience for me, both on a scientific and personal point of view. I learned a lot with you, acquired a rigorous approach of experiments and improved my scientific writing skills. Now, a few chips & beans and mushrooms later, looking back at what we have achieved in such a short period, I'm looking forward to other common work. Obviously, this is only the «tip of the iceberg» of what we are going to do together. Thanks for accepting to be one of my panel members and for your friendship.

Retour au français pour remercier chaleureusement quelqu'un qui le manie si bien, en la personne du professeur Michel Degrange. J'ai toujours admiré et pris comme exemple vos talents d'orateurs et la façon unique que vous avez de rendre passionnant pour nos confrères dentistes un sujet tel que les biomatériaux. Merci pour votre regard critique sur mon travail, pour votre motivation très communicative, et votre présence dans mon jury.

Les deux derniers membres de mon jury, les professeurs José Vreven et Jean-Pierre Van Nieuwenhuysen, ont également été mes professeurs respectivement de Dentisterie Opératoire et d'Endodontie, et sont pour beaucoup dans l'intérêt particulier que je porte à ces deux disciplines. Tous deux, vous avez été d'excellents enseignants et m'avez stimulé et encouragé à suivre votre voie vers une carrière universitaire. Mr Vreven, je vous souhaite encore de nombreux et beaux voyages. Mr Van Nieuwenhuysen, un merci tout particulier concernant vos efforts afin de créer une formation endo de grande qualité, qui m'a permis de m'épanouir cliniquement entre deux séjours au labo, et de garder ainsi le nécessaire contact avec la réalité clinique.

Ensuite, qui dit travail multidisciplinaire dit bien sûr collaborateurs venant de tous horizons. Ces différents collaborateurs ont chacun apporté des éléments essentiels à ce travail. Tout d'abord, merci à l'équipe CRIBIO. Guillaume, tu as été un véritable équipier, et je mesure ma chance d'avoir eu l'occasion de travailler avec quelqu'un comme toi et de refaire le monde (scientifique) ensemble. Tu es également et surtout un ami, toujours prévenant et prêt à rendre service. Thérèse et Ana, merci à toutes les deux

pour votre aide précieuse dans les manips parfois fastidieuses mais toujours impeccables, et pour votre bonne humeur au quotidien. Seb et Magali, vous m'avez tous deux montré d'une belle façon la voie à suivre. Merci pour vos conseils quand j'en avais besoin et pour les moments partagés.

J'en viens maintenant aux membres du labo POLY à Louvain-La-Neuve, qui m'ont accueilli d'une manière exceptionnelle. J'ai trouvé au sein de votre labo un esprit d'ouverture et d'accueil unique, où chacun était prêt à passer autant de temps qu'il le fallait pour expliquer l'un ou l'autre appareil. Merci à tous. Un clin d'oeil tout particulier à mes compères suivants pour les excellents délires et les projets révolutionnaires à venir: Guido Multifonctions, Xavier Nano-poils, Dimi ColosseAuxPolymèresDargile, Anne-Christine PlusBavardeQueMoi!, Vincent DessinateurHardcoreux.

Back to English to send special thanks to my British colleagues. Guys, my stay in Birmingham was incredible thanks to you. Mo, ready? you're the only one able to collect such a huge amount of data in one yEAr! Working with you was a real pleasure (except for the music ;). Naresh, master of the fillers, it was a pleasure to have so many interesting chats together. You're just Billiant! I wish you guys all the best for the rest of your PhD and your career. Yusuke, I spend such a great time with you along the trails of the English countryside, talking about anything, fighting against mud and wind. Ready for the next trip? Whenever you want! Jack, thanks a lot for your precious advice and for your pleasant company. Gareth, thanks a lot for your kindness and for the chats together. Next time we'll hike together! Finally, thanks to Owen, Sue, James and others for your friendship during my stay.

Merci aux membres du service de PATD et Endo qui m'ont soutenu durant cette thèse. Charlie, je te remercie particulièrement pour ton amitié et ton soutien depuis le tout début. Bon premier marathon, et quand tu veux bien sûr pour une bonne session course à pied. Gaetan, merci pour m'avoir motivé et aidé depuis le début, en clinique et à côté. Je n'oublierai jamais ce baptême du feu à l'ADF où tu m'as appris les ficelles. Bon vent pour tes projets, et à un de ces 4 pour une grimpe? Merci Patrick (le manuel) et Pierre (le mécanisé) pour vos conseils en clinique endo, et votre humour décapant. Thierry, merci pour ta sympathie, tes encouragements et pour nos discussions sportives. Merci aussi au Professeur Christian Vanzeveren pour votre soutien et pour m'avoir

permis de partir à Montréal. Enfin, à tous les membres de l'EMDS qui m'ont montré de la sympathie durant mon parcours.

Merci également à l'équipe du REMA à Woluwé et plus particulièrement Bénédicte et Philippe pour leur aide précieuse et leur gentillesse.

J'adresse aussi un merci plus global à tous mes amis proches, Gaumais, Bruxellois, Français, Montréalais, Américains... Vous avez non seulement supporté depuis des années mon humour plein de «finesse», mais aussi répondu présent quand il me faisait défaut.

Pour terminer, j'aimerais insister sur le fait qu'on mène difficilement à terme une thèse de doctorat sans un solide entourage de ses proches. Ce genre de parcours nécessite en effet un cadre solide, une éducation, et surtout un soutien permanent. Ces éléments m'ont été apportés par des gens exceptionnels, mes proches, ma famille, à qui j'aimerais exprimer ici toute ma reconnaissance.

J'ai une pensée particulièrement émue pour mes proches disparus, avec qui j'aurais tant aimé partager ce moment. Je pense à vous, pépé Robert, pépé Albert, mémé Sylvie et Tata. Mémé Yvonne, merci à toi aussi. C'est en grande partie grâce à vous, à votre exemple et vos conseils, que j'ai eu la chance de faire des études et de les pousser si loin. Je remercie également mon parrain qui m'a aidé à «slalomer» autour des difficultés. Lucas et Florent, merci pour votre soutien inconditionnel au cours de cette thèse et dans les moments difficiles. Flo, continue comme ça, tu peux être fier; Lu, à toi de jouer maintenant!

Anh cũng cảm ơn Quyên đã hỗ trợ hàng ngày của em. La force de la bulle est toujours avec nous!

Enfin, je remercie aussi et surtout mes parents qui m'ont offert une éducation exemplaire, m'ont permis de m'épanouir dans tous les domaines, m'ont transmis le goût des choses bien faites et surtout leur sens des valeurs. Père Lep et Mère Lep, c'est grâce à vous si le petit gourmand du lac Sainte-Croix en est arrivé là, et je mesure aujourd'hui tout ce que vous avez fait pour moi depuis 26 ans. Merci pour tout.

Summary

In modern dentistry, resin-based composites are about to definitely replace mercury amalgams in direct restorations, notably due to the clear aesthetic interest of tooth-like composites. However, authors have highlighted that the longevity of composite restorations is very dependent on the operator, which includes not only technical skills but also the respect of the material specificities, notably its light-responsive setting process. Therefore, the aim of the present work was to improve the understanding of the photopolymerization reaction of dimethacrylate-based dental resins and to develop strategies to improve this process.

To start with, a global reflection was conducted on the theoretical aspects of photopolymerization reaction of dimethacrylate-based resins. Notably, the emphasis was put on the incomplete conversion of such resins and the associated persistence in the polymer network of unconverted monomers and trapped free radicals. The kinetics of decay of the latter was then analyzed by Electron Paramagnetic Resonance, which firstly confirmed the identification of two distinct radical species with different reactivity, and secondly highlighted the oxygen-dependance of free radicals long-term decay. Finally, the use of spin-trapping methods produced evidence of hydroxyl radical release by dental resins, which is probably due to the reaction of oxygen with the remaining methacrylate groups.

As it appears that leaching of both free radicals and unconverted monomers are linked with the incomplete conversion of dimethacrylate-based resins, clinical procedures must be adapted appropriately to limit the amount of unconverted double bonds. Consequently, the second part of this thesis dealt with the two main ways to reach this goal: first, the use of a material containing a lower dimethacrylate fraction, second the adaptation of irradiation conditions in order to reach an optimal material conversion. Regarding the first method, the mechanical properties and filler fractions of different composite technologies were compared (ring-opening systems, ormocers and highly filled composites) and clinical guidelines were proposed for the use of each material. The second method focused on the evaluation of curing efficiency of new LED curing lights as well as their safety in terms of temperature rise in the pulp chamber. The results stressed the extreme importance of spectrum correspondence between light

emission spectrum and absorption spectrum of the photoinitiating system. Besides, new LED lights were also shown to enable a certain reduction of curing time.

Finally, the last part of this work was devoted to a frequent subject of debate in the photopolymerization of dental resin-based materials, i.e. applicability of the so-called Exposure Reciprocity Law, supporting the decrease of irradiation time by a proportional increase of irradiance. Again, the use of Electron Paramagnetic Resonance was very profitable, as it enabled to improve the understanding of the termination pathway through the measurement of trapped free radicals. Besides, the influence of photoinitiator type and filler content on the validity of this law were also investigated. These experiments revealed notably the very high curing efficiency of Lucirin-TPO, and underlined the impact of resin viscosity and filler content on the curing kinetics of Camphorquinone-based materials. These innovative approaches open the door to many other projects.

Table of Contents

Chapter 1 - Introduction **1**

1.1. Context **3**

1.2. Photo-polymerizable dimethacrylate-based materials used in dentistry **6**

1.3. Light-curing systems **10**

1.3.1. Historical background **10**

1.3.2. Technologies of visible light-curing units **11**

1.3.2.1. Quartz-tungsten Halogen (QTH) curing lights 11

1.3.2.2. Plasma-arc curing lights (PAC) 11

1.3.2.3. Argon Lasers 12

1.3.2.4. Light-emitting Diodes (LED) 12

1.3.3. Which technology should a dentist choose? **13**

1.3.4. Practical aspects **14**

1.3.5. Conclusion **16**

1.4. References **16**

Chapter 2 - Literature Review and Major Findings **21**

Foreword 23

2.1. Theoretical aspects of photopolymerization reaction **24**

2.1.1. Basics of photo-induced radical polymerization reaction **24**

2.1.2. Specificity of highly crosslinked polymer network **27**

2.1.3. Trapped free radicals: detection, identification, quantification and follow-up **30**

2.1.4. Elution of active species: monomers and free radicals **40**

Foreword 40

2.1.4.1. Unconverted monomers 41

2.1.4.2. Free radicals *43*

2.1.4.3. Strategies to limit free radical and monomer release 48

2.2. Investigation of commercial composites and light-curing units. **50**

2.2.1. Increased filler content and new monomer technologies **50**

2.2.2. New light-curing units and importance of spectrum match **57**

2.3. Exposure Reciprocity Law: Comprehension and Innovation **61**

2.3.1. Definition and Current knowledge **61**

2.3.2. Contribution of EPR technology in the understanding of the ER law **64**

2.3.3. Is ERL dependent on other factors than irradiation parameters? **67**

2.4. Perspectives **72**

2.5. References **77**

Chapter 3 - Kinetic study of free radicals trapped in dental resins stored in different environments **89**

3.1. Summary **91**

3.2. Introduction **93**

3.3. Materials and Methods **94**

3.3.1. Materials **94**

3.3.2. Preparation of samples **95**

3.3.3. Characterization **96**

3.4. Results **96**

3.5. Discussion **98**

3.5.1. General considerations **98**

3.5.2. Temperature **99**

3.5.2.1. Influence of storage temperature 99

3.5.2.2. Heating experiments 100

3.5.3. Storage environments **101**

3.5.3.1. Unfilled resin 101

3.5.3.2. Filled resin 103

3.5.4. Influence of fillers on free radical decay in air **103**

3.6. Conclusion **104**

3.7. Acknowledgments **105**

3.8. References **105**

Chapter 4 - Hydroxyl radical release from dental resins: EPR evidence **109**

4.1. Summary **111**

4.2. Introduction **112**

4.3. Materials and Methods **115**

4.3.1. Sample preparation **115**

4.3.2. EPR spectroscopy **116**

4.3.3. Kinetics of decay of trapped radicals in ethanol and water **116**

4.3.4. Spin trapping experiments **116**

4.3.4.1. Spin-adduct detection with EMPO and DEPMPO 116

4.3.4.2. Spectrum simulation 116

4.4. Results **117**

4.4.1. Kinetics of decay of trapped free radicals in ethanol and water **117**

4.4.2. Spin-trapping experiments in ethanol **118**

4.4.2.1. Free radical release by dental resin 118

4.4.2.2. Supplementary experiments 121

4.5. Discussion **122**

4.5.1. Free radicals trapped in the dental resin network disappear in ethanol **122**

4.5.2. Dental resins produce ethoxy radicals in ethanol **122**

4.5.3. Ethoxy radicals are secondary products from the reaction of hydroxyl radicals with ethanol 122

4.6. Conclusion 125

4.7. References 125

Chapter 5 - Investigating filler morphology and mechanical properties of new low-shrinkage resin composite types 129

5.1. Summary 131

5.2. Introduction 133

5.2. Materials and Methods 135

5.2.1. Characterization of the inorganic fraction 136

5.2.1.1. Filler morphology 136

5.2.1.2. Filler mass fraction 136

5.2.2. Mechanical properties 136

5.2.2.1. Dynamic modulus 137

5.2.2.2. Static modulus and flexural strength 137

5.2.2.3. Vickers microhardness 138

5.2.3. Photopolymerization efficiency 138

5.2.4. Statistical analysis 138

5.3. Results 139

5.3.1. Characterization of inorganic fillers 139

5.3.1.1. Filler morphology 139

5.3.1.2. Filler mass fraction 140

5.3.2. Mechanical properties 140

5.3.3. Photopolymerization efficiency 142

5.4. Discussion 143

5.4.1. Filler morphology 143

5.4.2. Filler mass fraction **143**

5.4.3. Mechanical properties **145**

5.4.4. Photopolymerization efficiency **148**

5.5. Acknowledgments **149**

5.6. References **149**

Chapter 6 - Pulpal-temperature rise and polymerization efficiency of LED curing lights **155**

6.1. Summary **157**

6.2. Introduction **159**

6.3. Materials and Methods **161**

6.3.1. Spectrum characterization **161**

6.3.2. Curing efficacy **161**

6.3.3. Temperature rise in the pulp chamber **162**

6.3.4. Statistical analysis **163**

6.4. Results **163**

6.5. Discussion **168**

6.6. Conclusion **172**

6.7. Acknowledgments **173**

6.8. References **173**

Chapter 7 - Irradiation Modes Impact on Radical Entrapment in Photoactive Resins **177**

7.1. Summary **179**

7.2. Introduction **181**

7.3. Materials and Methods **183**

7.4. Results **184**

7.5. Discussion **186**

7.6. Acknowledgments **188**

7.7. References **188**

Chapter 8 - Photoinitiator type and applicability of exposure reciprocity law in filled and unfilled photoactive resins **191**

8.1. Summary **193**

8.2. Introduction **195**

8.3. Materials and Methods **196**

8.4. Results **198**

8.5. Discussion **200**

8.6. Conclusion **204**

8.7. Acknowledgments **204**

8.8. References **204**

Main Abbreviations

ΔT: pulpal temperature rise

Bis-GMA: bisphenol A glycidyl dimethacrylate

CQ: camphorquinone

DC: degree of conversion (%)

DOC: depth of cure (mm)

I: irradiance

L: Lucirin-TPO®

LCU: light curing unit

LED: light-emitting diodes

PAC light: plasma arc curing light

PI: photoinitiator

R•: free radical

$R•_{Allyl}$: allylic radical

$R•_{Propag}$: propagating radical

$R•_{Trapped}$: trapped free radical

RE: radiant exposure

R_p: rate of polymerization

t: irradiation time

TEGDMA: triethylene glycol dimethacrylate

T_g: glass transition temperature

VHN: Vickers hardness number

Chapter 1

Introduction

1.1. Context

In 2010, no scientific evidence exists to prove that dental amalgam is responsible for any harmful effect, either for patient, for practitioner or for the environment. According to Jones (2008), mercury pollution from dentistry is insignificant compared with that from industrial use and natural sources. It was also stated that that banning "dental amalgam" is a political issue that will have no impact on total worldwide mercury pollution. However, throughout the last few years, a significant drift from mercury amalgam to resin composite has been observed. In Finland, a survey revealed that in 1997 dentists already used preferentially resin composites (74.9 %) compared to amalgam (4.8 %) for their restorations (Forss and Widström, 2001). In 2005 in the USA, resin composite was the material used most commonly for posterior restorations (Haj-Ali *et al.*, 2005). In England, the change from mercury amalgams to resin-based composites is nicely highlighted by two studies. In 2001, 49 % of questioned dentists in England rarely or never used resin composites for posterior restorations (Burke *et al.*, 2003). 70 % of them even stated that the stop of amalgam would restrict the dentists ability to adequately treat patients. On the opposite, in 2007, i.e. only 6 years later, the majority of the english dentists questioned affirmed that they place regularly extended resin-composites restorations on posterior teeth (Gilmour *et al.*, 2007). As for the most important factor they considered for their choice, the same trend can be observed in both papers (Burke *et al.*, 2001; Gilmour *et al.*, 2007): clinical indication (100 % in 2003, majority in 2009), esthetic demand of the patient (99 % in 2003, 89 % in 2009), choice of the patient (95 % in 2003, 78 % in 2009). Financial situation of patient (92 % in 2003) and preference of the dentist for one material (76 % in 2009) were not common to both studies.

Patient-related criteria, guided by the race for esthetics, and global scare campaigns regarding mercury, spread by lobbies and media, certainly played an important part in the composite success. But these criteria are not really scientifically-based, so what about clinical indications? Whereas «clinical indication» was revealed by both papers as the most important choice-factor, 61 % of the dentists questioned in 2009 report a decrease of amalgam use over the last 5 years, and 75 % of them an increase of resin-composite placement. Would this mean that the clinical indications have changed? Or that the materials have evolved?

A very interesting statistical analysis of clinical studies between 1998 and 2007 for posterior restorations was presented by Hickel at the 2008 ADM meeting. His results for studies longer than 2 years revealed a mean annual failure rate of 1.5 % for amalgam (10 studies) and 2.2 % for resin composite restorations (46 studies). Considering only long-term studies (≥ 10 years), the mean annual failure rate was 1.4 % for amalgam (4 studies) and 1.9 % for composite restorations (13 studies). As mentioned by the author, the studies differ in terms of study designs and evaluation criteria and the results should therefore be considered with caution. Though, the general trend is interesting and shows that over a 10 year period, both materials seem to present clinically sufficient results. Unfortunately, few papers compare both materials in the same study. In the few works doing so, the annual failure rates reported for amalgams and composites were respectively 0.6 and 0.7 % for Mair *et al.* (1998), 1.8 and 1.9 % for Van Nieuwenhuysen *et al.* (2003), 2.1 and 1.8 % for Opdam *et al.* (2007). These results seem to highlight that a comparable longevity between amalgam and resin composite can be achieved. Only on a very long term follow-up period were amalgam and composites longevity distinguished. Over a 17 year observation period, Van Nieuwenhuysen *et al.* (2003) indeed reported a median survival time of 12.8 years for amalgam and 7.8 years for composites. However, in the latter three considered studies (Mair *et al.,* 1998; Van Nieuwenhuysen *et al.,* 2003; Opdam *et al.*, 2007), it must be stressed that the restoration were performed by only one or two well-informed and experienced practitioners. On the contrary, in a very recent study in Sweden (Sunnegårdh-Grönberg *et al.*, 2009), the data came from 99 salaried dentists from Public Dental Health clinics (n = 2834). The longevity for amalgam restorations was higher than the one reported by Van Nieuwenhuysen *et al.* (2003) (16 years compared to 12.8) but the longevity of composites was lower, i.e. 6 years compared to 7.8. Interestingly, composite restorations showed a significantly increased longevity when performed by more experienced operators (Sunnegårdh-Grönberg *et al.*, 2009). This emphasizes that longevity of composite restorations might be more influenced by the operator skills than amalgam restorations. Operator skills not only relates to the technical ability of the practitioners, but also to a great extent to the «proper use» of resin composites, which implies the knowledge of the material characteristics and the comprehensive understanding of its specificity. In the same way, different reasons for failure between amalgam and composites were reported by Hickel in his review

(considering all studies longer than 2 years): for amalgam, tooth fractures (28 %) prevail on secondary caries (20.9 %), restoration loss (20.8 %), restoration fractures (15 %) and endodontic reasons (7.9 %); for composites, filling fractures (23.8 %) prevail on secondary caries (20.7 %), restoration loss (17.2 %), tooth fractures (9.4%), marginal adaptation (8.4 %), endodontic reasons (6.2 %) and hyper-sensitivities (4.8 %) (Hickel, 2008). It must be underlined that some reasons for failure are relatively specific to composites, i.e. marginal adaptation and hypersensitivity. Hence, these results highlight that the strategies to improve survival rates of composites must be designed according to the material particular characteristics. Notably, a major specificity of current composites is certainly their light-responsive setting process. Photopolymerization reaction of resin-composites is indeed complex and dentists need to take into account numerous factors to optimize the material performance. This leads the practitioners to numerous practical interrogations: What is currently the «best» choice of curing light? What is the appropriate choice among new photopolymerizable composites? What is the impact of alternative photoinitiators included in some composite formulations? Are photocuring procedures safe in terms of pulpal temperature rise? What are the optimal irradiation parameters? To what extent can the irradiation time be reduced thanks to an increase in irradiance? What are the potentially cytotoxic substances in photopolymerizable composites and how is it possible to limit their amount?

To sum up, this thesis will present fundamental research explanations and new findings in order to help answer these clinical issues that may rise when using photopolymerizable resin composites for a tooth restoration. The answers will revolve around the *photopolymerization reaction* and will be based on literature data completed with the new results obtained in this thesis.

«Photopolymerization» describes the conversion of a liquid monomer into a solid polymer under the action of light. Therefore, as underlined by the word itself, two different elements must be considered: the photo-responsive material (photo-POLYMERization) and the photon-emitting device (PHOTO-polymerization). Hence, in the next part of the introduction (**1.2.**), the constituents of the material will be described as well as the way they interact with light. Then, in the last part of the introduction (**1.3.**), the different lights-curing units that have been or are available for dentists will be reviewed, highlighting their respective strong and weak points.

1.2. Photopolymerizable dimethacrylate-based materials used in dentistry

Several kinds of materials available in dentistry contain photopolymerizable dimethacrylates: some adhesives and luting cements, resin-modified glass ionomers, compomers, and especially resin-based composites. The photopolymerization reaction occurs in the dimethacrylate-based organic matrix of the latter (Fig. 1), which will therefore be the central point of this thesis. Apart from resin, composites also contain different proportions of inorganic fillers, and a coupling agent («silane») enabling the bonding between fillers and resin (Fig. 1).

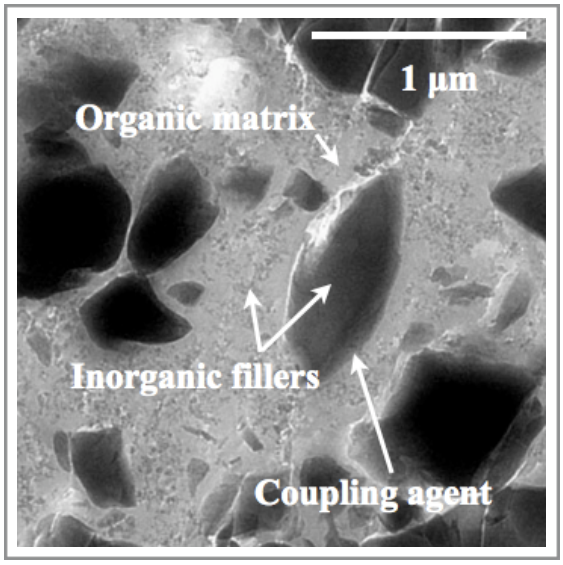

Figure I - TEM image of resin-based composite and its components

Organic matrix represents 25 to 50 vol% of the composite (12 to 40 mass%), and contains mainly monomers, but also photoinitiators in combination with co-intitiators, some inhibitors and pigments. Apart from minor exceptions (ring opening system Silorane®, 3M-Espe), the organic matrix is generally composed of dimethacrylate monomers. They differ from each other by the intermediate chain between two methacrylate groups (Fig. 2) and this intermediate chain determines their specificity. Bis-GMA (bisphenol A glycidyl dimethacrylate) is a heavy molecule (512 g/mol) with two aromatic groups, giving to the molecule a high rigidity. It was introduced by Bowen in 1962 to reduce polymerization shrinkage by reducing the amount of double bonds per volume unit. Bis-GMA is still today widely used in most commercially-available composites. Given its glass transition temperature (T_g = -7.7°C

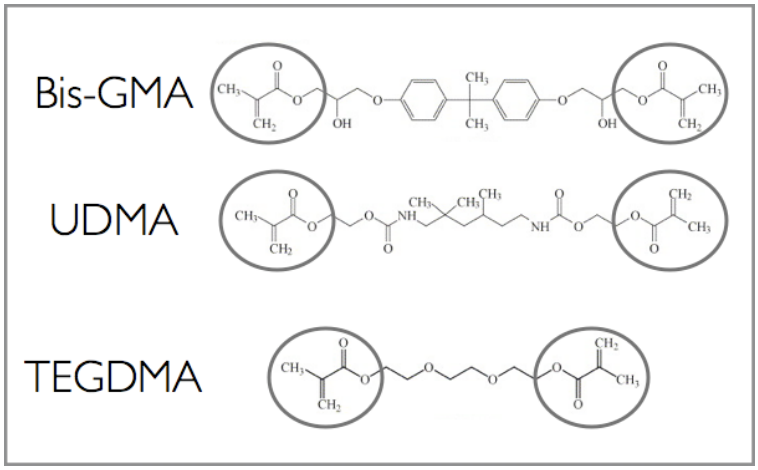

Figure 2 - Formulation of main monomers composing resin-based dental composites. Methacrylate-groups are circled in grey.

- Sideridou *et al.*, 2002), which is slightly below room temperature, Bis-GMA is highly viscous at room temperature, and cannot be used as such, especially considering the necessity to incorporate large amounts of inorganic fillers. Therefore, it must be diluted with low-molecular weight monomers, i.e. in most cases TEGDMA (triethylene glycol dimethacrylate; 286 g/mol; T_g = -83.4°C), which lead to higher conversion values due to their lower T_g and thus lower viscosity (Shobha *et al.*, 1996). UDMA (urethane dimethacrylate; T_g = -35.3°C) was also proposed as an alternative to Bis-GMA. Its intermediate molecular weight (470 g/mol) and more flexible intermediate chain confers more elasticity to the molecules, and therefore less viscosity to the resin compared to Bis-GMA. In this thesis, while UDMA can be found in several commercial formulations, a Bis-GMA / TEGDMA mix was chosen for experimental materials, in order to limit the variables.

In order to be converted from a liquid or paste into a solid, photoinitiator molecules present in the material have to absorb a certain amount of radiation energy $E = h\nu$ (h being the Planck's constant and ν the frequency of the radiation), i.e. a photon of specific wavelength. Then, a free radical can be created (R• in Fig. 3), thereby initiating the polymerization[1]. Currently, the most commonly used photoinitiator is a diketone - camphorquinone (CQ) - combined with a tertiary amine called co-initiator. Dimethyl amino-ethyl methacrylate (DMAEMA) and various other co-initiators have been investigated, but it is difficult to know which ones are used in commercial materials as manufacturers rarely divulge their photoinitiator systems. The «classical» CQ-amine system absorbs specifically blue light, i.e. roughly between 400 and 500 nm, with a peak of maximum absorption at 470 nm. While an increase of CQ concentration leads to an improvement of mechanical properties, this effect is limited. Above a certain value, generally between 0.5 and 1 mass% of the organic matrix, no further improvement is observed. On the opposite, the depth of cure decreases due to excessive absorption in the upper layers of the material (Schroeder *et al.,* 2008). Besides, excessive amounts of CQ also lead to a yellowish aspect to the material. Taira *et al.* (1988) found that CQ concentration in commercial composites ranged from 0.17 to 1.03 mass%. As for the tertiary amine, an improvement of the degree of cure was observed at higher concentrations but it also produced more yellowing of the resin composites (Schneider

[1] The initiation mechanism will be described more in details later (2.1.1.).

et al., 2009). A ratio of one to three times the concentration of CQ is generally used (Yoshida and Greener, 1993).

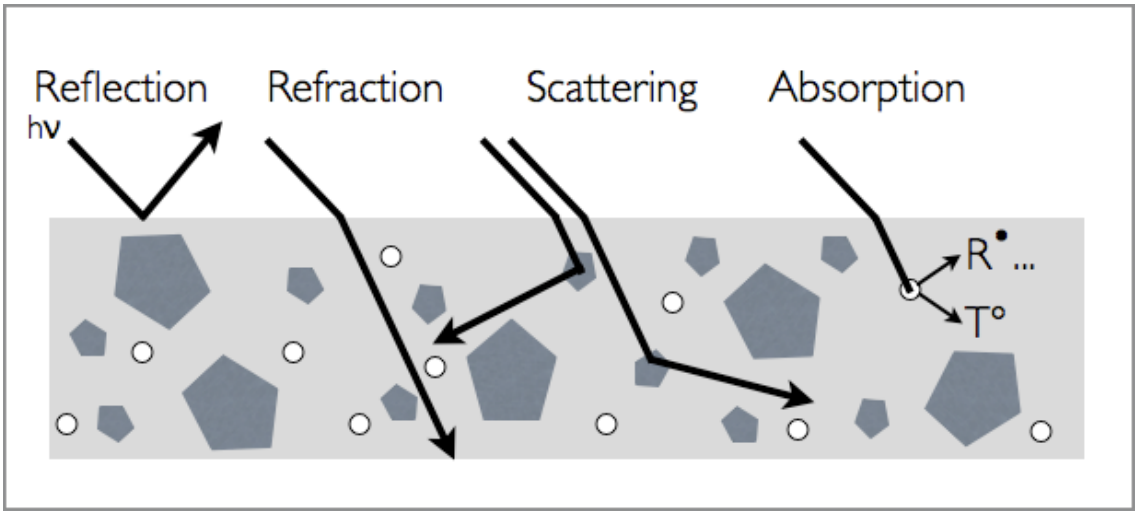

Figure 3 - Possible interactions of light (hν) with a resin-based composite. Light grey shade represents the organic matrix, white spots photoinitiator or pigment molecules, and dark grey polygonal shapes the inorganic fillers. R• stands for radical species, and T° for temperature rise.

Apart from CQ/amine systems, alternative photoinitiating systems appeared during the last few years, mostly due to the increasing popularity of whitening techniques. To restore whitened teeth, extremely white composite shades had to be developed. However, it was difficult to obtain due to the yellowish aspect of CQ powder. Therefore, other photoinitiating systems were incorporated into «bleach» shade composites, such as phenyl propane dione (PPD) or monoacylphosphine oxide (or Lucirin-TPO®). Besides aesthetic reasons, Lucirin is also used to improve the curing efficiency and curing depth. The use of 2 PIs, one with lower molar absorptivity (i.e. CQ) and another with higher absorptivity with maximum absorption at a different wavelength (i.e. Lucirin) can lead to more effective curing through depth, probably due to the broadening of the absorption spectrum, so that more photons are absorbed (Neumann *et al.,* 2008). However, lower quantum yields were measured for polymerization initiated by a mixture of L and CQ compared to systems in which L was used alone, probably due to a transfer from the more efficient photoinitiator (L) to the less efficient one (CQ). But besides these aspects, practitioners should keep in mind that the alternative photoinitiators absorb in other wavelength ranges than CQ. As a result, they should be aware of potential incompatibility between emission spectra of some curing lights and material absorption spectra, which could lead to insufficient

polymerization[2]. Unfortunately, information on commercial composite absorption spectrum is rarely communicated by manufacturers.

Then, it must also be pointed out that free radical generation by CQ/amine systems is not fully efficient. The number of converted photoinitators by absorbed photons - called the quantum yield (Φ) - equals to 0.07 in a 50/50 mass% Bis-GMA/ TEGDMA mixture, which means that 14 photons must be absorbed to create one free radical (Chen *et al.*, 2007). Hence, a certain proportion of photons is absorbed without resulting in radical production. In the same way, photons can be absorbed by pigments. In these cases, the emitted radiation will be transformed into thermal energy (T° in Fig. 3). Other factors than absorption can also prevent light from penetrating deep into the material. A part of the light can indeed be reflected, and photons can also be scattered by inorganic fillers. It has little impact on thin and slightly filled materials such as adhesives, but is a major issue in the case of highly filled composites in thick layers. At a depth of 2 mm, the initial light intensity is indeed reduced by 10–100 times (Phillips, 1991) depending on filler content, light supply and color of the material (Caughman *et al.*, 1991). It is generally admitted that maximum thickness of each composite layer should not exceed 2 mm (Van Noort, 1994; Pollington *et al.*, 2009; **Leprince *et al.*, 2010a - Chapter 5**). Consequently, deep restorations such as class II have to be build up in several layers («increments») photopolymerized separately, ideally each layer during 40 seconds irradiation. However, in case of large tissue loss, multi-increment resin composite restorations is time consuming and there is a clear demand for reduction in chairside procedure times. Some parts of this thesis will present current and new strategies to reduce curing time of each composite layer and other parts will address consequences of composite under-cure.

[2] This will be addressed in Section 2.2.2.

1.3. Light-curing systems[3]

1.3.1. Historical background

Photopolymerization of dental composites appeared in the early 1970s (Buonocore, 1970; Rock, 1974). This represented a significant breakthrough compared to auto-polymerizable resin-based materials, with major improvements such as single paste system requiring no mixing - thereby leading to lower air inclusion in the material - control of working time, reduction of setting time, and higher filler content. However, at that time, the light used to activate the polymerization was ultraviolet (λ = 365 nm, Fig. 4), which presented serious drawbacks. First, the safety aspects related to the use of UV-light were a source of concern for both patients (oral tissue damage) and practitioners (eye injury). Second, there was a serious limitation of the depth of cure of UV-light activated composites, due to increased scattering of shorter wavelengths of light (Cook, 1980). Then, practical problems were also reported, mainly concerning the short life-time of bulbs and the related progressive degradation of light irradiance. Altogether, these aspects led in the 1980s to the replacement of UV-light by «visible» light curing units (LCUs), which are still in use today.

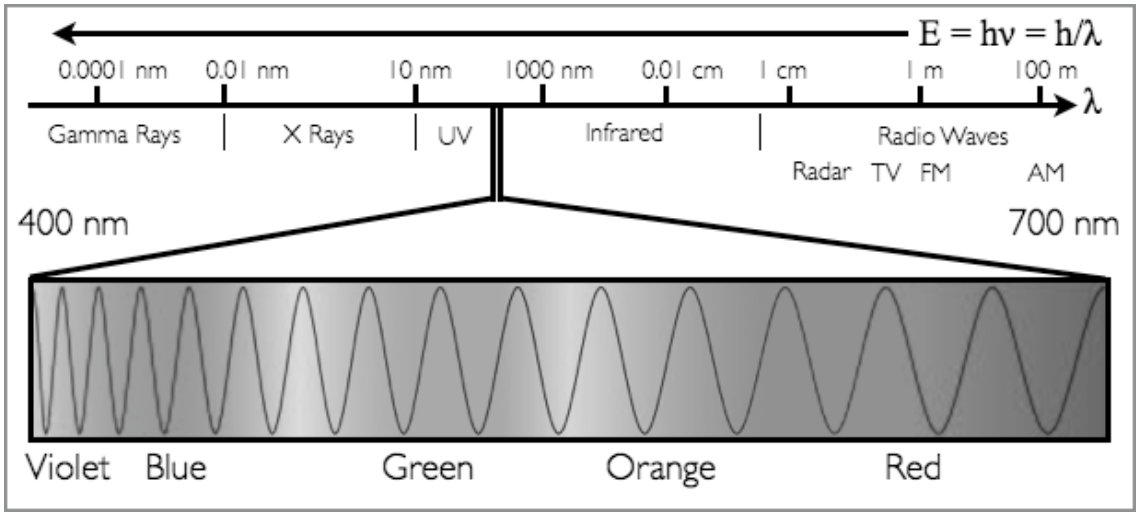

Figure 4 - visible light spectrum compared to global electromagnetic spectrum.

[3] Please note that some of the information below comes from a presentation that I wrote for dental practitioners, which I presented several times during my Ph.D. for continuous education courses. Besides, some of it was also used to write a chapter of the french Medico-Surgical Encyclopedia (EMC) entitled «Polymers and Resin-based Composites».

1.3.2. Technologies of visible light-curing units

1.3.2.1. Quartz-tungsten Halogen (QTH) curing lights

QTH curing lights were the first visible light curing systems available in dentistry. The bulb of this kind of light is made of a tungsten filament, sealed into a quartz envelope filled with an inert gas and a small amount of halogen (iodine, bromide or chloride). The flow of electric current through the filament heats it up to high temperatures so that it produces a continuous spectrum of white light, from near UV to infrared. However, as only blue light is useful to initiate polymerization, filters are used to get rid of light wavelengths above 500 nm and below 380 nm. Consequently, less than 1 % of the energy is delivered as light, most of it forms heat. This waste of energy constitutes the major drawback of halogen lights. First, heat generation leads to degradation of the filament over time, resulting in a progressive decline of light irradiance. To limit this decline, fans are integrated into the light-gun to cool down the bulb. Nevertheless, QTH lights require regular control of their irradiance, using a hand-held radiometer, and replacement of the bulb is frequently necessary (lifetime between 30 and 80 hours). For example, Barghi *et al.* (1994) found that 45 % of LCUs in 122 US dental offices had outputs below 300 mW/cm^2, which is generally considered as the minimum acceptable irradiance (Caughman *et al.*, 1995). The second important drawback of QTH lights, also related to high energy consumption, is the necessity to be plugged to commercial power supply. Hence, it prevents the use of batteries, and the units are generally quite bulky. This is reinforced by the presence of a fan, which is also noisy and requires slits that are difficult to clean. Despite these disadvantages, QTH LCUs are well-proven and are still today considered as a reference. Their spectrum is broad, which makes them efficient on all photoinitiators in commercial materials. They are also relatively low-cost, both on initial purchase and replacement of bulbs. The irradiance of halogen lights ranges from 300 to 800 mW/cm^2 for conventional systems, and from 800 to 1200 mW/cm^2 for the so-called «fast-curing» halogen lights. Besides, some units present a «turbo-tip», i.e. light guide whose exit diameter is smaller than the entrance diameter in order to concentrate light and locally increase irradiance. The pros and cons of this kind of tip will be addressed below (1.3.4.).

The increase in irradiance of LCUs was initiated in order to reduce curing time of each composite layer. This kind of strategy will lead to the development of Plasma

Arc Curing lights (PAC), laser lights and more recently high-power Light-emitting Diodes (LEDs). The interest and limitations of high irradiance curing protocols will be an important part of this thesis, and only the technical aspects are briefly evoked here.

1.3.2.2. Plasma-arc curing lights (PAC)

The light source of these systems is an electric arc produced between two electrodes separated by xenon gas. It produces a very intense white light, which requires light filters similar to QTH lights. With PAC technology, irradiation times as short as 3 s were supposedly sufficient to cure each composite layer. Besides, lower shrinkage values were reported. However, 10 s or even longer irradiation times were in fact necessary (Feng *et al.,* 2009) and the lower shrinkage reported for shorter times was actually related to a lower conversion of the material. In addition, this system is not convenient as it is very bulky, requires large power supply and presents a rigid and thick cord between light source and the tip. Above all, PAC lights are very expensive.

1.3.2.3. Argon Lasers

These systems are based on a laser produced by energy transitions of excited gas ions. The pros and cons of these LCUs are globally very similar to PAC lights. Argon lasers are indeed little convenient for the same reasons as PAC LCUs, and also for the narrowness of their light beam. They are extremely expensive, and their only interesting feature is the very low light dispersion over distance.

1.3.2.4. Light-emitting Diodes (LED)

This constitutes the newest and most popular technology. LEDs use junctions of doped semiconductors transforming electric energy directly into light. They emit a narrow light peak directly in the blue area of the visible spectrum, centered on the peak of maximum absorption of the main composite photoinitiator, CQ. Consequently, irradiation efficiency of these lights is increased compared to broad spectrum QTH lights (Neumann *et al.*, 2006) and filters are no longer necessary. This results in much lower power consumption, enabling the use of batteries, which led to significant ergonomic improvement (Antonson *et al.*, 2008). Then, as energy generated is not in the form of heat, the diodes have a much longer lifetime than other systems (thousands of

hours) (Dunn and Bush, 2002). Besides, light irradiance is very stable over time as long as batteries are full.

However, despite these interesting characteristics, the first generation of LED LCU did not meet with general approval. A large number of diodes was indeed required to reach quite low irradiance - around 300 mW/cm^2. Moreover, notwithstanding interesting reports of lower temperature rise and lower shrinkage, it then seemed that these results were due to their low irradiance, responsible for lower polymerization efficiency. Actually, when temperature rise is measured for LED and QTH curing units at the same irradiance, previous findings that LED curing units induce less temperature rise are not true in general; temperature rise is indeed mainly related to the irradiance (Asmussen and Peutzfeld, 2005). More recently, new diodes were created, reaching much higher irradiance, i.e. currently higher than 1500 mW/cm^2. This so-called second generation of LED lights has been shown to generate material properties comparable to QTH lights (Shortall, 2005; Soh *et al.*, 2004). Though, it must be pointed out that the high irradiance of new diodes led to the reappearance of cooling devices, which are however smaller and better-adapted than QTH fans. LED lights are now increasingly used by practitioners (Antonson *et al.,* 2008), notably due to their potential to reduce irradiation time without significant loss of mechanical properties (Yap and Soh, 2005; Schattenberg *et al.*, 2008). This potential mostly results from the narrower light peak of LEDs, which is better centered on the peak of maximum absorption of CQ. Nevertheless, with the introduction of new photoinitiators in some commercial composites, the narrow spectrum of blue LED lights, initially recognized as an asset, can become a problem because of spectrum mismatch (Price and Felix, 2009). To overcome this problem, the so-called “third generation” of LED LCUs was created, combining two different light peaks, a blue one (470 nm) and a violet one (400 nm). Initial results achieved with these lights have been promising, being similar to or better than those achieved with 2nd generation LED LCUs (Price *et al.*, 2006; **Leprince *et al.*, 2010b - Chapter 6**).

1.3.3. Which technology should a dentist choose?

QTH and LED lights are obviously the most valuable technologies, as they are both clinically validated and affordable. However, LED lights present several practical advantages over QTH lights: potential to some curing time reduction thanks to greater

effective irradiance, batteries, better emission consistency, longer lifetime of diodes, smaller and more convenient layout. The development of LED lights emitting several peaks in various wavelength ranges (LED 3rd generation) reduces the risk of spectrum mismatch (**Leprince *et al.*, 2010b - Chapter 6**). The creation of high irradiance diodes definitely gives the preference to LED technology compared to PAC and lasers, which are much less convenient to use and much more expensive. Nevertheless, the possibility to achieve very high irradiance should not directly result in their routine use. The interest and limitations of very high irradiance will be addressed later in this thesis.

1.3.4. Practical aspects

Here are some practical aspects dental practitioners should also be aware of. To start with, there are different types of light guide tips: different diameters, regular and «turbo» tips and diodes directly exposed behind a transparent cover (Fig. 5). The

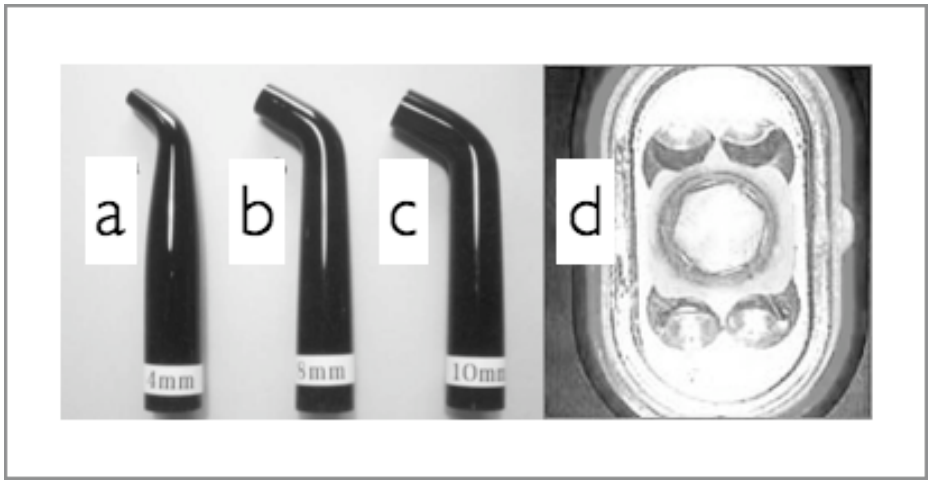

Figure 5 - Different light guides available; a) and b) are turbo tips, c) is the regular light guide and d) presents the diodes directly behind a simple transparent cover.

size and shape of the light exit can have important impact on the irradiance received by the material and its distribution across the surface. Vandewalle *et al.* (2005 and 2008) reported a greater light dispersion with turbo tips and diodes directly exposed, which leads to less uniform polymerization in case of large surface restorations. Moreover, it also leads to a higher decrease of irradiance with increasing material-tip distance, resulting in decreasing polymerization efficiency in depth. Therefore, regular tips with constant diameter should be preferred. It must also be mentioned that turbo tip were introduced to increase the irradiance directly at the exit of the tip - as irradiance is reported to the surface (mW/cm^2), it increases if the surface is reduced. However, the

irradiance of sources has become so high that the use of turbo tips to benefit from an additional increase is no longer justified, given the associated drawbacks cited above.

Then, another important drawback of some LED lights must be pointed out: the variability between manufacturer irradiance specifications and actual irradiance. For some lights, the mean measured irradiance is less than half the pretended value (Ernst *et al.,* 2006; ADA, 2006). As a matter of fact, it is more expensive for LCU manufacturers to ask their diode supplier for an accurate selection of diodes of the desired irradiance. As the appropriate irradiation time depends on the irradiance, dentists should ideally be able to verify the real irradiance of the LCU before purchase, which is unfortunately difficult, notably due to the little reliability of hand-held radiometers.

Last but not least, safety aspects related to the use of curing lights must be addressed. While concerns were clearly raised for UV-lights in the 1970s, UV diodes have now reappeared in 3rd generation LED units, which should certainly be considered on a safety point of view. Moreover, the potential damage by high irradiance visible LCUs to patients oral tissues and to dentist eyes are too often neglected. As already stated by Van Noort in 1994, the term «visible» light gives a feeling of safety because it is something that people are exposed to all the time. But blue light is not as safe as it might be thought. First, on a dentist point of view, hight intensity blue light can have a harmful effect on retina, due to «blue light hazard». Though blue light is less energetic than UV (Fig. 4), the use of very high irradiance combined with specific sensitivity of certain photoreceptors can certainly be harmful to retinal cells. Hence, dentists should request efficient and large shields for their curing unit. Then, concerning oral tissues of patients, the damage potential of UV light to skin is well-known. Contrary to more energetic radiations UVB (315 nm - 280 nm) and UVC (280 nm - 100 nm), which can directly damage DNA, the wavelengths used in dentistry (UVA - 400 nm to 315 nm) are usually associated with indirect DNA damage through creation of reactive oxygen species. Apart from UV light, there is also some evidence of cellular function disruption of fibroblasts *in vivo* under the action of visible dental curing lights (Wataha *et al.,* 2004; Hwang *et al.,* 2008). The identity of blue light targets that mediate the cell changes are unclear, but it seems to be linked with creation of reactive oxygen species (Omata *et al.*, 2006), possibly due to a thermal effect. Moreover, the effect is radiant energy dependent (Wataha *et al.,* 2004), which underlines the importance to optimize

irradiance and exposure time. It also highlights another interest of using a rubber dam during composite restoration procedures.

1.3.5. Conclusions

These different considerations can help dentists to choose the best light curing unit available. They should go for a LED light, for its convenience and efficiency, and favor regular light guides. QTH lights remain a valuable technology for those who do not care about their less convenient aspects, but the irradiance of these lights needs to be checked regularly. But besides the choice of light technology, uncertainties remain regarding the irradiance and curing time that should be used. In particular, the potential of high irradiance to enable curing time reduction needs to be addressed and will be one main topic in the present thesis. Moreover, another point that is not clear is the spectral correspondence between emission and absorption spectra. As explained above, the evolution of curing light spectrum started in the UV, then moved to a broad visible spectrum (QTH lights), then to a narrow blue peak (1st and 2nd generations LED lights). Now, emission spectra tend to broaden again (3rd generation LEDs), and near-UV wavelengths reappear. Such back-and-forth changes can certainly confuse dentists. Therefore, the latter need information on the efficiency of recent curing lights to cure materials containing new photoinitiators. This will be another main topic of this thesis. But in order to properly address these subjects, deep understanding of the photopolymerization reaction is necessary. Therefore, theoretical aspects will also be summarized in this work, and completed with new results obtained with innovative methods.

1.4. References

American Dental Association (2006). *Professional Product Review* vol 1.

Antonson SA, Antonson DE, Hardigan PC (2008). Should my new curing light be an LED?. *Oper Dent* 33:400-407.

Asmussen E, Peutzfeldt A (2005). Temprature rise induced by some light emitting diode and quartz-tungsten-halogen curing units. *Eur J Oral Sci* 113:96–98.

Barghi N, Berry T, Hatton C (1994). Evaluating intensity output of curing lights in private dental offices. *J Am Dent Assoc* 125:992-996.

Bowen RL (1962). Dental filling materials comprising of vinyl-silane fused silica and binder consisting of the reaction product of bispenol and glycidyl methacrylate. *US Patent* 3, 066, 112.

Buonocore M (1970). Adhesive sealing of pits and fissures for caries prevention, with use of ultraviolet light. *J Am Dent Assoc* 80:324-330.

Burke FJ, McHugh S, Hall AC, Randall RC, Widstrom E, Forss H (2003). Amalgam and composite use in UK general dental practice in 2001. *Br Dent J* 194:613-618

Caughman WF, Rueggeberg FA, Curtis JW Jr (1995). Clinical guidelines for photocuring restorative resins. *J Am Dent Assoc* 126:1280-2, 1284, 1286.

Caughman WF, Caughman GB, Shiflett RA, Rueggeberg F, Schuster GS (1991). Correlation of cytotoxicity, filler loading and curing time of dental composites. *Biomaterials* 12:737–740.

Chen Y-C, Ferracane JL, Prahl SA (2007). Quantum yield of conversion of the photoinitiator camphorquinone. *Dent Mater* 23:655-664.

Cook WD (1980). Factors affecting the depth of cure of UV-polymerized composites. *J Dent Res* 59:800-808.

Dewaele M, Truffier-Boutry D, Devaux J, Leloup G (2006). Volume contraction in photocured dental resins: the shrinkage-conversion relationship revisited. *Dent Mater* 22:359-365.

Dunn WJ, Bush AC (2002). A comparison of polymerization by lightemitting diode and halogen-based light-curing units. *J Am Dent Assoc* 133:335-341.

Ernst CP (2006). Feldtest zur Lichtemissionsleistung von Poly-merisationsgeräten in zahnärztlichen Praxen. *DZZ* 60:466-471.

Feng L, Carvalho R, Suh BI (2009). Insufficient cure under the condition of high irradiance and short irradiation time. *Dent Mater* 25:283-289.

Forss H, Widström E (2001). From amalgam to composite : selection of restorative materials and restoration longevity in Finland. *Acta Odontol Scand* 59:57-62.

Gilmour AS, Evans P, Addy LD (2007). Attitudes of general dental practitioners in the UK to the use of composite materials in posterior teeth. *Br Dent J* 202:E32.

Haj-Ali R, Walker MP, Williams K (2005). Survey of general dentists regarding posterior restorations, selection criteria, and associated clinical problems. *Gen Dent* 53:369-375.

Hickel R (2008). Long-term success of posterior restorations. Proceedings of the Academy of Dental Material Conference, Oct 2-4, 2008, Wurzburg, Germany. Academy of Dental Marterials.

Hwang IY, Son YO, Kim JH, Jeon YM, Kim JG, Lee CB, Park JS, Lee JC (2008). Plasma-arc generated light inhibits proliferation and induces apoptosis of human gingival fibroblasts in a dose-dependent manner. *Dent Mater* 24:1036-1042.

Jones DW (2008). Has dental amalgam been torpedoed and sunk? J Dent Res 87:101-102.

Leprince J, Palin WM, Mullier T, Devaux J, Vreven J, Leloup G (2010a). Investigating filler morphology and mechanical properties of new low-shrinkage resin composite types. *J Or Rehab*, doi: 10.1111/j.1365-2842.2010.02066.x

Leprince J, Devaux J, Mullier T, Vreven J, Leloup G (2010b). Pulpal-temperature rise and polymerization efficiency of LED curing lights. *Oper Dent* 35:220-230.

Mair LH (1998).Ten-year clinical assessment of three posterior resin composites and two amalgams. *Quint Int* 29:483-490.

Neumann MG, Schmitt CC, Ferreira GC, Correa IC (2006). The initiating radical yields and the efficiency of polymerization for various dental photoinitiators excited by different light curing units. *Dent Mater* 22:576-584.

Neumann MG, Schmitt CC, Horn MA Jr (2009). The effect of the mixtures of photoinitiators in polymerization efficiencies. *J Appl Pol Sci* 112:129-134.

Omata Y, Lewis JB, Rotenberg S, Lockwood PE, Messer RL, Noda M, Hsu SD, Sano H, Wataha JC (2006). Intra- and extracellular reactive oxygen species generated by blue light. *J Biomed Mater Res A* 77:470-7.

Opdam NJ, Bronkhorst EM, Roeters JM, Loomans BA (2007). A retrospective clinical study on longevity of posterior composite and amalgam restorations. *Dent Mater* 23:2-8.

Phillips RW. Science of Dental Materials. WB Saunders, Philadelphia,1991.

Pollington S, Kahakachchi N, van Noort R (2009). The influence of plastic light cure sheaths on the hardness of resin composite. *Oper Dent* 34:741-745.

Price RB, Felix CA (2009). Effect of delivering light in specific narrow bandwidths from 394 to 515nm on the micro-hardness of resin composites. *Dent Mater* 25:899-908.

Price RB, Felix CA, Andreou P (2006). Third-generation vs a second-generation LED curing light: effect on Knoop microhardness. *Compend Contin Educ Dent* 27:490-496.

Rock WP (1974). The use of ultra-violet radiation in dentistry. Br Dent J 136:455-458.

Schattenberg A, Lichtenberg D, Stender E, Willershausen B, Ernst CP (2008). Minimal exposure time of different LED-curing devices. *Dent Mater* 24:1043-1049.

Schneider LF, Cavalcante LM, Consani S, Ferracane JL (2009). Effect of co-initiator ratio on the polymer properties of experimental resin composites formulated with camphorquinone and phenyl-propanedione. *Dent Mater* 25:369-375.

Schroeder WF, Cook WD, Vallo CI (2008). Photopolymerization of N,N-dimethylaminobenzyl alcohol as amine co-initiator for light-cured dental resins. *Dent Mater* 24:686-693.

Shobha HK, Sankarapandian M, Schultz AR, McGrath JE, Kalachandra S, Taylor DF (1996). Recent advances in free radical polymerization. *Makromol Chem Macromol Symp* 111:73–83.

Shortall AC (2005). How light source and product shade influence cure depth for a contemporary composite. *J Or Rehab* 32:906-911.

Sideridou I, Tserki V, Papanastasiou G (2002). Effect of chemical structure on degree of conversion in light-cured dimethacrylate-based dental resins. *Biomaterials* 23:1819-1829.

Soh MS, Yap AU, Yu T, Shen ZX (2004). Analysis of the degree of conversion of LED and halogen lights using micro-Raman spectroscopy. *Oper Dent* 29:571-577.

Sunnegårdh-Grönberg K, van Dijken JW, Funegård U, Lindberg A, Nilsson M (2009). Selection of dental materials and longevity of replaced restorations in Public Dental Health clinics in northern Sweden. *J Dent* 37:673-678.

Taira M, Urabe H, Hirose T, Wakasa K, Yamaki M (1988). Analysis of photo-initiators in visible-light-cured dental composite resins. *J Dent Res* 67:24-28.

Van Nieuwenhuysen JP, D'Hoore W, Carvalho J, Qvist V (2003). Long-term evaluation of extensive restorations in permanent teeth. *J Dent* 31:395-405.

Van Noort (1994). Introduction to Dental Materials. Mosby editor. pp. 92-94

Vandewalle KS, Roberts HW, Andrus JL, Dunn WJ (2005). Effect of light dispersion of LED curing lights on resin composite polymerization. *J Esthet Restor Dent* 17:244-254.

Vandewalle KS, Roberts HW, Rueggeberg FA (2008). Power distribution across the face of different light guides and its effect on composite surface microhardness. *J Esthet Restor Dent* 20:108-117.

Wataha JC, Lockwood PE, Lewis JB, Rueggeberg FA, Messer RL (2004). Biological effects of blue light from dental curing units. *Dent Mater* 20:150-157.

Yap AU, Soh MS (2005). Curing efficacy of a new generation high-power LED lamp. *Oper Dent* 30:758-763.

Yoshida K, Greener EH (1993). Effects of two amine reducing agents on the degree of conversion and physical properties of an unfilled light-cured resin. *Dent Mater* 9:246-251.

Chapter 2

Literature Review

And

Major Findings

Foreword

During this PhD, several experimental projects were conducted to answer specific questions regarding photopolymerizable dimethacrylate-based dental materials. What is the fate of trapped free radicals? Are free radicals released by dental resins? What are the mechanical properties of new low-shrinkage composites? How efficient are new LED-lights? Are the latter capable of inducing pulp over-heating? Why is the positive effect of increased irradiance limited? Could new photoinitiators enable curing time reduction? The answers will be subsequently presented in chapters from 3 to 8.

At first sight, these different topics might seem somewhat disjointed. However, they are strongly connected together. Besides experimental projects, a global work of reflection was indeed conducted to understand the factors and principles governing photopolymerization reaction of dental resins. This work pointed out areas of the literature that needed clarification or development, and the experimental projects partially of totally filled in the blanks. Consequently, instead of presenting a mere summary of my main results, I wished to integrate them into a sort of literature review, which will be structured as follows.

I will first present my vision of the theoretical aspects of photopolymerization reaction. The accent will be placed on the specificity of polymers used for dental restoration, and on the potential consequences of their particular characteristics regarding their clinical use.

Secondly, more clinically connected aspects will be considered. Indeed, while very interesting on a researcher's point of view, theoretical characteristics of polymerization reaction lack to give clinicians guidelines and practical information connected to their daily practice. Hence, it was of prime interest to investigate new commercially available composites and light curing units. These works on commercial products - connected to clinician concerns - led to new fundamental research projects by highlighting areas requiring further understanding and by giving birth to new ideas of material development.

The third part of this review will present innovative approaches dealing with a frequent subject of debate in the photopolymerization of dental resin-based materials,

i.e. the applicability of the so-called Exposure Reciprocity Law, supporting the decrease of irradiation time by a proportional increase of irradiance.

Finally, I will put forward points of interest from the perspective of future research.

2.1. Theoretical aspects of photopolymerization reaction

2.1.1. Basics of photo-induced radical polymerization reaction

Basically, a polymerization process is a chemical reaction during which monomers connect to form polymers. But this reaction needs to be triggered. In the case of photosensitive dimethacrylate-based dental resins, free radicals generated by irradiation of a light-sensitive initiator open the double bonds at both ends of the

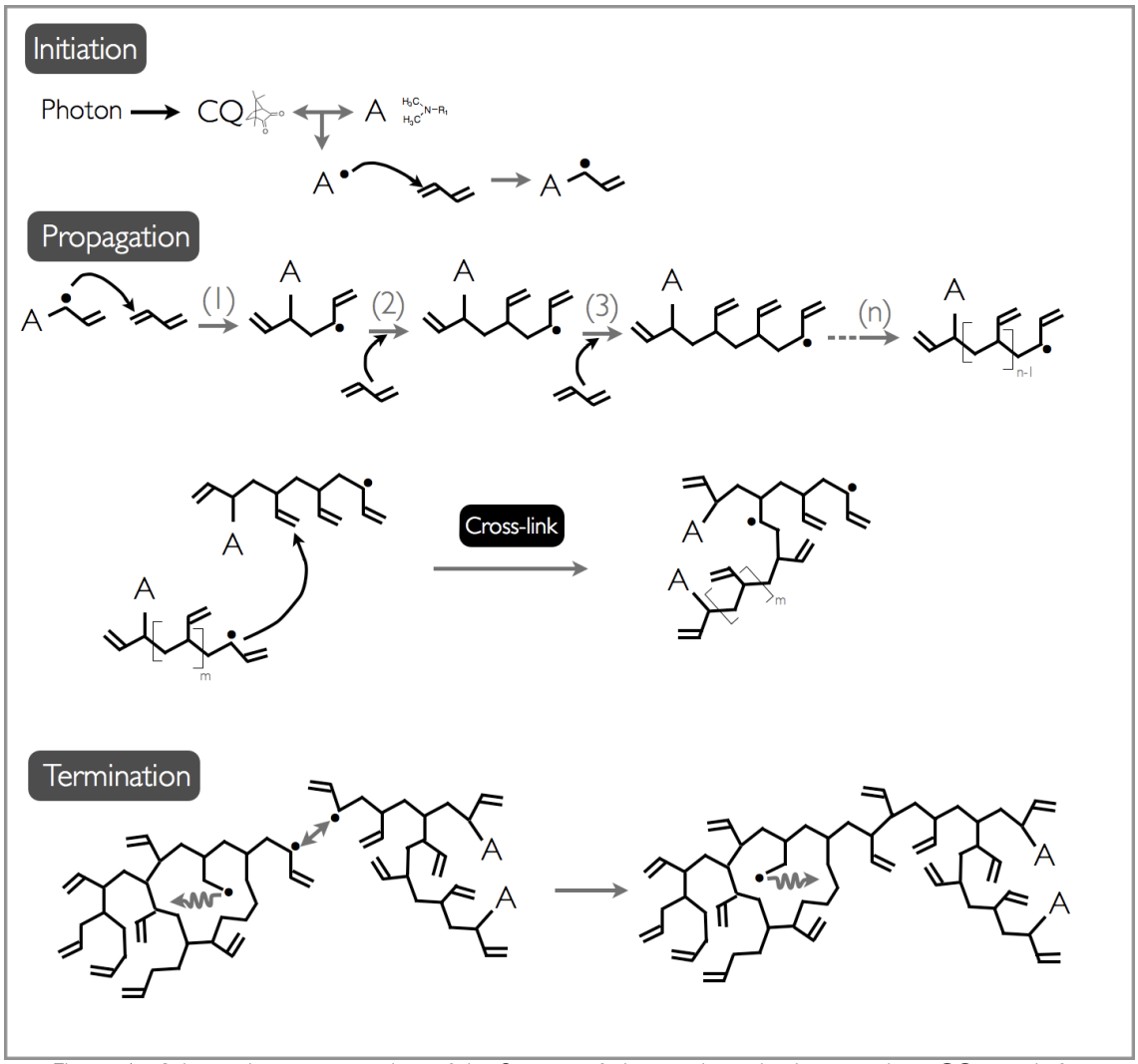

Figure 6 - Schematic representation of the 3 steps of photopolymerization reaction. CQ stands for Camphorquinone, A for a tertiary amine. • indicates a radical species. (1), (2), (3) and (n) represent the theoretical steps of linear monomer addition. n and m stand for a large amount of monomer units. A trapped radical is illustrated in the termnation section and segmental mobility is represented by a twisting grey arrow. A double grey arrow indicates radicals about to react together (bimolecular termination).

monomers, generating a cross-linking polymerization. Photopolymerization is classically described into 3 steps: initiation, propagation and termination, schematically represented in Fig. 6.

During the *initiation*, a free radical is generated through the activation of a photosensitive molecule by a photon of specific wavelength. In the case of dental composites, the most commonly used photoinitiating system is a combination of a photosensitive diketone, i.e. camphorquinone (CQ), with an electron donor called co-initiator, generally a tertiary amine. Other photoinitiators recently appeared in the dental composites, but they will be treated later in this work. After its interaction with a photon of specific wavelength (maximum efficiency at 467 nm), the excited ketone takes an electron from the tertiary amine inside an excited complex (or «exciplex») (Fig. 7a-b). Then, $H^{\bullet}$ is transferred from A to CQ (Fig. 7c-d), resulting in the creation of two free radicals: $A^{\bullet}$ and $CQH^{\bullet}$ (Fig. 7e). The latter is not an efficient initiator and dimerizes (Fig. 7f) (Cook, 1992; Jakubiak *et al.*, 2003), while the former is very reactive and is

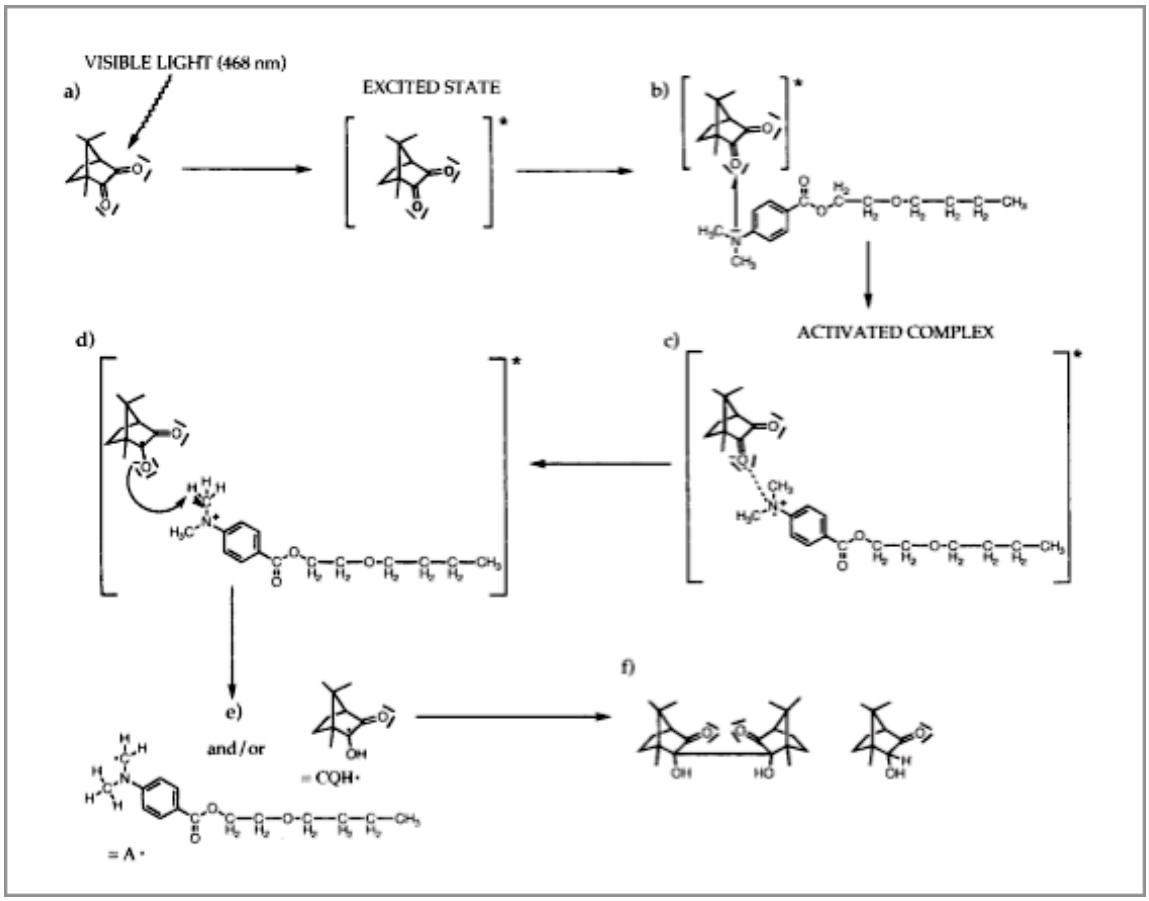

Figure 7 - First step of initiation and camphorquinone terminaison: a) light excitement of camphorquinone, b) camphorquinone reaction with tertiary amine, c) formation of an activated complex, d) rearrangements in the activated complex, e) creation of two kinds of radicals, f) two kinds of camphorquinone terminaisons. (Truffier-Boutry *et al.*, 2003)

generally considered as responsible for initiating the polymerization. It indeed quickly reacts with a nearby monomer, opening its C=C bond. Then follows a chain reaction, the *propagation*, by which the monomer grows by repetition of this C=C opening by the radical and addition of a large number of monomer units one after the other. The polymer can either grow linearly by reaction with monomers (Schematically represented in Fig. 6, reactions 1, 2, 3, n), leaving pendant double bonds, or react with another growing polymer chain, creating cross-links (Fig. 6). The addition of supplementary units continues until free radicals react with each other to form a stable covalent link through *bimolecular termination* reaction (Fig. 6). The latter can occur either by recombination (combination of two free radicals) or by dismutation (transfer of $H^{\bullet}$ with production of an unsaturated bond on one of both chains, and a saturated one on the other). However, bimolecular termination can only occur until the molecular mobility is high enough for species to meet. But as will be described below, the network builds up so quickly that all the radicals are not able to encounter other radicals. Radical growth centers add as much monomers as allowed by the system mobility, which is quickly decreasing. When no further addition is possible, they become trapped, which is referred to as *monomolecular termination*[4]. Note that these three steps, *initiation* - *propagation* - *termination*, are described separately for more clarity, but they all occur simultaneously throughout all the polymerization reaction. Only the relative importance of each one will vary with time, as will be described further.

The extent of polymerization can be quantified by comparing the initial amount of double bonds to the final one. This ratio, expressed in %, is called degree of conversion (DC) and can be calculated as follows: $DC = 1 - \frac{(C=C)_{Final}}{(C=C)_{Initial}}$. When this DC is represented as a function of time, the slope of the curve represents the speed of the reaction, called rate of polymerization (R_p). DC can be directly measured by

[4] This designation of «monomolecular termination» can be found in numerous polymer-related publications, notably Decker and Elzaouk (1995) and Andrzejewska (2001). For that reason, it will be used in the present work to describe the situation when, in contrast to «bimolecular termination», free radicals become inactive by immobilization in the polymer network due to the increasing viscosity. However, it is worth mentioning that this designation is somehow inappropriate as the free radicals that become trapped do not really terminate, as they still exist within the network. Moreover, if the mobility of the system increases (swelling by solvents, temperature increase, etc.), they regain the capacity to react with remaining double bonds and continue the reaction. Hence, one can find more accurate to talk about «radical immobilization» or «radical entrapment».

spectroscopic methods such as Raman (Pianelli *et al.*, 1999) or Fourier Transformed Infrared (FTIR - Mid IR or Near IR) spectroscopy and its value generally ranges from 35% to 77% (Schmalz and Arenholt-Bindslev, 2009) depending if unfilled or filled resins are considered. DC is a very important characteristics of the material as there is a significant and positive correlation between mechanical properties and degree of conversion (Ferracane and Greener, 1986). Stability and biocompatibility of the polymer are also related to DC, as will be explained further (2.1.4.).

2.1.2. Specificity of highly crosslinked polymer network

As mentioned above, it appears from DC values found in the literature that even in optimum irradiation conditions, DC is limited and a complete conversion (100%) cannot be obtained. This constitutes the specificity of the kind of polymers used in dental resins. The monomers used are indeed *tetrafunctional,* as each molecule has the potential to bind to 4 other molecules or structures (Fig. 8). As a result, a highly crosslinked network is formed, with covalent bonds between polymer chains, contrary to non-crosslinked polymer chains where long linear chains are not connected with each other, *e.g.* polyethylene. The cross-linked structure has major consequences on the material characteristics. Physical properties and structural stability of a polymer are indeed correlated nonetheless with degree of conversion, but also with cross-linking density (Lovell *et al.*, 2001). Increased cross-linking reduces molecular mobility, which can generally be highlighted by an increase of glass transition temperature (T_g, which represents the temperature at which the polymer vitrifies during polymerization process - above this temperature, the same polymer would return from a glassy to a rubbery state if heated up[5]). The cross-linked structure has also a considerable impact on the kinetic profile of the polymerization reaction. This is of prime interest as regards the topic of this thesis, as the polymerization kinetics must be clearly explained to properly understand the

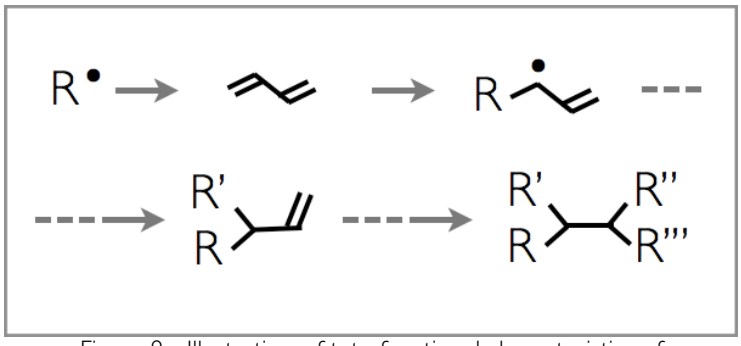

Figure 8 - Illustration of tetrafunctional characteristics of dimethacrylate monomers.

[5] The transition between glassy and rubbery state will be described further in more details.

consequences of curing protocol modifications. As mentioned above, *initiation, propagation* and *termination* are not really successive steps but co-exist during the polymerization process. The relative importance of each step varies during the reaction, mainly depending on the mobility of the system.

The kinetics of the polymerization reaction will now be described, with reference to Fig. 9 and to the following equations:

$$R_p = k_p [R\bullet] [M] \quad (1)$$

$$R_t = k_t [R\bullet]^2 \quad (2)$$

where R_p and R_t are respectively the rate of propagation and termination, k_p and k_t respectively the constants of propagation and termination, M stands for monomers and R• for radical species.

At the very beginning of the polymerization, both degree of conversion and cross-linking density are low, and the mobility of the system is high. Hence, according to the steady-state (quasi-stationary) approximation, it can be assumed that the free radical concentration is stable, i.e. there is an equilibrium between radicals created by initiation (R_i = rate of initiation) and radicals consumed by termination: $R_t = R_i$ and R_p = constant (Anseth *et al.*, 1996). This is illustrated by the quasi plateau of R_p for

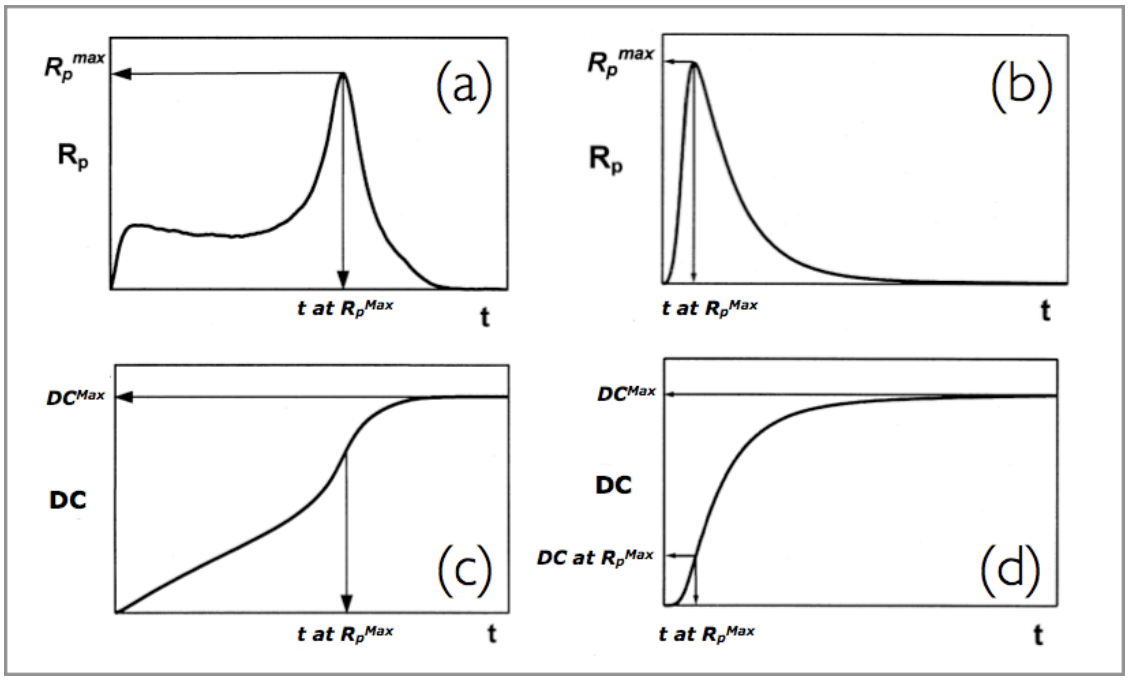

Figure 9 - Typical shape of kinetic curves for the polymerization of monomethacrylate monomers (a & c) and for dimethacrylate monomers (b & d): a & b represent the polymerization rate (R_p) as a function of irradiation time (t), c & d the degree of conversion (DC) as a function of time
(Charts modified from Andrzejewska, 2001)

monomethacrylate monomers in Fig. 9a, and by the relatively linear increase of DC with time in Fig. 9c. However, this plateau is generally not observed for dimethacrylate monomers (Fig. 9b), witnessing that the steady-state assumption is mainly invalid for cross-linked systems, except maybe during the very first instants of the reaction (below 10% conversion, according to Anseth *et al.* (1996).

As the propagation proceeds, DC (for mono- and dimethacrylate monomers) and crosslinking density (for dimethacrylate monomers) increase. Therefore, the system viscosity increases, and the mobility of the chemical species decreases accordingly: it is the *gelation*. As schematically represented in Fig. 10a, the mobility restriction firstly affects radicals, located on large molecules (growing polymer chains), whereas small monomer molecules can still diffuse easily. In other words, k_t decreases significantly while k_p scarcely changes (Fig. 11). Consequently, termination drops dramatically while new growth centers are still created by intiation ($R_i >> R_t$). Hence, [R•] increases (Eq. 1), which results in a spectacular increase of R_p (Fig. 9a and b), called *autoacceleration*. Due to this gel effect, termination occurs via reaction-diffusion, and therefore depends on propagation, as illustrated by the parallelism between k_t and k_p curves on Fig. 11. As demonstrated by Anseth *et al.* (1996), a higher concentration of double bonds and a higher crosslinking density both lead to an earlier onset of *autoacceleration*. In other words, variations of monomer nature (mono- or dimethacrylates, molecular weight, molecule stiffness, etc.) and proportions can result in various intermediate kinetic profiles between Fig. 9a-c and Fig. 9b-d.

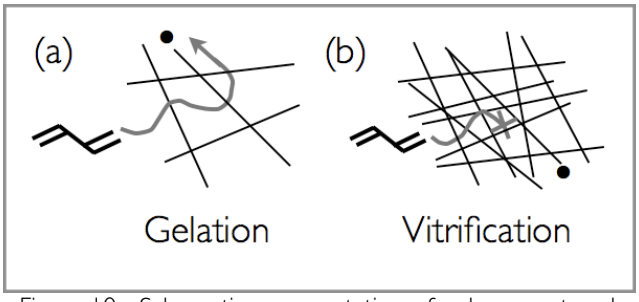

Figure 10 - Schematic representation of polymer network in gel- (a) and vitreous state (b).

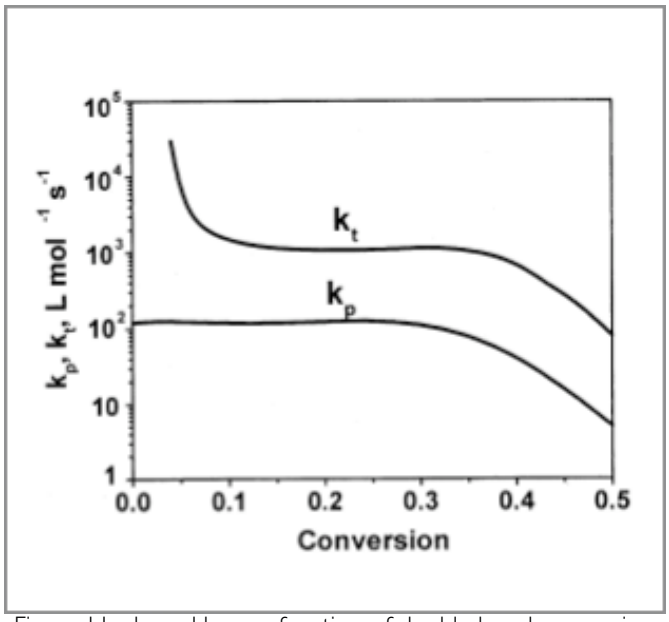

Figure 11 - k_t and k_p as a function of double bond conversion for diethylene glycol dimethacrylate at 30°C. (From Andrzejewska, Prog Polym Sci 2001)

Finally, at the end of the reaction, viscosity gets so high that diffusion becomes limited even for monomer molecules. As represented in Fig. 10b, monomers can no longer reach radicals to be added to the chain. At that time, k_p starts decreasing (Fig. 11), which results in a sharp drop of the propagation rate, called *autodeceleration*, while DC tends to plateau: it is the *vitrification.* As termination is reaction-diffusion controlled, k_t decreases concomitantly to k_p (Fig. 11). Vitrification takes place when T_g of the polymerizing material reaches reaction temperature, i.e. ambient temperature plus ΔT of the reaction exotherm. For example, T_g of a 50/50 mass% Bis-GMA - TEGDMA cured polymer lies around 47.5°C (Dewaele *et al.*, 2009). A major consequence of the vitrification, which occurs before the reaction was able to get to completion, is the entrapment of three kinds of active species: pendant double bonds, free monomers and free radicals (Fig. 12). While the presence of free monomers has already been widely described in the literature, it is not the case of trapped free radicals. The latter constituted a main interest in the present thesis, and several chapters were dedicated to their study (Chapters 3, 4 and 7). Their major findings will be discussed below.

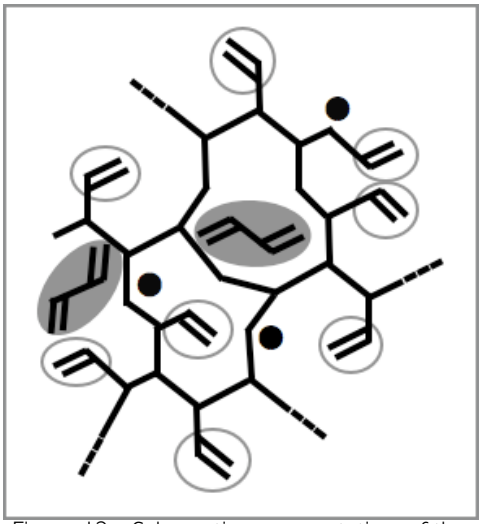

Figure 12 - Schematic representation of the active species that remain trapped in the network after vitrification: • indicate radical species, plain grey circles free monomers, and grey circles pendant double bonds

2.1.3. Trapped free radicals: detection, identification, quantification and follow-up

In general, it is extremely difficult to detect free radicals, as they are extremely reactive, and therefore disappear very quickly in solution. However, as explained above, the decrease in molecular mobility during the polymerization is associated with a progressive entrapment of radical growth centers. Thanks to this unique feature of dental resins, free radicals can be detected days or even months after photopolymerization (Kloosterboer *et al.,* 1986; Truffier-Boutry *et al.*, 2006; **Leprince *et al.*, 2009 - Chapter 3**) by means of electron paramagnetic resonance (EPR) spectroscopy. This technique, also called electron spin resonance (ESR)[6], is adapted for

[6] For more clarity, EPR will be used throughout all this work.

the study of chemical species with unpaired electrons. Once submitted to a magnetic field ($\vec{B}$), the average electron magnetic moment aligns itself either parallel or antiparallel to the field (Fig. 13). Both orientations correspond to two energy levels and the energy difference between the two spin states (ΔE) is proportional to the magnetic field. An unpaired electron can change its energy level either by absorbing or by emitting electromagnetic radiation of energy hν. As there are more electrons in the lower energy state (Maxwell-Boltzmann distribution), energy absorption is favored. Therefore, when a microwave radiation is supplied to the sample, resonance occurs when hν corresponds to ΔE, which is monitored and converted into a spectrum, usually represented by its first derivative in EPR (Fig. 13). Atoms surrounding the electron can influence the electron if they possess a magnetic moment, which leads to the splitting of the EPR signal into 2 or more peaks[7]. In the same way, the environment of the electron also influences the shape of the signal, which was nicely highlighted for dimethacrylate-based materials in the work of Anseth *et al.* (1996). In the latter, the EPR spectrum presents 13 lines at low conversion values (Fig. 14a) - liquid environment - and then switches sharply to a 9-line spectrum (Fig. 14b) as the system vitrifies. In that work, the free radical concentration was followed in real time, which is very interesting conceptually. However, two limitations must be underlined for real-time follow-up of free radical concentrations.

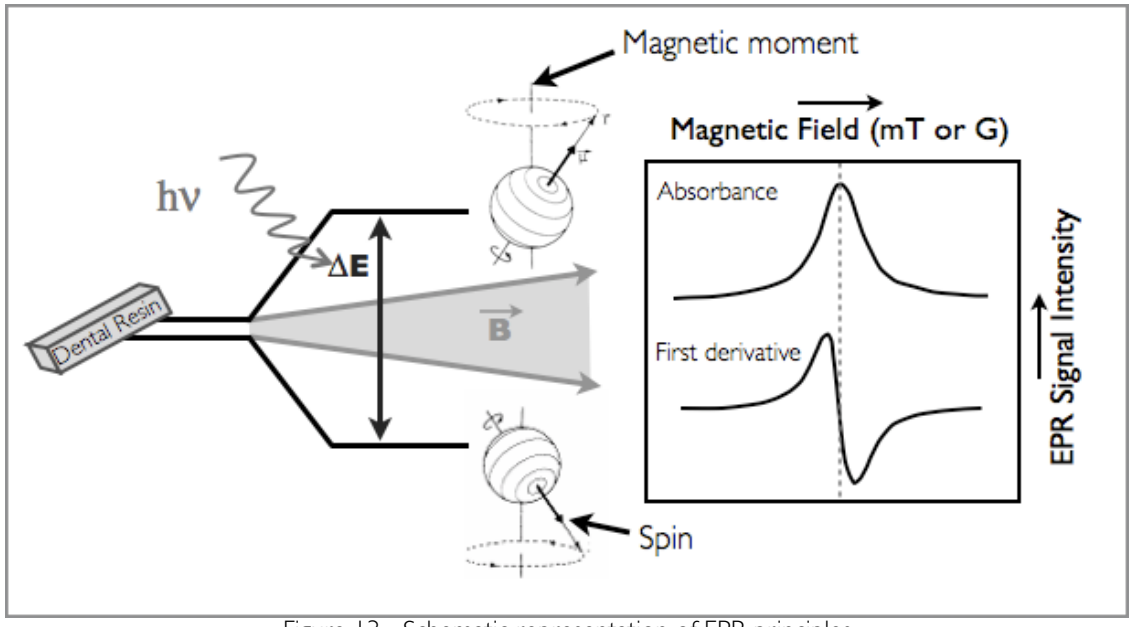

Figure 13 - Schematic representation of EPR principles

[7] The resulting spectrum is characterized by values called hyperfine constants.

First, very low light irradiance is generally used, i.e. 0.2 mW/cm^2 (Anseth *et al*., 1996) or 5 mW/cm^2 (Berchtold *et al.* 2005), which is irrelevant compared to the irradiance of dental curing lights (from 400 to 3000 mW/cm^2). The reason for this choice is the need to slow down the reaction to be able to follow it by EPR. Even though, in some cases, they were not able to do so by scanning the entire spectrum, as a temporal resolution of only about 7 s was obtained (Berchtold *et al.* 2005). This temporal resolution represents a major limitation when studying polymerization reactions that occur in seconds or tens of seconds like in the case of dimethacrylate-

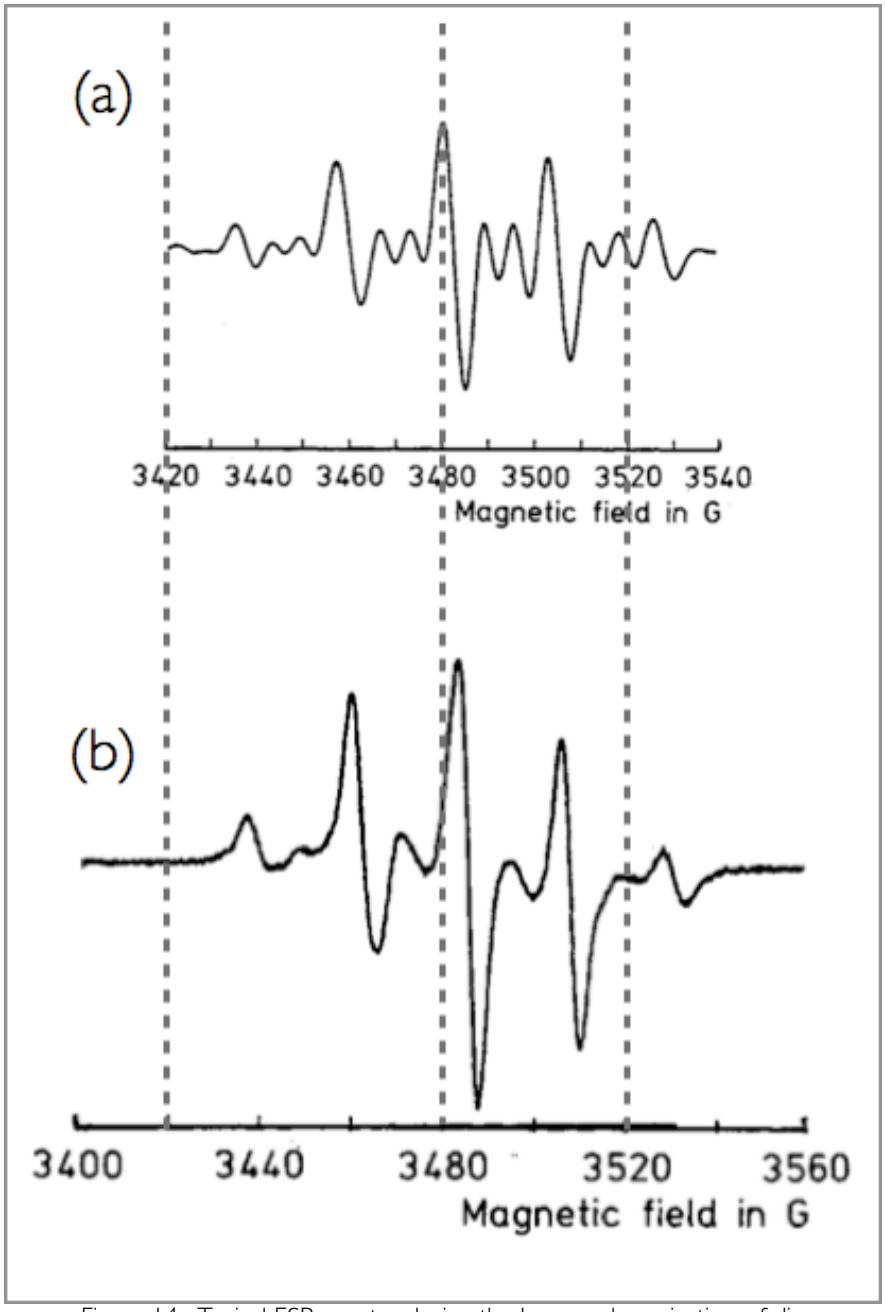

Figure 14 - Typical ESR spectra during the homopolymerization of di-methacrylates: (a) typical 13-line spectrum and (b) 9-line spectrum corresponding to low and high polymer conversion respectively.
(Charts modified from Anseth *et al.,* 1996)

based systems. For that reason, they fixed the magnetic field at the value of the central line peak and the changes in the peak height were related to the relative changes in radical concentrations. However, as it can be observed by comparing both spectra on Fig. 14 (a versus b - grey dotted lines were added and scale of figures modified for comparative purposes), the position of the central peak shifts between the 9 and 13-line spectrum. Therefore, it is difficult to adequately follow the concentration during the polymerization, and the static measurement after vitrification is certainly more accurate.

The second limitation of EPR experiments on dental resins was that the radical species giving rise to the 9-line spectrum had not been properly identified. This was done later by Truffier-Boutry *et al.* (2003), who demonstrated by using computer simulated spectra that vitrified dental resins contain two types of trapped free radicals ($R^{\bullet}_{Trapped}$), namely a propagating radical ($R^{\bullet}_{propag}$) and an allylic radical type ($R^{\bullet}_{allyl}$) (Fig. 15). The 9-line spectrum was described for the first time as a superposition of 9 weak

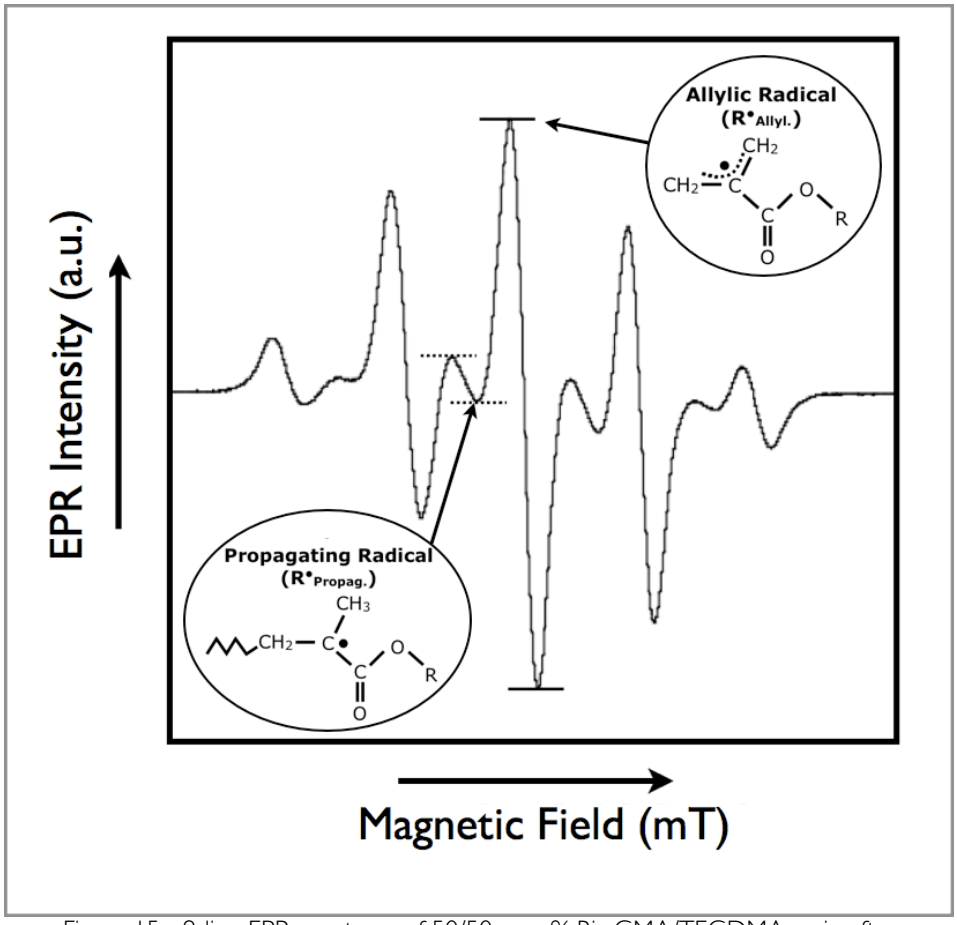

Figure 15 - 9-line EPR spectrum of 50/50 mass% Bis-GMA/TEGDMA resin after polymerization and chemical structure of both radical species. R stands either for a pendant monomer, carrying the second and unreacted methacrylated group, or for a polymer chain. The respective concentrations of both radical species were assessed by the height measurement of peaks indicated by arrows.
(Leprince, Lamblin *et al.*, 2010a)

peaks and 5 strong peaks corresponding to $R^{\bullet}_{propag}$ and $R^{\bullet}_{allyl}$ respectively. As peak width does not significantly vary with time, EPR peak height can be used to determine the relative concentration of $R^{\bullet}_{Trapped}$. Measurement of peaks that are least influenced by the signal of the other radical can be conducted to compare the abundance of both species: height of the fifth (from 334,9 to 335,5 mT) and fourth peaks (from 336,1 to 336,6 mT of the magnetic field) for $R^{\bullet}_{allyl}$ and $R^{\bullet}_{propag}$, respectively (Fig. 15). From the spectrum, it is obvious that the signal of $R^{\bullet}_{propag}$ is much less intense than the one of $R^{\bullet}_{allyl}$. This is not surprising as the latter are products of transfer reactions and do not propagate but accumulate during the polymerization. On the contrary, propagating radicals are the true active species, undergoing propagation and termination unless their further reaction is limited by vitrification.

Following the identification, it was of prime interest to study the fate of $R^{\bullet}_{Trapped}$:[8] firstly, on a biocompatibility point of view, and secondly given the impact that they might have on the long-term material properties of a polymer product (Berchtold *et al.* 2005). It has indeed been hypothesized that their presence could lead to property deterioration over time due to the formation of peroxyl radicals via reaction with atmospheric oxygen. Additionally, they can facilitate further reaction when the polymer is exposed to environmental changes such as temperature increase, which can also significantly affect the material properties.

Hence, a long-term follow-up of $R^{\bullet}_{trapped}$ concentrations was conducted in the present thesis (**Leprince *et al.*, 2009 - Chapter 3)**, analyzing the impact of different storage environments and temperature on the $R^{\bullet}_{trapped}$ kinetics of decrease. From what can be observed on Fig. 16, in the case of an unfilled resin (Bis-GMA/TEGDMA 70/30 mass%), two periods can be determined in the free radicals concentration decrease: firstly from 0 to 24 hours, where the slope is independent of storage conditions, and secondly more than one day after irradiation.

The first period was already investigated by Truffier-Boutry *et al.* (2006) and $R^{\bullet}_{trapped}$ decay was assigned to the post-irradiation shrinkage phenomenon. The latter is linked to the free volume relaxation in the organic matrix, resulting in increased

[8] The EPR measurements performed in this work are mass measurements, i.e. the peak intensity corresponds to the whole amount of trapped free radicals present in the sample placed in the spectrometer cavity. As samples were covered by acetate films prior to polymerization, the oxygen inhibited layer can be neglected.

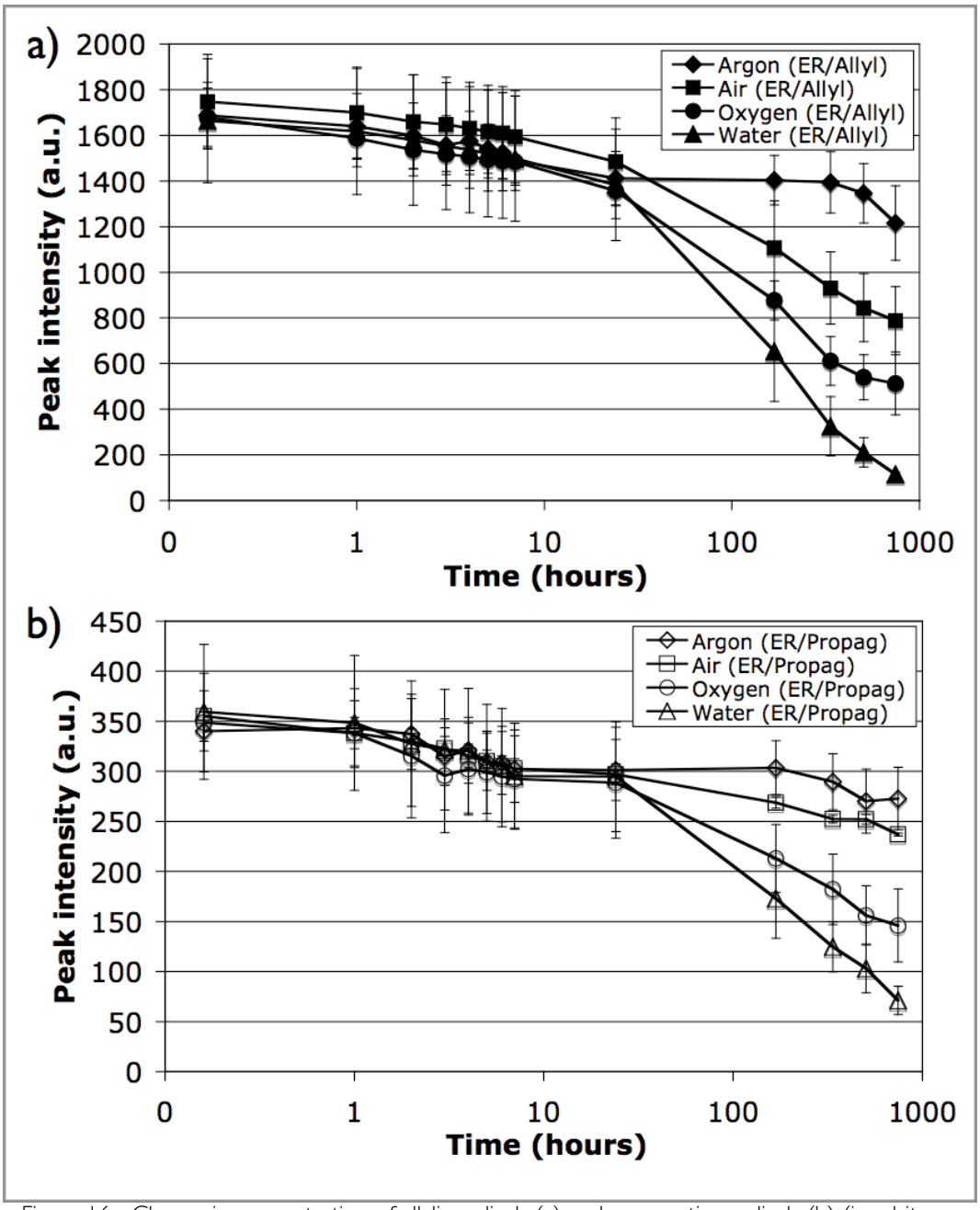

Figure 16 - Change in concentration of allylic radicals (a) and propagating radicals (b) (in arbitrary units) in samples of experimental resin (ER) stored in different environments. Time is presented on a logarithmic scale.
(Leprince *et al.*, 2009)

proximity of the chemical species. In this way, recombination of radicals can occur, either by bimolecular termination or due to reaction-diffusion (Anseth *et al.*, 1994). As a result, an increase of the degree of conversion (DC) was measured (2%) during the 24 h after photocuring. However, this effect is limited, as no additional change in DC was observed from 24 to 48 h. This may be due to the end of the free volume relaxation and/ or to the influence of oxygen, competing with additional propagation (Pavlinec and Moszner, 2003; Pavlinec *et al.*, 2009).

In another work being part of this thesis (**Leprince, Lamblin *et al.*, 2010a - Chapter 7**), additional evidence was found to support the identification of both radical species and to explain the additional propagation during the first hours post-cure. From what appears on Fig. 17, $R^{\bullet}_{propag}$ concentrations decrease at higher rates than $R^{\bullet}_{allyl}$ during approximately the first 4 hours. According to the above explanation, the local molecular mobility due to free volume relaxation enables some $R^{\bullet}_{Trapped}$ to move closer to each other, thereby increasing the probability of termination. Moreover, whilst $R^{\bullet}_{allyl}$ are unable to react with species other than free radicals (higher stability due to a resonance phenomenon, Fig. 15), $R^{\bullet}_{propag}$ exhibit sufficient reactivity to interact with remaining double bonds (either pendant double bonds or free monomers). In this way, additional propagation reactions can repeat locally, slightly increasing DC (Truffier-Boutry *et al*., 2006) and local radical mobility, which leads to some bimolecular radical termination through reaction-diffusion, as schematically represented in Fig. 18.

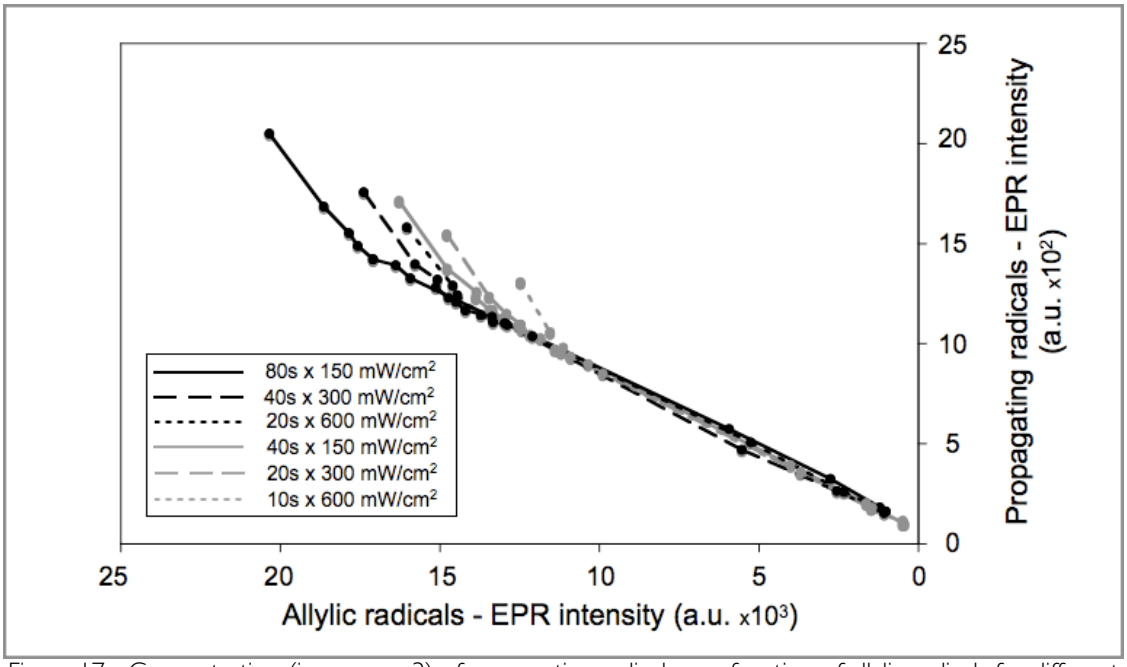

Figure 17 - Concentration (in a.u., n = 3) of propagating radicals as a function of allylic radicals for different continous curing modes. Each point indicates the respective concentrations of both radical types at a given storage time (5 minutes, 1 to 6 hours, 1 day and 1 to 3 months).
(Leprince, Lamblin *et al.*, 2010a)

Moving on to the period from 1 day to 1 month, the decrease rate of free radical concentrations clearly depends on the storage environment (**Leprince *et al.*, 2009 - Chapter 3**). For samples stored in argon, the decay is very limited. By contrast, the decrease rate is very high in oxygen, and even higher in water (Fig. 16). The free radical concentrations in samples stored in air decrease at intermediate rates. In the time range investigated (1 day to 1 month), no physical phenomenon can be invoked

(Truffier-Boutry *et al*., 2006). On the contrary, reactions with species coming from the external environment are most likely involved, and the presence of oxygen is clearly the determining factor of radical decay (**Leprince *et al.*, 2009 - Chapter 3**). This is in accordance with Li *et al.* (1993) who observed no decay of the trapped free radicals over a two-year period in the absence of oxygen (room temperature). This undoubtedly denotes the occurrence of an oxidation reaction in dental resins after photopolymerization.

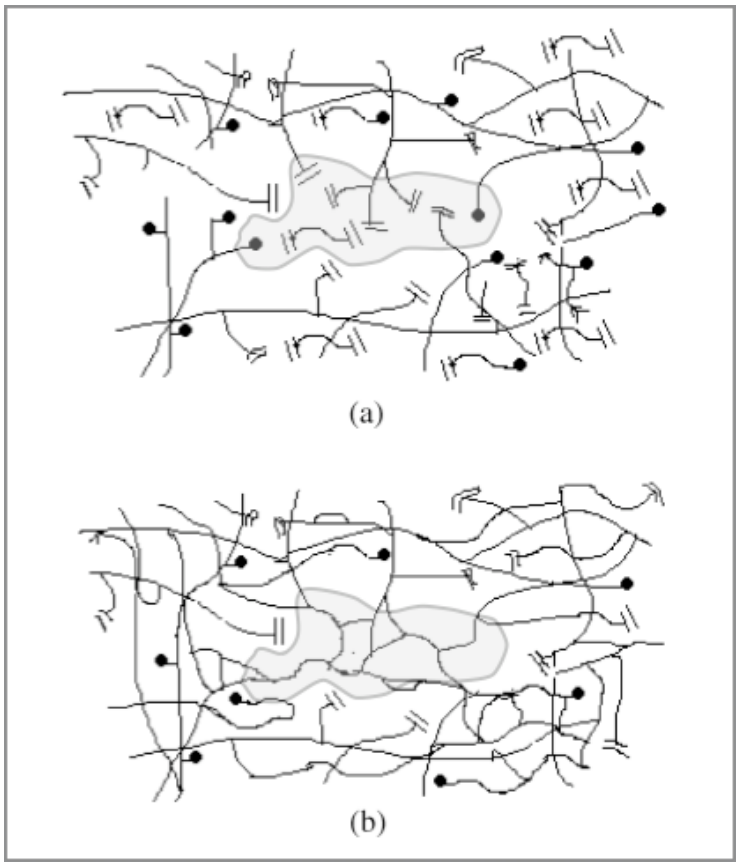

Figure 18 - Illustration of reaction-diffusion termination
(a) Example of network structure at the time that the light is extinguished. (b) Same network structure some time after, when slight increase in chain mobility due to free volume relaxation has enabled additional propagation and subsequent termination of both radicals in the grey-shaded area.
(Modified from Berchtold *et al.*, 2005)

Nevertheless, the exact chemical process has not been clearly identified yet. According to the high reactivity of free radicals, peroxide radicals necessarily form by the addition of oxygen on the trapped free radicals (Eq. 3):

$$R\bullet + O2 \rightarrow ROO\bullet \quad (3)$$

Accordingly, Kaptan *et al.* (1992), who followed the decrease of the trapped radicals by EPR, suggested that it would be the same to measure the increase of peroxyl radical signal with time. Besides, Pavlinec *et al.* (2009) reported an accumulation of hydroperoxides using chemiluminescence. However, peroxyl radicals were never detected by EPR spectroscopy (Kloosterboer *et al.*, 1986; **Leprince *et al.*, 2009 - Chapter 3**). This may be due to the impossibility to simultaneously observe the EPR spectra of both trapped radicals (allylic / propagating) and peroxide radicals under the same setting conditions. It could also be explained by their high reactivity and their

possible reaction with a slightly mobile hydrocarbon species (R'H), e.g. neighboring unconverted monomers (Eq. 4):

$$ROO\bullet + R'H \rightarrow ROOH + R'\bullet \quad (4)$$

This hypothesis would lead to the reformation of an allyl radical (R'• in Eq. 2) and of an hydroperoxide, which is in line with the observation of Pavlinec *et al*. (2009). Finally, peroxide radicals could also be terminated by mobile radical species, as will be explained further (*2.1.4.1.*).

Besides the differences between argon-, oxygen- and air-storage, the effect of water on free radicals is of particular interest, as dental resins are permanently exposed *in vivo* to an aqueous environment. It was observed (Fig. 16) that the radical concentration in water-stored samples decays even faster than in oxygen. As mentioned by many authors (Sideridou *et al.,* 2003; Diaz-Arnold *et al.,* 1992; Malacarne *et al.,* 2006), water sorption results in a swelling of the polymer, which increases molecular mobility, reduces T_g and can lead to a faster diffusion of oxygen. As a result, free radicals disappear faster. In the same way, heating experiments accelerated the decrease in $R^{\bullet}_{trapped}$ concentrations (Fig. 19) (**Leprince *et al.*, 2009 - Chapter 3**), which is not surprising as at high temperatures (above T_g), trapped radicals are well-known to be reactivated by an increase in network mobility (Andrzejewska, 2001). This increase enables some bimolecular termination as well as additional propagation and subsequent

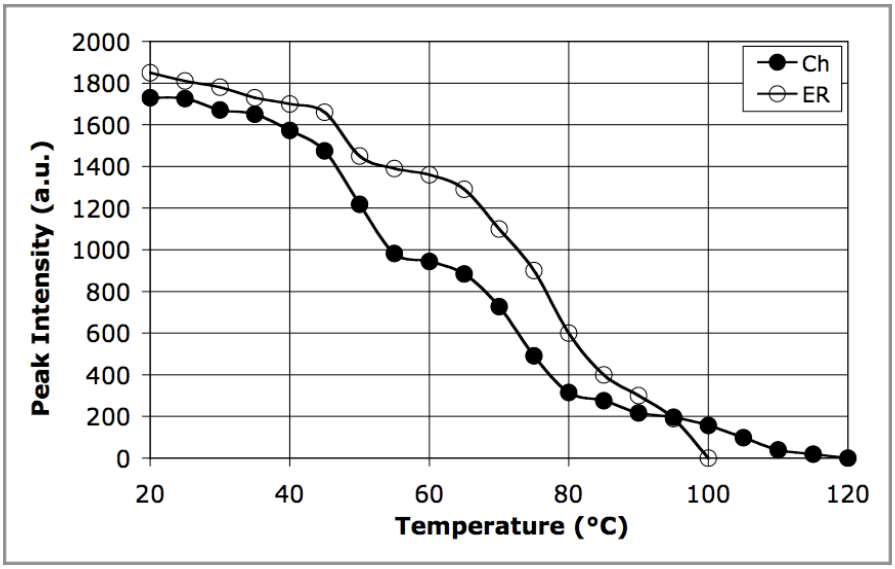

Figure 19 - Change in concentration of allylic radicals (in arbitrary units) with temperature in the experimental resin (ER) and in the commercial composite Charisma® (Ch).
(Leprince *et al.*, 2009 - Chapter 3)

reactive-diffusion termination. On the contrary, below T_g, bimolecular termination cannot be expected. However, Fig. 19 shows a slow free radical decrease between 20 and 40°C. While a slight increase of reactive-diffusion termination can not be excluded, this observation principally supports the effect of oxygen, as temperature increase favors the diffusion of small molecules into the polymer network.

Interestingly, discordances were observed between the observations made with an unfilled resin and a commercial composite (**Leprince *et al.*, 2009 - Chapter 3**). When a filled resin (commercial composite Charisma® [9]) was considered, only the stability of the signal in argon was confirmed, whereas the results for the three other environments are less clear. Notably, the kinetic curve of samples stored in water shows a decrease rate surprisingly lower than in air. The reason could be the presence of inorganic fillers in Charisma®, which can influence the sorption phenomena by the presence of interfaces. Besides, a preferential affinity of water to fillers and/or silanes compared to the organic matrix could be responsible for the different effect of water storage. Hence, only the effect of oxygen is confirmed for Charisma® (stability in argon) and further experiments on filled resins are required to highlight the differences between water-, air- and oxygen-storage.

Nevertheless, a general statement can be made on the impact of fillers on $R^{\bullet}_{trapped}$ concentration and their kinetics of decay. Free radical concentrations were nearly 3 times higher in the organic fraction of the composite (after volume standardization[10]) than in the unfilled resin (**Leprince *et al.*, 2009 - Chapter 3**). This could firstly be due to the spatial confinement of the radicals during the polymerization in filled resins, preventing their recombination. It could indeed be assumed that the organic fraction is located in small interstices between inorganic particles, which could restrict the diffusion of radicals to a relatively small area. Then, it could also be related to an increase in local viscosity, as suggested by Beun *et al.* (2009). According to the latter, the large contact area between fillers and resin results in a significant local increase in viscosity. Consequently, it may be assumed that the local molecular mobility

[9] Composition of organic matrix comparable to the experimental resin used (Bis-GMA/TEGDMA 70/30 wt %); filler content: 64 vol%

[10] As organic matrix of Charisma represents about 36 vol%, free radical concentration must be ratioed to the organic content using a multiplication factor of 100/36 (or 2.78) in order to compare them adequately with radical concentrations in unfilled resin samples.

is reduced, thereby favoring a «monomolecular termination» pathway, i.e. radical entrapment. This notion is very important and will be useful to explain observations being part of the last chapter of this thesis (**Leprince *et al.*, 2010b - Chapter 8**), where it was observed that high irradiance modes are more efficient in filled than in unfilled systems. This will be discussed in more details later in this review (2.3.3.).

Finally, the rate of decay of $R^{\bullet}_{trapped}$ is much higher in composites than in unfilled resins, regardless of the storage condition (**Leprince *et al.*, 2009**). This is in accordance with other papers, where it was also observed that inorganic fillers accelerated the decay of $R^{\bullet}_{trapped}$ concentrations (Ottaviani *et al.,* 1992; Burtscher, 1993). Two main explanations can be proposed, associated with the two different phases described above for the $R^{\bullet}_{trapped}$ kinetics of decrease. During the first phase (free volume relaxation), as $R^{\bullet}_{trapped}$ concentration is about 3 times higher in the organic fraction of filled resins, the probability for two radical species to meet and terminate is higher than in unfilled materials. During the second phase (oxidation), as stated above, oxygen diffusion into the material is certainly influenced by the presence of organic-inorganic interfaces. Besides, the probability for oxygen - or for the products resulting from oxygen interaction with the polymer[11] - to react with $R^{\bullet}_{trapped}$ is proportional to their concentration (linearly or not, depending on the kinetics), i.e. in this case higher in filled resins.

2.1.4. Elution of active species: monomers and free radicals

Foreword

By active species, I mean species that are potentially capable of inducing biological effects on the living tissues surrounding the material. Among these species, on the one hand, unconverted monomers have already been the subject of a large amount of publications. Therefore, no additional experiments on their leaching has been conducted in this thesis. Nevertheless, they are of prime interest on a biocompatibility point of view. For that reason, I reviewed the principal information on this subject. It is indeed important to highlight the consequences of a lack of polymerization. On the other hand, contrary to monomer elution that has been widely documented, the results

[11] This topic relates to chapter 4 and will be discussed further in this review (2.1.4.1.)

presented below (2.1.4.2.) highlight for the first time an elution of free radicals out of dental resins.

2.1.4.1. Unconverted monomers

It was extensively explained that vitrification prevents complete conversion of dental dimethacrylate-based resins, with DC roughly ranging from 35 to 75 %. As a result, a significant amount of double bonds (from 25 to 65 %) are still present in the set resin. Among these double bonds, some are connected to the network and called «pendant», some are not, which corresponds to a given amount of free monomers (statistically, a minimum of 6.25 % - $(0.25)^2$ - Anseth *et al.* 1995). The remanence of these species in the cured materials represents a major concern due to their potential impact on both the biocompatibility and the structural stability of the restoration. They indeed act as plasticizers, therefore weakening the mechanical properties of the material. They were also demonstrated to be cytotoxic and responsible for harmful effects (Lin and Lin-Gibson, 2009; Schweikl *et al.,* 2005). For instance, they can induce tooth pulp damage, mucosal irritation, contact dermatitis and allergic reactions (Kawahara *et al.,* 2004). Of course, as being part of the material, their mobility is very restricted below T_g. However, once stored in a solvent such as water or ethanol, the material swells and monomers can more easily leach out. The elution of unconverted monomers, i.e. their diffusion out of the resin matrix into various extraction media, has been extensively studied. It appears that, in appropriate liquid media, elution of leachable components from composites is rapid and declines asymptotically over time, with the majority being released within a matter of hours. The amount of these leachable substances has been correlated to DC and weight losses of up to 2% of the mass of the composite have been reported under certain conditions (organic solvents) **(**Ferracane, 1994).

The extent and rate of elution of components from composites is dependent upon several factors: size and chemical characteristics of the leachable species, and extraction media, which can be water, physiological saline solution, ethanol, or mixed (e.g., 75% ethanol and 25% water) (Schmaltz and Arenholt-Bindslev, 2009). On the one hand, Tanaka *et al*. (1991) found a good correlation between conversion rate and the release of TEGDMA and Bis-GMA into an aqueous medium. On the other hand, Ferracane (1994) reported a weak correlation between conversion rates and eluted

residual monomers if water was used as extraction medium, while a better correlation was found in case of an ethanol - water mixture. In organic solvents, the amount of Bis-GMA extracted ranges from 0.4 % to 1.5 % of the composite mass (Geurtsen, 1998; Inoue and Hayashi, 1982), while the amount of eluted TEGDMA goes from 0.04 to 2.3 mass% of the composite (Spahl *et al.,*1998). By comparison, in water, significantly lower amounts of Bis-GMA are eluted (0.03 - 0.07 mass% of the composite) (Inoue and Hayashi, 1982) compared to lower molecular weight and more hydrophilic monomers such as TEGDMA (up to 0.4 mass% of the composite - Spahl *et al.,*1998), which generally represents the principal eluted substances (Schmaltz and Arenholt-Bindslev, 2009). Taken together, approximately 2 mass% of the organic matrix is elutable in aqueous media (Ferracane and Condon, 1990).

Speaking of monomer type, a recent fear has been raised in the media concerning the potentially oestrogenic effect of Bisphenol A. In consequence, the potential release of this compound by dental resins was investigated. Some papers reported the detection of Bisphenol A in extracts of Bis-GMA-based composites and sealants and in saliva in contact with these materials (Pulgar *et al.*, 2000). However, these investigations have been criticized due to methodological problems by other authors, who defended that a Bis-GMA-based pit and fissure sealant containing no primary Bisphenol A contamination (which probably depends on the initial purity) did not release any into saliva (Arenholt-Bindslev D *et al.*, 1999; Schmaltz and Arenholt-Bindslev, 2009). Moreover, according to Imai and Komabayashi (2000), little or no estrogenic effect due to long-term elution of Bisphenol A from commercial Bis-GMA-based resins is expected in practice, but this is far beyond the scope of the present work.

That being said, it appears that monomer elution and cytotoxicity on human gingival fibroblast cultures are inversely correlated with DC (Caughman *et al.*, 1991). Therefore, in case of insufficient material polymerization, adverse biologic effects may be feared, both for the oral and pulp tissues. However, regarding the latter, biologically active molecules must first penetrate from the cavity floor through the dentin to the pulp in order to cause an inflammatory pulpal reaction. Interestingly, dentin was shown to act as a diffusion barrier (Pashley, 1984; Pashley *et al.,* 1981; Schmalz *et al.,* 2001), which is specifically due to the smear layer generated during cavity preparation. Moreover, permeability is logically lower in dentin distant from the pulp compared with dentin

close to the pulp (Pashley *et al.,* 1988; Schmalz *et al.,* 2001), and an obliteration of dentin tubules beneath a carious lesion (dentinal sclerosis) can also reduce permeability. Though, relatively hydrophilic substances, such as HEMA or TEGDMA, are able to diffuse through dentin, specifically in the case of a thin dentin layer (Bouillaguet *et al.*, 1996 and 1998).

Clinically, it is very difficult to discern whether pulp damage is due to cavity preparation, e.g. due to insufficient water cooling, to damage related to bacterial toxins subsequent to the carious lesion, or to direct toxic effect of substances that leach from the material (Schmaltz and Arenholt-Bindslev, 2009). Nevertheless, the concentration of leachable compounds at the target cells was found to be high enough to induce pulp cell damage *in vivo* (Bouillaguet *et al.*, 1998).

Besides biocompatibility matters, studies have shown that ethylene glycol-based co-monomers such as EGDMA and TEGDMA may promote the proliferation of important cariogenic microorganisms such as Lactobacillus acidophilus and Streptococcus sobrinus (Hansel *et al.*, 1998). More recently, it has been shown that saliva can catalyze the degradation of ethyleneglycol-based monomers, forming biodegradation by-products such as methacrylic acid, and triethyleneglycol (Khalichi *et al.,* 2009). Interestingly, the latter seem to accelerate the growth of Streptococcus mutans, a major etiological agent of dental caries. Hence, chemical species derived from dimethacrylate monomers can potentially influence biofilm formation and microbial survival on surfaces in the oral cavity. This is an additional element in favor of the limitation of the unconverted monomers remaining in the material.

In conclusion, though the clinical significance of incomplete polymerization has not yet been fully clarified (Schmaltz and Arenholt-Bindslev, 2009), several concerns have been raised and the photopolymerization procedures must therefore be directed at achieving DC as high as possible.

2.1.4.2. Free radicals

As demonstrated above, free radicals remain trapped for a long time in dental resins. From a biocompatibility viewpoint, it is of prime interest to determine if their progressive decay is linked with the release of radical species into the environment. The

fate of trapped free radicals is also interesting to better understand the aging process of the material.

Given the macromolecular dimensions of most trapped free radicals, their mobility into the polymeric network is strongly limited by entanglement and connection to the network. Even free radicals hypothetically carried by small molecules (monomers or oligomers) that are not connected to the network are included in a material, which is below T_g in air and at room temperature. Similarly to what was explained above for monomer leaching, this excludes their free diffusion out of the material without any swelling solvents. Nevertheless, $R^{\bullet}_{trapped}$ concentrations decrease was observed in air at ambient temperature, which could only be explained by radical reactions (distinct from typical methacrylate photopolymerization) occurring within the resin and depending on the presence of oxygen (**Leprince *et al.*, 2009 - Chapter 3**). This led to an innovative work (**Lamblin, Leprince *et al.*, 2010 - Chapter 4**) whose objective was to highlight if these radical reactions can produce and release mobile secondary free radicals into the environment. Given the high reactivity and therefore short half-life of free radicals in a liquid storage media, spin-trapping methods are necessary to stabilize and enable detection and identification of unstable free radicals (Gallez and Beghein, 2002; Teshima *et al.,* 2003).

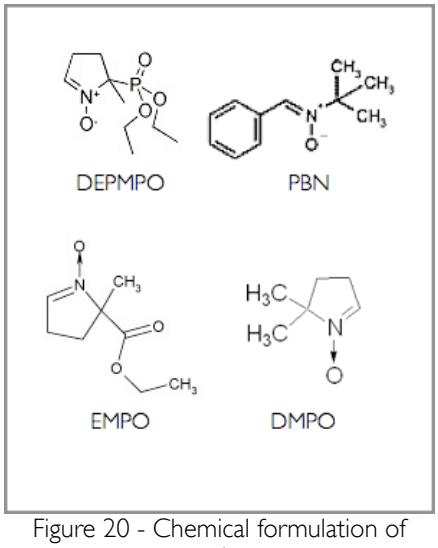

Figure 20 - Chemical formulation of some spin-traps.

A spin-trap is an unsaturated non-radical molecule reacting with an unstable free radical to form a product called the spin-adduct. The half-life of the latter is longer than the one of the radical (Bosnjakovic and Shulamith, 2006; Taniguchi and Madden, 2000), allowing its detection by EPR. The spectrum of the adduct and its hyperfine constants are characteristic, enabling them to be identified. Nevertheless, due to the variable half-lives of spin-adducts, which depend on many parameters (nature of the trapped free radical and spin-traps, solvent, pH, temperature, etc.), detection may be more or less difficult. Typical spin-traps are nitroso compounds, like 5,5-dimethyl-1-pyrroline-N-oxide (DMPO) or phenyl-butylnitrone (PBN) (Fig. 20). Spin-traps with longer spin-adduct half-lives have recently been synthesized, e.g. 5-ethoxycarbonyl-5-

methyl-1-pyrroline N-oxide (EMPO) and 5-diethoxyphosphoryl 5-methyl-1-pyrrolyne N-oxide (DEPMPO), which were chosen for this work (Fig. 20). Ethanol was used as a solvent for immersion of resin samples as it induces better swelling of methacrylated polymer than water, thereby maximizing the diffusion of species in and out of the material. A comparison of the different spectra obtained with EMPO (Fig. 21a, b and c) clearly demonstrates for the first time that dental resins release ethoxy radicals when they are stored in ethanol. This was confirmed by the experiments with the other spin-trap - DEPMPO (**Lamblin, Leprince *et al.*, 2010 - Chapter 4**). Interestingly, the signals obtained with EMPO for the commercial composite and the unfilled experimental resin were similar (Fig. 21 a and b), supporting the fact that only the organic part of the dental resin is involved in the release of ethoxy radicals.

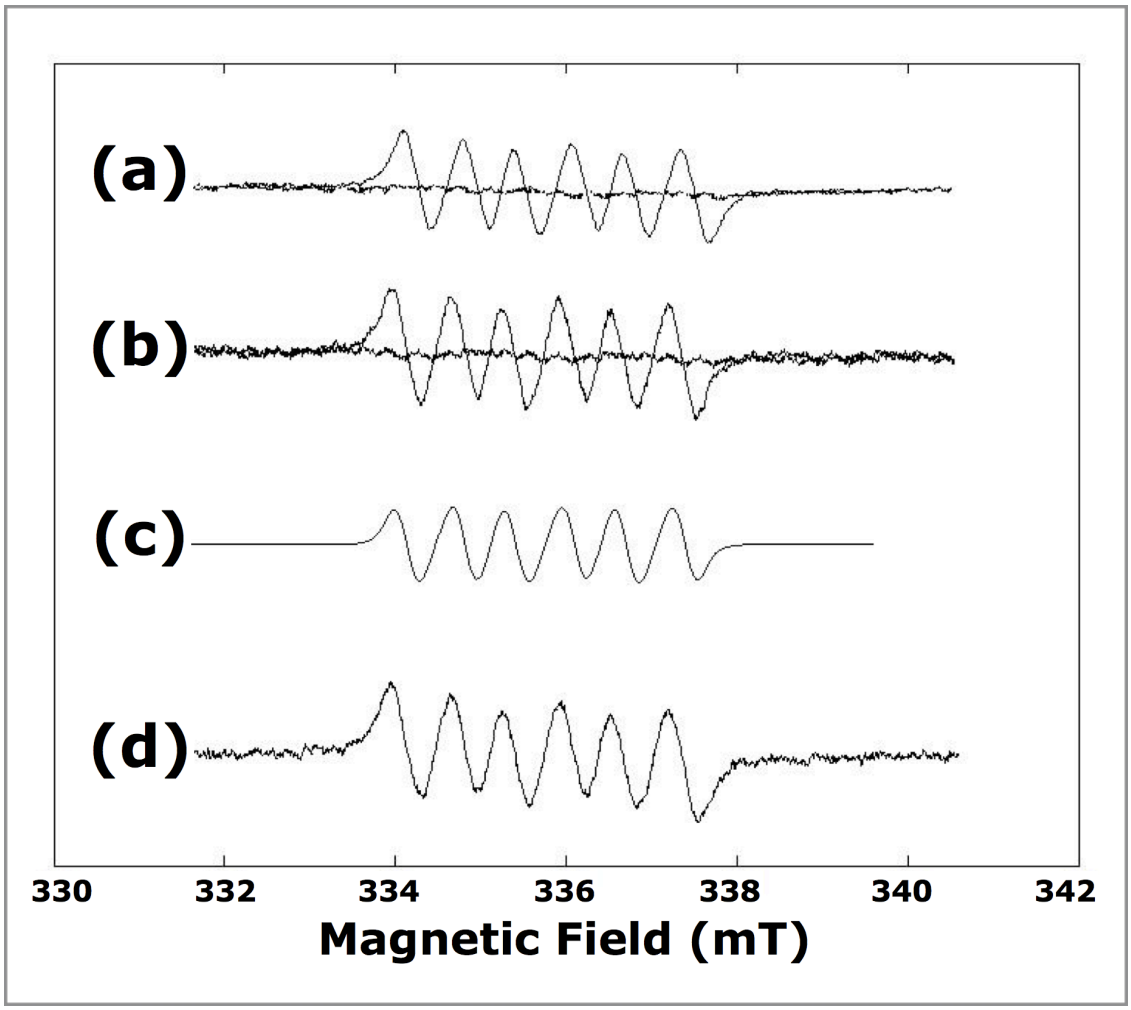

Figure 21 - EPR spectrum obtained with EMPO spin-trap. (a) Solution of EMPO (50 mM) and pure ethanol in which unfilled cured dental resin was incubated for 15 minutes; (b) Similar experiment as (a) but with commercial composite instead of unfilled resin; (c) Computer simulated spectrum of EMPO-ethoxy radical spin-adduct. (d) EMPO incubated in a Fenton system in pure ethanol.
(**Lamblin, Leprince *et al.*, 2010 - Chapter 4**)

Considering ethoxy radical kinetics of release, the major observation was the significant decrease in EPR signal intensity when a hydroxyl radical scavenger was introduced (Fig. 22). This suggests that ethoxy radicals are secondary products of the reaction between hydroxyl radicals (OH•) and ethanol molecules. The results obtained with the Fenton system[12] in ethanol (Fig. 21d) also support this assumption. Indeed, ethanol is known to be an efficient scavenger of OH•, which are typically produced by the Fenton reaction and rapidly converted into ethoxy-derived free radicals in ethanol (Yamazaki and Piette, 1991; Reinke, 2002). Therefore, the simple detection of ethoxy radicals suggests the release of OH•.

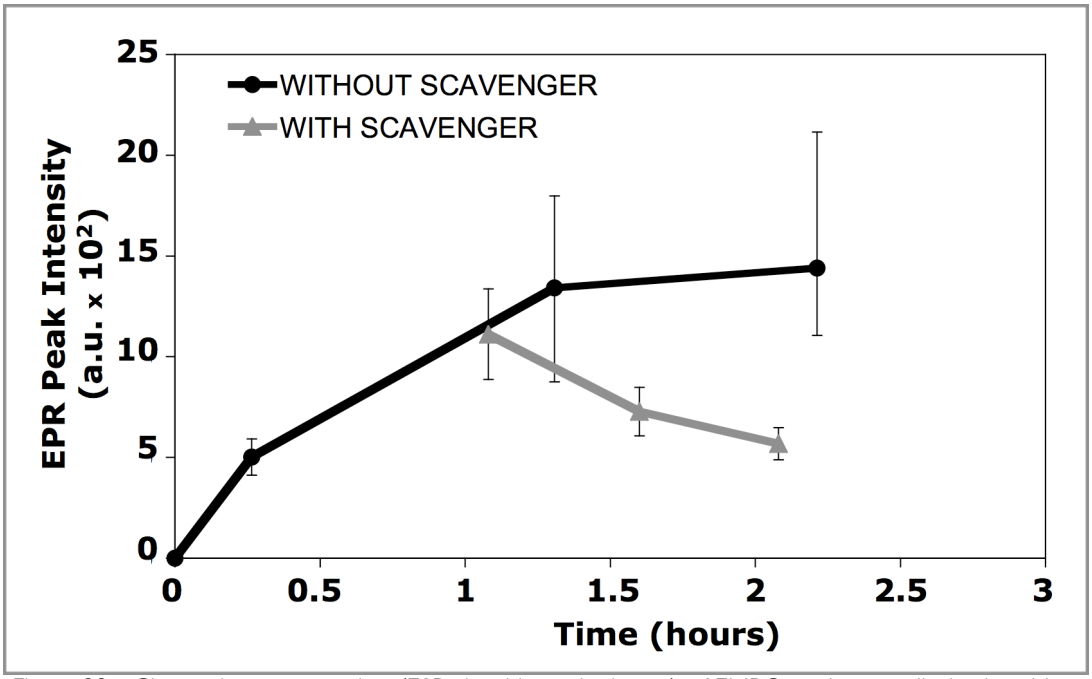

Figure 22 - Change in concentration (ESR signal intensity, in a.u.) of EMPO - ethoxy radical spin-adducts over time, with or without hydroxyl radical scavenger. (**Lamblin, Leprince *et al.*, 2010 - Chapter 4**)

OH• release by dental resins has already been suggested in the literature. Lee *et al.* (1995ab) hypothesized that OH• production could explain the chemical degradation of dental composites stored in a food simulating environment (water/ ethanol 25/75). These authors proposed the hydroperoxidation of the methyl group in the α position of a methacrylate group (Eq. 5).

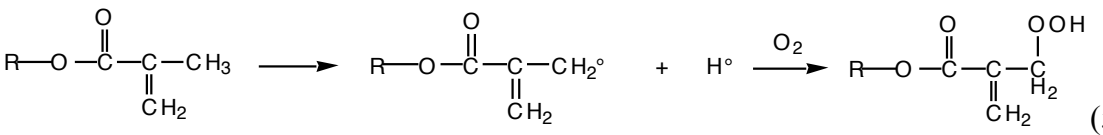

(5)

[12] Fenton reaction is the iron-salt-dependent decomposition of hydrogen peroxide generating hydroxyl radical:
$Fe^{2+} + H_2O_2 \rightarrow Fe^{3+} + OH^{\bullet} + OH^-$. It is used notably to destroy certain organic compounds or to oxidize contaminants or waste waters.

It has to be noted that the allyl radical produced in the first step of Eq. 5 is the same as the allyl radical trapped in the resin. However, the one produced by Eq. 5 is accompanied by a H• abstraction, which can give a hydroperoxide. The trapped allyl radical can only transform into a hydroperoxide with the assistance of another "mobile" hydrocarbon. The hydroperoxide produced can then decompose into OH• and acyl radicals (Eq. 6). The latter could provide new cross-linking or decompose into aldehyde species.

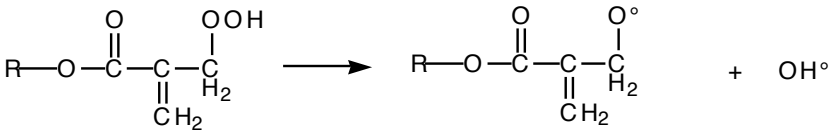

(6)

Hence, according to Eq. 5 and 6, hydroperoxidation of the methyl group in a methacrylate depends on two major parameters: the presence of oxygen and unconverted double bonds. This is in accordance with supplementary experiments conducted with EMPO. Firstly, ethoxy radical release was shown to be independent of the presence of trapped free radicals in the resin samples, but dependent on the presence of oxygen (**Lamblin, Leprince *et al.*, 2010 - Chapter 4**). Secondly, fully converted methacrylate polymers (PMMA[13]) revealed no EPR signal, contrary to unpolymerized resin, which confirms that ethoxy radical release depends on the presence of unconverted double bonds (**Lamblin, Leprince *et al.*, 2010 - Chapter 4**).

Interestingly, the release of OH• could explain the long term decay of $R^{\bullet}_{trapped}$ in dental resins. Contrary to radicals carried by polymers, oligomers or even monomers, OH• can easily diffuse through resin network - even in air at room temperature - and terminate $R^{\bullet}_{trapped}$ by addition. Hence, according to the hydroperoxidation mechanism, $R^{\bullet}_{trapped}$ kinetics of decrease would depend on the diffusion of oxygen in the sample, which corresponds quite well with the observations by **Leprince *et al.* (2009 - Chapter 3)**. However, this termination mechanism involving OH• is not the most likely. As explained above (2.1.3.), a more obvious mechanism would start by direct oxidation of the trapped radicals, leading to peroxyl radicals (Eq. 3). However, no EPR signal corresponding to peroxy radicals was ever detected in dental resins. Three hypotheses can then be proposed. The first and second ones, referring respectively to a potential impossibility to observe simultaneously the spectra of different radical types, and to the

[13] polymethylmethacrylate, DC = 100%

transformation into hydroperoxide compounds, were previously described (2.1.3.). The third hypothesis relates to the fact that the amount of unconverted double bonds remaining after polymerization is by far higher (>10^2) than the one of $R^{\bullet}_{trapped}$ in the resin. As a consequence, oxygen molecules are much more likely to react with an unconverted methacrylate group to create hydroperoxides (Eq. 5) than with free radicals trapped in the polymer (Eq. 3).

To conclude, the present results improve the understanding of material aging process. In addtion, as free radicals are implicated in many diseases, the evidence of their release out of the material raises a new source of concern for dimethacrylate-based resins. Free radical and monomer leaching demonstrate that these biomaterials, which are becoming increasingly popular to dentists in place of mercury amalgams, are far from inert. Though evaluation of toxicity requires to take into account other elements (dose, distance and nature of structures between release location and potential target tissue, etc.), it is reasonable to reduce the amount of reactive species as much as possible.

2.1.4.3. Strategies to limit free radical and monomer release

From the above sections (*2.1.4.1. and 2.1.4.2.)*, it appears that the leaching of free radicals and unconverted monomers is linked with the incomplete conversion of dimethacrylate-based resins. Therefore, in order to limit the amount of eluted species, clinical procedures must be adapted appropriately to limit the amount of unconverted double bonds.

The first and more obvious way to reduce their amount is to choose a material containing less dimethacrylate groups, either by increasing filler fraction or by using other kinds of monomers, i.e. other technologies or larger dimethacrylate monomers. As mentioned above, larger molecules such as Bis-GMA, are indeed less expected to diffuse out of the material than smaller ones (TEGDMA or HEMA). Going further, larger molecules combining inorganic (Silica) and organic parts (dimethacrylate group) were developed. For materials based on these molecules - called Ormocers® [14] - lower cytotoxicity was reported compared to conventional resins (Moszner *et al.,* 2008).

[14] ORganically MOdified CERamics, Fraunhofer-Gesellschaft zur Förderung der angewandten Forschung e. V., Munich (FRG), Germany.

Another promising approach would be to give up using dimethacrylate-based organic matrices, and move on to other monomer technologies. The most striking example is the ring-opening system Silorane® [15] - developed to reduce polymerization shrinkage - but to date, no publications are available on monomer elution and cytotoxicity of Silorane-based composites. Despite these different alternative technologies that could be promising for biocompatibility improvement, dentists can not afford to use less resistant materials. Therefore, their mechanical properties and filler fraction were compared in this thesis to the «classical» dimethacrylate-based composites (**Leprince *et al.*, 2010c - Chapter 5**) and the main results will be presented in the next section of this review (2.2.1.).

The second manner to limit the amount of unconverted double bonds in dimethacrylate-based composites is to reach the highest possible DC. For example, the introduction of a new commercial composite (N'Durance by Septodont) claims to reduce residual double bonds by phase-separation[16]. Besides, the most obvious way to obtain DC as high as possible is certainly to choose appropriate irradiation conditions. Several factors can lead to a decreased DC: excessive thickness of composite layers, which should generally not exceed 2 mm (Van Noort, 1994; Pollington *et al.,* 2009), lack of overlap between curing light emission and material absorption spectra, and insufficient light exposure due to a shortage of curing time and/or light irradiance. These different aspects have to be explored in two different ways. Firstly, in order to make their choice for their daily practice, dentists need direct information on curing lights and composites that are currently commercially available. For that reason, the next part of this review (2.2.) will be dedicated to the investigation of recent commercially available composites (Chapter 5) and light curing units (Chapter 6). Secondly, the impact on the polymerization process of light irradiance, irradiation time and their product, i.e. radiant exposure, needs clarification. Besides, the curing efficiency of alternative photoinitiators also require investigation in experimental materials, where the material composition is controlled. The third part of this review (2.3.) and chapter 8 will deal with these matters.

---

[15] The term coined from the combination of SILOxane and oxiRANE moieties (3M-Espe)

[16] This material has been introduced very recently and its presumably higher DC has not yet been confirmed.

2.2. Investigation of commercial composites and light-curing units.

Dental materials are in constant evolution. In a way, the situation can be compared with informatics: as soon as a client receives his new computer, it is already old-fashioned. The real problem with dental materials is the difficulty to sort out which new products are really innovative. Therefore, the purpose of this chapter was to give clinicians independent information regarding firstly new materials, and secondly recent light curing units, and help dentists to chose among the products available. At the same time, it is a good way to highlight problems and thereby lead to new fundamental approaches.

2.2.1. Increased filler content and new monomer technologies

Considering the resin-based composites recently introduced to the market, it is legitimate to ask what real progress have been achieved compared to previous generations. Regarding inorganic fillers, though so-called "nano-composites" have been introduced, it might be argued that nanotechnology has been used since the mid-1970s (colloidal silica < 100 nm diameter). Rather than the filler size, improvement regarding the filler fraction has more to do with optimization of filler morphology and size distribution to optimize their packing. Then, concerning the organic matrix, research has mainly focused on new monomer formulations to reduce volumetric shrinkage. The most significant evolution since the synthesis of Bis-GMA by Bowen in 1962 was the development of the ring-opening system Silorane® (Guggenberger and Weinmann, 2000). Initial *in vitr*o studies on this composite confirmed a reduction in polymerization stress (Eick *et al.*, 2007; Palin *et al.*, 2005a) and shrinkage, reaching values of less than 1 vol% (Weinmann *et al.,* 2005). Another alternative to dimethacrylate monomers is the inorganic-organic resin Ormocers®, for which interesting characteristics were also reported, notably a limited shrinkage, ranging from 1.46 to 2.64 vol% depending on the material and measurement method (Uhl *et al.*, 2005; Gerdolle *et al.,* 2008). Finally, a new composite based on phase-separation (N'Durance®, Septodont) has been introduced very recently to reduce volumetric shrinkage. Initial results revealed around 2.3 % volumetric shrinkage and intermediate stress values compared to dimethacrylate- and silorane-based materials (Boaro *et al.*, 2010)[17].

[17] Apart from this reference, no literature data was found on this material. Therefore, it will not be further discussed in the present work.

Table 1 - General description of investigated composites

Materials	Manufacturer	Composite Type*	General Description	Filler type and dimensions*
Tetric Evo Ceram	Ivoclar-Vivadent (Schaan, Liechtenstein)	Nano-Hybrid	Commercial dimethacrylate-based composite	Barium glass, ytterbium trifluoride, mixed oxide and prepolymer – range of particle size: 40 to 3000 nm; average particle size: 550 nm
Synergy D6	Coltène-Whaledent (Langenau, Germany)	Nano-Hybrid	Commercial dimethacrylate-based composite	Prepolymerized fillers, Glass fillers, Nanofillers – range of particle size: 20 to 2500nm – average particle size: 600nm
Admira	Voco (Cuxhaven, Germany)	Micro-Hybrid	Commercial Ormocer-based composite	Ormocers, Glass-Ceramic Micro-fillers (average particle size: 700 nm)
V35694	Voco (Cuxhaven, Germany)	Nano-Hybrid-Ormocer	Experimental Ormocer based and highly filled composite	Ormocers, SiO_2 nanoparticles - range of particle size: 20 to 50 nm and silicate glass - average particle size: 1000 nm
V34930	Voco (Cuxhaven, Germany)	Nano-Hybrid	Experimental dimethacrylate-based and highly filled composite	SiO_2 nanoparticles - range of particle size: 20 to 50 nm and silicate glass - average particle size: 1000 nm
Grandio	Voco (Cuxhaven, Germany)	Nano-Hybrid	Commercial dimethacrylate-based and highly filled composite	Glass-ceramic micro-fillers - average particle size: 1000 nm - and nanofillers – range of particle size: 20 to 50nm
Filtek Supreme XT	3M-Espe (St. Paul, MN, USA)	Nanofilled	Commercial dimethacrylate-based nano- composite	Silica nanofillers - average particle size: 75nm - zirconia nanofillers - average particle size: 5 to 10 nm - and agglomerated zirconia/silica nanoclusters – range of particle size: 600 to
Filtek Silorane	3M-Espe (St. Paul, MN, USA)	Micro-Hybrid	Composite based on ring-opening monomer technology	Quartz Microfillers (0,1-1 μm) – range of particle size: 40 to 1700 nm – average particle size: 470nm

* Based on information from the manufacturer ** Experimental materials

Despite the interesting features of new materials in terms of shrinkage reduction and/or potentially improved biocompatibility mentioned in the previous section, mechanical properties should not be compromised. To our knowledge, there exists no study comparing in the same protocol the mechanical properties and inorganic fraction of Ormocer-, Silorane-based materials and the most recent highly filled dimethacrylate-based composites. Such a work was conducted in the present thesis (**Leprince *et al.*, 2010c - Chapter 5**) (see Table 1 for general description of each material). To start with, significant differences of filler fraction were observed between the different so-called "nanocomposites". Grandio and both experimental Voco

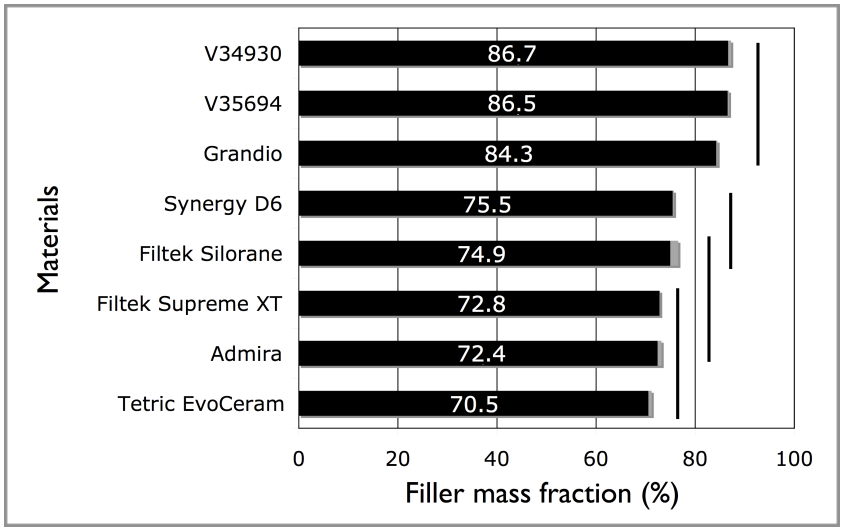

Figure 23 - Filler mass fraction (%) measured by TGA (n=3). The materials are ranked in descending order according to their means (black horizontal bars) and the standard deviations are added in the form of grey bars. Vertical bars connect materials that are not statistically different ($p<0.05$).
(Leprince *et al.*, 2010c - Chapter 5)

materials (composite V34930 and ormocer V35694) presented a significantly increased filler load (84.3 - 86.7 mass%) compared with the other materials (70.5 - 75.5 mass%) (Fig. 23). Assuming no particle agglomeration, a possible explanation for such differences in the filler content is a better adapted combination of particles of different sizes, reducing inter-particulate distances and enabling higher filler packing in Grandio, V34930 and V35694. Nevertheless, as the filler content here was measured in mass percentage, it should be noted that filler load could also be partly related to the nature of the particles. Indeed, denser particles are responsible for improving filler load without increasing the volume percentage and quoting volume filler percentages is probably more relevant for overall performance of the composite material.

Considering the mechanical properties (Fig. 24a-d), there were no significant differences observed in flexural strength (σ_s) between each material although Grandio and V34930 exhibited significantly higher elastic moduli (E_d and E_s) compared with other material types, which can be explained by a significantly increased filler content (**Leprince *et al.*, 2010c - Chapter 5**). Consequently, in the case of Grandio and V34930 (experimental composite), the mechanical characteristics may favour their use in high occlusal stress locations. As both materials exhibit a high elastic modulus, which

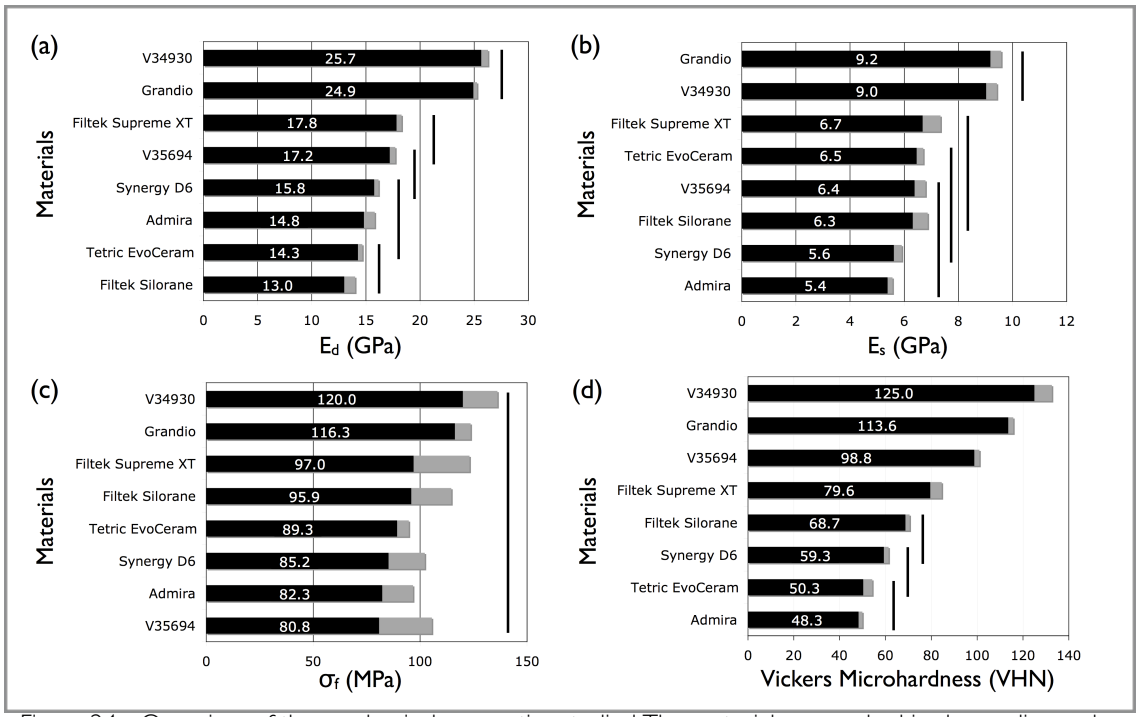

Figure 24 - Overview of the mechanical properties studied. The materials are ranked in descending order according to their means (black horizontal bars) and the standard deviations are added in the form of grey bars. Vertical bars connect materials that are not statistically different ($p < 0.05$). (a) Dynamic modulus (E_d in GPa) (n = 5); (b) static modulus (E_s in GPa) (n = 5); (c) flexural strength (σ_s in MPa) (n = 5); (d) Vickers microhardness (in VHN) (n = 5). **(Leprince *et al.*, 2010c - Chapter 5)**

may result in the generation of high polymerization shrinkage stress, their use in cavities with a low configuration factor might be suggested, e.g. in extended cavities for which a high modulus material is also important. Although the mass percentage of filler in V35694 (experimental Ormocer-based composite) was statistically equivalent to Grandio and V34930, a significant reduction in elastic modulus (E_d and E_s) was observed, which can be associated with the difference in the proprietary matrix composition of the experimental material. Consequently, the ormocer-based V35694 might be more suitable to fill in cavities where a lower elastic modulus is preferred (class III or V). Still, it must be pointed out that the experimental V35694 represents an interesting evolution compared to the the commercially available Ormocer-based parent Admira. Firstly, V35694 exhibits a significant increase in E_d and upper surface microhardness, which can be attributed in part to a significantly increased filler content. Admira exhibits statistically inferior mechanical properties compared with several of the methacrylates tested here (Figure 24a-d), which has also been demonstrated in the literature (Manhart *et al.,* 2000). The increase in mechanical properties of the experimental material V35694 highlights the potential of Ormocer-based composites to surpass the properties of several methacrylate-based materials. Secondly, while Admira contains TEGDMA, it is not the case of V35694 (information from the manufacturer). In the former, TEGDMA was necessary to compensate the high viscosity of the inorganic-organic network, to aid rheological properties and filler inclusion. Unfortunately, this addition of low molecular weight methacrylate-monomers may counteract improved biocompatibility if cytotoxicity of eluted residual monomer is considered. Hence, this constitutes an interesting progress of Ormocer-based materials regarding biocompatibility, as elution of TEGDMA should no longer be feared, which might go along with the lower cytotoxicity and reduced water solubility reported by Moszner *et al.* (2008).

In our investigation (**Leprince *et al*., 2010c - Chapter 5**), Filtek Supreme XT was the only material reported as “nano-composite”, the others being considered as micro- or nano-hybrids. It exhibited high strength values (Fig. 24c) (although not significant), in accordance with Ilie and Hickel (2009). Interestingly, it could be due to its unique spherical shape of its particles, which are known to exhibit improved fracture resistance compared with irregular-shaped morphologies as regions of high stress-concentrations at the filler particle edge are avoided (Suzuki *et al.*, 1995). Filtek

Supreme XT also showed high values of E_d and E_s. Unlike Masouras *et al.* (2008), the present results suggest the potential of a composite with spherical fillers to generate equal or better modulus than some materials of higher filler content but with irregular particles (Synergy D6, V35694). One possible explanation could be silane infiltration into porosities of the nanoclusters as proposed by Curtis *et al.* (2008). However, it must be pointed out that nano-composites seem to be more degraded by longer storage in water and saliva than the micro-hybrids (Ilie and Hickel, 2009; Curtis *et al.*, 2008).

Regarding Filtek Silorane, it can be stated that this material compares favourably to some clinically well-accepted methacrylate-based composites in terms of mechanical properties, which is in agreement with other studies (Weinmann *et al.,* 2005; Ilie and Hickel, 2006 and 2009; Lien and Vandewalle, 2010). However, while Lien and Vandewalle (2010) reported a better flexural modulus for Filtek Silorane than for Filtek Supreme XT, our work (**Leprince *et al.*, 2010c - Chapter 5**) showed the opposite, with lower E_d and E_s for Filtek Silorane. This, in association with lower surface hardness (Palin *et al.*, 2005b; Lien and Vandewalle, 2010; **Leprince *et al.*, 2010c - Chapter 5**), and reduced wear resistance ((Palin *et al.*, 2005b) might be considered as a clinical disadvantage in areas with high occlusal force. Though, this material presents another very interesting aspect: higher stability of its mechanical properties after storage in aqueous and ethanol solutions compared to methacrylate-based composites (Ilie and Hickel, 2009; Yesilyurt *et al.,* 2009). Finally, it must be underlined that even if Silorane was developed as a low shrinkage composite, decreased shrinkage does not necessarily result in reduced marginal gap formation. The stress generated at the tooth-restoration interface is a result of a complex process of shrinkage, curing speed and elastic modulus of the material. In addition, it also depends on the configuration factor of the cavity and on the compliance of the surrounding tooth tissue. In the case of Silorane, the lower elastic modulus combined with different curing characteristics associated with its cationic ring-opening polymerization and resultant low shrinkage reported in the literature (Eick *et al.,* 2007) may work in combination to reduce gap formation. As a result, this new material might be recommended for cavities with high configuration factor (where low shrinkage and shrinkage stress are required). Better marginal adaptation (Papadogiannis *et al.*, 2009) and lower microleakage (Bagis *et al.,* 2009) was indeed highlighted for Silorane compared to dimethacrylate-based composites. However, in a recent paper from Van Ende *et al.* (2010), no significant

difference in microtensile bond strength was observed between Silorane and the methacrylate-based composite Z100 (3M-Espe) on flat dentin (C-factor = 0.17). Surprisingly, in a class I cavity (C-factor = 3.5), microtensile bond strength only decreased for Silorane and not for Z100, whereas the latter is among the fastest curing and highest shrinking composites with a relatively high E-modulus ('worst-case scenario' regarding shrinkage stress). According to the authors, factors other than polymerization shrinkage influenced these results, such as problems of adaptation of Silorane in narrow cavities due to high stiffness of uncured material, which can lead to air bubbles inclusion. It was also concluded that adequate polymerization, especially at the bottom of the cavity, is more important than the cavity configuration. Therefore, layering technique remains recommended, even for these low-shrinking composites (Van Ende *et al.,* 2010).

Speaking of adequate polymerization, it must be mentioned that mechanical characterization of composites are usually conducted using "maximum cure" procedures, i.e. 60 s irradiation on both sides of the samples with a halogen light-curing unit[18]. In addition, the samples are generally prepared according to ISO specification 4049 with a material thickness limited to 2 mm (sample size: 25 × 2 × 2 mm). However, both sample configuration and irradiation conditions are far from clinical situation. Even if information obtained with such an experimental protocol can certainly help practitioners in their material choice, dentists also need to know if clinically relevant curing procedures are suitable for each material. New curing protocols using new light curing units for shorter irradiation time have indeed been validated in certain conditions. Besides, an ultimate goal of low-shrinkage resin composite materials might be the possibility to cure thicker layers of composite (> 2 mm) without bonding failure, gap formation and without deterioration of tooth structure. Therefore, despite the difficulty to thoroughly analyze the impact of each parameter on the curing extent, it was interesting to investigate the polymerization of thicker composite layers of low-shrinkage resin composites with two commonly accepted curing protocols -

[18] XL3000 (3M-Espe, St-Paul, MN, USA) operating at 544 mW/cm^2 (+/- 17 mW/cm^2)

conventional halogen light[19] during 40s and third generation LED light[20] during 20s (**Leprince *et al.*, 2010c - Chapter 5**). The results presented in Fig. 25 indicate that both irradiation procedures induce a suitable polymerization through all the studied materials within the first two millimeters, which confirms the potential of the new generation LED lights to reduce irradiation time to some extent (Price *et al.,* 2005). In the same way, current standards state that a composite layer is properly cured when the bottom microhardness is higher than or equal to 80 % of the top microhardness (Price *et al.,* 2005). In this case, the materials of the different technologies fulfill these requirements for both photoinitiating procedures (XL3000 40 s / G-Light 20 s) (**Leprince et al., 2010c - Chapter 5**). However, for the deepest layers (3 – 4 mm), the differences between the composites increase and all values but Grandio /3 mm / G-Light / 20 s are lower than 80%. This confirms that, for the materials and curing protocols considered, practitioners should limit the thickness of each composite layer to 2 mm. Finally, as will

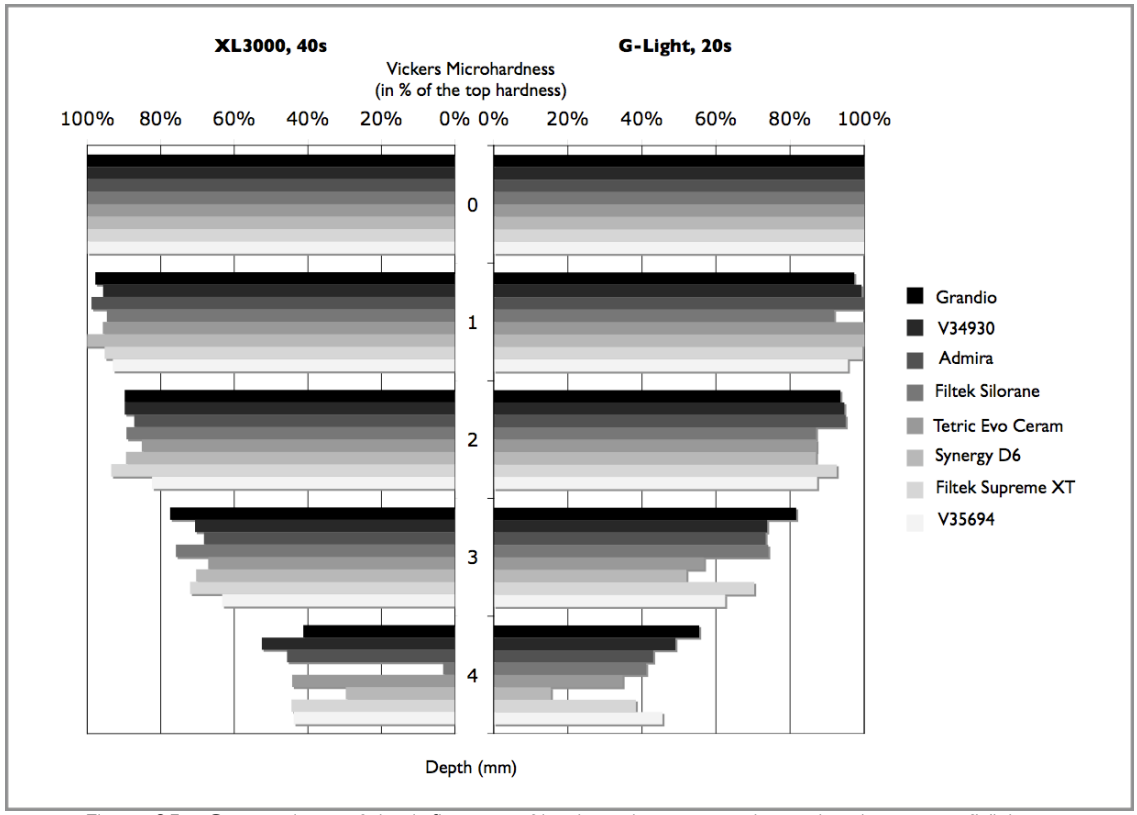

Figure 25 - Comparison of the influence of both curing protocols on the decrease of Vickers microhardness with depth. The values are presented in percentage of uppermost surface microhardness (n=5). The values to the left refer to samples cured during 40s with XL3000, and those to the right refer to samples cured during 20s with G-Light. (**Leprince *et al.,* 2010c - Chapter 5**)

[19] XL3000 (3M-Espe, St-Paul, MN, USA) operating at 544 mW/cm^2 (+/- 17 mW/cm^2)

[20] G-Light (GC, Leuven, Belgium) operating at 1166 mW/cm^2 (+/- 78 mW/cm^2). The third generation LED light was preferred to a second generation LED to limit the impact of potential spectrum incompatibility on the results.

be explained in details further (6.5), it is worth mentioning that the validation of a curing protocol based on this 80 % ratio between top and bottom hardness must be considered with caution. This can indeed lead to the validation of a curing protocol responsible for low absolute hardness values (**Leprince *et al.*, 2010d - Chapter 6**).

2.2.2. New light-curing units and importance of spectrum match

Dental practice and materials must evolve concomitantly with the demands of the society: more time efficiency, more aesthetics. Several works have highlighted the potential of the new generation LED lights to reduce irradiation time to some extent (Price *et al.,* 2005; Felix *et al.,* 2006; **Leprince et al. 2010c - Chapter 5**). However, dentists need to know to what extent, which depends on the type of LED lights they use. Moreover, as mentioned in the introduction (1.2.), alternative photoinitiators are now incorporated in some commercial composite formulations - mainly for aesthetic reasons (yellowish aspect of CQ/amine systems) - which modifies the absorption spectrum of composites. Consequently, problems of incompatibility can raise, notably when using 2nd generation of LED lights with a single narrow blue peak (Price and Felix, 2009). To overcome this problem, the 3rd generation of LED lights were developed, combining two different light peaks, a blue one (470 nm) and a violet one (400 nm) (Fig. 26, G and BG2). Besides, some LED lights belonging to the 2nd generation present a shifted peak,

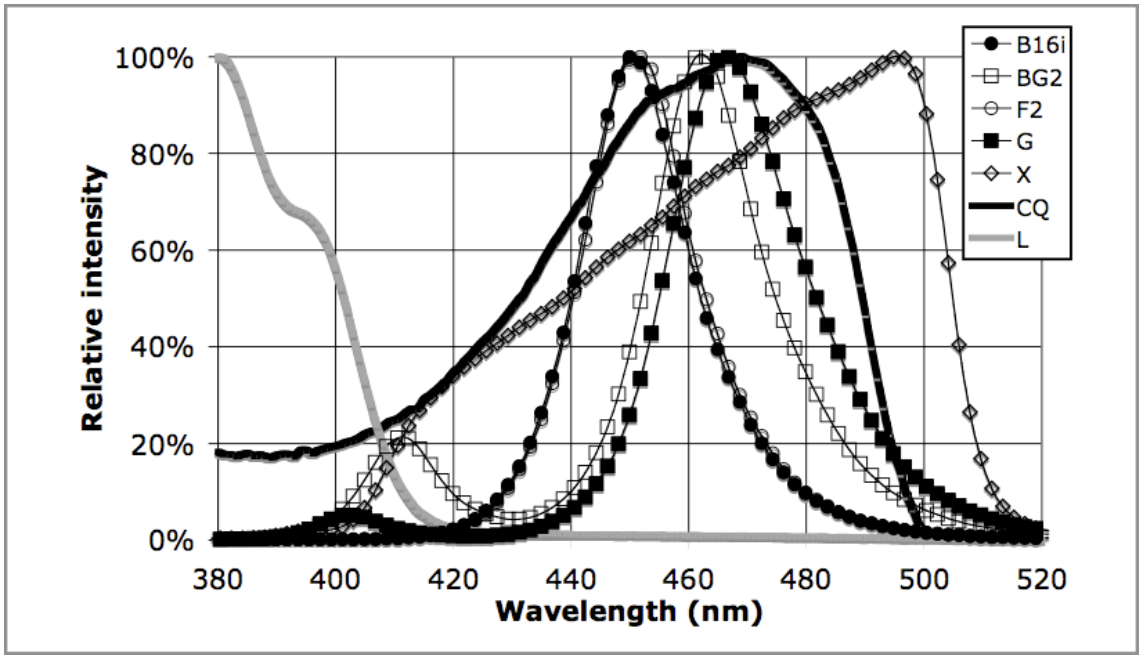

Figure 26 - Absorption spectra of the photoinitiators (pure CQ and L) and emission spectra of the light-curing units (in relative intensity of their respective maximum). B16i stands for Bluephase 16i (Ivoclar-Vivadent, Schaan, Liechtenstein), BG2 for Bluephase G2 (Ivoclar-Vivadent, Schaan, Liechtenstein), F2 for Freelight 2 (3M-Espe, St-Paul, MN, USA), G for G-Light (GC, Japan), X for XL3000 (3M-Espe, St-Paul, MN, USA), CQ for Camphorquinone and L for Lucirin-TPO. (**Leprince *et al.*, 2010d - Chapter 6**)

centered on 450 nm rather than the usual 470 nm (Fig. 26, B16i and F2), which probably attests the presence of phenylpropanedione in some materials of the curing light manufacturers. Given the lack of information from manufacturers on the photoinitiating systems of commercially available composites, dentists face a difficult choice among the diverse light curing systems. Therefore, a study was conducted in the present thesis to provide practitioners with some indications (**Leprince *et al.*, 2010d - Chapter 6**). Two main objectives were pursued: the first one was to evaluate the potential of curing time reduction of 4 different types of recent LED lights (Table 2) in comparison with a commonly accepted curing protocol - conventional halogen light[21] during 40 s (Torno *et al.,* 2008; Peutzfeldt and Asmussen, 2005). The second aim was to highlight potential lack of polymerization and/or excessive temperature rise in the pulp

Table 2 - Tested lights

Name	Code	Manufacturer	Light type	Mode*	Expected irradiance** (mW/cm^2)	Measured irradiance (mW/cm^2)	Recommended curing time ** ***
BluePhase 16i	B16i	Ivoclar-Vivadent (Schaan, Liechtenstein)	LED 2nd generation	High	1600 +/- 100	1622 (+/-78)	10s
BluePhase G2	BG2	Ivoclar-Vivadent (Schaan, Liechtenstein)	LED 3rd generation	High	1200 +/- 10%	1050 (+/-14)	10s
G-Light	G	GC (Japan)	LED 3rd generation	-	1200	1166 (+/-78)	10 or 20s
Freelight 2	F2	3M-Espe (St. Paul, MN, USA)	LED 2nd generation	-	1000	644 (+/-26)	50% reduction vs conventional halogen
XL3000	X	3M-Espe (St. Paul, MN, USA)	Halogen	-	data not found	544 (+/-17)	40s

* When choice possible between Low & High power mode

** Based on information from the manufacturer

*** For 2mm micro-hybrid composite, at high power when different modes available

chamber due to spectrum mismatch between LCU and composite. Therefore, two shade variants of the same composite - Tetric Evo Ceram® A2 and Bleach XL (Ivoclar-Vivadent, Schaan, Liechtenstein) - were chosen for their different photoinitiating system. Both shade variants indeed contain camphorquinone (CQ) and lucirin-TPO (L) but in different ratios. In shade A2, CQ is dominant while in Bleach shade, L is present in greater concentrations. Globally[22], Vickers microhardness results (VHN) for shade A2 composite seem to validate[23] the use of the four LED lights for irradiations of as short as 10 s as an alternative to the reference protocol (X – 40 s) (**Leprince *et al.*,**

[21] XL3000 (3M-Espe, St-Paul, MN, USA) operating at 544 mW/cm^2 (+/- 17 mW/cm^2)

[22] The results will be fully described in Chapter 6, and only the main conclusions will be presented here.

[23] For composite layers of 2 mm

2010d - Chapter 6). Indeed, VHN values were statistically comparable to or higher than values of the reference (except for F2 – 10 s, significantly lower at 2 mm depth). In case of higher values, the balance between microhardness improvement and pulpal temperature rise (ΔT) must be considered. Temperature rise is indeed mainly related to the irradiance (Asmussen and Peutzfeld, 2005) and despite the fact that dentin is an excellent thermal insulator, it cannot be excluded that the pulp will be thermally damaged during extended irradiation times, especially with a thin remaining dentin layer (Schmalz and Arenholt-Bindslev, 2009). Withworth *et al*. (2004) indeed reported increased incidence of pulpal problems for deep restorations and found that composite restorations were more likely to be associated with pulpal breakdown than amalgam, which could be partly explained by thermal damage (Jakubinek *et al.,* 2008). Hence, even if there is no consensus on the critical temperature above which pulpal damage can occur, an improvement in mechanical properties (as a result of an increase in irradiance and/or time) should only be validated if the associated ΔT is reasonable. Despite the better microhardness values for shade A2 composite obtained with 40 s irradiations with B16i, BG2 and G lights, ΔT[24] was significantly higher, with respectively 5.98, 5.22 and 4.96°C, i.e. nearly twice ΔT of the reference (3.09°C). When irradiation time was reduced to 20 s, B16i still induced a significantly higher ΔT (3.98°C) than the standard, while for BG2 and G there were no significant differences in ΔT compared to X – 40 s. Therefore, 3rd generation LED lights BG2 and G should be preferred and used for a maximum of 20 s for greater safety. However, a time of 40 s could be recommended in endodontically treated teeth. Considering Bleach shade, a reduction of curing time is also possible with LED lights, but only when using G and BG2 and for an irradiation time of 20 s (**Leprince *et al.*, 2010d - Chapter 6**). The latter curing protocols were also validated by temperature measurements: as there is no significant improvement in VHN with 40 s irradiation, 20 s could be preferred given the lower ΔTs.

Besides the determination of these clinical guidelines, several interesting observations must be highlighted. To start with, a perfect correspondence between light and material spectra is of prime concern, both to insure optimal polymerization (Price and Felix, 2009; **Leprince *et al.*, 2010d - Chapter 6**) and to limit heating in the pulp

[24] Tooth partially immersed in water at ambient temperature (+/- 23°C), thermocouple placed in the pulp chamber, temperature measurements performed during irradiation of the tooth either covered or uncovered by 2 mm composite layer. Please see Chapter 6 for complete description of the experimental setup.

chamber (**Leprince *et al.*, 2010d - Chapter 6**). For example, despite the much higher irradiance of B16i compared to BG2 (1622 mW/cm^2 versus 1050 mW/cm^2), the surface hardness of shade A2 cured with BG2 – 40 s was significantly greater (63.40 +/- 1.73 versus 56.61 +/- 2.31 VHN), probably thanks to the better alignment of the BG2 blue peak on the CQ peak of maximum absorption (Fig. 26). In addition, the effect of BG2's additional violet peak on the small amount of L in shade A2 composite must certainly not be neglected. The less adapted spectrum of B16i also results in a higher ΔT than BG2. Manufacturers should, therefore, inform practitioners carefully regarding the correspondence of light and material spectra.

Then, ΔT of uncovered teeth were higher (about 1°C) than when teeth were covered with 2 mm composite (**Leprince *et al.*, 2010d - Chapter 6**), which highlights, in accordance with other studies (Stewardson *et al.,* 2004; Millen *et al.,* 2007), the insulatory effect of composite, despite the exothermicity of the polymerization reaction. In other words, the heating induced by the light has more impact on the temperature rise in the pulp chamber than the exothermicity occurring as a result of the polymerization reaction of the 2 mm composite. It also underlines that the polymerization of the adhesive layer (assimilated to uncovered teeth) is probably the most critical step for the pulp. Notably, the most powerful LCU may represent a risk for the pulp when they are used for too long. Hence, dentists should limit the irradiation time with these lights for the polymerization of the adhesive or favour LED LCU with low irradiance mode. This is supported by the observation that the impact of irradiation time and irradiance is less important at the surface in terms of microhardness (**Leprince *et al.*, 2010d - Chapter 6**), but this trend should of course be supported by measurement of adhesion properties.

Finally, reduction in curing time is feasible with the new LED LCUs investigated as a result of a better-centered spectrum of LED and a higher irradiance. Nevertheless, despite the limited importance of irradiation time at the surface, time was very important at depth in order to obtain optimum polymerization (**Leprince *et al.*, 2010d - Chapter 6**). Hence, the potential to reduce irradiation time is limited by the need to maintain microhardness values as high as possible, especially at depth. In addition, time, and particularly irradiance, must be optimized to insure reasonable levels of pulpal heating. Notably, practitioners should remember that the effect of an increase in irradiance on microhardness is limited. An evocative example is the case of B16i and

F2, which can reasonably be compared as their spectra overlap perfectly (Fig. 26). On the surface of A2 shade, even though microhardness for B16i – 40 s was statistically higher than that of F2 – 40 s (56.61 +/- 2.31 versus 50.4 +/- 1.91 VHN), the difference is not proportional to the huge difference in irradiance (644 mW/cm^2 for F2 versus 1622 mW/cm^2 for B16i); between B16i – 20 s and F2 – 20 s or B16i – 10 s and F2 – 10 s, the differences were not significant. At a depth of 2 mm, there was no statistical difference either between B16i – 40 s and F2 – 40s, or between B16i – 20 s and F2 – 20 s. This is in accordance with the results of Musanje and Darvell (2003), who state that there seems to be little use to exceed 1000 mW/cm^2 for 2 mm layers. In addition, ΔT values of B16i were significantly higher (5.98 +/- 0.04, 3.98 +/- 0.13, 2.68 +/- 0.30) than with F2 (2.63 +/- 0.66, 1.71 +/- 0.28, 1.30 +/- 0.13), which is excessive compared to the slight and generally not significant increase in microhardness values.

To conclude, this highlights the importance to consider the relationship between the degree of conversion of a composite and the photoinitiation parameters: irradiation time, irradiance and the product of both, i.e. radiant exposure. This will be the topic of the next chapter, dealing with the exposure reciprocity law. Finally, as any excess irradiance can result in unjustified pulp heating in the same way as spectrum mismatch, data on thermal effects should clearly be available for light-curing units that are on the market.

2.3. Exposure Reciprocity Law: Comprehension and Innovation

2.3.1. Definition and Current knowledge

As underlined in the previous section, dental practice has to adapt to society changes and its new requirements. One of them and no the least is the need to save time, and there exists a demand for reduction in curing exposure to minimize chairside procedure times of multi-increment resin composite restorations. This is interesting for patients, who are understandably reluctant to stay for a long time with open mouth, and for the dentists, who wish to increase the yield of their practice.

In order to reach this time reduction, the general trend among manufacturers was to produce light curing units with increased irradiance. This was based on the assumption that the total energy of the irradiation, i.e. Radiant Exposure (*RE*, J/cm^2), is the main determining factor of the degree of conversion and mechanical properties of

the photoactive material. As *RE* is the product of irradiance (*I*, mW/cm^2) and irradiation time (*t*, s), it supposes that to reach a certain property, no matter how *RE* is obtained (different combinations of *I* and *t*) as long as it remains the same: it is the seducing principle known as *Exposure Reciprocity Law* (ERL). ERL is originated from a very old work from Bunsen and Roscoe (1859), stating that all photochemical reaction mechanisms depend only on the total absorbed energy and are independent of *I* and *t*.

It = constant

This law was applied later in photography and radiography, where the behavior of the films was observed to be uniformly constant if the exposure times to which the films are exposed vary reciprocally with the intensities of the exposing radiation (Morgan, 1944). In other words, considering radiography, the mass of the photoproduct resulting from X-ray radiation of silver grains in an emulsion is determined by the time integral of the exposure, i.e. the product of the X-ray radiation flux and the exposure time.

However, failures to this law were reported, and to account for them, Schwarzschild (1900) proposed a modification of this law:

$I^p t$ = constant

where *p* is the Schwarzschild coefficient that he thought was constant. It then appeared that p varied from material to material, within the same material, and in some cases with a change in irradiance (Martin et al., 2003). In their review, Martin et al. (2003) concluded that the law proposed by Schwarzschild models adequately the photoresponse of a wide range of materials as a function of I. In an large majority (97%), p fell between 0.5 and 1.0, the latter corresponding to the validity of the reciprocity law.

Now, in relation to dental dimethacrylate-based materials, ERL has been tested with regard to several material properties: degree of conversion, flexural strength and modulus, hardness and depth of cure (Feng and Suh, 2007); in certain cases, the law held quite well (Emami and Söderholm, 2003; Halvorson *et al.,* 2002; Price *et al.,* 2004; Sakaguchi and Ferracane, 2001). Based on this observation, as mentioned by Feng and Suh (2007), it was tempting to adopt ERL as a guideline to select the proper *t* based on

the available *I.* Unfortunately, several elements prevent from doing so. First of all, there seems to be no consensus on the adequate *RE* to cause acceptable polymerization, though such recommendations as 400 mW/cm^2 for 60 s (Rueggeberg *et al.,* 1993) or 600 mW/cm^2 for 40 s (Vandewalle *et al.,* 2004) with conventional halogen lights are usually considered as a standard for less than 2 mm increments. Musanje and Darvell (2003) even declare that the absence of consensus is not surprising given the variety of resin-based composite composition, light source spectra and responsivity of detectors. In addition, in contradiction with previous assumptions (Caughman *et al.,* 1995), they demonstrate that there is no «minimum irradiance» under which no effective polymerization can be achieved. Nevertheless, the necessary irradiation time may sometimes be clinically inconvenient at low *I.* Besides, there is clearly a need to specify *I* and *t* values at a given incremental thickness to generate «sufficient» material properties, i.e. competitive in its clinical purpose. Several studies have indeed reported that although *RE* plays an important role, *I* and *t* independently influence polymer chain length, extent of crosslinking and mechanical properties, and as such, exposure reciprocity law does not hold under all conditions. Notably, Musanje and Darvell (2003) highlighted that globally, apart from extremes (unset regions, i.e. gel state, and regions where properties have roughly attained their maximum), properties increase with *RE.* But on four investigated materials, only one seemed to roughly satisfy the reciprocity between *I* and *t*. This seems to demonstrate the prime importance of the particular composition and reactivity of the products. In the same way, DC, flexural strength, and flexural modulus were shown to increase with increasing *RE*. For each *RE,* DC was shown to decrease with increasing *I,* while flexural strength and modulus showed a maximum at intermediate *I* (Peutzfeldt and Asmussen, 2005). According to Peutzfeldt and Asmussen (2005), the effect of DC and cross-linking frequency on mechanical properties is of opposite direction. As DC decreases at higher *I* and shorter *t,* kinetic chain length decreases at the same time, and the frequency of cross-linking increases. This may explain the parabolic relationship found between *I,* and flexural strength and modulus. Finally, Dewaele *et al.* (2009) confirmed that DC, elastic modulus and T_g of a light-curing polymer-based material are mainly influenced by and positively correlated with *RE,* while there is negative correlation between *I* and DC and between *I* and elastic modulus. Their explanation relates to initial premature termination of free radicals, which is proportional to their squared concentration, hence proportionally more in case

of high *I*. Consequently, one interesting approach to better grasp the chemical process of photopolymerization is the observation of trapped free radical concentration, which can bring further clarification to conditions that lead to applicability of exposure reciprocity law. This will be detailed below.

2.3.2. Contribution of EPR technology in the understanding of the ER law

The study of trapped free radicals ($R\bullet_{Trapped}$) is particularly relevant regarding dimethacrylate-based resins as their polymerization leads to highly crosslinked networks, where «monomolecular termination» (or rather radical entrapment/ immobilization) becomes the dominant pathway (Andrzejewska, 2001). A strong relationship between autoacceleration and radical trapping was also established (Zhu *et al.,* 1990). This highlights the importance of considering the amount of trapped radicals when studying the impact of photoirradiation protocols, which to our knowledge, has never been investigated with clinically relevant irradiation parameters. For that reason, a work was conducted to test the impact of different curing modes of similar *RE* (either 6 or 12 J/cm^2) but different *I* (150, 300 and 600 mW/cm^2) and *t*, with or without a delay[25], on concentrations of $R\bullet_{Trapped}$ (**Leprince, Lamblin *et al.*, 2010a - Chapter 7**).

From Fig. 27 *a* and *b*, both distinct phases of $R\bullet_{Trapped}$ concentration decrease can be observed, as described earlier (3.1.3.): from 0 to 24 h, quick decay[26] associated with post-cure volumetric shrinkage (Truffier-Boutry *et al.,* 2006), and from 24 h to 3 months, slower decay assigned to oxidation by atmospheric oxygen (**Leprince *et al.*, 2009 - Chapter 3**). To compare $R\bullet_{Trapped}$ concentrations, the period from 5 minutes to 1 day post-cure should be considered, since the ratio of concentrations between curing regimes remains constant within this timeframe (parallel evolution with time). For continuous curing modes, the increase in $R\bullet_{Trapped}$ concentration following twice the *RE*, either by doubling *I* or *t* (Fig. 27 *a* and *b*), can be explained by the creation of a higher concentration of free radicals (generated by an increase in number of photons), which are more likely to become trapped (**Leprince, Lamblin *et al.*, 2010a - Chapter 7**).

---

[25] one second irradiation - 1, 2 or 3 min delay - rest of the irradiation

[26] Please keep in mind that the scale is logarithmic; with such a scale, the slope of the second phase appears sharper, but the decay is actually slower than during the first phase.

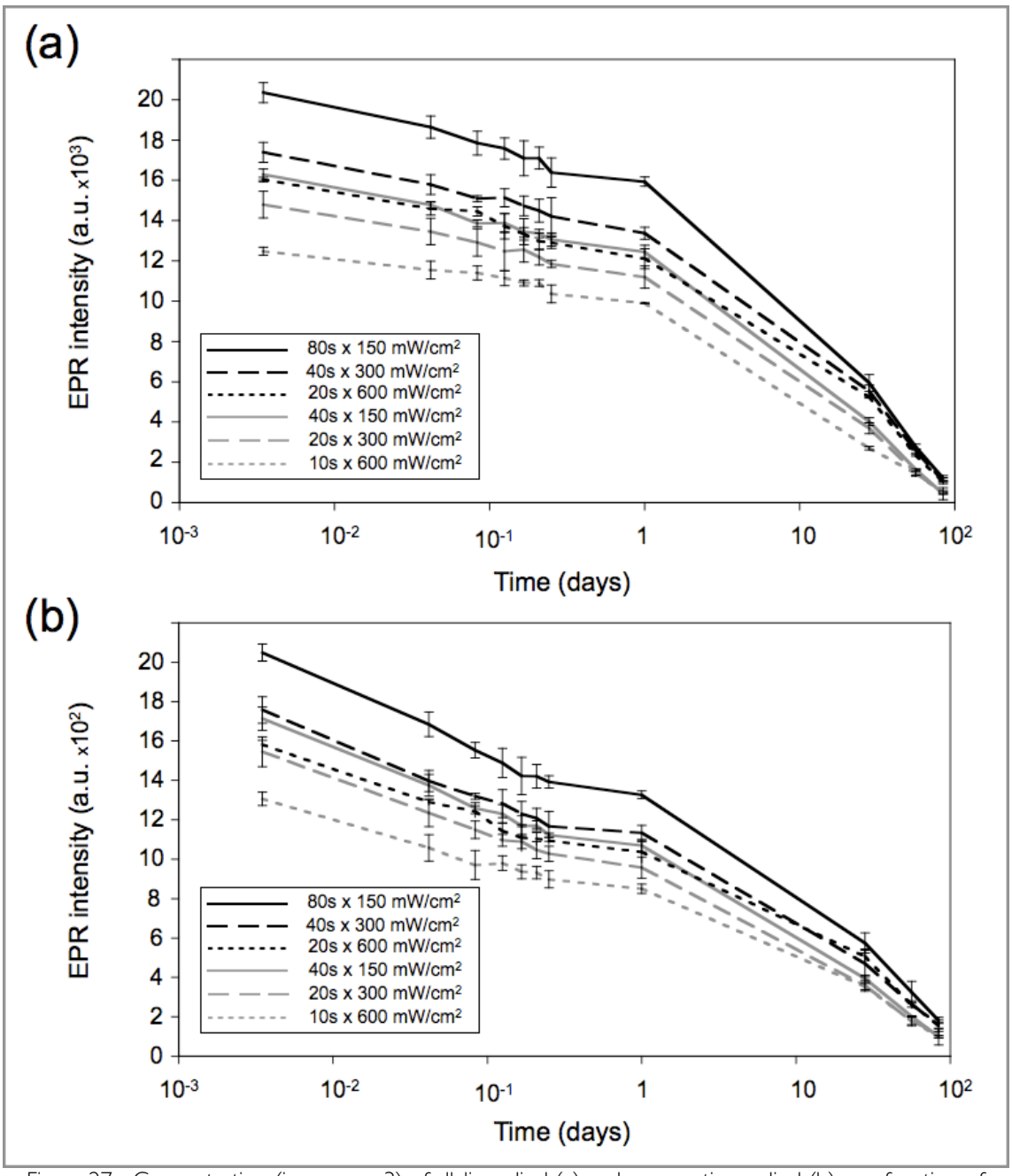

Figure 27 - Concentration (in a.u., n = 3) of allylic radical (a) and propagating radical (b) as a function of time (means +/- SD at 5 minutes, 1 to 6 hours, 1 day and 1 to 3 months – logarithmic scale) for continous-modes. Due to similar but overlapping profiles, pulse-mode curves are not displayed here for more clarity. Black lines represent modes of 12 J/cm^2 and grey lines modes of 6 J/cm^2.
(**Leprince, Lamblin *et al.*, 2010a - Chapter 7**)

However, for similar *RE*, higher concentrations of $R\bullet_{Trapped}$ were measured for longer *t* and lower *I* (**Leprince, Lamblin *et al.*, 2010a - Chapter 7**). This observation is in apparent contradiction with the reciprocity observed between *I* and *t* (ERL) for CQ quantum yield of photoinitiator conversion (number of converted photoinitiator molecules per number of absorbed photons) (Chen *et al.*, 2007). However, it cannot be excluded that the photoinitiating system may become saturated as *I* is increased, resulting in no improvement in the initiation rate (Musanje and Darvell, 2003). Indeed,

while the *I* in the work by Chen *et al.* (2007) was limited to 345 mW/cm^2, the works of Munsanje and Darvell (2003) investigated up to 1500 mW/cm^2, highlighting that there seems useless to exceed 1000 mW/cm^2 in 2 mm increments. Then, even assuming that the same total amount of radicals are created, it does not necessarily result in the same number entrapped. This can be explained by considering both types of termination mechanisms co-existing during polymerization (Lovell *et al.,* 1999): while bimolecular termination probably prevails during the very initial stages of the reaction, «monomolecular termination» (or rather radical immobilization/entrapment) dominates when molecular diffusion becomes limited (autoacceleration) (2.1.2.). There is probably a loss of a given amount of radicals during the early stages by bimolecular termination. This loss (or early termination) is higher for high irradiance protocols, as termination is proportional to $[R\bullet]^2$ (Eq. 2 in 2.1.2.). As a result, at constant *RE* but higher *I* and shorter *t*, the amount of growth centers created during auto-acceleration is lower, leading to a lower final concentration of $R\bullet_{Trapped}$ (**Leprince, Lamblin *et al.*, 2010a - Chapter 7**). In other words, the amount of $R\bullet_{Trapped}$ measured in the present work may provide an indication of the quantity of effective growth centers created during auto-acceleration. In light of theses results, the use of EPR to measure $R\bullet_{Trapped}$ gives valuable information on radical immobilization («monomolecular termination»), which is critical in highly crosslinked systems. It must be underlined that other factors than irradiation parameters alone could also determine whether exposure reciprocity law (ERL) holds or not, for example temperature, filler content, or viscosity. This will be discussed in the next section of this review (2.3.3.).

Regarding pulse-delay modes, no influence of any delay time (1, 2 or 3 minutes with no irradiation) was observed on the concentration of $R\bullet_{Trapped}$ or compared with continuous mode curing with similar *RE* (**Leprince, Lamblin *et al.*, 2010a - Chapter 7**). However, DC values associated with pulse-delay protocols were lower than those associated with the continuous mode of similar *RE* (Dewaele *et al.*, 2009), which can be explained by differences in polymer chain growth. The initial pulse probably results in microgels with relatively linear polymer chains (few pendant double bonds available) (Poshusta *et al.,* 2002; Dewaele *et al.,* 2009) and where most free radicals probably terminated. During final irradiation, these microgel regions, in which unreacted double bonds are less available, are certainly less reactive. Therefore, they may disturb the polymerization reaction compared with a continuous irradiation, leading

to reduced DC. However, as discussed above, most of the free radicals are trapped when propagation becomes diffusion-controlled. Therefore, it might be assumed that the irradiation parameters at the time of auto-acceleration govern the final amount of trapped radicals, leading to comparable amounts of $R\bullet_{Trapped}$ with or without a delay (**Leprince, Lamblin *et al.*, 2010a - Chapter 7**).

Prospectively, it clearly appears from the results presented in this section that the measurement of $R\bullet_{Trapped}$ is very useful in further understanding complex photopolymerization processes.

2.3.3. Is ERL dependent on other factors than irradiation parameters?

As explained above (2.3.1.), ERL states that different combinations of irradiance and exposure time provide similar «effect» for a same radiant exposure. The law was initially proposed for non-dental applications related to photochemistry, notably in connection with the behaviour of photographic films. In the latter field, the «effect» expected is the darkening of silver pigments under the action of visible light, and apparently, ERL holds quite well in general. The case of photography is very interesting, as it basically depends only on the emitted radiation and the photosensitive molecules. Each silver grain must indeed absorb a certain number of photons in order for the reaction to occur and the image to appear. However, even in this seemingly simple case, reciprocity law failures were reported in case of very high or very low irradiance. For example, in the latter case, the given number of photons required arrive one after the other, but over a longer interval. As a consequence, the partial change due to the first one or two photons is not stable enough to survive before enough photons arrive to induce a permanent change.

By analogy with photography, the «effect» of light expected in dental resin-based materials is the creation of free radicals. Hence, ERL should hold if the same total amount of efficient radicals were created by different irradiation protocols, which was verified by Chen *et al*. (2007) by measuring CQ quantum yield of conversion. However, again in relation with photography, very low or very high irradiances might lead to reciprocity failures. Notably, as mentioned earlier, it cannot be excluded that the photoinitiating system may become saturated at very high irradiance, resulting in no

improvement in the initiation rate (Musanje and Darvell, 2003). Besides, the amount of radicals created by absorbed photons, i.e. quantum yield efficiency, critically depends on the photoinitiator type. Hence, ERL should be verified with photoinitiators of different quantum yield, such as Lucirin-TPO (L) (Neumann *et al.*, 2006). Finally, the «effect» expected from irradiation of dental resins is not really the creation of an equal amount of free radicals but rather the build-up of a polymer network with equivalent properties. Given the specific characteristics of the dimethacrylate network growth explained above (**2.1.2.**), it is easily conceivable that the network development not only depends on free radical creation, but also on the conditions in which radicals are created, notably temperature, viscosity and filler load. Actually, all the factors that have an impact on the free radical termination pathway (bi-molecular termination or radicals immobilization) may influence achievement of reciprocity. In fact, it might be stated that failure to ERL occurs when the influence of the squared radical concentration can play a significant part in termination kinetics. This does not occur in two situations: either when [R•] is very low or when there is no termination at all, which can be due to free radicals immobilization, spatial confinement, etc.

Currently, few works exist on the impact of these different parameters on the applicability of ERL, as most work on reciprocity concerned commercial composites. Regarding viscosity, Feng and Suh (2007) highlighted that photopolymerization of CQ dimethacrylate-based resins with viscosity higher than 100 - 200 mPa.s, i.e. with a Bis-GMA/TEGDMA ratio equal to or above a 60/40 mass%, obeyed ERL for DC, while a resin with a ratio under 40/60 mass% did not. In the latter work, however, intermediate ratios were not investigated.

In recent work comparing three different I / t combinations of similar RE (**Leprince *et al.*, 2010b - Chapter 8**), the differences in DC observed in CQ-based 70/30 mass% Bis-GMA/TEGDMA resin (from 56.5 to 62.7 %; Table 3), were much smaller than in CQ-based 50/50 mass% Bis-GMA/TEGDMA resin (from 43.9 to 72.1 %; Table 3). This underlines that a relatively high viscosity can increase the efficiency of high I protocols, i.e. approach reciprocity, in CQ-based unfilled resins. This is probably due to a decrease of premature bimolecular termination explained in the previous section (2.3.2.). The results also support, in accordance with previous literature

(Peutzfeldt and Asmussen, 2005; Dewaele *et al.,* 2009), that for CQ-based materials, DC is higher at longer *t* and lower *I*.

Material	Mode		Radiant Exposure (J/cm^2)	DC (%)			DOC (mm)		
	Time (s)	Irradiance (mW/cm^2)		Mean	SD	*	Mean	SD	*
U 55 CQ	45	400	18	72.1	0.7	c	18.2	0.2	b
U 55 CQ	12	1500	18	65.8	0.5	e, f	16.9	0.1	c
U 55 CQ	6	3000	18	43.9	1.2	l	14.4	0.1	d
U 55 L	45	400	18	76.0	0.1	b	9.6	0.3	h
U 55 L	12	1500	18	83.3	0.5	a	11.8	0.2	e
U 55 L	6	3000	18	85.0	0.3	a	10.4	0.2	g, h
U 73 CQ	45	400	18	62.7	0.3	g	19.8	0.1	a
U 73 CQ	12	1500	18	58.9	0.5	h	20.0	0.3	a
U 73 CQ	6	3000	18	56.5	0.5	h, i, j	18.3	0.2	b
U 73 L	45	400	18	68.8	0.5	d	8.2	0.2	i
U 73 L	12	1500	18	73.2	1.0	c	12.1	0.4	e
U 73 L	6	3000	18	78.1	0.6	b	10.2	0.4	g, h
F 55 CQ	45	400	18	57.6	0.7	h, i	10.6	0.2	g
F 55 CQ	12	1500	18	54.9	0.9	j	10.8	0.2	f, g
F 55 CQ	6	3000	18	50.8	0.2	k	10.1	0.3	g, h
F 55 L	45	400	18	62.7	0.5	g	3.2	0.2	k
F 55 L	12	1500	18	65.2	2.5	f, g	3.7	0.1	j, k
F 55 L	6	3000	18	68,0	0.3	d, e	3.9	0.3	j, k
F 73 CQ	45	400	18	49.3	0.2	k	11.4	0.2	e, f
F 73 CQ	12	1500	18	44.7	0.8	l	10.1	0.2	g, h
F 73 CQ	6	3000	18	48.4	0.4	k	11.4	0.2	e, f
F 73 L	45	400	18	55.8	1.5	i, j	3.7	0.3	j, k
F 73 L	12	1500	18	54.3	1.1	j	4.3	0.2	j
F 73 L	6	3000	18	63.1	0.8	f, g	4.2	0.2	j

* Similar letters within columns indicate no significant difference ($p<0.05$)

Table 3 - Results for degree of conversion (DC, %) in 1.4 mm thickness samples and depth of cure (DOC, mm) for unfilled (U) or filled resins (F) cured with different irradiation parameters of similar radiant exposure. 55 and 73 indicate a 50/50 and 70/30 Bis-GMA/TEGDMA ratio respectively. L stands for Lucirin-TPO and CQ for Camphorquinone.
(Leprince *et al.*, 2010b - Chapter 8)

In L-based unfilled systems, contrary to CQ-based resins, the DC range between low and high *I* protocols were comparable for both 50/50 and 70/30 Bis-GMA/ TEGDMA ratios (from 76.0 to 85 % and from 68.8 to 78.1 respectively; Table 3), which underlines that viscosity has less impact on the reactivity of L-based materials. Besides, regarding the latter, the trend is opposite to CQ-based materials: higher DC are reached at higher *I* and shorter *t*. This can be explained by an increased generation of free

radicals resulting from the vastly higher molar absorptivity (**Leprince *et al.*, 2010b - Chapter 8**) and quantum yield efficiency of L, the latter being about five times higher than for CQ with a halogen light (Neumann *et al.*, 2006). Hence, despite some possible radical loss by early recombination evoked in the previous section for CQ-based resins (2.3.2.), there is probably a much quicker build-up of the polymer network into a gel-phase, favouring radical entrapment and leading to an earlier onset of autoacceleration. During autoacceleration, which is characterized by a low termination rate, L-based materials generate many more polymer growth centers. At high irradiance, this results in a significantly increased rate of polymerization compared with CQ-systems (**Leprince *et al.*, 2010b - Chapter 8**), which can compensate time reduction and lead to high DC. In addition, the influence of temperature must certainly not be neglected. As high rate of polymerization is associated with a higher and quicker reaction exotherm, it further improves DC by increasing monomer mobility. DC and maximum temperature reached were indeed highly correlated for unfilled resins ($R^2 = 0.95$; $p<0.0001$) (**Leprince *et al.*, 2010b - Chapter 8)**. Hence, it can be stated that resins containing a highly efficient photoinitiator system such as Luririn-TPO can obey quite well to ERL, even at low initial viscosity.

Now, in filled resins, the same trends as the ones highlighted for unfilled materials were observed, i.e. higher DC at longer *t* and lower *I* for CQ-based materials, and the opposite for L-based materials. In both cases, filler inclusion resulted in a decrease of DC ($p < 0.05$), except surprisingly, at 3000 mW/cm^2 for 50/50 Bis-GMA/ TEGMA CQ-based resin, whose filled parent exhibited a significantly higher DC (50.8 versus 43.9 %). Inclusion of filler particules may for example have affected light scattering properties through the limited specimen thickness (1.4 mm) and/or provided some insulating effect which improved final conversion of the filled composite. The reasons of this exception are not clear, and require further investigation.

Regardless of the latter exception, it is very interesting to consider the impact of fillers on the reciprocal effect of *I* and *t* in CQ-based materials. Compared to unfilled CQ-based 50/50 mass% Bis-GMA/TEGDMA resin, for which the DC range was quite large (from 43.9 to 72.1 %; Table 3), it is striking to observe more subtle DC differences in the same resin but filled with 75 mass% fillers (from 50.8 to 57.6 %; Table 3), approaching a reciprocal relationship with respect to *I* and *t*. This suggests that filler

inclusion seems to somehow reduce early bimolecular termination and favour radical entrapment. This may well be supported by previous findings (**Leprince *et al.*, 2009 - Chapter 3**) demonstrating that trapped free radical concentrations were nearly three times higher in the organic matrix of a filled composite than in a corresponding unfilled resin. The explanatory hypothesis proposed in that work was spatial confinement of radicals in filled resins, preventing their recombination. It could indeed be assumed that the organic fraction is located in small interstices between inorganic particles, which could restrict the diffusion of radicals to a relatively small area. But, it could also be related to an increase in local viscosity, reducing molecular mobility, thereby favoring monomolecular termination pathway. As mentioned earlier (2.1.3.), Beun *et al*. (2009) suggested that the large contact area between fillers and resin probably results in a significant local increase in viscosity. Consequently, in light of the present results, an increase of local viscosity of the resin due to fillers may partly explain the better efficiency of higher irradiance for CQ-based filled materials compared to their unfilled counterparts. Finally, it cannot be excluded that growing radicals can be immobilized by bonding to fillers though reaction with silane functions on their surface. Further work is required to fully elucidate this synergistic effects of filler particles on local resin viscosity and curing kinetics.

Finally, it must be underlined that DC measurements reported above for CQ- and L-based experimental materials (**Leprince *et al.*, 2010b - Chapter 8)** were obtained in 1.4 mm thick samples. However, considering the absorption characteristics of L and the increased scattering of light of shorter wavelength by fillers, inferior curing depth of materials that replace CQ with L may be a cause for concern (Price *et al.,* 2009; **Leprince *et al.*, 2010d - Chapter 6**). This was indeed verified (**Leprince *et al.*, 2010b - Chapter 8)**, as L-based materials exhibit inferior curing efficiency through depth, for unfilled and even more for filled materials (Table 3). Since L is a colourless photoinitiator and has been shown to exhibit efficient photobleaching properties with no absorbance of photolysis products above 360 nm (Stephenson *et al.,* 2008), negligible light attenuation through unfilled L-based resin might be assumed, although high exotherm and increasing UV radiation may cause some oxidation and discolouration of the polymer resin (any oxidative effect was visibly imperceptible following examination of the cured samples). The more likely explanation for inferior cure depth of L-based materials is related to the much higher molar absorptivity of L (Neumann *et al.,* 2005).

At similar PI concentration, L absorbs many more photons than CQ, which reduces the penetration of light through depth. The ratio of CQ / amine used in our study (**Leprince *et al.*, 2010b - Chapter 8)** was selected as an optimum combination to produce maximum DC (Yoshida and Greener, 1994) and CQ concentration represented that used in commercial composites (Taira *et al.*, 1988). An equimolar concentration was used for L for comparative purposes. However, given the very high polymerization efficiency of L, its concentration could probably be reduced, thereby improving the depth of cure (DOC). As for the additional decrease of DOC in filled materials, it is probably related to increased light scattering at the shorter wavelengths that correspond with the effective absorption of L (Price *et al.,* 2009). Though, the effective spectral irradiance of the curing-unit in the absorption range of L is several times lower than the one of CQ. As there is a linear correlation between irradiance and DOC (Lindberg *et al.,* 2004), a higher DOC for L-based materials might be achieved using a higher intensity source emitting specifically around 400 nm.

In conclusion, some interesting trends have been highlighted in this section: First, the opposite trend in L- and CQ-based materials - better efficiency at high *I* and short *t* for the former, and at low *I* and long *t* for the latter - and second, the positive effect of high viscosity and filler inclusion on the efficiency of high *I* in CQ-based materials. Obviously, this is only the tip of the iceberg and further works must be conducted to properly describe the influence on the polymerization kinetics and on polymer properties of the different parameters evoked in the present section. These future works and other work perspectives will be described in the next and last part of this review.

2.4. Perspectives

The present thesis has led to a deeper understanding of the photopolymerization of dimethacrylate-based dental resins, and opened the door to innovating approaches, which are promising and should certainly be pursued.

To start with, electron paramagnetic resonance (EPR) spectroscopy is clearly a very useful tool to study the termination pathway through measurement of radical entrapment. In particular, this technique provides complementary information to DC measurement methods (Raman spectroscopy, FTIR spectroscopy) when analyzing the

effect of various irradiation modes on the polymerization kinetics. For example, as illustrated by Fig. 28, $R\bullet_{Trapped}$ concentration evolves differently whether *RE* is increased through increase of *I* (*t* = constant - 30 s) or through increase of *t* (*I* = constant - 100 mW/cm²). In the former case, $R\bullet_{Trapped}$ concentration plateaus around 6 J/cm² (corresponding to 200 W/cm²), which indicates that for a given *t*, there is probably a maximum *I* above which no additional creation of growth centers can be expected. On the contrary, an increase of irradiation time leads to an increase of $R\bullet_{Trapped}$ concentration up to 15 J/cm² (corresponding to 150 s). Moreover, the impact of photoinitiator concentration is obvious, as doubling the concentration leads to a significant increase of $R\bullet_{Trapped}$ concentration at each *RE*.

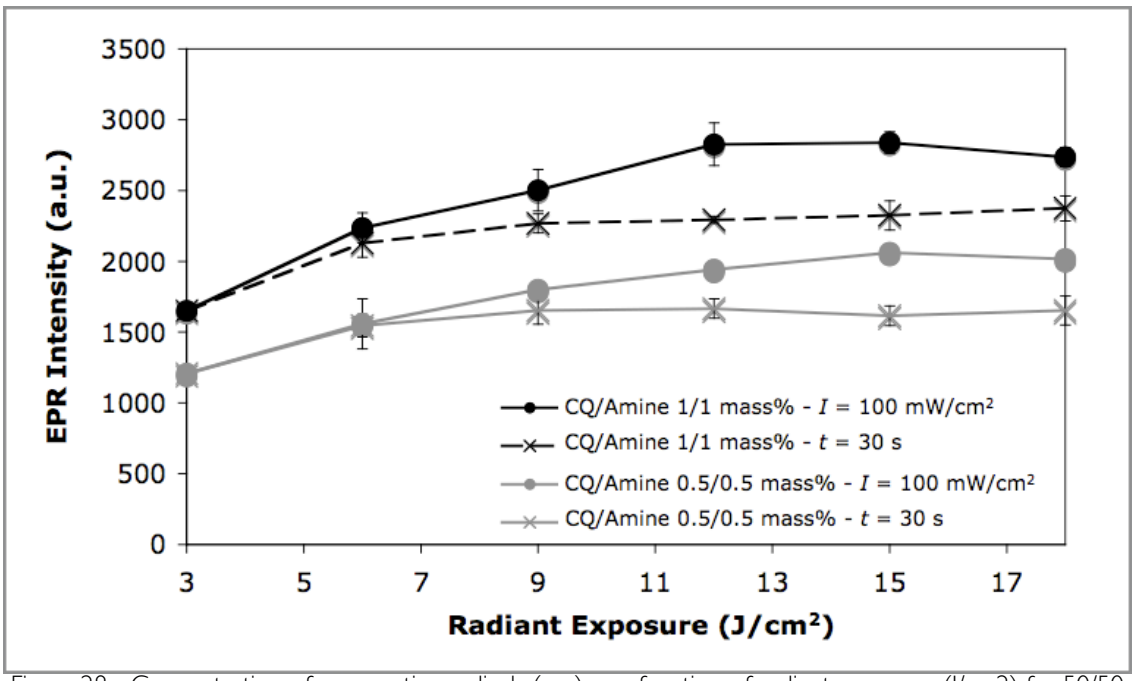

Figure 28 - Concentration of propagating radicals (a.u.) as a function of radiant exposure (J/cm2) for 50/50 bis-GMA/TEGDMA mass% resin cured in 1 x 1 x 7 mm brass molds.

Besides quantitative information on $R\bullet_{Trapped}$ concentration for a given resin volume, EPR spectroscopy can also provide bi- and tridimensional information on $R\bullet_{Trapped}$. As illustrated by the 2D-mapping of $R\bullet_{Trapped}$ in Fig. 29, EPR imaging can reveal differences of $R\bullet_{Trapped}$ concentration in the thickness of the material depending on the curing time. Moreover, using spectral imaging, it is possible to recover the EPR spectrum of each point of the sample, which enables to compare the proportion of allylic and propagating radicals at different depths (Fig. 30). Very interestingly, their respective proportions vary with curing depth: while allylic radical concentration slowly decreases with depth, the concentration of propagating radicals drops sharply around 1 mm depth. According to the increased reactivity of propagating radicals over allyl

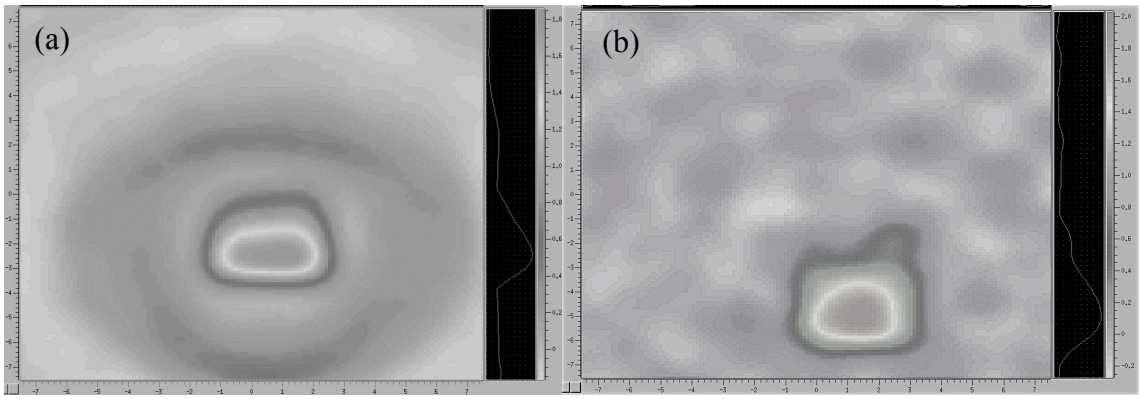

Figure 29 - Cross-section of a 3D-mapping of $R^{\bullet}_{Trapped}$ concentration (a.u.) in commercial composite Tetric Evo Ceram® cured with Bluephase G2 at low irradiance mode during 10 s (a) or 40 s (b). Color scale indicates variations of signal intensity. (Images gratefully from P. Leveque, REMA, UCL)

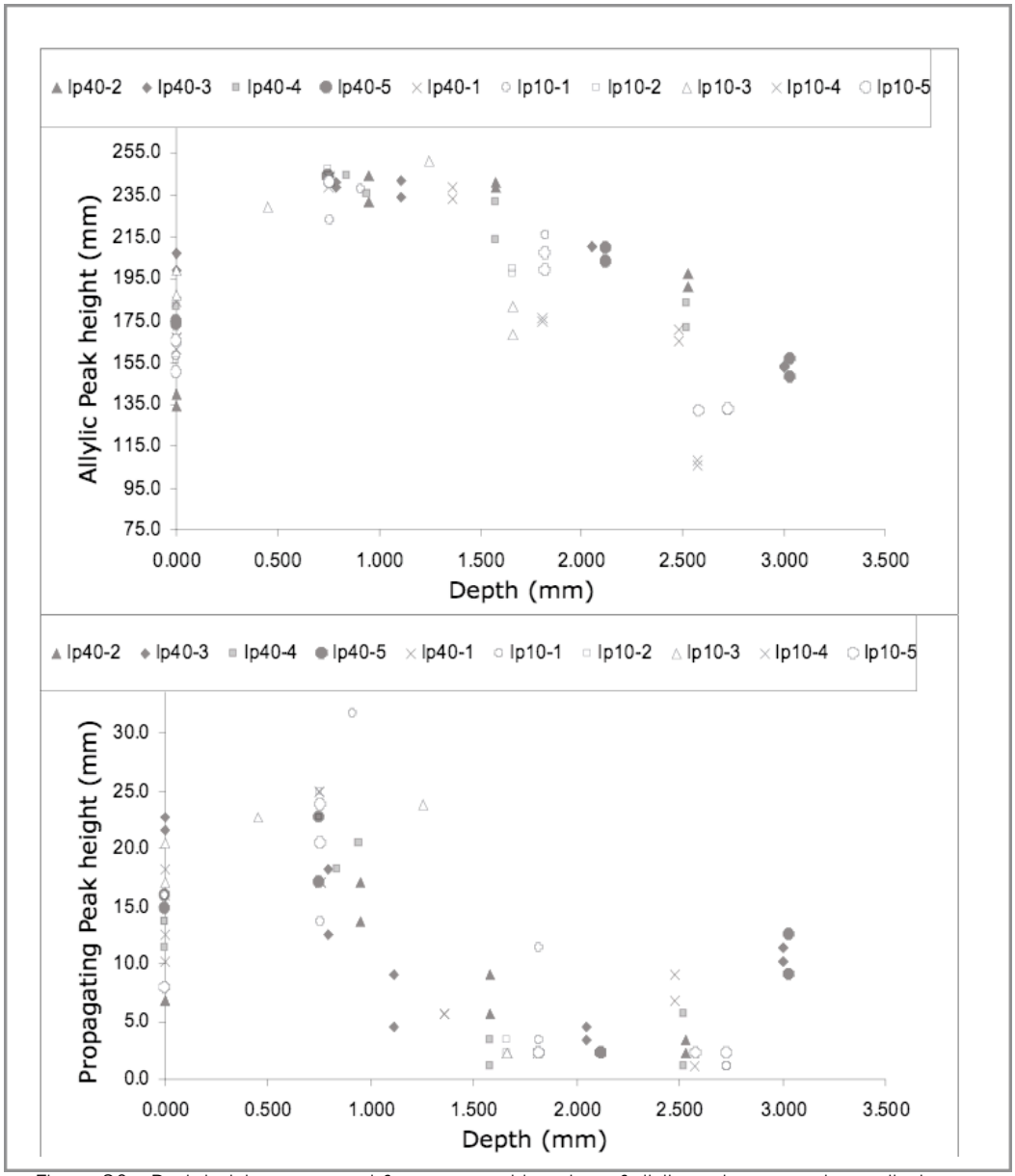

Figure 30 - Peak height recovered from spectral imaging of allylic and propagating radicals as a function of curing depth of composite Tetric Evo Ceram® cured with Bluephase G2 at low irradiance mode during 10 s (Ip10) or 40 s (Ip40).
(Images gratefully from P. Leveque, REMA, UCL)

radicals described above (**Leprince, Lamblin *et al.*, 2010a - Chapter 7**), this might be due to a difference of physical state of the polymer. Given the higher stability of allylic radicals, it is conceivable that they might persist in a gel state, while the more reactive propagating radicals would terminate. Hence, EPR spectral imaging could enable to determine a border between gel and vitrified state. Additional experiments using techniques such as atomic force microscopy (AFM) or nano-indentation are required in order to verify this hypothesis by the observation of a significant drop of the elastic modulus in the resin phase.

A second interesting topic for further research relates to the use of Lucirin-TPO as photoinitiator in dental resins. The alternative photoinitiator indeed presents several advantages over the classical CQ/amine system. First, L is a type I Norrish photoinitiator nature, producing radicals by photochemical cleavage, hence without any co-initiator (Fig. 31). This would certainly ease the optimization of L concentration,

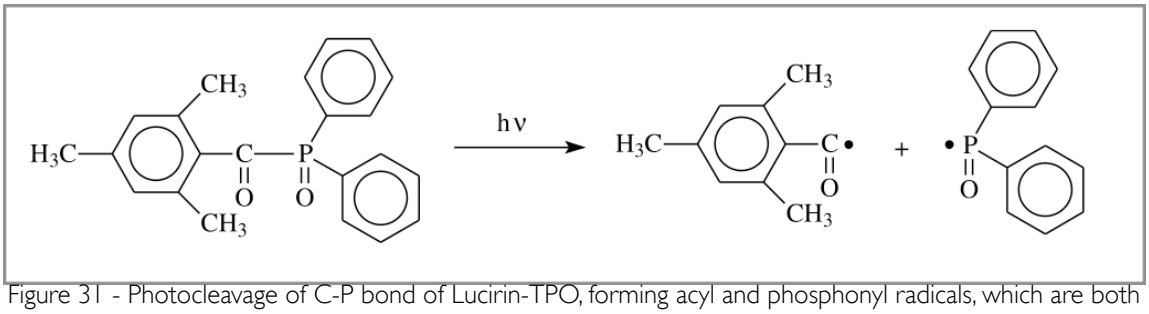

Figure 31 - Photocleavage of C-P bond of Lucirin-TPO, forming acyl and phosphonyl radicals, which are both capable of initiating polymerization. (Neumann *et al.*, 2006)

contrary to CQ/amine systems for which optimization is difficult as both components must be considered (Musanje *et al.,* 2009). An inappropriate proportion of amine can not only lead to lower mechanical properties and detrimental yellowing of margins like CQ, but can also represent a risk of toxicity (Schroeder *et al.,* 2008). For example, Cimpan *et al.* (2005) demonstrated that the coinitiator DMABEE[27] was able to induce cellular death by apoptosis and necrosis, and Seiss *et al.* (2009) stressed the dose- and time-dependence of the deleterious effects. The second obvious advantage of L is it increased curing efficiency, which enables significant curing time reduction thanks to the use of modern high-irradiance curing lights (**Leprince *et al.*, 2010b - Chapter 8)**. In the present thesis, the efficiency of L was tested regarding DC, which was shown to be significantly higher for L-based materials than for CQ-based ones, regardless of the curing protocol. However, mechanical properties and solvent sorption need to be

[27] 4-N,N-Dimethyl amino benzoic acid ethylester

investigated, as well as shrinkage stress, which might be a source of concern given the high rate of polymerization of L-based materials. Besides, L-based composites present a serious drawback: a limited DOC. This needs to be improved to enable the cure of thick layers (2 mm). As mentioned earlier (**2.3.3.**), several options should be considered: the reduction of L concentration, the use of a higher intensity source emitting specifically around 400 nm, or the adaptation of filler size to reduce light scattering. Nevertheless, DOC is not a problem in thin layers such as flowable composites and adhesive systems, and an increase of L concentration might even allow an additional reduction of curing time and/or irradiance. This could also play a part in the limitation of temperature rise in the pulp chamber during placement of the adhesive layer, which was shown to be the most critical step for the pulp (**Leprince *et al.*, 2010d - Chapter 6**). Besides, the interest of L high molar absorptivity is obvious in deep class II cavities or in the root canal during the placement of adhesive prior to fiber post luting. Ilie and Hickel (2008) already demonstrated the potential of L to replace CQ in adhesives in terms of DC and hardness. Hence, further works should now consider bonding performances of L-based adhesives cured with different curing protocols.

Another interesting area deserving further experimentation relates to the factors determining whether exposure reciprocity law is upheld or not in CQ-based resins. Notably, the understanding of the synergistic effects of filler particles on local resin viscosity and curing kinetics of CQ-based resins requires additional work. Different curing protocols should be tested on resins of various viscosities (different Bis-GMA / TEGDMA ratios), in which different ratios of micro- and nano-fillers would be incorporated. Volume fraction of fillers should be kept constant to test the influence of larger specific surface area by increasing the nano-filler part. Again, the contribution of EPR spectroscopy would certainly provide useful information on the extent of monomolecular termination.

To end up with, speaking of viscosity, another kind of dimethacrylate-based resin would be really worth investigating. Dewaele *et al.* (2010) recently investigated resin formulations containing hyperbranched polymers (HBPs)[28] in order to reduce volumetric shrinkage. In the latter work, it was observed that the higher the HBP

[28] The resins contained 5, 10, 20, 30 and 40 mass% of HBPs, combined with Bis-GMA and TEGDMA in equivalent mass percentages; they were compared to a 50 / 50 mass% Bis-GMA / TEGDMA resin.

content, the lower the volumetric shrinkage. This is explained by the increased size of such molecules, which consequently decreases the number of double bonds per unit volume of resin matrix (Dewaele *et al.*, 2006). DC was generally not affected, and an increase in elastic modulus was even observed up to 20 mass% of HBPs (Dewaele *et al.,* 2010). Very interestingly, despite the high molecular weight of HBPs, their addition to Bis-GMA / TEGDMA mixtures induced a lower-than-expected increase of the resin viscosity. For example, considering resins containing 30 mass% TEGDMA, the viscosity of resins containing HBPs (30 mass% Bis-GMA / 40 mass% HBPs) was lower (0.99, 1.33 or 2.15 Pa.s, depending on HBP type) than the corresponding 70 / 30 mass% Bis-GMA / TEGDMA resin (2.29 Pa.s - Beun *et al.,* 2009). Hence, once mixed to Bis-GMA / TEGDMA, HBPs seem to behave more like a diluent, contrary to what was expected given their high molecular weight. As a result, their amount might be increased as a replacement of TEGDMA, thereby possibly reducing volumetric shrinkage even more. Moreover, given the importance of viscosity on resin reactivity of CQ-based resins, the applicability of ERL needs to be tested on HBP-based resins, either unfilled or filled. In addition, it is certainly worth testing the efficiency of Lucirin-TPO as a photoinitiator in these systems, which could compensate for higher shrinkage stress that may be feared with L.

2.5. References

Andrzejewska E (2001). Photopolymerization kinetics of multifunctional monomers. *Prog Polym Sci* 26:605-665.

Anseth KS, Anderson KJ, Bowman CN (1996). Radical concentration, environments, and reactivities during crosslinking polymerizations. *Macromol Chem Phys* 197:833-848.

Anseth KS, Newman SM, Bowman CN (1995). Polymeric Dental Composites: Properties and Reaction Behavior of Multimethacrylate Dental Restorations. *Adv Polym Sci* 122:177-217.

Anseth KS, Wang CM, Bowman CN (1994). Kinetic evidence of reaction diffusion during the polymerization of multi(meth)acrylate monomers. *Macromol* 27:650–655.

Arenholt-Bindslev D, Breinholt V, Preiss A, Schmalz G (1999). Time-related bisphenol A content and estrogenic activity in saliva samples collected in relation to placement of fissure sealants. *Clin Oral Invest* 3:120–125.

Asmussen E, Peutzfeld A (2005). Temperature rise induced by some light emitting diode and quartz-tungsten-halogen curing units. *Eur J Oral Sci* 113:96–98.

Bagis YH, Baltacioglu IH, Kahyaogullari S (2009). Comparing microleakage and the layering methods of silorane-based resin composite in wide Class II MOD cavities. *Oper Dent* 34:578-585.

Berchtold KA, Randolph TW, Bowman CN (2005). Propagation and Termination Kinetics of Cross-Linking Photopolymerizations Studied Using Electron Paramagnetic Resonance Spectroscopy in Conjunction with Near IR Spectroscopy. *Macromol* 38:6954-6964.

Beun S, Bailly C, Dabin A, Vreven J, Devaux J, Leloup G (2009). Rheological properties of experimental Bis-GMA/TEGDMA flowable resin composites with various macrofiller/microfiller ratio. *Dent Mater* 25:198-205.

Boaro LCC, Gonçalves F, Guimarães TC, Braga RR, Ferracane JL (2010). Shrinkage and polymerization stress of silorane- and dimer acid-based composites. *Dent Mater* 26, e128-e129.

Bosnjakovic A, Shulamith S (2006). Spin trapping by 5,5-dimethylpyrroline-N-oxide in fenton media in the presence of nafion perfluorinated membranes: limitations and potential. *J Phys Chem B* 110:10720-10728.

Bouillaguet S, Virgillito M, Wataha JC, Ciucchi B, Holz J (1998). The influence of dentine permeability on cytotoxicity of four dentine bonding systems, in vitro. *J Oral Rehab* 25:45–51.

Bouillaguet S, Wataha JC, Hanks CT, Ciucchi B, Holz J (1996). In vitro cytotoxicity and dentin permeability of HEMA. *J Endod* 22:244–248.

Bowen RL (1962). Dental filling materials comprising of vinyl-silane fused silica and binder consisting of the reaction product of bispenol and glycidyl methacrylate. *US Patent* 3, 066, 112.

Bunsen RW, Roscoe HE (1859). Photochemische untersuchungen. *Ann Phys* 108:193.

Burtscher P (1993). Stability of radicals in cured composite materials. Dent Mater 9:218-221.

Caughman WF, Rueggeberg FA, Curtis JW Jr (1995). Clinical guidelines for photocuring restorative resins. *J Am Dent Assoc* 126:1280-2, 1284, 1286.

Caughman WF, Caughman GB, Shiflett RA, Rueggeberg F, Schuster GS (1991). Correlation of cytotoxicity, filler loading and curing time of dental composites. *Biomaterials* 12:737–740.

Chen YC, Ferracane JL, Prahl SA (2007). Quantum yield of converion of the photoinitiator camphorquinone. *Dent Mater* 23:655-654.

Cimpan MR, Matre R, Skaug N, Lie SA, Lygre H (2005). The coinitiator DMABEE induces death by apoptosis and necrosis in human monoblastoid cells. *Clin Oral Invest* 9:168-172.

Cook WD (1992). Photopolymerization kinetics of dimethacrylates using the camphoroquinone/amine initiator system. *Polymer* 33:600-609.

Curtis AR, Shortall AC, Marquis PM, Palin WM (2008). Water uptake and strength characteristics of a nanofilled resin-based composite. *J Dent* 36:186–193.

Decker C and Elzaouk B (1995). Photopolymérisation de monomères multifonctionnels - VII. Evaluation des constantes de vitesse de propagation et de terminaison. *Eur Polym J* 31:1155-1163.

Dewaele M, Asmussen E, Peutzfeldt A, Munksgaard EC, Benetti AR, Finné G et al. (2009). Influence of curing protocol on selected properties of light-curing polymers: degree of conversion, volume contraction, elastic modulus, and glass transition temperature. *Dent Mater* 25:1576-1584.

Dewaele M, I. Fallais, J. Leprince, J. Devaux, G. Leloup (2010). Hyperbranched polymers: Their use in dental resins to reduce polymerization contraction. *Dent Mater* 26:e131.

Diaz-Arnold AM, Arnold MA, Williams VD (1992). Measurement of water sorption by resin composite adhesives with Near-Infrared Spectroscopy. *J Dent Res* 71:438-442.

Eick JD, Kotha SP, Chappelow CC, Kilway KV, Giese GJ, Glaros AG et al (2007). Properties of silorane-based dental resins and composites containing a stress-reducing monomer. *Dent Mater* 23:1011–1017.

Emami N and Söderholm KJ (2003). How light irradiance and curing time affect monomer conversion in light-cured resin composites. *Eur J Oral Sci* 111:536-542.

Felix CA, Price RB, Andreou P (2006). Effect of reduced exposure times on the microhardness of 10 resin composites cured by high-power LED and QTH curing lights. *J Can Dent Assoc* 72:147

Feng and Suh (2007). Exposure reciprocity law in photopolymerization of multi-functional acrylates and methacrylates. *Macromol Chem Phys* 208:295-306.

Ferracane JL, Greener EH (1986). The effect of resin formulation on the degree of conversion and mechanical properties of dental restorative resins. *J Biomed Mater Res* 20:121-31.

Ferracane JL ((1994). Elution of leachable components from composites. *J Oral Rehab* 21:441–452.

Ferracane JL, Condon JR (1990). Rate of elution of leachable components from composite. *Dent Mater* 6:282–287.

Gallez B, Beghein N (2002). Noninvasive in vivo EPR monitoring of the methyl methacrylate polymerization during the bone cement formation. *Biomaterials* 23:4701-4704.

Gerdolle DA, Mortier E, Droz D (2008). Microleakage and polymerization shrinkage of various polymer restorative materials. *J Dent Child* 75:125–133.

Geurtsen W (1998). Substances released from dental resin composites and glass ionomer cements. *Eur J Oral Sci* 106:687–695.

Guggenberger R, Weinmann W (2000). Exploring beyond methacrylates. *Am J Dent* 13:82D-84D.

Halvorson RH, Erickson RL, Davidson CL (2002). Energy dependent polymerization of resin-based composite. *Dent Mater* 18:463-469.

Hansel C, Leyhausen G, Mai UE, Geurtsen W (1998). Effects of various resin composite (co)monomers and extracts on two caries-associated micro-organisms in vitro. *J Dent Res* 77 :60-67.

Ilie N, Hickel R (2006). Silorane-based dental composite: behavior and abilities. *Dent Mater J* 25:445-454.

Ilie N, Hickel R (2008). Can CQ be completely replaced by alternative initiators in dental adhesives?. *Dent Mater* J 27:1-8.

Ilie N, Hickel R (2009). Macro-, micro- and nano-mechanical investigations on silorane and methacrylate-based composites. *Dent Mater* 25:810-819.

Imai Y, Komabayashi T (2000). Elution of bisphenol A from composite resin: a model experiment. *Dent Mater* J 19:133–138.

Inoue K, Hayashi I (1982). Residual monomer (Bis-GMA) of resin composites. *J Oral Rehab* 9:493–497.

International Organization for Standardization (1988). Specification of dentistry-resin-based filling materials. ISO-4049.

Jakubiak J, Allonas X, Fouassier JP, Sionkowska A, Andrzejewska E, Linden LA, Rabek JF (2003). Camphorquinone-amines photoinitiating systems for the initiation of free radical polymerization. *Polymer* 44:5219.

Jakubinek MB, O'Neill C, Felix C, Price RB, White MA (2008). Temperature excursions at the pulp-dentin junction during the curing of light-activated dental restorations *Dent Mater* 24:1468-1476.

Kaptan Y, Pekcan O, Güven O (1992). Determination of diffusion coefficient of oxygen into polymers by using electron spin resonance spectroscopy. II. Poly(vinyl acetate). *J Appl Polym Sci* 44:1595–1599.

Kawahara T, Nomura Y, Tanaka N, Teshima W, Okazaki M, Shintani H (2004). Leachability of plasticizer and residual monomer from commercial temporary restorative resins. *J Dent* 32:277-283.

Khalichi P, Singh J, Cvitkovitch DG, Santerre JP (2009). The influence of triethylene glycol derived from dental composite resins on the regulation of Streptococcus mutans gene expression. *Biomaterials* 30:452-459.

Kloosterboer JG, Lijten GFCM, Greidanus FJAM (1986). Structure and stability of polyacrylate radicals trapped in a network. *Polym Commun* 27:268–271.

Lamblin G, Leprince J, Devaux J, Mestdagh M, Gallez B, Leloup G (2010). Free radical release from dental resins: ESR evidences. Submitted to *Acta Biomater*.

Lee S-Y, Greener EH, Menis DL (1995b). Detection of leached moieties from dental composites in fluid simulating food and saliva. *Dent Mater* 11:348-353.

Lee S-Y, Greener EH, Mueller HJ (1995a). Effect of food and oral simulating fluids on structure of adhesive composite systems. *J Dent* 23:27-35.

Leprince J, Lamblin G, Truffier-Boutry D, Demoustier-Champagne S, Devaux J, Mestdagh M, Leloup G (2009). Kinetic study of free radicals trapped in dental resins stored in different environments. *Acta Biomater* 5:2518-2524.

Leprince J, Lamblin G, Devaux J, Dewaele M, Mestdagh M, Palin WM, Gallez B, Leloup G (2010a). Irradiation Modes Impact on Radical Entrapment in Photoactive Resins. Submitted to J *Dent Res*.

Leprince J, Hadis M, Shortall AC, Ferracane JL, Devaux J, Leloup J, Palin WM (2010b). Photoinitiator type and applicability of exposure reciprocity law in filled and unfilled photoactive resins. Submitted to *Dent Mater*.

Leprince J, Palin WM, Mullier T, Devaux J, Vreven J, Leloup G (2010c). Investigating filler morphology and mechanical properties of new low-shrinkage resin composite types. *J Or Rehab*, In Press.

Leprince J, Devaux J, Mullier T, Vreven J, Leloup G (2010d). Pulpal-temperature rise and polymerization efficiency of LED curing lights. *Oper Dent* 35:220-230.

Li D, Zhu S, Hamielec AE (1993). ESR study on permeation of oxygen in crosslinked polymers. *Polymer* 34:1383-1387.

Lien W, Vandewalle KS (2010). Physical properties of a new silorane-based restorative system. *Dent Mater* doi:10.1016/j.dental.2009.12.004

Lin NJ, Lin-Gibson S (2009). Osteoblast response to dimethacrylate composites varying in composition, conversion and roughness using a combinatorial approach. *Biomaterials* 30:4480-4487

Lindberg A, Peutzfeldt A, van Dijken JW (2004). Curing depths of a universal hybrid and a flowable resin composite cured with quartz tungsten halogen and light-emitting diode units. *Acta Odontol Scand* 62:97-101.

Lovell LG, Lu H, Elliott JE, Stansbury JW, Bowman CN (2001). The effect of cure rate on the mechanical properties of dental resins. *Dent Mater* 17:504-511.

Lovell LG, Newman SM, Bowman CN (1999). The effects of light intensity, temperature, and comonomer composition on the polymerization behavior of dimethacrylate dental resins. *J Dent Res* 78:1469-1476.

Malacarne J, Carvalho RM, De Goes MF, Svizero N, Pashley DH, Tay FR, Yiu CK, MR Carrilho (2006). Water sorption/solubility of dental adhesive resins. *Dent Mater* 22:973-980.

Manhart J, Kunzelmann KH, Chen HY, Hickel R (2000). Mechanical properties of new composite restorative materials. *J Biomed Mater Res* 53:353-361.

Martin JW, Chin JW, Tinh N (2003). Reciprocity law experiments in polymeric photodegradation: a critical review. *Progress Org Coat* 47:292–311.

Masouras K, Akhtar R, Watts DC, Silikas N (2008). Effect of filler size and shape on local nanoindentation modulus of resin-composites. *J Mater Sci Mater Med* 19:3561–3566.

Millen C, Ormond M, Richardson G, Santini A, Miletic V, Kew P (2007). A study of temperature rise in the pulp chamber during composite polymerization with different light-curing units. *J Contemp Dent Pract* 8:29-37.

Morgan RH. Reciprocity law failure in X-ray films (1944) Radiology 42:471.

Moszner N, Gianasmidis A, Klapdohr S , Fischer UK, Rheinberger V (2008). Sol-gel materials 2. Light-curing dental composites based on ormocers of cross-linking alkoxysilane methacrylates and further nano-components. *Dent Mater* 24:851-856.

Musanje L, Darvell BW (2003). Polymerization of resin composite restorative materials: exposure reciprocity. Dent Mater 19:531-541.

Musanje L, Ferracane JL, Sakaguchi RL (2009). Determination of the optimal photoinitiator concentration in dental composites based on essential material properties. *Dent Mater* 25:994-1000.

Neumann MG, Miranda WG Jr, Schmitt CC, Rueggeberg FA, Correa IC (2005). Molar extinction coefficients and the photon absorption efficiency of dental photoinitiators and light curing units. *J Dent* 33:525-532.

Neumann MG, Schmitt CC, Ferreira GC and Correa IC (2006). The initiating radical yields and the efficiency of polymerization for various dental photoinitiators excited by different light curing units. *Dent Mater* 22:576-584.

Ottaviani MF, Fiorini A, Mason PN, Corvaja C (1992). Electron spin resonance studies of dental composites: effects of irradiation time, decay over time, pulverization, and temperature variations. *Dent Mater* 8:118-124.

Palin WM, Fleming GJ, Nathwani H, Burke FJ, Randall RC (2005a). In vitro cuspal deflection and microleakage of maxillary premolars restored with novel low-shrink dental composites. *Dent Mater* 21:324–335.

Palin WM, Fleming GJ, Burke FJ, Marquis PM, Pintado MR, Randall RC, Douglas WH (2005b). The frictional coefficients and associated wear resistance of novel low-shrink resin-based composites. Dent Mater 21:1111-8.

Papadogiannis D, Kakaboura A, Palaghias G, Eliades G.Setting characteristics and cavity adaptation of low-shrinking resin composites. *Dent Mater* 25:1509-1516.

Pashley DH, Derkson GD, Tao L, Derkson M, Kalathoor S (1988). The effects of a multi-step dentin bonding system on dentin permeability. *Dent Mater* 4:60–63.

Pashley DH, Michelich V, Kehl T (1981). Dentin permeability: effects of smear layer removal. *J Prosth Dent* 46:531–537.

Pashley DH (1984). Smear layer: physiological considerations. *Oper Dent* 3:13–29.

Pavlinec J, Moszner N, Mikova G, Placeka J, Slovak K (2009). Light emission on heating polymer networks formed by radical polymerization. *Polym Degrad Stab* 94:49-56.

Pavlinec J, Moszner N (2003). Dark reactions of free radicals trapped in densely crosslinked polymer networks after photopolymerization. *J Appl Polym Sci* 89:579-588.

Peutzfeldt A and Asmussen E (2005). Resin composite properties and energy density of light cure. *J Dent Res* 84:659-662.

Pianelli C, Devaux J, Bebelman S, Leloup G (1999). The micro-raman spectroscopy, a useful tool to determine the degree of conversion of light-activated composite resins. *J Biomed Mater Res Appl Biomater* 48:675–681.

Pollington S, Kahakachchi N, van Noort R (2009). The influence of plastic light cure sheaths on the hardness of resin composite. *Oper Dent* 34:741-745.

Poshusta AK, Bowman CN, Anseth KS (2002). Application of a kinetic gelation simulation to the characterization of in situ cross-linking biomaterials. *J Biomater Sci Polym Ed* 13:797-815.

Price RB, Felix CA (2009). Effect of delivering light in specific narrow bandwidths from 394 to 515nm on the micro-hardness of resin composites. *Dent Mater* 25:899-908.

Price RB, Felix CA, Andreou P (2004). Effects of resin composite composition and irradiation distance on the performance of curing lights. *Biomaterials* 25:4465-4477.

Price RB, Felix CA, Andreou P (2005). Knoop hardness of ten resin composites irradiated with high-power LED and quartz-tungsten-halogen lights. *Biomaterials* 26:2631-2641.

Pulgar R, Olea-Serrano MF, Novillo-Fertrell A, Rivas A,Pazos P, Pedraza V, Navajas JM, Olea N (2000). Determination of bisphenol A and related aromatic compounds released from Bis-GMA-based composites and sealants by high performance liquid chromatography. *Environ Health Perspect* 108:21–27.

Reinke LA (2002). Spin trapping evidence for alcohol-associated oxidative stress. *Free Rad Biol Med* 32:953-957.

Rueggeberg FA, Caughman W, Curtis J (1993). Factors affecting cure at depths within light-activated resin composite. *Am J Dent* 6:91-95.

Sakaguchi RL and Ferracane JL (2001). Effect of light power density on development of elastic modulus of a model light-activated composite during polymerization. *J Esthet Restor Dent* 13:121-130.

Schmalz G and Arenholt-Bindslev D (2009). Biocompatibility of Dental Materials. Springer.

Schmalz G, Hiller, K-A, Nunez LJ, Stoll J, Weis K (2001). Permeability characteristics of bovine and human dentin under different pretreatment conditions. *J Endod* 27:23–30.

Schroeder WF, Cook WD, Vallo CI (2008). Photopolymerization of N,N-dimethylaminobenzyl alcohol as amine co-initiator for light-cured dental resins. *Dent Mater* 24:686-693.

Schwarzschild K (1900). On the law of reciprocity for bromide of silver gelatin. *Astrophys J* 11:92-99.

Schweikl H, Altmannberger I, Hanser N, Hiller K-A, Bolay C, Brockhoff G, et al (2005). The effect of triethylene glycol dimethacrylate on the cell cycle of mammalian cells. *Biomaterials* 26:4111-4118.

Seiss M, Langer C, Hickel R, Reichl FX (2009). Quantitative determination of TEGDMA, BHT, and DMABEE in eluates from polymerized resin-based dental restorative materials by use of GC/MS. *Arch Toxicol* 83:1109-1115.

Sideridou I, Tserki V, Papanastasiou G (2003). Study of water sorption, solubility and modulus of elasticity of light-cured dimethacrylate-based dental resins. *Biomaterials* 24:655-665.

Spahl W, Budzikiewics H, Geurtsen W (1998). Determination of leachable components from four commercial dental composites by gas and liquid chromatography/mass spectrometry. *J Dent* 26:137–145.

Stephenson Kenning N, Ficek BA, Hoppe CC, Scranton AB (2008). Spatial and temporal evolution of the photoinitiation rate for thick polymer systems illuminated by polychromatic light : selection of efficient photoinitiators for LED or mercury lamps. *Polymer Int* 57:1134-1140.

Stewardson DA, Shortall AC, Harrington E, Lumley PJ (2004). Thermal changes and cure depths associated with a high intensity light activation unit. *J Dent* 32:643-651.

Suzuki S, Leinfelder KF, Kawai K, Tsuchitani Y (1995). Effect of particle variation on wear rates of posterior composites. *Am J Dent* 8:173–178.

Taira M, Urabe H, Hirose T, Wakasa K, Yamaki M (1988). Analysis of photo-initiators in visible-light-cured dental composite resins. *J Dent Res* 67:24.

Tanaka K, Taira M, Shintani H, Wasaka K, Yamaki M (1991). Residual monomers (TEG-DMA and Bis-GMA) of a set visiblelight-cured dental resin composite when immersed in water. *J Oral Rehab* 18:353–362.

Taniguchi H, Madden KP (2000). DMPO-alkyl radical spin trapping: an in situ radiolysis steady-state ESR study. *Rad Res* 153:447-453.

Teshima W, Nomura Y, Tanaka N, Urabe H, Okazaki M, Nahara Y (2003). ESR study of camphorquinone/amine photoinitiator systems using blue light-emitting diodes. *Biomaterials* 24:2097-2103.

Torno V, Soares P, Martin JM, Mazur RF, Souza EM, Vieira S (2008). Effects of irradiance, wavelength, and thermal emission of different light curing units on the Knoop and Vickers hardness of a composite resin. *J Biomed Mater Res B* 85:166-171.

Truffier-Boutry D, Demoustier-Champagne S, Devaux J, Biebuyck JJ, Mestdagh M, Larbanois P, et al (2006). A physico-chemical explanation of the post-polymerisation shrinkage in dental resins. *Dent Mater* 22:405–412.

Truffier-Boutry D, Gallez XA, Demoustier-Champagne S, Devaux J, Mestdagh M, Champagne B, Leloup G (2003). Identification of free radicals trapped in solid methacrylated resins. *J Polym Sci A* 41:1691-1699.

Uhl A, Mills RW, Rzanny AE, Jandt KD (2005). Time dependence of composite shrinkage using halogen and LED light curing. *Dent Mater* 21:278–286.

Van Ende A, De Munck J, Mine A, Lambrechts P, Van Meerbeek B (2010).Does a low-shrinking composite induce less stress at the adhesive interface? *Dent Mater* 26:215-222.

Van Noort (1994). Introduction to Dental Materials. Mosby editor.

Vandewalle KS, Ferracane JL, Hilton T, Erikson RL, Sakaguchi RL (2004). Effect of energy density on properties and marginal integrity of posterior resin composite restorations. *Dent Mater* 20:96–106.

Weinmann W, Talacker C, Guggenberger R (2005). Siloranes in dental composites. *Dent Mater* 21:68–74.

Whitworth JM, Myers PM, Smith J, Walls AW, McCabe JF (2005). Endodontic complications after plastic restorations in general practice. *Int Endod J* 38:409-416.

Yamazaki I, Piette LH (1991). EPR spin-trapping study on the oxidizing species formed in the reaction of the ferrous ion with hydrogen peroxide. *J Am Chem Soc* 113:7588-7593.

Yesilyurt C, Yoldas O, Altintas SH, Kusgoz A (2009). Effects of food-simulating liquids on the mechanical properties of a silorane-based dental composite. *Dent Mater J* 28:362-367.

Yoshida K, Greener EH (1994). Effect of photoinitiator on degree of conversion of unfilled light-cured resin. *J Dent* 22:296-299.

Zhu S, Tian Y, Hamielec AE, Eaton DR (1990). Radical concentrations in free radical copolymerization of MMA/EGDMA. *Polymer* 31:154-159.

Chapter 3

Kinetic study of free radicals trapped in dental resins stored in different environments

Available online at www.sciencedirect.com
ScienceDirect
Acta Biomaterialia 5 (2009) 2518–2524
Acta BIOMATERIALIA
www.elsevier.com/locate/actabiomat

Kinetic study of free radicals trapped in dental resins stored in different environments

Julian Leprince [a,b,d,*], Guillaume Lamblin [a,b,d], Delphine Truffier-Boutry [a,b,d], Sophie Demoustier-Champagne [b,d], Jacques Devaux [b,d], Michèle Mestdagh [c,d], Gaetane Leloup [a,d]

[a] *School of Dentistry and Stomatology, Université catholique de Louvain, Brussels, Belgium*
[b] *Unité de Physique et de Chimie des Hauts Polymères (POLY), Université catholique de Louvain, Louvain-la-Neuve, Belgium*
[c] *Interfacial Chemistry Laboratory, Université catholique de Louvain, Louvain-la-Neuve, Belgium*
[d] *CRIBIO (Center of Research and Engineering of Odontologic Biomaterials), Brussels, Belgium*

Received 14 January 2009; received in revised form 8 April 2009; accepted 17 April 2009
Available online 3 May 2009

3.1. Summary

In this work, we followed by EPR (Electron Paramagnetic Resonance) the decrease kinetics of free radicals trapped in an experimental resin (ER) and in a commercial composite (Charisma® - Ch) stored in different conditions (air – 25 and 37°C, argon, oxygen and water – 25°C). During the first day, the decay was fast (0 to 24h - rate of decay of allylic radical: 1700 to 1000a.u. for Ch, 1700 to 1500a.u. for ER) and the storage conditions had no influence on the kinetics. This phase was assigned to a post-polymerization phenomenon. From 1day to 1month, the rate of decay depended on the storage environment. In argon, free radicals were quite stable (1day to 1 month – rate of decay of allylic radical: 1200 to 1000a.u. for Ch, 1400 to 1200a.u. for ER). For the other storage environments, in ER, the rate of decay was higher in water, then in oxygen and in air (1day to 1 month – rate of decay of allyl radical: 1400a.u; to 100, 500 and 800a.u. respectively). In Ch, free radicals faded quicker than in ER, as undetectable levels were reached before 1month, which attests the influence of fillers on radical decrease kinetics. Heating experiments were also performed, and free radical concentrations decreased faster at higher temperatures, especially above the glass transition temperature. In conclusion, ambient oxygen is mainly involved in the free radicals termination process. Therefore, conditions influencing oxygen diffusion have an impact on radical kinetics as well.

3.2. Introduction

Free radicals are created during the photopolymerization of methacrylated dental resins. Some terminate by encountering other radical species, but others become trapped by vitrification of the system [1, 2, 3]. A work studying the reaction mechanism and comparing experimental EPR (Electron Paramagnetic Resonance) spectra with simulated ones resulted in the identification of two free radical species [1]. The first one, a propagating radical (Fig. 1a), gives rise to 9 weak and broad peaks on the EPR spectrum and the second one, an allylic species (Fig. 1a), to 5 strong and sharp peaks. Both spectra superimpose, resulting in an "overall" 9-line spectrum with peaks of alternated intensities (Fig. 1b). As these free radicals are trapped in the solid matrix, they cannot recombine and the 9-lines ESR spectrum persists during a period ranging from a few days to a few months depending on the storage conditions.

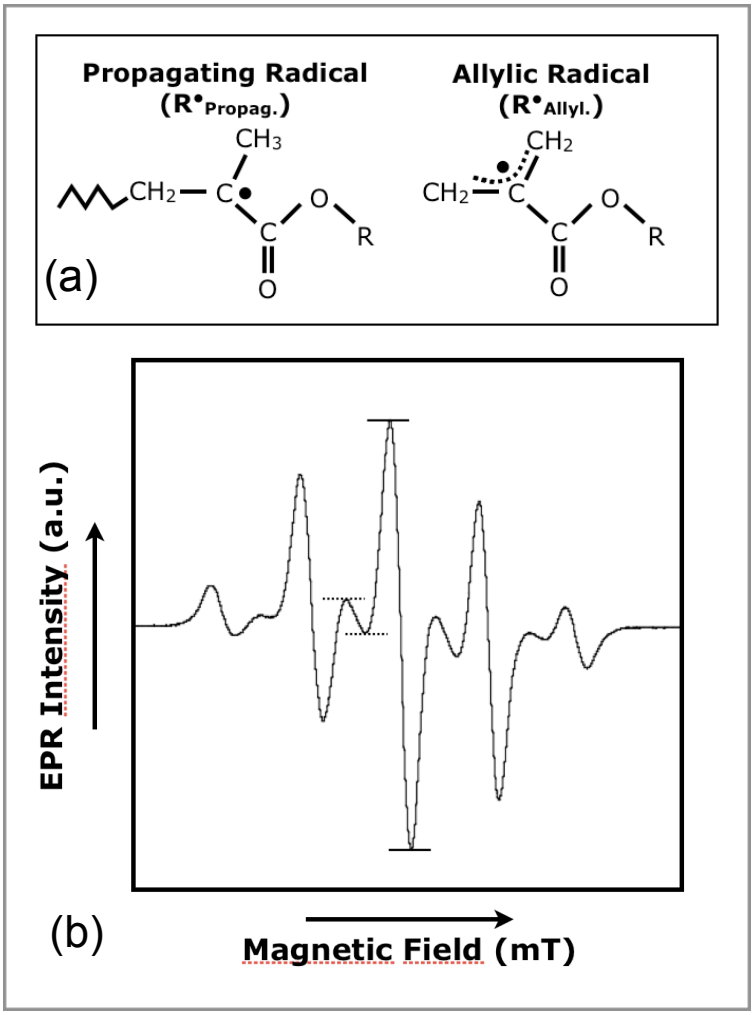

Figure 1 - a) chemical structure of both trapped radical species (R represents either an end group or a connection to the network); b) 9-line EPR spectrum of the experimental resin after polymerization; assessment of the respective intensities of both radical species by the measurement of the two peaks indicated by two lines, plain for the peak corresponding to the allylic radical and dotted for the one corresponding to the propagating one respectively.

The fate of these trapped radicals during the first 24 hours after photocuring was investigated in a previous publication [4]. In this paper, an exponential decrease of the concentration of both trapped free radicals was observed. This was assigned to the shrinkage phenomenon linked to the free-volume relaxation in the organic matrix,

resulting in increased proximity and mobility of the chemical species. In this way, recombination of radicals can occur, either by bimolecular termination or due to reactive diffusion. As a result, an increase of the degree of conversion (DC) was measured (2%) during the 24h after photocuring. However, this effect is limited, as no additional change in DC was observed from 24 to 48h. This may be due to the end of the free-volume relaxation and/or to the influence of oxygen [5, 6], competing with additional propagation. For that reason, the long-term kinetics of decrease of the trapped free radicals must be analyzed, as well as the impact of different storage environment.

To begin with, the effect of atmospheric oxygen on the trapped free radicals surely has to be taken into account. Generally speaking, the reaction of oxygen with free radical species is indeed very likely. For example, during the polymerization process, it acts as an inhibitor by reacting with the radicals created by irradiation [7], ending in the creation of an inhibition layer at the surface of the composite [8]. Regarding trapped free radicals, the impact of oxygen has also been established [5, 6, 9]. Moreover, the follow-up of free radical fading by EPR was previously used to determine the diffusion coefficient of oxygen in the bulk of polymers [10]. Besides oxygen, other substances of the oral environment such as water [11, 12] or saliva [13, 14] can also interact with the organic matrix, which could have an impact on free radical decay. For example, saliva can cause damage e.g. through the reaction of enzymes with compounds of the organic matrix. The rate of these different reactions increases with temperature [2, 12, 15], which is thus another interesting parameter to take into account. In this work, the effect of different storage conditions on free radical kinetics of decrease was studied: two different temperatures, i.e. 25°C (ambient) and 37°C, and 4 environments (water, argon, air and oxygen) were investigated. An experimental resin (ER) and a commercial resin-composite (Charisma® - Ch) were both used to study the impact of inorganic fillers on free radical decay.

3.3. Materials and Methods

3.3.1. Materials

The commercial resin-composite studied was Charisma® (A3, batch n °090054, Heraeus Kulzer, Dormagen, Germany). The organic matrix represents about

36 vol% of the dental composite, and the mineral fillers the remaining 64 vol%. For that reason, free radical concentration of Ch (assessed by EPR intensities) can be ratioed to the organic content using a multiplication factor of 100/36 (or 2.78) in order to compare them adequately with radical concentrations in pure resin samples. Besides inorganic fillers, Ch was found to contain Bisphenol A Glycidyl diMethAcrylate (Bis-GMA) and TriEthylene Glycol diMethAcrylate (TEGDMA) in a weight ratio close to 70:30%. It also includes an initiator system (camphorquinone – CQ), pigments and antioxidants in undetermined concentrations.

In order to imitate the organic phase of the Ch, the experimental resin used in this work was a mix of Bis-GMA (Heraeus Kulzer, Wehrheim, Germany) and TEGDMA (Aldrich, Belgium) in the same 70:30 wt% ratio, with an addition of 1 wt% of photoinitiating mix, i.e. CQ (97% Camphorquinone, Aldrich, Belgium) and DABE (97% N,N-Dimethyl-p-AminoBenzoic acid ethyl Ester, Aldrich), both with 0.5wt%.

3.3.2. Preparation of samples

The resin was inserted in moulds of 25 x 2 x 2 mm and the samples were photopolymerized with the light Translux Energy (Heraeus Kulzer, Dormagen, Germany) used under conventional mode with an irradiance of 900 mW/cm^2. Four irradiations of 40 seconds each were performed on both sides of the sample in order to cover its full length and to insure optimum polymerization. The degree of conversion of the samples was assessed by Raman spectroscopy [4]. After the light cure, the samples were removed from the mould, inserted in an EPR tube, and immediately analyzed. The samples were then removed and stored in opaque vials in different storage conditions. They were periodically recovered (after 2, 4, 6, 24 hours, 1, 2, 3, 4 weeks) for analysis. A replacing device was used to ensure an identical position of the sample in the EPR cavity for each measurement, enabling the accurate long-term comparison of the peak intensities. Thereafter, the samples were reintroduced in their specific storage environments, i.e. air (25 and 37°C), argon, oxygen, and water. For air storage, a steam room was used to maintain a constant temperature of either 25 or 37°C. For the analyses under argon or oxygen, samples were stored in a glove bag where argon or oxygen atmospheres were maintained. As for water storage, the samples were placed in a thermostatic bath.

EPR analyses were also performed to study the effect of temperature increase on free radicals decay. For those experiments, the resin samples were placed in the spectrometer, where temperatures were increased by steps of 5°C. A JEOL JES-VT-3A system stabilized the temperature during 10 minutes before each EPR measurement.

3.3.3. Characterization

EPR spectra were recorded by JEOL JES-RE 2X spectrometer, equipped with an ES-UCX2 cylindrical cavity. Given that the width of the peaks did not significantly vary with time, it was considered as a constant. Therefore, the evolution of the free radial concentrations was assessed by the measurement of the height of the peaks of interest. The magnetic field was centered on 334,9 or 336,1 mT, which corresponds to the position of peaks belonging to the part of the spectrum due respectively to propagating and allylic radicals (Fig. 1b). Other settings were: microwave frequency, 9.4616 GHz; microwave power, 0.5 mW; modulation frequency, 100 kHz; modulation amplitude, 0.1 mT; scan range, 0.01 mT; scan time, 120 s; receiver gain, 20; time constant, 0.01 s. For all observations, the microwave irradiation power and the modulation amplitude were set to avoid signal saturation and were kept constant. The scan range was limited to the lowest value so that the decrease of the signal could only be attributed to the kinetic effect. A calibration of the magnetic field was operated before each measurement using a reference signal coming from Mn2+ (calibration sample from JEOL). All data were treated with the JEOL "Esprit330;01.521version" software. Five samples per storage condition were analyzed.

3.4. Results

Degree of conversion calculated by Raman spectroscopy was 62% for the experimental resin samples and 50% for commercial composite Ch. Hence, the amount of remaining double bonds is 38 and 50%, respectively, which includes pendant double bonds as well as free monomers. Figure 1a presents the chemical structure of both radical species and Figure 1b is an image of the 9-line spectrum obtained by EPR analysis of the dental resins. Note that the shape of the spectrum is identical for both materials, i.e. ER and Ch. From the observation of the spectrum, it is clear that the relative concentration of propagating radicals is much smaller than the one of allylic radical. Figure 2 presents the change in concentration of both radical species in ER and

Ch samples conserved in ambient atmosphere (air) at two different storage temperatures (25 and 37°C). The curves have quite a linear aspect, which means that the first phase of the decrease kinetics is quicker given the logarithmic time scale. Besides, free radicals clearly decay more quickly in the commercial composite. For ER, a rise in storage temperature from 25 to 37°C barely has any effect on radical decay, while for Ch, the decay is slightly faster at 37°C at the end of the kinetics. The effect of temperature is clearer in Figure 3, reporting the change in signal intensity (in arbitrary units) of the allylic radicals in ER and Ch samples during heating from 20 to 120°C. It confirms the slight effect of temperature observed in Fig. 3 between 25 and 37°C, and shows the extinction of the signal at high temperatures. Figure 4 shows the influence of the

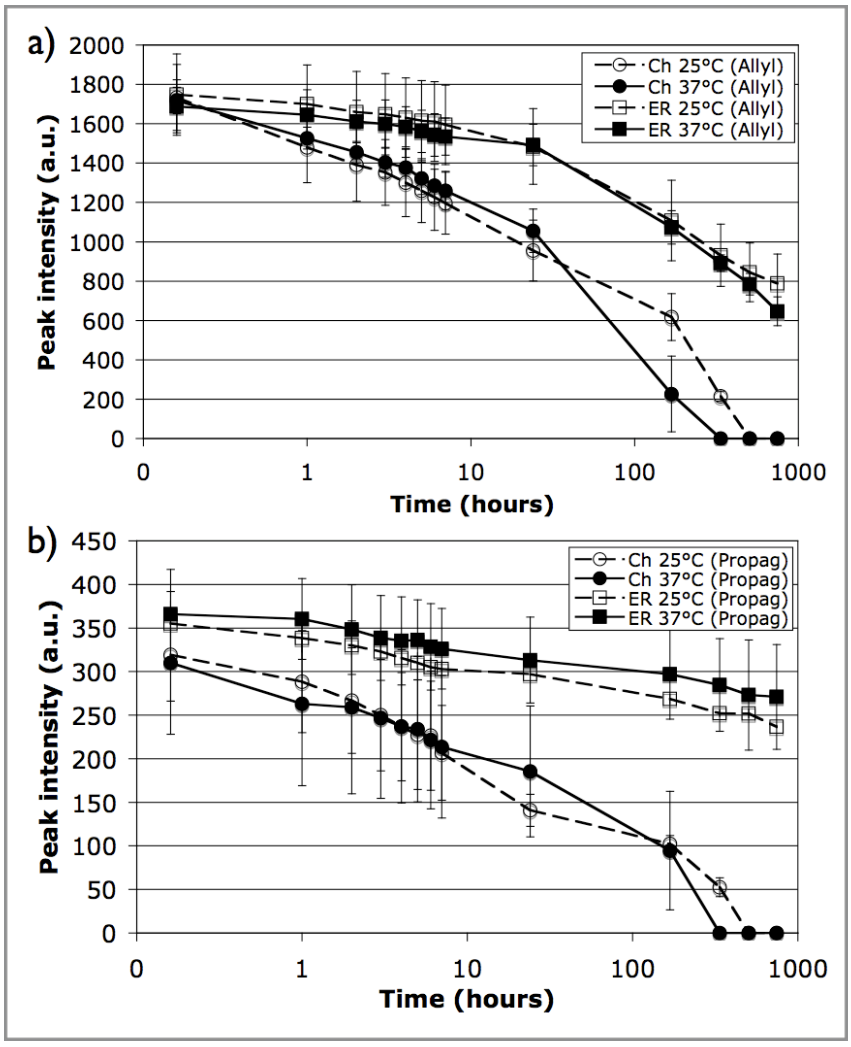

Figure 2 - Change in concentration of allylic radicals (a) and propagating radicals. (b) (in arbitrary units) in samples of experimental resin (ER) and commercial composite Charisma® (Ch) conserved in air at two different storage temperatures (25 and 37°C). Time is presented on a logarithmic scale.

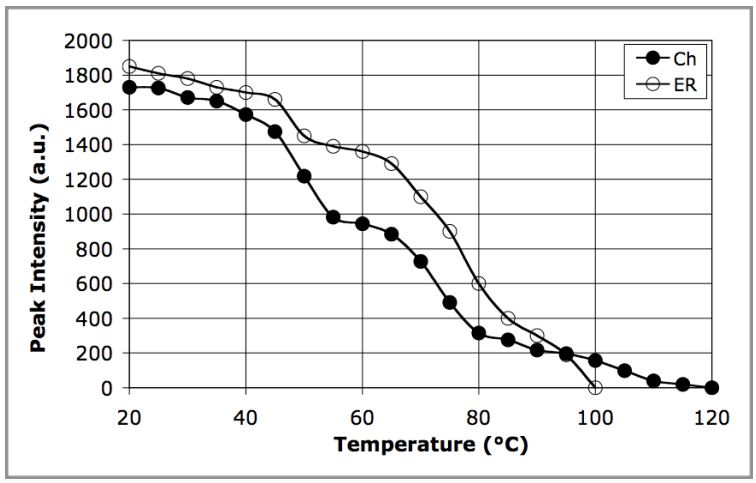

Figure 3 - Change in concentration of allylic radicals (in arbitrary units) with temperature in the experimental resin (ER) and in the commercial composite Charisma® (Ch).

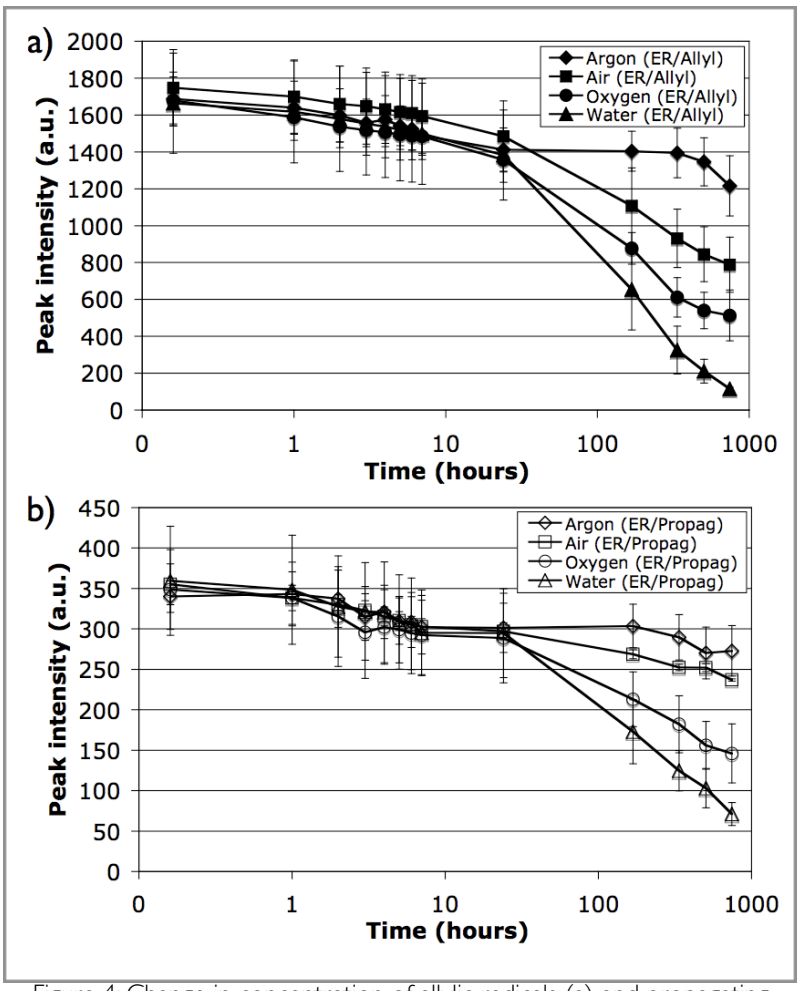

Figure 4: Change in concentration of allylic radicals (a) and propagating radicals. (b) (in arbitrary units) in samples of experimental resin (ER) stored in different environments. Time is presented on a logarithmic scale.

different storage environments on the concentration of the free radicals in ER at 25°C. The behavior of allylic radicals (Fig. 4a) and propagating radicals (Fig. 4b) is similar and a clear distinction of the kinetics in two phases can be done. In the first phase (0 to 24h), the storage conditions had no influence on the kinetics. In the second one (1day to 1month), the rate of decay depended on the storage environment. In argon, free radicals were stable and for the other storage environments, the rate of decay was higher in water, then in oxygen and in air. In Figure 5, the same results are displayed but for Ch. Even if the stability of the signal in argon is confirmed, the results for the three other environments are less clear. The rate order changes to water < air < oxygen.

3.5. Discussion

3.5.1. General considerations

In all the measurements, the initial signal intensity (at t_0) was much less intense for propagating radicals than for allylic ones. This is not surprising as the latter are products of transfer reactions and do not propagate but accumulate during the polymerization while propagating radicals are the true active species, undergoing initiation, propagation and termination unless their further reaction is limited by vitrification.

As explained before, two periods have to be taken into account in the free radicals concentration decrease: 0 to 24 hours, and more than one day after irradiation. The first period was already considered in a previous publication [4], and the second one (> 1 day) will be discussed here. The influence of temperature and storage atmosphere on the radical kinetics of decrease from 1 day to one month will be discussed hereunder.

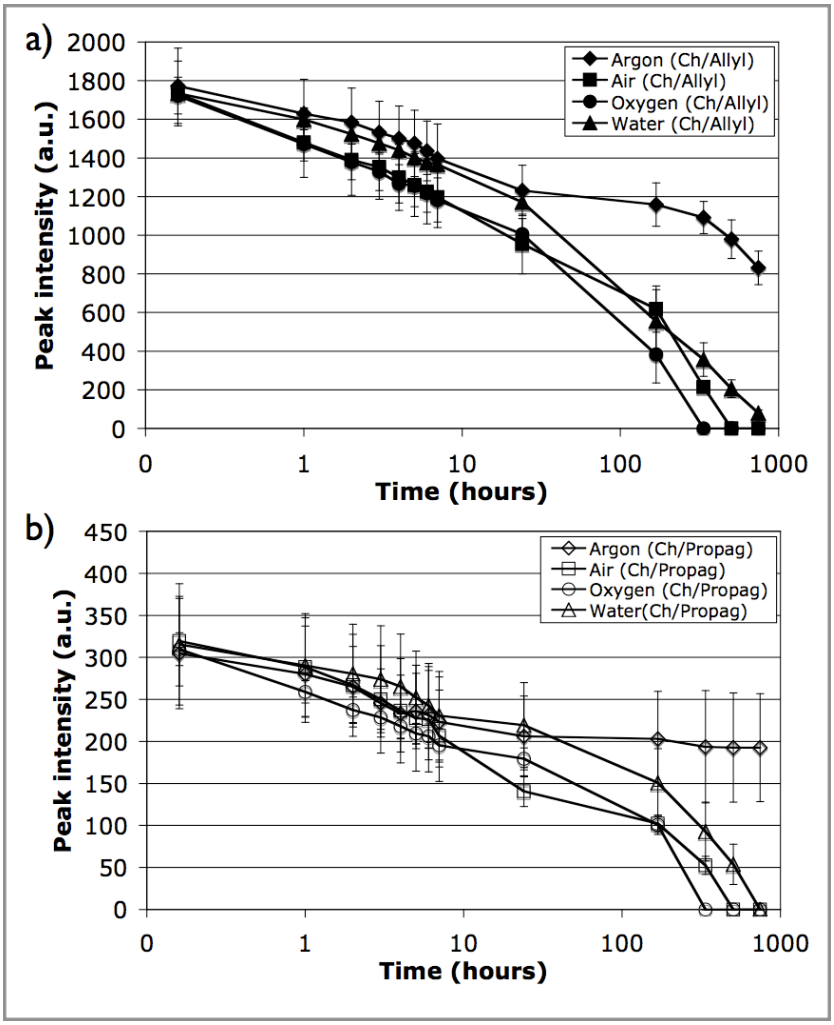

Figure 5: Change in concentration of allylic radicals (a) and propagating radicals (b) (in arbitrary units) in samples of commercial composite Charisma (Ch) stored in different environments. Time is presented on a logarithmic scale.

3.5.2. Temperature

3.5.2.1. Influence of storage temperature

Increasing the storage temperature from 25 to 37°C for ER barely has any effect on radical decay, but there is a slightly faster decay at 37°C for Ch (Fig. 2a an 2b). Two hypotheses can be proposed to explain the impact of the storage temperature on the radical decay.

Firstly, this temperature effect could be related to the glass transition temperature. As reported in a previous publication [4], the glass transition temperature (Tg) of such an organic matrix is close to 55°C. The storage of the samples at higher temperatures closer to Tg could increase the molecular mobility in the matrix, which

should allow radical recombination to occur. However, the increase of mobility below Tg is probably rather low as the system remains in a vitrified state. Moreover, this is insufficient to explain the differences observed between Ch and ER as regards the storage temperature.

A second possible explanation of the effect of storage temperature can be put forward using diffusion phenomena. It is well known that the diffusion of a substance into a material depends on the temperature. In this case, it could be possible that a small molecule diffuses into the polymer network and induces radical termination either directly or after intermediate reactions. While this (these) hypothetic reaction(s) has(ve) not yet been identified, the influence of storage temperature is obviously an argument in favor of the second hypothesis [13]. The nature of the reaction at stake will be discussed further when we deal with the different storage atmospheres. Contrary to the first hypothesis, this second one gives an explanation for the differences between Ch and ER as the presence of fillers can disturb the reaction(s) at stake, for example diffusion, as explained further.

3.5.2.2. Heating experiments

Temperature analyses have been performed by a follow-up of the EPR signal intensities while gradually heating the samples from 20°C to 120°C (Fig. 3). In both cases (ER and Ch), increasing temperature accelerates the decay of radical species, as it was already shown in a previous publication [15]. Again, the two same hypotheses can be proposed. To begin with, a discontinuity was observed in the evolution of the allylic radical concentrations (Fig. 3). EPR peak intensities decrease rather slowly under 50°C, while they drop at higher temperatures. This temperature value is interestingly close to Tg of the material determined by DMA (Dynamic Mechanical Analysis), i.e. 55°C [4], which indicates that Tg undoubtedly plays a part in free radicals decay in these experiments. As observed in DSC experiments (Differential Scanning Calorimetry) on polymers, the polymerization reaction indeed restarts at temperatures above Tg. At those temperatures, the increase in molecular mobility allows radical recombination [16] as well as additional propagation [17]. This latter effect can also account for radical termination due to reaction-diffusion. On the other hand, below Tg, the system is frozen due to vitrification. It is thus quite unlikely that an increase in temperature below Tg could create enough mobility for radicals to terminate, either trough simple

diffusion or by reaction-diffusion. However, Fig. 3 shows a slow free radical decrease even under Tg. As stated before, this is in favor of the implication of another chemical reaction in the termination process, as heating affects the diffusion of small molecules into the polymer network [15]. In any case, temperature is clearly an important factor involved in the termination of the free radicals trapped in dental resins.

3.5.3. Storage environments

As shown in Fig. 4 and 5, storage environment influences the decrease rate of radical concentrations. In these experiments, sample temperature was kept constant at 25°C to limit thermal influence on molecular mobility. During the first phase of the kinetics (0 to 24h), the storage conditions had no influence on the kinetics. This phase was assigned to a post-polymerization phenomenon, i.e. free volume relaxation [4], which is physical phenomenon and is not affected by the storage environment investigated. Moving on to the period from 1 day to 1 month, the decrease rate of free radical concentrations is very different according to the environment, and discordances are also perceptible between the experimental resin and the commercial composite.

3.5.3.1. Unfilled resin

For samples stored in argon, the decay is very limited. By contrast, this decrease rate is very high in oxygen, and even higher in water. Free radical concentrations in samples stored in air decrease at intermediate rates (Fig. 4). In the time range investigated in the present paper (from 1 day to 1 month), no physical phenomenon can be invoked [4]. On the contrary, reactions with species coming from the external environment are most likely involved. As it can clearly be seen on Fig. 4, the presence of oxygen is the determining factor of radical decay. It is confirmed by Li *et al.* [18] who observed no decay of the trapped free radicals over a two-year period in the absence of oxygen (room temperature). This undoubtedly denotes the occurrence of an oxidation reaction in dental resins from 1 day to 1 month after photopolymerization. As the uptake of oxygen in polymers is diffusion controlled [10], this supports the second hypothesis evoked earlier, referring to an Arrhenius-type reaction to explain the influence of temperature. Nevertheless, while an oxidation reaction is probably at stake, the exact chemical process has not been clearly brought to light yet. According to a theoretical explanation based on the high reactivity of free radicals, a possible initial

reaction could be the formation of peroxide radicals by the addition of oxygen on the trapped free radicals (Eq. 1):

$$R\bullet + O2 \rightarrow ROO\bullet \quad (1)$$

For example, Kaptan *et al*. [13] followed the decrease of the trapped radicals by EPR but suggested that it would be the same to measure the increase of peroxyl radical signal with time. The results of Pavlinec *et al*. [5, 6, 9] support the formation of hydroperoxides to explain the decay of trapped free radicals. However, peroxyl radicals were never observed during the experiments of this study. Kloosterboer *et al*. [19] did not observe any EPR signal for peroxide radicals either. This may be due to their high reactivity and/or to the impossibility to simultaneously observe the EPR spectra of both trapped radicals (allylic / propagating) and peroxide radicals under the same setting conditions. The fate of peroxyl radicals could depend on their reaction with hydrocarbon species (R'H), which could for example come from the external environment (eq. 2):

$$ROO\bullet + R'H \rightarrow ROOH + R'\bullet \quad (2)$$

Highly mobile low molecular mass R'• radicals would rapidly terminate by recombination or disproportionation.

Besides the differences between argon-, oxygen- and air-storage, the effect of water on free radicals is of particular interest, as dental resins are permanently exposed in vivo to an aqueous environment, i.e. the saliva in the mouth. It was observed (Fig. 4) that the radical concentration in water-stored samples decays even faster than in oxygen (for ER). As mentioned by many authors [11, 20, 21], water sorption results in a swelling of the polymer. In a way, the effect of water is similar to the temperature effect developed earlier: the polymer expansion increases molecular mobility, reduces Tg and leads to a faster diffusion of oxygen. As a result, free radicals disappear faster. Sideridou *et al.* [11] suggested a dual mode-theory assuming that the amount of sorbed water molecules in a resin in glassy state can be divided into two populations. The first one is a molecular dissolution of water in the polymer matrix, which applies to volume fractions of the network in equilibrium state. The second one is the trapping of water molecules in polymer frozen microvoids in the polymer fraction that is in a non-

equilibrium state. As the latter group does not cause the swelling of the polymer, only the first molecular population is of interest here.

3.5.3.2. Filled resin

Concerning the kinetic results in Charisma® (Fig.5), even if the stability of the signal in argon is confirmed, the results for the three other environments are less clear. The decrease rate of the radical concentrations is still clearly higher in air and even more in oxygen than in argon (Fig.5). However, the kinetic curve of samples stored in water shows a decrease rate surprisingly lower than in air. The reason could be the presence of inorganic fillers in Ch, which can influence the sorption phenomena by the presence of interfaces. For instance, Rüttermann *et al*. [22] compared two experimental composites, one microhybrid and the other nanofilled, in terms of water sorption. The nanofilled composite was found to absorb nearly two times more water than the microhybrid of same volumetric filler content and same organic matrix. Moreover, a preferential affinity of water to fillers and/or silanes compared to the organic matrix could be responsible for the different effect of the water storage. Finally, only the effect of oxygen is confirmed for Charisma® (stability in argon) and further experiments on filled resins are required to highlight the differences between water-, air- and oxygen-storage.

3.5.4. Influence of fillers on free radical decay in air

Comparing the results in Ch (Fig. 5) and in ER (Fig. 4), EPR intensities are nearly the same. Nevertheless, free radical concentrations in Ch have to be corrected by a 2.78 multiplication as organic matrix only represents 36% of its volume. Hence, after this correction, initial concentrations in Ch are nearly 3 times higher than in ER (without fillers). This can be due to the spatial confinement of the radicals in Charisma® which leads to increased radical lifetime [23]. Indeed, due to the high filler content in Ch, the organic fraction is located in small interstices between inorganic particles and the diffusion of the radicals attached to the polymer chain is thus spatially restricted to a relatively small area. Hence, the rate of radical-radical termination reactions is very low during the polymerization process, as the radicals reach each other with great difficulties.

That being said, the radical kinetics of decay in Ch and in ER can be compared in Fig. 2. It is clear that the rate of decay is much higher in the commercial material and this is the case from the very beginning of the kinetics. Two reasons can account for it. Firstly, as more unreacted double bonds remain in Ch after irradiation (50% to 38% for ER), there are also statistically more free monomers. During free volume relaxation, this additional amount of free monomers can account for a greater reactive diffusion, leading to a quicker termination of trapped free radicals during the free volume relaxation. Secondly, as stated before, the organic-inorganic interface can influence the sorption phenomena. Moreover, Burtscher [17] already observed that fillers significantly altered free radicals half-life: at constant temperature, their half-life was shown to depend on the type of filler, the filler fraction and their surface treatment. Burtscher concluded that filler surface had a catalytic effect on radical decay while surface coating reduces this effect. Ottaviani *et al*. [2] also observed that inorganic fillers accelerated the radical concentration decrease.

3.6. Conclusion

The incomplete conversion of dental polymers due to vitrification is a well-known problem in the field of dental resins. The persistence of reactive species in the materials has been the subject of numerous publications, especially concerning free monomers that can cause tooth pulp damage, mucosal irritation, contact dermatitis and allergic reactions [24]. In the same way, the aim of the present work was to study the behavior of free radicals, i.e. another important species regarding both biocompatibility and material properties. Several factors influence the decay of free radicals trapped in dental resins, and some of them were investigated in this work.

First, the filler content and/or coating has an impact on both initial concentration and decrease kinetics of free radicals. Further studies are required to confirm it, but these effects must undoubtedly be taken into account given the permanent evolution of filler technologies.

Second, the long-term radical termination clearly depends on the presence of oxygen. Its effect is promoted by factors likely to increase molecular mobility such as temperature rise or swelling by solvents, i.e. water in this case. A higher mobility indeed promotes oxygen diffusion in the polymer.

Finally, some aspects must still be investigated in the fields of free radicals. For example, the influence of resin formulation or light irradiation on free radicals concentrations should provide valuable information. Furthermore, the leaching capacity of free radical species from the bulk to the oral environment should also be examined. These perspectives draw the lines of future publications.

3.7. Acknowledgments

J. Leprince and S. Demoustier-Champagne thank the Funds for Scientific Research (F.R.S.-FNRS) for their research fellow and Senior Research Associate positions, respectively.

3.8. References

1. Truffier-Boutry D, Gallez XA, Demoustier-Champagne S, Devaux J, Mestdagh M, Champagne B, Leloup G. Identification of free radicals trapped in solid methacrylated resins. *J Polym Sci Part A: Polym Chem* 2003; 41:1691-99.
2. Ottaviani MF, Fiorini A, Mason PN, Corvaja C. Electron spin resonance studies of dental composites: effects of irradiation time, decay over time, pulverization, and temperature variations. *Dent Mater* 1992; 8:118-24.
3. Anseth KS, Anderson KJ, Bowman CN. Radical concentrations, environments, and reactivities during crosslinking polymerizations. *Macromol Chem Phys* 1997; 197:833-48.
4. Truffier-Boutry D, Demoustier-Champagne S, Devaux J, Biebuyck JJ, Mestdagh M, Larbanois P, Leloup G. A physico-chemical explanation of the post-polymerisation shrinkage in dental resins. *Dent Mater* 2006; 22:405-12.
5. Pavlinec J, Moszner N. Dark reactions of free radicals trapped in densely crosslinked polymer networks after photopolymerization. *J Appl Polym Sci* 2003; 89:579-88.
6. Pavlinec J, Moszner N, Mikova G, Placeka J, Slovak K. Light emission on heating polymer networks formed by radical polymerization. *Polym Degrad Stab* 2009; 94:49-56.
7. Anseth KS, Newman SM, Bowman CN. Polymeric dental composites: Properties and reaction behavior of multimethacrylate dental restorations. *Ad Polym Sci* 1995; 122:177-217.

8. Rueggeberg FA, Margeson DH. The effect of oxygen inhibition on an unfilled/ filled composite system. *J Dent Res* 1990; 69:1652-8.
9. Pavlinec J, Moszner N, Placek J. The Stability of Free Radicals in Densely Crosslinked Acrylate Polymer Networks. *Macromol Chem Phys* 2001; 202:2387-93.
10. Kaptan Y, Pekcan O, Güven O. Determination of diffusion coefficient of oxygen into polymers by using electron spin resonance spectroscopy. II. Poly(vinyl acetate). *J Appl Polym Sci* 1992; 44:1595-99.
11. Sideridou I, Tserki V, Papanastasiou G. Study of water sorption, solubility and modulus of elasticity of light-cured dimethacrylate-based dental resins. Biomaterials 2003; 24:655-65.
12. Söderholm KJ. Water sorption in a Bis(GMA)/TEGDMA resin. *J of Biomed Mater Res* 1984; 18:271-9.
13. Atkinson JC, Diamond F, Eichmiller F, Selwitz R, Jones G. Stability of bisphenol A, triethylene-glycol dimethacrylate, and bisphenol A dimethacrylate in whole saliva. *Dent Mater* 2002; 18:128-35.
14. Eiriksson SO, Pereira PN, Swift EJ Jr, Heymann HO, Sigurdsson A. Effects of saliva contamination on resin-resin bond strength. *Dent Mater* 2004; 20:37-44.
15. HY Kaptan. ESR study on the effect of temperature on the diffusion of oxygen into PMMA and PVAC polymers. *J Appl Polym Sci* 1999; 71:1203-7.
16. Burtscher P. Stability of radicals in cured composite materials. Dent Mater 1993; 9:218-21.
17. Bağis YH, Rueggeberg FA. Effect of post-cure temperature and heat duration on monomer conversion of photo-activated dental resin composite. *Dent Mater* 1997; 13:228-32.
18. Li D, Zhu S, Hamielec AE. ESR study on permeation of oxygen in crosslinked polymers. *Polymer* 1993; 34:1383-7.
19. Kloosterboer JG, Lijten GFCM, Greidanus FJAM. Structure and stability of polyacrylate radicals trapped in a network. *Polym Com* 1986; 27:268-271.
20. Diaz-Arnold AM, Arnold MA and Williams VD. Measurement of water sorption by resin composite adhesives with Near-Infrared Spectroscopy. *J Dent Res* 1992; 71:438-442.

21. Malacarne J, Carvalho RM, De Goes MF, Svizero N, Pashley DH, Tay FR, Yiu CK, MR Carrilho. Water sorption/solubility of dental adhesive resins. *Dent Mater* 2006; 22:973-80.

22. Rüttermann S, Wandrey C, Raab WH, Janda R. Novel nano-particles as fillers for an experimental resin-based restorative material. *Acta Biomater* 2008 Jun 27 [Epub ahead of print].

23. Zachary M., Camara S., Whitwood A.C., Gilbert B.C., van Duin M., Meier R.J., Chechik V. EPR study of persistent free radicals in cross-linked EPDM rubbers. *Eur Polym J* 2008; 44:2099-2107.

24. Kawahara T, Nomura Y, Tanaka N, Teshima W, Okazaki M and Shintani H. Leachability of plasticizer and residual monomer from commercial temporary restorative resins. *J Dent* 2004; 32: 277-283.

Chapter 4

Hydroxyl radical release from dental resins: Electron paramagnetic resonance evidence

Acta Biomaterialia xxx (2010) xxx–xxx

Contents lists available at ScienceDirect

Acta Biomaterialia

journal homepage: www.elsevier.com/locate/actabiomat

Hydroxyl radical release from dental resins: Electron paramagnetic resonance evidence

Guillaume Lamblin [a,c,e,1], Julian Leprince [a,b,e,1], Jacques Devaux [b,e], Michèle Mestdagh [c,e], Bernard Gallez [d], Gaëtane Leloup [a,b,e,*]

[a] School of Dental Medicine and Stomatology, Université catholique de Louvain, Avenue Hippocrate 10/5721, Brussels B-1200, Belgium
[b] Institute of Condensed Matter and Nanosciences – Bio & Soft Matter (IMCN/BSMA), Université catholique de Louvain, Croix du sud 1, Louvain-la-Neuve B-1348, Belgium
[c] Unité de chimie des interfaces, Université catholique de Louvain, Croix du sud 1, Louvain-la-Neuve B-1348, Belgium
[d] Unité de résonance magnétique biomédicale, Louvain Drug Research Institute, Université catholique de Louvain, Avenue Mounier 73, Brussels B-1200, Belgium
[e] CRIBIO (Centre de Recherche et d'Ingénierie en Biomatériaux), Avenue Hippocrate 10/5721, Brussels B-1200, Belgium

4.1. Summary

It is well known that polymeric free radicals remain trapped inside dental resins for a long time after photopolymerization. Moreover, although these high molecular mass compounds have very limited mobility, there is evidence to suggest that they disappear progressively over time. The purpose of this study was to provide new experimental data to help understand this phenomenon. To determine whether low molecular mass free radicals are released by dental composites stored in hydrophilic media, we used electron paramagnetic resonance (EPR) spectroscopy to perform spin-trapping experiments on experimental and commercial samples stored in ethanol. Under these conditions, ethoxy radicals were produced. Further experiments demonstrated that hydroxyl radicals were firstly released from the methacrylated resin and secondly that they reacted with ethanol molecules to produce "secondary" ethoxy free radicals. In addition to the well-known monomer toxicity of methacrylated resins, we may have identified a new source of concern for these biomaterials.

4.2. Introduction

Resin composites, made of inorganic fillers within an organic matrix, are widely used for dental restoration. The organic matrix is produced by a photoinitiated radical copolymerization of dimethacrylate monomers. Light induces crosslinking of the difunctional monomers, which progressively leads to the vitrification of the material. As a result, two kinds of free radical are trapped in the network: Allylic and propagating radicals (Fig. 1) [1]. It is well known that these compounds can remain stable for several months in the polymer network [2-4]. Nevertheless, they disappear more or less rapidly, depending on the storage environment, until they reach undetectable levels on electron paramagnetic resonance (EPR) spectroscopy [5, 6]. For instance, Leprince *et al*. [7] recently investigated the fate of the trapped free radicals in dental resins stored in water, air, oxygen or argon. They demonstrated that the rate of disappearance decreased in the following order: Water > oxygen > air > argon.

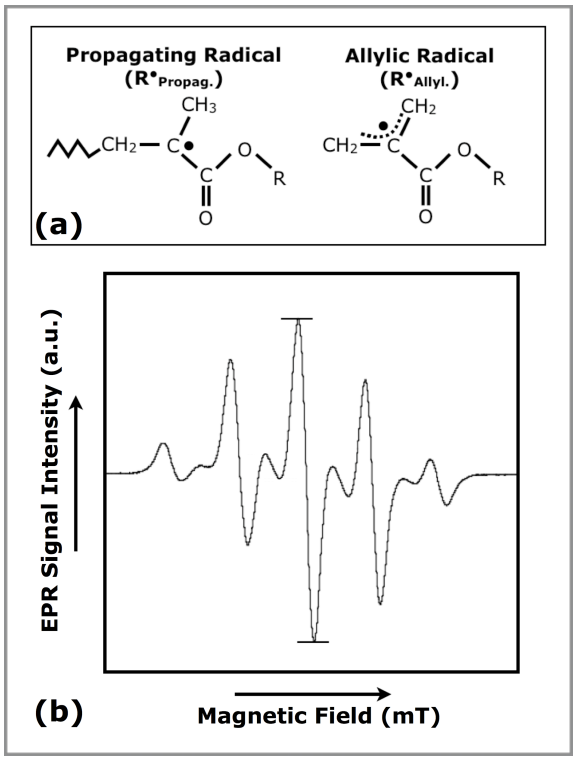

Figure 1 - (a) Chemical structure of both trapped radical species (R represents either an end group or a connection to the network). (b) Nine-line EPR spectrum of the experimental resin after polymerization. Plain line on the spectrum corresponds to the position (allylic radical) where the intensity was measured for kinetic experiments.

Given the macromolecular dimensions of these trapped free radicals, their mobility into the polymeric network is strongly limited by entanglement and they cannot diffuse out of the resin. The decrease in trapped free radical concentration can, therefore, only be explained by radical reactions (distinct from typical methacrylate photopolymerization) occurring within the resin. It is then important, especially from a biocompatibility viewpoint, to know whether these reactions can produce and release mobile secondary free radicals into the environment. It has already been demonstrated that unconverted monomers are cytotoxic and can have harmful effects [8, 9]. For instance, they can induce tooth pulp damage, mucosal irritation, contact dermatitis and

allergic reactions [10]. Similarly, local release of free radicals could be another source of concern.

There are relatively few publications devoted to the stability of trapped free radicals in dental materials, and most of them have focused on the study of postpolymerization (or dark polymerization) [2, 5, 11, 12]. The latter reaction occurs when the illumination is stopped and the resin stored in the dark. In this case, a slow decrease in the concentration of trapped free radicals can be observed due to termination phenomena (the rate of which depends on the crosslink density and on the storage temperature) associated with a certain increase in the degree of conversion [2, 6].

In addition to postpolymerization effects, Leprince *et al*. studied the impact of the storage environment on the kinetics of the trapped free radicals [7]. Twenty-four hours after irradiation, oxidation was the main phenomenon involved in the decrease in radical concentration. Moreover, conditions influencing oxygen diffusion inside the polymer network (e.g., swelling in solvent) have an impact on radical kinetics. This effect of atmospheric oxygen was also noted by Pavlinec *et al*. [4]. Nevertheless, the exact mechanism involved has not yet been described. A generally accepted first step of the reaction leads to the formation of peroxyl radicals (Eq. 1):

$$R\bullet + O2 \rightarrow ROO\bullet \quad (1)$$

Unfortunately, most studies have not detected these species by EPR spectroscopy despite the fact that evidence of the existence of peroxides has been published [7]. For example, Pavlinec *et al*. [4] recently noted, using chemiluminescence, that accumulation of these compounds occurred concomitantly with trapped free radical decay. Leprince *et al*. [7] hypothesized that low molecular mass radicals may terminate trapped species by recombination or disproportionation. In line with this hypothesis, Lee *et al*. [13, 14] proposed that hydroxyl radicals could be released by hydroperoxidation of the methacrylated double bonds. If this hypothesis is valid, spin-trapping experiments are required to detect the hydroxyl radicals.

EPR spectroscopy and, more precisely, spin-trapping methods indeed enable the detection and identification of unstable free radicals [15, 16]. This technique was first employed in the 1960s and has become increasingly popular because of the key role of radicals in many biological mechanisms and in deleterious processes in disease

and ageing [17]. An unsaturated non-radical (diamagnetic) molecule, M, called the spin-trap, reacts with the unstable free radical, R•. The product, called the spin-adduct, M-R•, has a longer half-life than R• [18, 19] allowing its detection by EPR. The hyperfine constants of the adducts (M-R•) are characteristic, enabling them to be identified. Nevertheless, due to the variable half-lives of spin-adducts, which depend on many parameters (nature of the trapped free radical and spin-traps, solvent, pH, temperature etc...), detection may be more or less difficult. Typical spin-traps are nitroso compounds, like 5,5-dimethyl-1-pyrroline-N-oxide (DMPO) or phenyl-butylnitrone (PBN). Currently, research is being conducted to synthesize new spin-traps with longer spin-adduct half-lives [20, 21]. For instance, the spin-traps 5-ethoxycarbonyl-5-methyl-1-pyrroline N-oxide (EMPO) and 5-diethoxyphosphoryl 5-methyl-1-pyrrolyne N-oxide (DEPMPO) have been synthesized recently [22-25].

The objective of the present article was to assess the potential release of free radicals from dental resin using spin-trapping methods. Ethanol was used as a solvent for immersion as it induces better swelling of methacrylated polymer than water, thus maximizing the diffusion of species in and out of the material. Because of the long half-lives of their spin-adducts, EMPO and DEPMPO spin-traps were chosen to characterize the free radicals released.

4.3. Materials and Methods

4.3.1. Sample preparation

Experimental dental resins were prepared from a blend of Bisphenol A Glycidyl diMethAcrylate (Bis-GMA, from Heraeus Kulzer, Dormagen, Germany) and TriEthylene Glycol diMethAcrylate (TEGDMA, from Sigma-Aldrich) in a 70:30 weight ratio. A photoinitiator system (1% by weight of camphorquinone and tertiary amine obtained from Sigma-Aldrich) was added to initiate the polymerization. Point 4 (Kerr, Orange County, USA) was used as the commercial resin composite, which contains inorganic fillers. The resins (experimental or commercial) were inserted in moulds (7 mm long, 1 mm wide, 1 mm thick) and photopolymerized with a visible light device, “Curing Light XL 3000” (3M-Espe,St Paul, MN, USA). A constant intensity of 450 mW/cm^2 was applied for 40 seconds to one side of the samples. The mould not only allows the same sample geometry to be used for each experiment but also for the same

amount of resin to be placed in the EPR cavity. These dimensions were chosen to ensure that the full area of the sample was covered by the diameter of the optic fiber of the lighting device.

4.3.2. EPR spectroscopy

The X-band EPR spectra were recorded at room temperature, using a Magnettech MINISCOPE MS200 spectrometer, equipped with a rectangular cavity (TE102). For kinetics experiments, the following instrument settings were applied: Magnetic centre field, 336.7 mT; microwave frequency, 9.5 GHz; microwave power, 0.5 mW (23 dB); modulation frequency, 100 kHz; modulation amplitude, 0.1 mT; field sweep 19.8 mT, sweep time, 120 s; receiver gain, 100. For the spin-trapping experiments, all the parameters were identical except the sweep and centre of the magnetic field, which were adjusted to 9.8 mT and 335.6 mT, respectively. For all observations, the microwave irradiation power and the modulation amplitude were set to avoid signal saturation and were kept constant. Three samples were analyzed for each experimental condition. Except for experiments with reduced oxygen pressure, the linewidth of the spectra was constant. The radical concentration could, therefore, be assessed by measurement of the peak height. In cases where the linewidths changed, the free radical quantity was determined by the double integration of the peaks.

4.3.3. Kinetics of decay of trapped radicals in ethanol and water

Experimental samples were removed from the mould and inserted in an EPR tube for measurement five minutes after the end of the illumination process to ensure the same zero time for all kinetics analyses. Then samples were stored in the appropriate environment, ethanol or water, in the dark, at 25°C. The EPR spectra were recorded at different times after photopolymerization until complete extinction of the EPR signal intensity.

4.3.4. Spin trapping experiments

4.3.4.1. Spin-adduct detection with EMPO and DEPMPO

An average of 30 minutes after photopolymerization, two rods of resin were immersed in ethanol (170 µL, HPLC grade, Sigma Aldrich) which contained dissolved EMPO or DEPMPO (50 mM, Alexis Biochemicals) spin-traps. The presence of spin-

adduct peaks was noted 15 minutes after immersion by sampling the spin-traps solution with a capillary tube. For the kinetic study of released free radicals, the measurement was extended to 1 and 2 hours. The content of the capillary tube was replaced in the spin-traps solution after each ESR measurement. The intensity was determined by measurement of the first peak of the spectrum.

Additional experiments were also performed with 3 month old rods instead of freshly polymerized ones. For experiments under limited pressure of oxygen, nitrogen gas was bubbled in the pure unpolymerized resin and in the ethanol spin-trap solution prior to photopolymerization and EPR analyses, respectively. To assess the possible effect of methacrylated double bond concentration on the detection of spin-adducts, three polymethylmethacrylate (Oroglas,) rods or unpolymerized resins were introduced in place of the two freshly photopolymerised rods.

Three specific reactions were performed with EMPO only. Firstly, some experiments were performed with methanol in place of ethanol for spin-adduct detection. Secondly, a Fenton reaction was conducted by adding FeCl2 (1 mM, Acros) to ethanol containing EMPO (50 mM) and H2O2 (1 mM, Merck). Finally, a hydroxyl radical scavenger, N,N-dimethylthiourea (50 mM, Sigma Aldrich), was introduced at a given time in the spin-trapping kinetics experiments.

4.3.4.2. Spectrum simulation

Computer simulations were performed using hyperfine constants found in the literature. Matlab software was used and upgraded with the "Easyspin toolbox".

4.4. Results

4.4.1. Kinetics of decay of trapped free radicals in ethanol and water

It can be observed in Fig. 2 that the free radicals trapped in the dental resins disappeared much more quickly in ethanol than in water. In ethanol, the rate of decrease of free radicals was nearly linear in the logarithmic representation and complete extinction is obtained after four days. In water, two steps could be clearly identified in the kinetics and the EPR signal was undetectable after a few months.

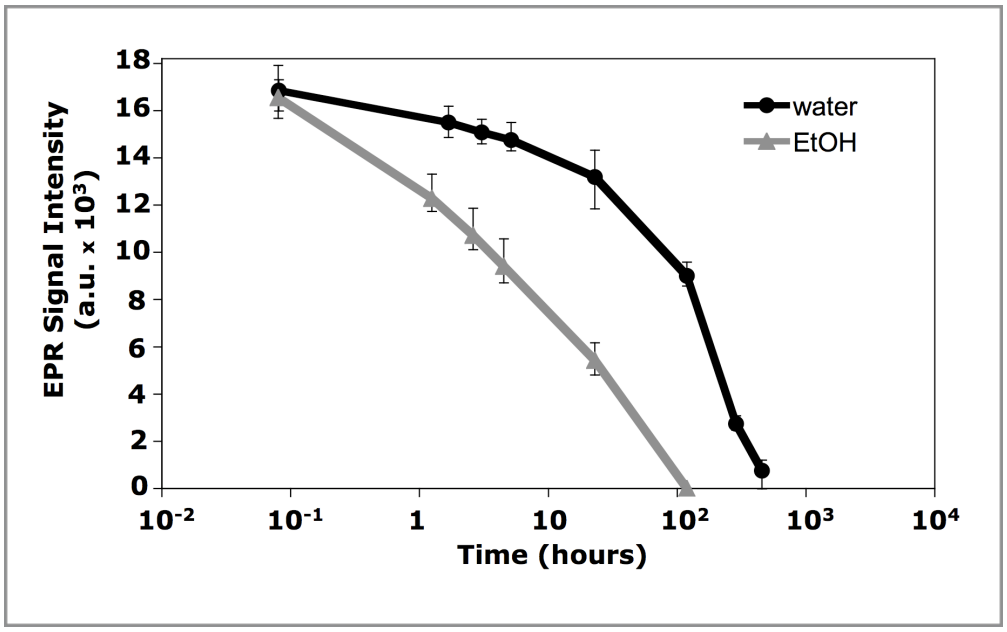

Figure 2 - Change in the concentrations of the trapped allylic radical over time for experimental dental resin stored in water or ethanol. Time is presented on a logarithmic scale.

4.4.2. Spin-trapping experiments in ethanol

4.4.2.1. Free radical release by dental resin

The signal obtained with EMPO for experimental resins is shown in Fig. 3a. This six peak signal has the following characteristics: Peaks are fairly broad and the hyperfine constants are aN=1.29 mT and aH=0.68 mT. A similar signal was obtained with methanol as a solvent, i.e. a six peak signal with approximately the same hyperfine constants: aN=1.31 mT, aH=0.71 mT (data not shown) corresponding to MeO• radical. This is in accordance with previous work [26], and contrary to what was initially expected, did not enable to directly detect hydroxyl radical spin-adducts. The same signal was obtained with a commercial resin, Point 4 (Fig.3b). These characteristics are

Radical	spin-trap	trans/cis	aP (mT)	aN (mT)	aH β (mT)	aH γ (mT)	source	reference
EtO•	EMPO		—	1,265	0,685	—	Fenton system in ethanol	this work
EtO•	EMPO		—	1,29	0,68	—	dental resin in ethanol	this work
EtO•	EMPO	*trans 50%*	—	1,375	1,088	—	Fenton type system	[26]
		cis 50%	—	1,375	0,808	—		
EtO•	DEPMPO		4,56	1,27	0,5-0,7	—	dental resin in ethanol	this work
EtO•	DEPMPO	*trans 85%*	4,621	1,296	0,69	—	NO• bubbling in EtOH	[27]
		cis 15%	3,824	1,307	0,782	—		

Table I - Comparison of the EPR parameters of ethoxy radicals trapped by EMPO and DEPMPO

similar to recently published values [26] for ethoxy radicals (EtO•), spin-adducts of EMPO (Table 1), and were used to simulate a spectrum (Fig. 3c), which was very close to the experimental one. Finally, Fig. 3d shows the EPR spectrum of EtO• produced by the Fenton reaction, which was very similar to both experimental and simulated spectra.

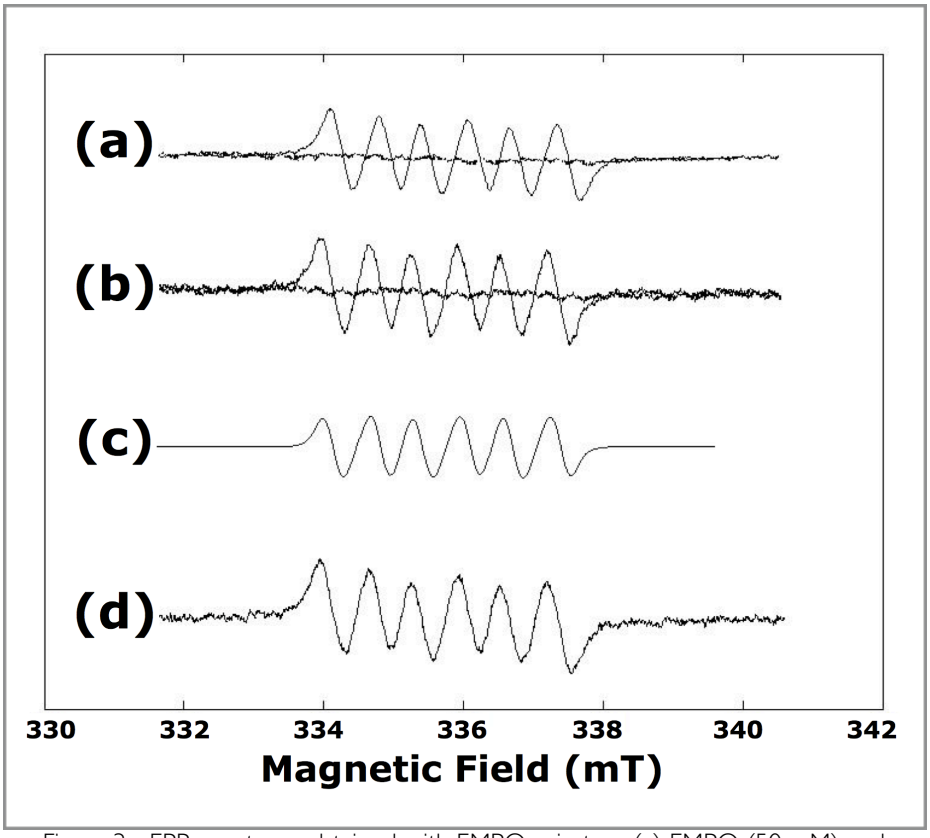

Figure 3 - EPR spectrum obtained with EMPO spin-trap (a) EMPO (50 mM) and experimental dental resin incubated 15 minutes in pure ethanol (baseline : without resin) (b) same as a with commercial resin (baseline : without resin) (c) simulation of the ethoxy radical spectrum with aN= 1.29 mT, aH=0.68 mT. (d) EMPO incubated in a Fenton system in pure ethanol.

Fig. 4 shows the results of similar experiments conducted with the DEPMPO spin-trap on experimental resin. A 14 peak signal with the following hyperfine constants was obtained: aP=4.56 mT, aN=1.27 mT and aH=0.6 mT. As for EMPO, these values were very similar to published ones [27] for ethoxy free radicals (Table 1). The computer simulation based on these values led to a spectrum (Fig. 4b) similar to the experimental one (Fig. 4a).

These results show that ethoxy radicals are released by dental resins; their kinetic of release is shown in Fig. 5. The addition of a specific hydroxyl radical scavenger (N,N-dimethylthiourea) [28, 29] resulted in a significant decrease in signal intensity (Fig. 6).

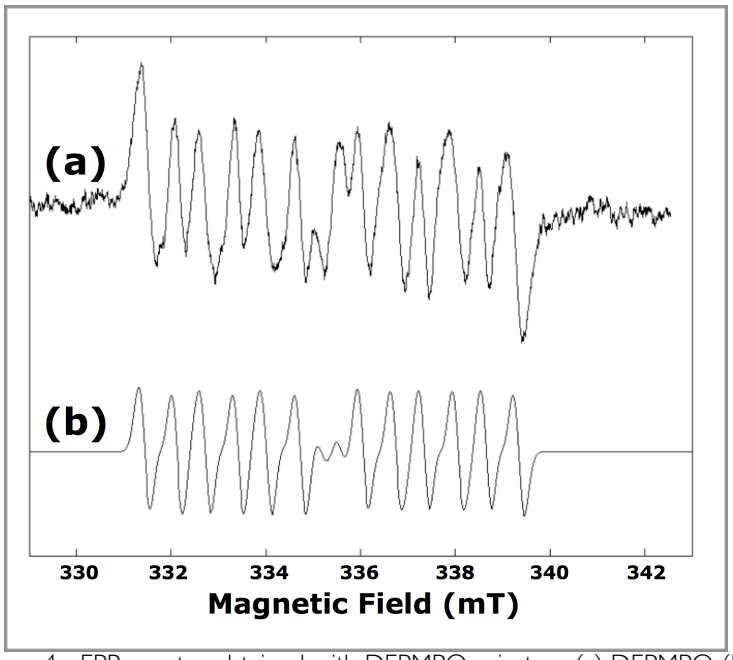

Figure 4 - EPR spectra obtained with DEPMPO spin-trap (a) DEPMPO (50 mM) and experimental dental resin incubated 15 minutes in pure ethanol (b) simulation of the ethoxy radical spectrum with aP=4.56 mT, aN=1.27 mT, aH=0.6 mT.

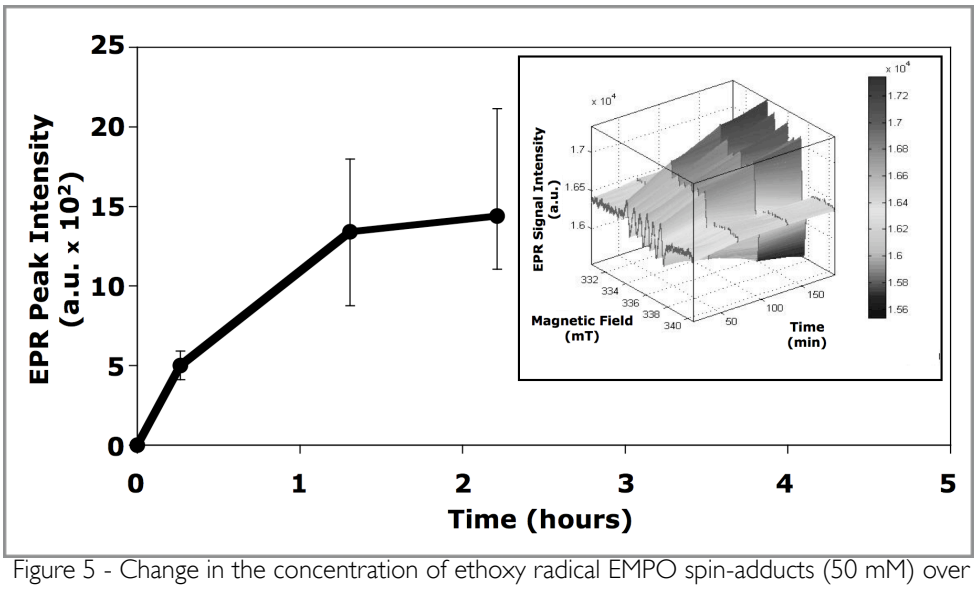

Figure 5 - Change in the concentration of ethoxy radical EMPO spin-adducts (50 mM) over time. Inset: evolution of the spectrum over time in a 3D representation.

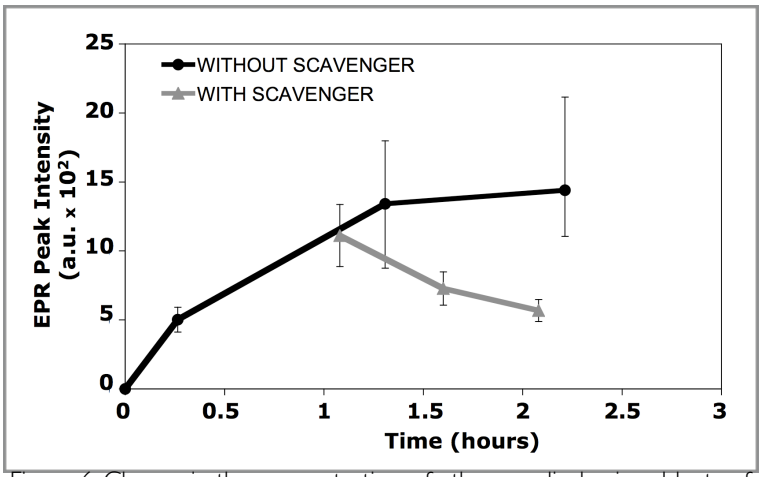

Figure 6: Change in the concentration of ethoxy radical spin-adducts of EMPO (50 mM) over time, with and without hydroxyl radical scavenger .

4.4.2.2. Supplementary experiments

Supplementary experiments were conducted with experimental resins to examine the influence of three factors on the production of ethoxy radicals: Trapped free radicals, oxygen concentration, and double bonds. Replacing freshly photopolymerised samples with old (> 3 months) samples had no effect on the shape or on the intensity of the six peak signals (data not shown). This 3-month ageing period has been shown to lead to the extinction of the EPR signal attributed to the trapped free radicals [7]. Consequently, it can be stated that EtO• release is independent of the presence of trapped free radicals. When oxygen concentration was reduced (in photopolymerised resins and in spin-trap solutions) there was a significant change in the spectrum (Fig. 7): The six peaks were narrower and split, and their double integral was reduced by half (Table 2). This latter observation demonstrates the key role of oxygen: Without oxygen, no ethoxy radicals would be released. The signal is only reduced and not completely extinguished because deoxygenation was not complete, being technically more difficult to achieve. The effects of methacrylated double bond concentration were also examined. Using completely converted PMMA (no remaining double bonds), no peak was detected. On the contrary, an ethoxy spectrum was detected when unpolymerized experimental resin (maximum double bond concentration) was used.

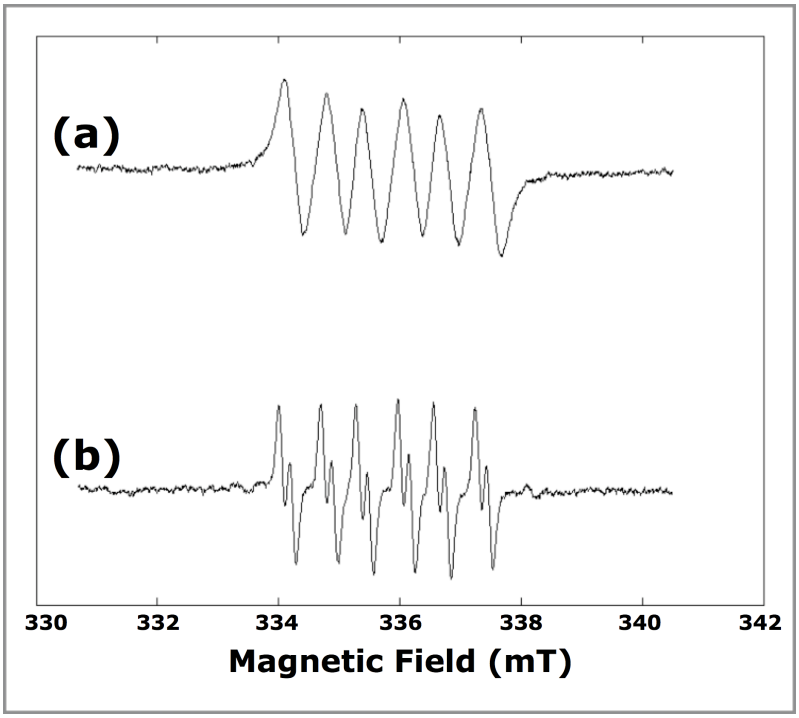

Figure 7 - EPR spectrum obtained with EMPO spin-trap (a) EMPO (50 mM) and experimental dental resin incubated 150 minutes in pure ethanol (b) same as (a) except that oxygen concentration has been reduced.

experiment	double integrale (a.u)
EMPO in ethanol	15 +/- 6
EMPO in deoxygenated ethanol	7,6 +/-2

Table 2 - Comparison of the concentrations of ethoxy radical EMPO spin-adducts in ethanol and in partially deoxygenated ethanol

4.5. Discussion

4.5.1. Free radicals trapped in the dental resin network disappear in ethanol

As is clearly shown in Fig. 2, the trapped free radicals disappeared most rapidly when dental resins were stored in ethanol. This is not surprising as ethanol is well known to induce better swelling of methacrylated polymer than water. Therefore, as briefly stated above, the diffusion mass transfers in and out of the resin are fast. In view of the spin-adduct half-lives of EMPO and DEPMPO spin-traps, ethanol clearly offers the better option for detecting spin-adduct accumulation.

4.5.2. Dental resins produce ethoxy radicals in ethanol

Comparison of the different spectra obtained with EMPO (Fig. 3a, b and c) clearly demonstrates for the first time that dental resins release ethoxy free radicals (EtO•) when they are stored in ethanol. This is confirmed by the DEPMPO spectra (Fig 4. a, b). Interestingly, the signals obtained with EMPO for commercial and experimental resins were similar, supporting the fact that the organic part of the dental resin is the only part involved in the release of ethoxy radicals.

4.5.3. Ethoxy radicals are secondary products from the reaction of hydroxyl radicals with ethanol

When considering the kinetics of decay of EtO•, the major observation was the significant decrease in the double integral when a hydroxyl radical scavenger was introduced (Fig. 6). This suggested that ethoxy radicals are secondary products of the reaction between hydroxyl radicals and ethanol molecules. The results obtained with the Fenton system (Fig. 3d) in ethanol support this assumption. Indeed, ethanol is known to be an efficient scavenger of hydroxyl radicals, which are rapidly converted into ethoxy-derived free radicals [30-32]. For example, ethanol was used to demonstrate the decomposition of superoxide radicals into hydroxyl radicals, based on the fact that ethyl alcohol reacts only with hydroxyl radicals to form EtO•, which is not the case with superoxide radicals. Therefore, the simple detection of ethoxy radicals suggests the release of hydroxyl radicals. The results obtained in methanol supports these conclusion

as they produce methoxy radicals which was also reported for Fenton system in methanol.

The release of hydroxyl radicals (OH•) by dental resins has already been suggested in the literature. Lee *et al*. hypothesized that OH• production could explain the chemical degradation of dental composites stored in a food simulating environment (water/ethanol (25/75) [13, 14]. These authors proposed the hydroperoxidation of the methyl group in the α position of a methacrylate group (eq 2).

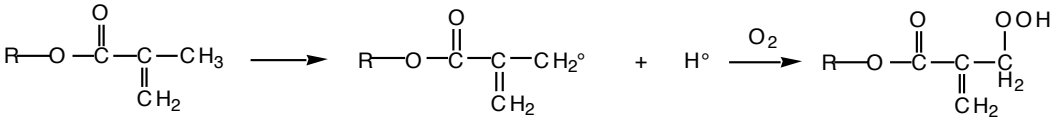

(2)

It has to be noted that the allyl radical produced in the first step of reaction (2) is the same as the allyl radical trapped in the resin. However the one produced by reaction (2) is accompanied by a H• abstraction which can give a hydroperoxide. The trapped allyl radical can only do so with the assistance of another "mobile" hydrocarbon. The hydroperoxide produced can then decompose into hydroxyl and acyl radicals (eq 3). The latter could provide new cross-linking or decompose into aldehyde species.

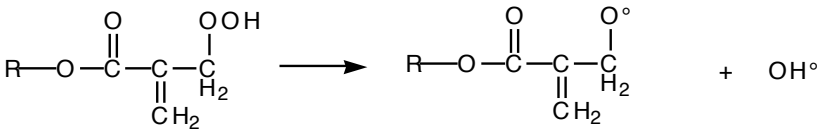

(3)

Hydroperoxidation of the methyl group in a methacrylate, therefore, depends on two major parameters, the presence of oxygen and of unconverted double bonds. This is exactly what was highlighted in the supplementary experiments conducted with EMPO to investigate the mechanism of EtO• release. Firstly, ethoxy radical release was shown to be independent of the presence of trapped free radicals in resin rods, but dependent on oxygen. Secondly, the qualitative experiments conducted with unpolymerized experimental resin and fully converted methacrylated polymers revealed the dependence of ethoxy radical release on the concentration of double bonds.

The release of hydroxyl radicals could explain the long term decay of trapped free radicals in dental resins. It is indeed conceivable that, once created, small OH• radicals diffuse then combine with trapped radicals by addition. The decreased kinetics of the trapped free radicals would then depend on the diffusion of oxygen in the sample.

This was demonstrated in an earlier paper [7], in which water was shown to accelerate radical decay more than oxygen and air. It, therefore, seems reasonable that hydroperoxidation may also explain the decrease in trapped free radicals when dental materials are stored in other environments, such as air and water.

However, as already mentioned, this mechanism involving OH• is not the most likely. A more obvious mechanism would start by direct oxidation of the trapped radicals, leading to peroxyl radicals (eq 1). Nevertheless, no EPR signal corresponding to peroxyl radicals has been detected, in the present study or in other papers on dental resins. Two hypotheses can then be proposed. Firstly, this may be explained by their transformation into hydroperoxide compounds, as detected by Pavlinec *et al*. [7]. This transformation from peroxyl radicals to hydroperoxides requires the intervention of "mobile" hydrocarbons, e.g. those present on neighbouring "free" monomers (only slightly mobile under T_g). Secondly, it is well known that the amount of non-converted pendant methacrylated functions is higher than the one of trapped radicals in the resin. Indeed the degree of conversion of dimethacrylate resins is limited as it only reach 60-65% maximum [2], and therefore contains many unreacted methacrylate functions after photopolymerization. As a consequence, oxygen molecules are much more likely to react with a methacrylate double bond than with free radicals trapped in the polymer.

While the detection of free radical release is of prime interest in the understanding of material ageing process, it should not be misinterpreted in terms of potential toxicity. Indeed, this paper only displays qualitative work, demonstrating that small free radicals are released by dental resin. Even if the quantity of the released free radicals is probably small, the precise determination of their concentrations was not in the scope of this paper. Though very tempting to evaluate the amount of released radicals, the direct comparison of the concentrations of trapped free radicals (Fig. 2) and hydroxyl radicals (Fig. 5-6) must be considered cautiously for several reasons: different spectrometer settings, different physical environments – respectively liquid for hydroxyl radicals and solid for trapped radicals – and intrinsic variability of spin-trapping experiments, which prevents accurate quantitative measurements. Moreover, as explained by Schmaltz and Arenholt-Bindslev, toxic reactions depend not only on the dose of the chemical species, but also on other parameters like the distance and the nature of the structures between release location and potential target tissue. Therefore,

the present results do not enable to come to any conclusion regarding potential biological effects. In vitro investigations are required to determine the impact of the released hydroxyl radicals on the local biological environment of dental restorations.

4.6. Conclusion

The results of this paper present sufficient evidence to affirm that dental resins release hydroxyl radicals. This gives new insight into the resin ageing process and should be taken into consideration in biological studies.

4.7. References

1. Truffier-Boutry Delphine, A. Gallez Xavier, Demoustier-Champagne Sophie, Devaux Jacques, Mestdagh Michèle, Champagne Benoît, Leloup Gaëtane Identification of free radicals trapped in solid methacrylated resins. *Journal of Polymer Science Part A: Polymer Chemistry* 2003;41:1691-1699.
2. Anseth K. S., Anderson K. J., Bowman C N. Radical concentrations, environments, and reactivities during crosslinking polymerizations. *Macromolecular Chemistry and Physics* 1996;197:833-848.
3. Li D., Zhu S., Hamielec A. E. E.s.r. study on permeation of oxygen in crosslinked polymers. *Polymer* 1993;34:1383-1387.
4. Pavlinec J., Moszner N., Miková G., Plaček J., Slovák K. Light emission on heating polymer networks formed by radical polymerization. *Polymer Degradation and Stability* 2009;94:49-56.
5. Pavlinec J., Moszner N., Placek J. The stability of free radicals in densely crosslinked acrylate polymer networks. *Macromolecular Chemistry and Physics* 2001;202:2387-2393.
6. Pavlinec J., Moszner N. Dark reactions of free radicals trapped in densely crosslinked polymer networks after photopolymerization. *Journal of applied Polymer Science* 2003;89:579-588.
7. Leprince Julian, Lamblin Guillaume, Truffier-Boutry Delphine, Demoustier-Champagne Sophie, Devaux Jacques, Mestdagh Michèle, Leloup Gaetane Kinetic study of free radicals trapped in dental resins stored in different environments. *Acta Biomaterialia* 2009;5:2518-2524.

8. Lin Nancy J., Lin-Gibson Sheng Osteoblast response to dimethacrylate composites varying in composition, conversion and roughness using a combinatorial approach. *Biomaterials* 2009;30:4480-4487.
9. Schweikl Helmut, Altmannberger Inge, Hanser Nico, Hiller Karl-Anton, Bolay Carola, Brockhoff Gero, Spagnuolo Gianrico, Galler Kerstin, Schmalz Gottfried The effect of triethylene glycol dimethacrylate on the cell cycle of mammalian cells. *Biomaterials* 2005;26:4111-4118.
10. Kawahara T., Nomura Y., Tanaka N., Teshima W., Okazaki M., Shintani H. Leachability of plasticizer and residual monomer from commercial temporary restorative resins. *Journal of Dentistry* 2004;32:277-283.
11. Lecamp L., Youssef B., Bunel C., Lebaudy P. Photoinitiated polymerization of a dimethacrylate oligomer: Part 3. Postpolymerization study. Polymer 1999;40:6313-6320.
12. Truffier-Boutry D., Demoustier-Champagne S., Devaux J., Biebuyck J-J., Mestdagh M., Larbanois P., Leloup G. A physico-chemical explanation of the post-polymerization shrinkage in dental resins. *Dental Materials* 2006;22:405-412.
13. Lee S.-Y., Greener E. H., Mueller H. J. Effect of food and oral simulating fluids on structure of adhesive composite systems. *Journal of Dentistry* 1995;23:27-35.
14. Lee S.-Y., Greener E. H., Menis D. L. Detection of leached moieties from dental composites in fluid simulating food and saliva. *Dental Materials* 1995;11:348-353.
15. Gallez Bernard, Beghein Nelson Noninvasive in vivo EPR monitoring of the methyl methacrylate polymerization during the bone cement formation. *Biomaterials* 2002;23:4701-4704.
16. Teshima Wataru, Nomura Yuji, Tanaka Nobuyuki, Urabe Hidenori, Okazaki Masayuk, Nahara Yukinori ESR study of camphorquinone/amine photoinitiator systems using blue light-emitting diodes. *Biomaterials* 2003;24:2097-2103.
17. Davies M. J. Recent developments in EPR spin-trapping. *Electron paramagnetic resonance* 2002;18:47-73.
18. Bosnjakovic A., Shulamith S. Spin Trapping by 5,5-Dimethylpyrroline-N-oxide in Fenton Media in the Presence of Nafion Perfluorinated Membranes: Limitations and Potential. *Journal of Physical Chemistry B* 2006;110:10720-10728.

19. Taniguchi Hitoshi, Madden Keith P. DMPO-alkyl radical spin trapping: an in situ radiolysis steady-state ESR study. *Radiation Research* 2000;153:447-453.

20. Janzen Edward G., Sankuratri Nagaraju, Kotake Yashige Chiral Spin Traps. The Spin Trapping Chemistry of 5-Methyl-5-phenylpyrroline-N-oxide (MPPO). *Journal of Magnetic Resonance*, Series B 1996;111:254-261.

21. Villamena Frederick A., Rockenbauer Antal, Gallucci Judith, Velayutham Murugesan, Hadad Christopher M., Zweier Jay L. Spin Trapping by 5-Carbamoyl-5-methyl-1-pyrroline N-Oxide (AMPO): Theoretical and Experimental Studies. *The Journal of Organic Chemistry* 2004;69:7994-8004.

22. Villamena Frederick A., Hadad Christopher M., Zweier Jay L. Kinetic Study and Theoretical Analysis of Hydroxyl Radical Trapping and Spin Adduct Decay of Alkoxycarbonyl and Dialkoxyphosphoryl Nitrones in Aqueous Media. J*ournal of physical Chemistry* 2003;107:4407-4414.

23. Olive Gilles, Mercier Anne, Le Moigne Francois, Rockenbauer Antal, Tordo Paul 2-ethoxycarbonyl-2-methyl-3,4-dihydro-2H-pyrrole-1-oxide: evaluation of the spin trapping properties. *Free Radical Biology and Medicine* 2000;28:403-408.

24. Roubaud Valérie, Sankarapandi Sornampillai, Kuppusamy Periannan, Tordo Paul, Zweier Jay L. Quantitative Measurement of Superoxide Generation Using the Spin Trap 5-(Diethoxyphosphoryl)-5-methyl- 1-pyrroline-N-oxide. *Analytical Biochemistry*. 1997;247:404-411.

25. Stolze Klaus, Rohr-Udilova Natasha, Rosenau Thomas, Hofinger Andreas, Kolarich Daniel, Nohl Hans,Spin trapping of C- and O-centered radicals with methyl-, ethyl-, pentyl-, and phenyl-substituted EMPO derivatives. *Bioorganic & Medicinal Chemistry* 2006;14:3368-3376.

26. Stolze Klaus, Rohr-Udilova Natascha, Hofinger Andreas, Rosenau Thomas Spin trapping experiments with different carbamoyl-substituted EMPO derivatives. *Bioorganic & Medicinal Chemistry* 2008;16:8082-8089.

27. Culcasi Marcel, Muller Agnès, Mercier Anne, Clement Jean-Louis., Payet Olivier, Rockenbauer Antal, Marchand Véronique, Pietri Sylvia Early specific free radical-related cytotoxicity of gas phase cigarette smoke and its paradoxical temporary inhibition by tar: An electron paramagnetic resonance study with the spin trap DEPMPO. *Chemico-Biological Interactions* 2006;164:215-231.

28. Dos Santos Neife Aparecida Guinaim, Martins Nádia Maria, Curti Carlos, Pires Bianchi Maria de Lourdes, Dos Santos Antonio Cardozo Dimethylthiourea protects against mitochondrial oxidative damage induced by cisplatin in liver of rats. *Chemico-Biological Interactions* 2007;170:177-186.
29. Kato Akihiko, Hishida Akira, Nakajima Toshiaki Effects of oxygen free radical scavengers on uranium-induced acute renal failure in rats. *Free Radical Biology and Medicine* 1994;16:855-859.
30. Reinke Lester A. Spin trapping evidence for alcohol-associated oxidative stress. *Free Radical Biology and Medicine* 2002;32:953-957.
31. Pou Sovitj, Ramos Carroll L., Gladwell Tim, Renks Erik, Centra Michelle, Young David, Cohen Myron S., Rosen Gerald M. A Kinetic Approach to the Selection of a Sensitive Spin Trapping System for the Detection of Hydroxyl Radical. *Analytical Biochemistry* 1994; 217:76-83.
32. Yamazaki Isao, Piette Lawrence H. EPR spin-trapping study on the oxidizing species formed in the reaction of the ferrous ion with hydrogen peroxide. *Journal of the American Chemical Society* 1991;113:7588-7593.
33. Schmaltz G and Arenholt-Bindslev D. Biocompatibility of Dental Materials 2009, chapter 1, pg 7-8.

Chapter 5

Investigating filler morphology and mechanical properties of new low-shrinkage resin composite types

Journal of Oral Rehabilitation

Journal of Oral Rehabilitation 2010

Investigating filler morphology and mechanical properties of new low-shrinkage resin composite types

J. LEPRINCE*,†, W. M. PALIN‡, T. MULLIER*,†, J. DEVAUX†,§, J. VREVEN* & G. LELOUP*,† *School of Dentistry and Stomatology, Université catholique de Louvain, Brussels, †CRIBIO (Center of Research and Engineering of Odontologic Biomaterials), Brussels, Belgium, ‡Biomaterials Unit, The University of Birmingham School of Dentistry, St Chad's Queensway, Birmingham, UK and §Laboratory of Chemistry and Physics of High Polymers, Université catholique de Louvain, Louvain-la-Neuve, Belgium

5.1. Summary

Three types of low-shrinkage composites are today commercially available: Ormocers, cationic ring-opening curing systems and highly-filled methacrylate-based materials, which cure via free-radical polymerization mechanisms. The aim of this study was to characterize the inorganic fraction of materials belonging to each type and to compare their mechanical properties. Two Ormocers (Admira and an experimental Ormocer V35694), one ring-opening composite (Filtek Silorane) and five methacrylate-based composites (Filtek Supreme XT, Tetric EvoCeram, Grandio, Synergy D6 and an experimental material, V34930) were tested. Inorganic fillers were quantified by thermogravimetric analysis and morphologically characterized by scanning-electron microscopy. Dynamic modulus was determined by an impulse excitation technique, static elastic moduli and flexural strength by a three-point bending method. The results were analyzed using ANOVA tests ($p<0.05$) and linear correlations. Grandio, V34930 and V35694 exhibited significantly higher filler mass fractions. Both dynamic and static moduli of Grandio and V34930 were significantly higher than the other materials ($p<0.05$), although no significant difference in flexural strength was observed between material type ($p>0.05$). From the present findings, it was suggested that V35694 and Filtek Silorane exhibit comparable properties to conventional methacrylate-based composites, although clinically the cavity type and location must guide material choice. Under high occlusal load, the use of Grandio and V34930 might be favoured. For small cavities, alternative technologies could be preferred as the need for mechanical resistance is lower and the potential for stress generation is greater.

5.2. Introduction

Since the introduction of dental resin-based composites, intense research has attempted to develop materials with acceptable mechanical and physical properties in order to significantly improve their longevity and aesthetic quality. For many cavity types, resin composite materials are perceived as versatile and reliable materials for direct and indirect restorations and have become widely used. However, some problems remain, which include the deleterious effects of polymerization shrinkage (1), inadequate mechanical properties (2, 3) and poor wear resistance (4) of large occlusal restorations during service. To solve or at least reduce such drawbacks, numerous investigations have been conducted, including alternative curing protocols ("soft-start", "pulse-delay" polymerization) (5), or material combinations (stress absorbing "flowable" layers or sandwich techniques with resin hybrid or conventional ionomers).

Regarding the development of intrinsic resin composite material properties, research has focused on the optimization of filler particle morphology and more recently, modification of the organic matrix. The introduction of so-called "nanohybrid" composites during the last 5 years presents a good example of the aggressive marketing and prolific product cycle of dental resin composite materials. It might be argued that nanotechnology has been utilized in resin composites since the use of colloidal silica (<100nm particle diameter) in homogenous and heterogeneous microfills introduced in the mid-1970s. As such, the smallest filler size does not differ greatly from that of modern nanohybrid types (6) and any improvement in material properties compared with conventional types is debated in the literature (7-10). Nevertheless, optimized filler morphology and a range of filler particle sizes (usually a bimodal distribution) and smaller average particle size reduces polymerization shrinkage and improves mechanical and aesthetic material properties (11-15).

In terms of the organic matrix, high molecular weight dimethacrylate monomers such as Bis-GMA (bisphenol A glycidyl dimethacrylate) are commonly used in most commercially-available composites and their chemistry has not significantly changed since the pioneering work by Bowen in 1962 (16). To improve cross-linking and structural integrity and to aid the incorporation of filler particles, lower viscosity diluent monomers such as TEGDMA (triethylene glycol dimethacrylate) are used in various proportions, although they contribute to additional shrinkage. A recent

alternative is the replacement of methacrylate-based monomers by epoxy-based ring opening systems (Filtek Silorane™, 3M ESPE Dental Products, Seefeld, Germany). Silorane chemistry (the term coined from the combination of SILOxane and oxiRANE moieties) exhibits a cationic ring-opening polymerization mechanism and initial in vitro studies confirm a reduction of polymerization stress (17, 18) and shrinkage, reaching values of less than 1 %vol (19).

An alternative inorganic-organic resin type was developed many years ago for the polymer industry and has subsequently been adapted for dental use. ORMOCER™ (ORganically MOdified CERamics) technology consists of an organic reactive species, which is bound by the in-situ formation of an inorganic (Si-O-Si) network, which may result in reduced shrinkage ranging from 1.46 to 2.64 vol %, depending on the material and measurement method (20, 21).

Although much is known concerning the shrinkage properties of new, commercially available resin composite restoratives, the effect of filler morphology on mechanical properties of these new materials is not widely reported. Consequently, the present investigation aims to explore the effect of filler particle morphology on static and dynamic modulus, and on flexural strength. Furthermore, the fillers of a resin-composite are well-known to be responsible for light-scattering, and therefore limit the depth of cure (22). In addition, besides filler content, major differences exist between the investigated materials, which can have an impact on the depth of cure, i.e. nature of resin phase (ring-opening systems, Ormocer- and methacrylate-based composites), type of initiating system (radical or cationic polymerization), type and concentration of photoinitiator. Despite the difficulty to thoroughly analyze the impact of each parameter on the curing extent, clinicians need information about the validity of commonly accepted curing protocols on these materials. For that reason, the photopolymerization efficiency of two different commonly accepted curing protocols, i.e. conventional halogen light during 40s and third generation LED light during 20s, was tested on 4 mm layers of each composite.

5.2. Materials and Methods

Eight resin composites including 6 commercially available and 2 experimental materials were tested in the present work (Table 1). Usually, the fillers are distinguished on the basis of manufacturing techniques, the average particle size and chemical composition (13). In the present work, they were classified according to the manufacturer's appellation. The terms 'micro' or 'nano' refer to the size of the smallest fillers and 'hybrid' is used to describe products containing fillers of different size.

Besides fillers, the composites used can also be differentiated according to the nature of their organic matrix. Most of the products contain only dimethacrylate-based monomers, except for Filtek Silorane, which contains a "Silorane"-based organic matrix (3,4-epoxycyclohexyl cyclopolymethylsiloxane) and TEGDMA. Admira and V35694 contain Ormocers, with an addition of TEGDMA for Admira only.

Table 1. Characteristics of tested materials

Materials	Manufacturer	Composite Type*	Shade	Batch	Filler Content* (wt%)	Filler type and dimensions*
Tetric Evo Ceram	Ivoclar-Vivadent (Schaan, Liechtenstein)	Nano-Hybrid	A3	2859	75–76	Barium glass, ytterbium trifluoride, mixed oxide and pre-polymer – range of particle size: 40–3000 nm; average particle size: 550 nm
Synergy D6	Coltène-Whaledent (Langenau, Germany)	Nano-Hybrid	A3/D3	150177	80	Pre-polymerized fillers, glass fillers, nanofillers – range of particle size: 20–2500 nm – average particle size: 600 nm
Admira	Voco (Cuxhaven, Germany)	Micro-Hybrid	A3	791340	77	Ormocers, glass–ceramic microfillers (average particle size: 700 nm)
V35694	Voco (Cuxhaven, Germany)	Nano-Hybrid-Ormocer	A3	**	86	Ormocers, SiO_2 nanoparticles – range of particle size: 20–50 nm and silicate glass – average particle size: 1000 nm
V34930	Voco (Cuxhaven, Germany)	Nano-Hybrid	A3	**	91	SiO_2 nanoparticles – range of particle size: 20–50 nm and silicate glass – average particle size: 1000 nm
Grandio	Voco (Cuxhaven, Germany)	Nano-Hybrid	A3	803031	87	Glass-ceramic micro-fillers – average particle size: 1000 nm – and nanofillers – range of particle size: 20–50 nm
Filtek Supreme XT	3M-ESPE (St. Paul, MN, USA)	Nanofilled	A3	20071029	65–75	Silica nanofillers – average particle size: 75 nm – zirconia nanofillers – average particle size: 5–10 nm – and agglomerated zirconia/ silica nanoclusters – range of particle size: 600–1400 nm
Filtek Silorane	3M-ESPE (St. Paul, MN, USA)	Micro-Hybrid	A3	20071108	76	Quartz microfillers (0·1–1 mm) – range of particle size: 40–1700 nm – average particle size: 470 nm

*Based on information from the manufacturer ** Experimental materials

5.2.1. Characterization of the inorganic fraction

5.2.1.1. Filler morphology

Scanning electron microscopy (SEM) was used to observe the filler morphology and size in each composite. Prior to the SEM observation, the composites samples underwent successive dilutions in order to eliminate the organic phase, with the exception of the polymer fraction in prepolymerized fillers. Firstly, 0.5 g of each material were dissolved in 4 ml of acetone and centrifuged for 5 min at 700 × g and the process repeated three times with acetone and three times with chloroform. The remaining fillers – including prepolymerized fillers – were suspended in 2.5 ml of absolute ethanol, smeared on a glass slide (7.5 cm × 2.5 cm) and dried at 37°C for 6 h. After gold coating, the samples were observed by SEM (Leica Stereoscan S-260, Cambridge, UK) at 10000x magnification.

5.2.1.2. Filler mass fraction

Thermogravimetric analysis (TGA/SDTA861e, Mettler-Toledo, Greinfensee, Switzerland) was used to determine the filler mass fraction. The resin composites were subject to a temperature rise from 30 to 900°C at the rate of 10°C/min followed by air-cooling to room temperature. The inorganic fraction was determined by the ratio of the final and initial sample mass. Three samples of each material were analyzed.

5.2.2. Mechanical properties

Five specimens of each material were prepared in tin moulds of 25 × 2 × 2 mm according to ISO specification 4049 (23). The specimen surfaces were covered by glass slides and irradiated using a halogen light-curing unit (LCU) (XL 3000, 3M-ESPE, St. Paul, MN, USA) operating at 544 mW/cm2 (+/-17 mW/cm2). Four, 60 s overlapping irradiations were applied on both sides of the samples. Each specimen was carefully removed from the mould and stored for 24 h in the dark at 23 ± 1°C prior to testing. The same specimen was used to measure dynamic modulus, static modulus, flexural strength and Vickers microhardness.

5.2.2.1. Dynamic modulus

The dynamic modulus of elasticity (E_d) was measured non-destructively by an impulse excitation technique (24). Each sample (n=5) was set in flexural vibration by a small mechanical impulse. The signal produced was collected using a signal analyzer via a microphone placed underneath the sample (Grindosonic, Lemmens Elektronics, Haasrode, Belgium). The dynamic elastic modulus (E_d) was calculated by the following Equation

$$E_d = 0.9465 \frac{m f_t^2}{b} \frac{L^3}{t^3} T_l \qquad \text{Equation 1}$$

where m was the mass of the sample (g), L was specimen length, b specimen width and t specimen thickness (mm), f_t was the fundamental frequency of the bar (Hz) and T_l a correction factor for fundamental flexural mode accounting for finite thickness of the bar, Poisson's ratio and other constants.

5.2.2.2. Static modulus and flexural strength

The static modulus (E_s) and flexural strength (σ_f) were measured using a three-point bend test according to ISO4049 (23). Samples (n=5) were loaded in a universal testing machine (Instron 5566, High Wycombe, UK) at a strain rate of 0.75 mm/min until fracture occurred. E_s was expressed in GPa and calculated according to Equation 2

$$E_s = \frac{F l^3}{4 b h^3 d} \qquad \text{Equation 2}$$

where F was the load (N), l the distance between the supports (mm), b the width of the sample, h thickness (mm) and d is the mid-span deflection corresponding to the load F. Flexural strength (σ_f) was calculated according to Equation 3 and expressed in MPa

$$\sigma_f = \frac{3}{2} \frac{F l}{b h^2} \qquad \text{Equation 3}$$

5.2.2.3. Vickers microhardness

Vickers microhardness measurements were carried out on the fractured samples recovered from the previous analyses. A 200 g load was applied for 30 s on the cured surface using a Durimet microhardness tester (Leitz, Wetzlar, Germany). The length of the diagonal of each indentation was measured directly using a graduated eye-lens. The Vickers Hardness Number (VHN) was obtained using the following Equation (average of 3 indents per sample):

$$H = 1854.4\frac{P}{d} \qquad \text{Equation 4}$$

where H was Vickers hardness (kg/mm^2), P the load (g) and d diagonal length of the indent (μm).

5.2.3. Photopolymerization efficiency

Each material was placed in 4 similar brass moulds (3 mm diameter, 1 mm depth). Each mould was superimposed, isolated from each other by a thin Mylar film, and the material was light-cured from the top surface in order to assess the curing efficiency through a 4 mm depth. Two different LCUs were used to cure each material: the halogen LCU (used in Section **5.2.2.**) for 40 s and a third generation LED (G-Light, GC, Japan, 1166 +/- 78 mW/cm^2) for 20 s. To assess curing extent throughout the sample depth, Vickers microhardness measurements (as described in *5.2.2.3.*) were performed at the upper surface of the first cylinder and at the lower surface of each of the four cylinders, providing 5 measurements (from 0 to 4 mm depth).

5.2.4. Statistical analysis

Filler mass fraction and mechanical properties were analyzed by one-way ANOVA and post hoc Scheffe's tests at a significance level of 0.05. Three-way ANOVA and Tukey's test at a signifiance level of 0.05 was performed to analyze the results of photopolymerization efficiency. Linear regression analysis was performed to study the relationship between both elastic moduli, and between the elastic moduli and the filler mass fraction.

5.3. Results

5.3.1. Characterization of inorganic fillers

5.3.1.1. Filler morphology

The SEM images are displayed in Figure 1. For each material, fillers were observed at 10000x magnification. Except for Filtek Supreme XT containing spherical particles and spherical aggregates of various sizes, each other material showed irregular shaped particles. Those composites can be divided in two approximate groups according to the proportion of particles of different sizes (Figure 1). In the first group, V34960, V35694, Admira and Tetric EvoCeram show homogeneous particles with an apparent average particle size of less than 1 μm. However, Tetric EvoCeram differs by the presence of large filler aggregates. The composites of the second group (incl. Grandio, Filtek Silorane and SynergyD6) display less homogeneity and appear to contain a number of smaller fillers (< 1 μm) but with an addition of larger particles (> 1 μm).

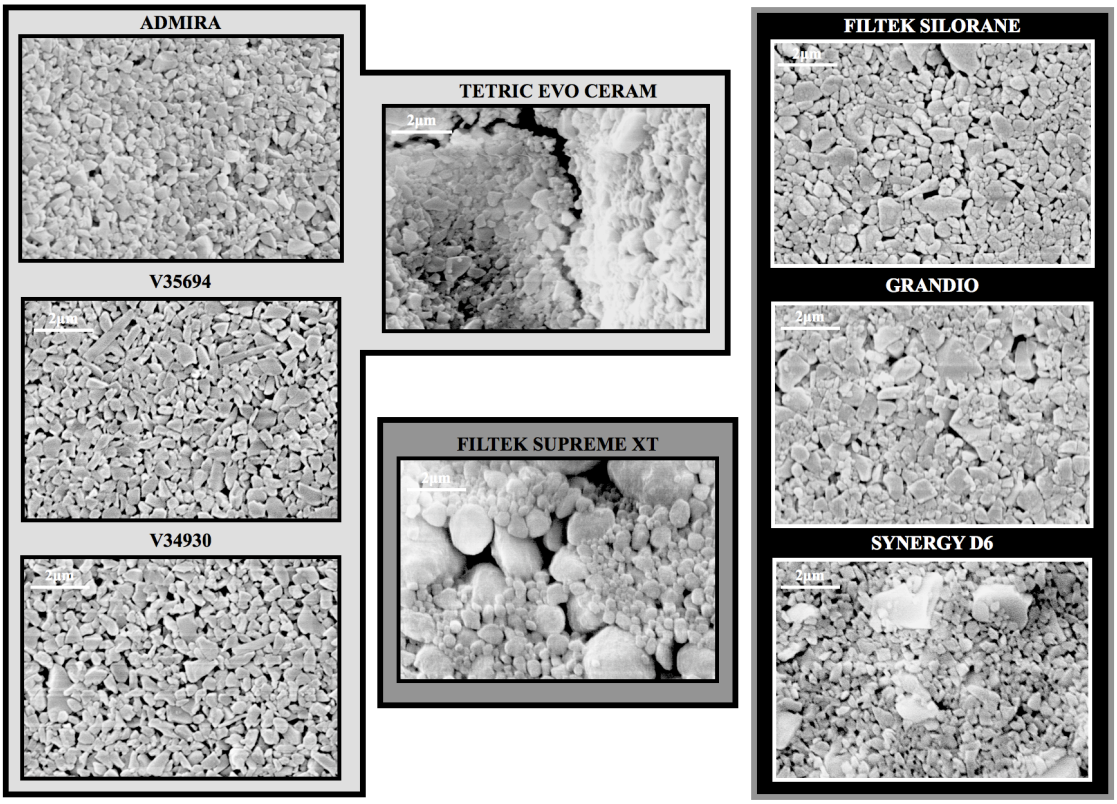

Figure 1 - SEM images of the fillers at 10000x magnification

5.3.1.2. Filler mass fraction

Means, standard deviations and statistical associations are presented in Figure 2. Both Voco experimental materials and Grandio exhibit a significantly higher filler content compared with other materials ($p<0.05$), with values ranging from 84.3 to 86.7 wt% compared with 75.5 and 70.5 wt%, respectively.

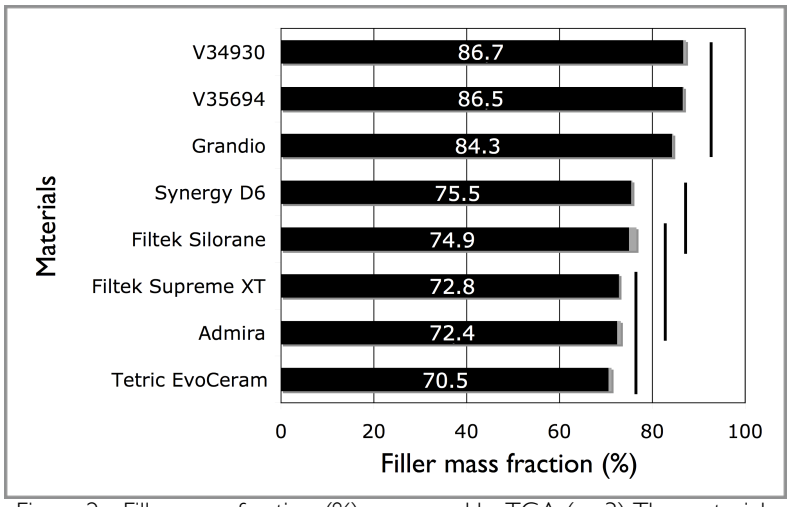

Figure 2 - Filler mass fraction (%) measured by TGA (n=3). The materials are ranked in descending order according to their means (black horizontal bars) and the standard deviations are added in the form of grey bars. Vertical bars connect materials that are not statistically different ($p<0.05$).

5.3.2. Mechanical properties

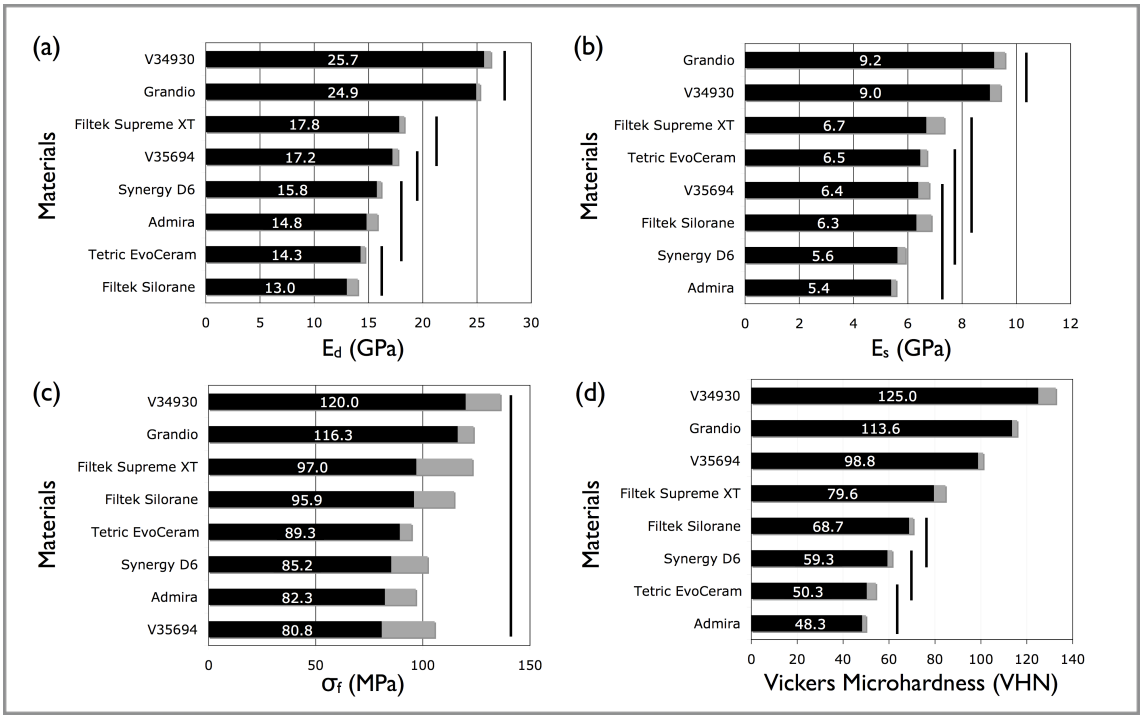

Figure 3 - Overview of the mechanical properties studied. The materials are ranked in descending order according to their means (black horizontal bars) and the standard deviations are added in the form of grey bars. Vertical bars connect materials that are not statistically different ($p<0.05$).
(a) Dynamic modulus (GPa) (n=5); (b) Static modulus (GPa) (n=5); (c) Flexural strength (MPa) (n=5); (d) Vickers microhardness (VHN) (n=5)

Means, standard deviations and statistical associations are presented in Figures 3a to 3d. For E_d (Figure 3a), Grandio and V34930 exhibit statistically higher moduli values compared with each other material ($p<0.05$), amongst which the differences in dynamic moduli are less marked. Similarly, a significant increase in E_s (Figure 3b) is observed for Grandio and V34930 compared with each other material ($p<0.05$). Concerning σf (Figure 3c), the same trend is observed for Grandio and V34930, but no statistically significant difference between any composite was recorded ($p>0.05$). The surface microhardness values (Figure 3d) are higher for the experimental composites and Grandio, and except Filtek Supreme XT, each other material exhibits a significantly reduced surface hardness ($p<0.05$)

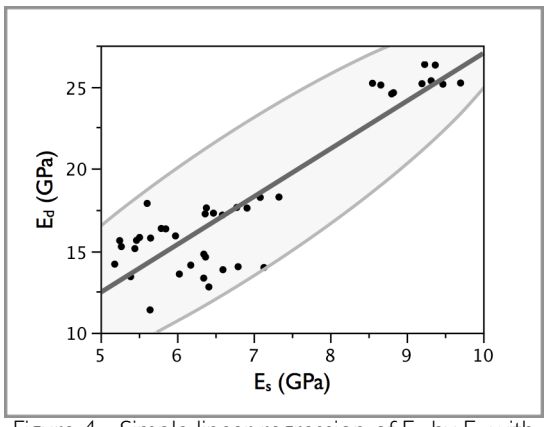

Figure 4 - Simple linear regression of E_d by E_s with a density ellipse ($p=0.95$); $R^2 = 0.815$; $p<0.0001$

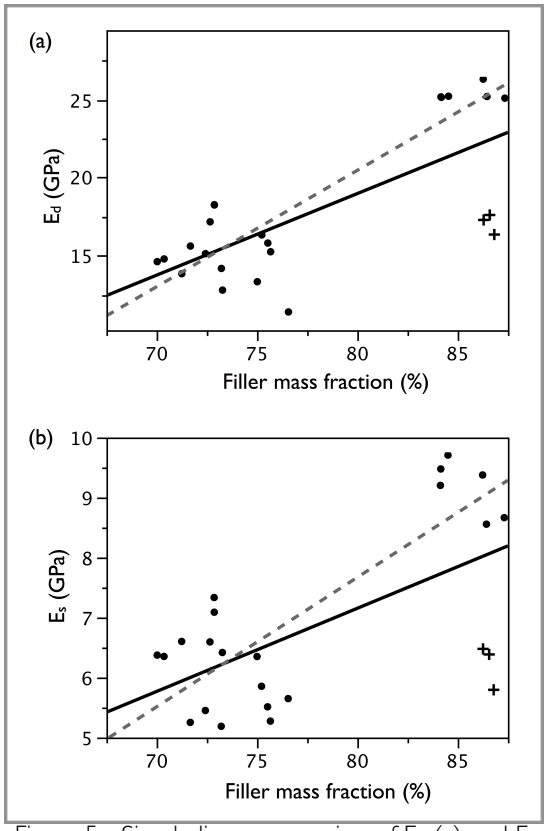

Figure 5 - Simple linear regression of E_d (a) and E_s (b) by filler mass fraction, with (plain lines; $R^2 = 0.52$; $p<0.0001$ for E_d and $R^2 = 0.37$ – $p=0.0017$ for E_s) or without (dashed grey lines; $R^2 = 0.90$ - $p<0.0001$ for E_d and $R^2 = 0.70$ - $p<0.0001$ for E_s) taking into account V35694 (+).

E_d was significantly correlated to E_s ($R^2 = 0.815$; $p<0.0001$) (Figure 4). The linear regression coefficient between E_d / E_s and the filler mass fraction (Figures 5a and 5b, respectively) was fairly low ($R^2 = 0.52$ for E_d and $R^2 = 0.37$ for Es). However, this can be mainly attributed to the results of V35694, which shows a much lower filler content than Grandio and V34930 despite a comparable filler mass fraction. Besides

V35694 (Figure 5, dashed grey lines), the regression coefficients are much higher: R^2 = 0.90 for E_d and R^2 = 0.70 for E_s.

5.3.3. Photopolymerization efficiency

Figure 6 illustrates the decrease in Vickers microhardness with depth (presented in percentage of uppermost surface value, whose absolute values can be found in Fig. 3d) and highlights a similar distribution of the values to the left (samples cured with halogen LCU) and those to the right (samples cured with LED LCU). Analysis of variance of upper-to-lower surface hardness ratio as a function of curing protocol, depth and material was highly significant ($p<0.0001$). The related statistical comparisons are presented in Table 2, where it appears that at 1 and 2 mm depth, the hardness ratio of all materials (except V35694 – 2mm – XL3000 – 40s) were statistically comparable, regardless of the curing protocol. At 3 and 4 mm depth, a significant drop of hardness ratios is observed; at 3mm, all the ratios but one (Grandio – G-Light – 20s) are below 80%.

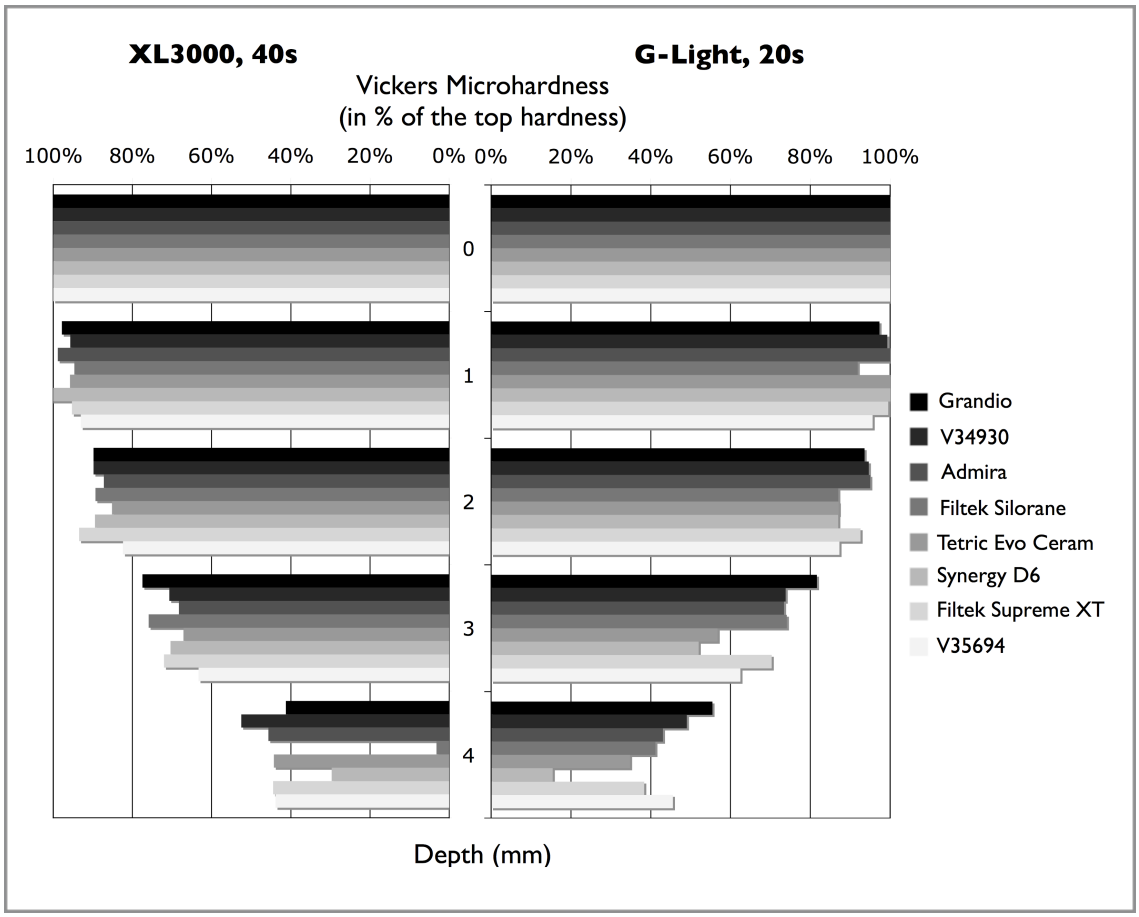

Figure 6 - Comparison of the influence of both curing protocols on the decrease of Vickers microhardness with depth. The values are presented in percentage of uppermost surface microhardness (n=5). The values to the left refer to samples cured during 40s with XL3000, and those to the right refer to samples cured during 20s with G-Light.

5.4. Discussion

5.4.1. Filler morphology

Filtek Supreme XT is the only composite in this study to contain spherical particles and aggregates (Figure 1). This spherical form of the particles was already observed in composites of the same manufacturer, i.e. in Filtek Z100, Supreme XT (12, 24), Z250 and P-60 (25). Filtek Supreme XT is marketed as a "nanocomposite", and according to the manufacturers, contains 8 wt% silica nanoparticles (20-75 nm diameter) and 71 wt% silica/zirconia "nanoclusters" (0.6-1.4 μm diameter). Since it is impossible to perceive the smallest particles using SEM, all the particles are assumed to be aggregates, whose diameter ranges from about 0.1 to 2-3 μm. For Filtek Silorane, the SEM images confirm a distinct filler morphology (irregularly shaped fillers from 0.1 to 1μm) compared with the other resin composite (Filtek Supreme XT) of the same manufacturer. Such radical change in filler content is surprising although specific characteristics of the silorane-based organic matrix may account for this. The necessity for an epoxy-functional silane agent may restrict the use of particular filler types. Silorane is known to contain quartz particles which cannot be processed by a sol-gel technique and may explain the more irregular morphology compared with other materials provided by the same manufacturer.

Currently, there is no consensus on the positive effect of a certain particle size and shape (spherical or irregular) on the mechanical properties. According to Rueggeberg *et al*. (26), it is difficult to distinguish the effect of filler size and shape on mechanical properties of commercial composites. Even the comparison of experimental composite formulations has resulted in unclear findings (14, 27). Masouras *et al*. (28) suggested that the filler load was the main factor for determining elastic modulus properties, while filler size and shape should be considered as secondary "fine-tuning" factors for altering material properties.

5.4.2. Filler mass fraction

For V35694, Filtek Silorane and Supreme XT, the mean values obtained were close to that reported by the manufacturers. For the remaining materials, larger differences of up to 5 wt% were observed. For Tetric Evo Ceram and Synergy D6, an underestimation of filler load may be attributed to the presence of pre-polymerized

particles and the TGA method used here, which relies on removal of the composite organic fraction. A further explanation may be related to filler silanization. As reported by Sabbagh *et al*. (25), some manufacturers assess the fillers mass fraction before the silanization process, while others include the percentage of silane coating in their calculations.

Despite the close similarity of SEM images (except for Filtek Supreme XT), large differences in filler fraction are observed between the different, so-called "nanocomposites". Grandio and both experimental Voco materials exhibit a significantly increased filler load (84.3-86.7 wt%) compared with the other materials (70.5-75.5 wt%; Figure 2). Assuming no particle agglomeration, a possible explanation for such differences in the filler content is a better adapted combination of particles of different sizes, reducing inter-particulate distances and enabling higher filler packing in Grandio, V34930 and V35694. Although the size of nanofillers precludes their examination using SEM, they may account for the high filler content of these 3 composites. However, other materials also contain nanoparticles (Table 1) but exhibit significantly reduced filler content. The extent of filler loading will be dependent upon many factors including the size and amount of the smallest filler, particle morphology, the type and extent of silanisation and viscosity and hydrophobicity of the resin matrix. As filler size decreases to the nanoscale region, surface area increases and viscosity will rapidly increase compared with the same volume percentage of fillers with larger diameter. Consequently, surface area to volume effects will limit filler wettability and reduce filler content, which was a significant drawback of homogeneous microfill types introduced in the 1970s. Addition of discrete spherical nanoparticles is known to cause a decrease in viscosity by reducing polymer entanglement, which contradicts Einsteinian theory (29). However, nanoparticle dispersion is very difficult to control, especially in highly filled, viscous systems such as resin composite restoratives. As the diameter of a particle decreases, the surface free energy increases and therefore agglomeration occurs where interparticulate forces exceed the particulate mass. Filler particle agglomerates may act as critical flaws as the interaction between fillers and polymer is reduced (9, 30).

As the filler content here was measured in mass percentage, it should be noted that filler load and consequential mechanical and physical properties could also be

partly related to the nature of the particles. Indeed, denser particles are responsible for improving filler load without increasing the volume percentage and quoting volume filler percentages is probably more relevant for overall performance of the composite material.

5.4.3. Mechanical properties

Dental restorative materials should mimic as much as possible the physical behavior of the tooth and approximate the mechanical properties of enamel and dentin. In the present study, the mechanical properties of all the composites did not approach the values generally reported for enamel with elastic moduli of 80 to 94 GPa depending on prism orientation (31), which is in agreement with previous investigations (12, 32). Similarly, but to a lesser extent, no material tested in the present study exhibited a modulus value similar to that of dentine (19 GPa determined by an indentation method (31). Balooch *et al*. (33) reported that the elastic modulus of dentine is dependent upon its microstructure, ranging from 17 to 23 GPa for intertubular dentine and 40 to 50 GPa for peritubular dentine. Moreover, the tooth is a complex heterogeneous graded structure, which combines hardness and toughness, wherein the modulus of dentine will vary through depth due to the sigmoidal nature of tubules. Although the use of restorative materials with similar elastic modulus to tooth tissue will allow efficient load transfer between structures, no resin composite material can replicate the combination of hardness and toughness exhibited by the graded structure of enamel and dentine. That said, the elastic modulus of resin composites must be high enough to resist occlusal forces, especially in class I and II cavities (32). However, a high elastic modulus can also lead to more brittle materials. Therefore, an increase in elastic modulus must be combined with suitable mechanical characteristics, such as fracture toughness, flexural and fatigue strength in order to resist occlusal loads.

In the present work, E_d was significantly correlated to E_s ($R^2 = 0.815$), which concurs with previous work (32). In the latter, it was also observed that all materials showed a higher E_d than E_s. As explained by Sabbagh *et al*. (32), the high values for E_d are to be attributed to the high strain rate applied on the specimen during testing. This impulse excitation technique gives low standard deviations as the frequency is recorded only when three consecutive and similar values (within 1% of each other) are obtained.

There were no significant differences observed in flexural strength between each material although Grandio and V34930 exhibited significantly higher E_d and E_s compared with other material types, which can be explained by a significantly increased filler content. Consequently, in the case of Grandio and V34930, the mechanical characteristics may favour their use in high occlusal stress locations. As both materials exhibit a high elastic modulus, which may result in the generation of high polymerization shrinkage stress, their use in cavities with a low configuration factor might be suggested, e.g. in extended cavities for which a high modulus material is also important. Although the mass percentage of filler in V35694 was statistically equivalent to Grandio and V34930, a significant reduction in E_d, E_s was observed, which can be associated with the difference in the proprietary matrix composition of the experimental material. Ormocer materials are known to reach lower conversion compared with conventional methacrylate-based resin composites (34), which could partly account for lower mechanical properties of Ormocers with equal filler content. Nevertheless, V35694 might be indicated for cavities where a lower elastic modulus is preferred (class III or V).

Although non-significant differences were observed in flexural strengths between any material tested in the present investigation, a reason that Filtek Supreme exhibited high strength values despite visibly large areas of agglomeration (Figure 1) might be due to its distinct filler particle morphology. Spherical-shaped particles are known to exhibit improved fracture resistance compared with irregular-shaped morphologies as regions of high stress-concentrations at the filler particle edge are avoided (35). Filtek Supreme XT also shows high values of E_d (statistically equivalent to V35694) and E_s. Unlike Masouras *et al*. (28), the present results suggest the potential of a composite with spherical fillers to generate equal or better modulus than some materials of higher filler content but with irregular particles (Synergy D6, V35694). One possible explanation could be silane infiltration into porosities of the nanoclusters as proposed by Curtis *et al*. (6). However, the comparison of commercial material properties is challenging since full constituents are rarely disclosed where filler morphologies, resin types and photoinitiation chemistries vary greatly between products.

Some previous studies have reported the potential of Ormocer materials to reach equal or improved properties than methacrylate-based composites (34, 36, 37). However, Admira exhibits statistically inferior mechanical properties compared with several of the methacrylates tested here (Figure 3a-d), which has also been demonstrated in the literature (38). The increase in mechanical properties of the experimental material, V35694, highlights the potential of Ormocer composites to surpass the properties of several methacrylate-based materials. Also, V35694 exhibits a significant increase in E_d and upper surface microhardness compared with Admira, which can be attributed in part to a significantly increased filler content. Besides their potential low shrinkage, Ormocer materials present other potential interests, such as lower cytotoxicity and lower water solubility compared to conventional resins (34). The inorganic-organic network of conventional Ormocer materials (Admira) exhibits a similar viscosity to bisGMA and therefore dilution is required for dental purposes to aid rheological properties and filler inclusion. Unfortunately, this addition of low molecular weight methacrylate-monomers (TEGDMA) may negate improved biocompatibility if cytotoxicity of eluted residual monomer is considered. However, while Admira contains TEGDMA, it is not the case of the experimental Ormocer V35694 (information from the manufacturer). This constitutes an interesting progress of Ormocer-based materials regarding biocompatibility, as elution of this diluent monomer should no longer be feared.

Regarding Filtek Silorane, it can be stated that this material compares favourably to some clinically well-accepted methacrylate-based composites in terms of mechanical properties, which is in agreement with other studies (19, 39). However, Silorane exhibits relatively low E_d and E_s, which might be considered a clinical disadvantage in areas with high occlusal force. Although Silorane was developed as a low shrinkage composite, it should be noted that decreased shrinkage does not necessarily result in reduced marginal gap formation. The stress generated at the tooth-restoration interface is a result of a complex process of shrinkage, curing speed and elastic modulus of the material. In addition, it also depends on the configuration factor of the cavity and on the compliance of the surrounding tooth tissue. In the case of Silorane, the lower elastic modulus combined with different curing characteristics associated with its cationic ring-opening polymerization and resultant low shrinkage reported in the literature (17) may work in combination to reduce gap formation. As a

result, this new material might be recommended for cavities with high configuration factor (where low shrinkage and shrinkage stress are required).

5.4.4. Photopolymerization efficiency

An ultimate goal of low-shrinkage resin composite materials might be the possibility to cure thicker layers of composite (> 2 mm) without bonding failure, gap formation and without deterioration of tooth structure. However, even if this goal is reached, which is not yet the case, another limiting factor is the depth of cure. Several

Table 2. Percentage of the upper surface microhardness for each material/curing protocol/depth association

Material	Curing protocol	Depth (mm)																							Least Sq Mean (%)
Synergy D6	XL3000 - 40s	1	A																						102
Admira	G-Light - 20s	1	A																						102
Tetric Evo Ceram	G-Light - 20s	1	A	B																					101
Synergy D6	G-Light - 20s	1	A	B																					101
Filtek Supreme XT	G-Light - 20s	1	A	B	C																				100
V34930	G-Light - 20s	1	A	B	C																				99
Admira	XL3000 - 40s	1	A	B	C																				99
Grandio	XL3000 - 40s	1	A	B	C																				98
Grandio	G-Light - 20s	1	A	B	C																				97
V35694	G-Light - 20s	1	A	B	C	D																			96
V34930	XL3000 - 40s	1	A	B	C	D																			96
Tetric Evo Ceram	XL3000 - 40s	1	A	B	C	D																			96
Filtek Supreme XT	XL3000 - 40s	1	A	B	C	D																			95
Admira	G-Light - 20s	2	A	B	C	D																			95
Filtek Silorane	XL3000 - 40s	1	A	B	C	D																			95
V34930	G-Light - 20s	2	A	B	C	D																			95
Grandio	G-Light - 20s	2	A	B	C	D	E																		94
Filtek Supreme XT	XL3000 - 40s	2	A	B	C	D	E																		94
V35694	XL3000 - 40s	1	A	B	C	D	E																		93
Filtek Supreme XT	G-Light - 20s	2	A	B	C	D	E	F																	93
Filtek Silorane	G-Light - 20s	1	A	B	C	D	E	F	G																92
Synergy D6	XL3000 - 40s	2	A	B	C	D	E	F	G	H															90
V34930	XL3000 - 40s	2	A	B	C	D	E	F	G	H															90
Grandio	XL3000 - 40s	2	A	B	C	D	E	F	G	H	I														90
Filtek Silorane	XL3000 - 40s	2	A	B	C	D	E	F	G	H	I	J													89
V35694	G-Light - 20s	2	A	B	C	D	E	F	G	H	I	J	K												88
Synergy D6	G-Light - 20s	2	A	B	C	D	E	F	G	H	I	J	K												87
Filtek Silorane	G-Light - 20s	2	A	B	C	D	E	F	G	H	I	J	K												87
Tetric Evo Ceram	G-Light - 20s	2	A	B	C	D	E	F	G	H	I	J	K												87
Admira	XL3000 - 40s	2	A	B	C	D	E	F	G	H	I	J	K												87
Tetric Evo Ceram	XL3000 - 40s	2	A	B	C	D	E	F	G	H	I	J	K	L											85
V35694	XL3000 - 40s	2		B	C	D	E	F	G	H	I	J	K	L											82
Grandio	G-Light - 20s	3			C	D	E	F	G	H	I	J	K	L	M										82
Grandio	XL3000 - 40s	3				D	E	F	G	H	I	J	K	L	M	N									77
Filtek Silorane	XL3000 - 40s	3					E	F	G	H	I	J	K	L	M	N									76
Filtek Silorane	G-Light - 20s	3						F	G	H	I	J	K	L	M	N	O								74
V34930	G-Light - 20s	3						F	G	H	I	J	K	L	M	N	O	P							74
Admira	G-Light - 20s	3							G	H	I	J	K	L	M	N	O	P							73
Filtek Supreme XT	XL3000 - 40s	3								H	I	J	K	L	M	N	O	P							72
V34930	XL3000 - 40s	3									I	J	K	L	M	N	O	P	Q						71
Synergy D6	XL3000 - 40s	3										J	K	L	M	N	O	P	Q	R					71
Filtek Supreme XT	G-Light - 20s	3											K	L	M	N	O	P	Q	R					70
Admira	XL3000 - 40s	3												L	M	N	O	P	Q	R					68
Tetric Evo Ceram	XL3000 - 40s	3												L	M	N	O	P	Q	R	S				67
V35694	XL3000 - 40s	3													M	N	O	P	Q	R	S	T			63
V35694	G-Light - 20s	3														N	O	P	Q	R	S	T	U		63
Tetric Evo Ceram	G-Light - 20s	3															O	P	Q	R	S	T	U	V	57
Grandio	G-Light - 20s	4																P	Q	R	S	T	U	V	55
V34930	XL3000 - 40s	4																	Q	R	S	T	U	V	W	53
Synergy D6	G-Light - 20s	3																		R	S	T	U	V	W	52
V34930	G-Light - 20s	4																			S	T	U	V	W	49
Admira	XL3000 - 40s	4																				T	U	V	W	X	46
V35694	G-Light - 20s	4																				T	U	V	W	X	46

elements can limit the curing extent at depth, i.e. mostly fillers (responsible for light-scattering), pigments and photoinitiator molecules. Due to the difficulty to get information from the manufacturer regarding the latter, it is difficult to thoroughly analyze the impact of each parameter on the curing extent. However, it is important for clinicians to know if the commonly accepted curing protocols are valid on the investigated materials. For that reason, the photopolymerization efficiency of two different commonly accepted curing protocols, i.e. conventional halogen light during 40s and third generation LED light during 20s, was tested on 4 mm layers of each composite. The third generation LED light was preferred to a second generation LED to limit the impact of potential spectrum incompatibility on the results.

The present results indicate that both irradiation procedures induce a suitable polymerization through all the studied materials within the first two millimeters, which confirms the potential of the new generation LED lights to reduce irradiation time to some extent (40). In the same way, current standards state that a composite layer is properly cured when the bottom microhardness is higher than or equal to 80% of the top microhardness (40). In this case, all materials fulfill these requirements for both photoinitiating procedures (XL3000 40s / G-Light 20s). However, the differences are huge when considering the absolute VHN values, with means ranging from 125 to 48.3. In addition, for the deepest layers (3 – 4 mm), the differences between the composites increase and all values but one are lower than 80%. This confirms that, for the materials and curing protocols considered, practitioners should limit the thickness of each composite layer to 2mm.

5.5. Acknowledgments

J. Leprince thanks the Funds for Scientific Research (F.R.S.-FNRS) for his research fellow position. The authors would also like to thank Voco GmbH for supporting this study as well as the other manufacturers who supplied us with materials. The authors are grateful to L. Thibon for her participation in the experiments.

5.6. References

1. Davidson CL, Feilzer AJ. Polymerization shrinkage and polymerization shrinkage stress in polymer-based restoratives. *J Dent* 1997; 25: 435-440

2. Hickel R, Manhart J. Longevity of restorations in posterior teeth and reasons for failure. *J Adhes Dent* 2001; 3: 45-64
3. Van Nieuwenhuysen J.-P., D'Hoore W, Carvalho J and Qvis V. Long-term evaluation of extensive restorations in permanent teeth. *J Dent* 2003; 31: 395-405
4. Yesil ZD, Alapati S, Johnston W, Seghi RR. Evaluation of the wear resistance of new nanocomposite resin restorative materials. *J Prosthet Dent* 2008; 99: 435-443
5. Fleming GJP, Cara RR, Palin WM, Burke FJT. Cuspal movement and microleakage in premolar teeth restored with posterior filling materials cured using 'soft-start' polymerization. *Dent Mater* 2007; 23: 637-643
6. Curtis AR, Shortall AC, Marquis PM, Palin WM. Water uptake and strength characteristics of a nanofilled resin-based composite. *J Dent* 2008; 36: 186-193.
7. Curtis AR, Palin WM, Fleming GJ, Shortall AC, Marquis PM. The mechanical properties of nanofilled resin-based composites: characterizing discrete filler particles and agglomerates using a micromanipulation technique. *Dent Mater*, 2009; 25: 180-187
8. Curtis AR, Palin WM, Fleming GJ, Shortall AC, Marquis PM. The mechanical properties of nanofilled resin-based composites: the impact of dry and wet cyclic pre-loading on bi-axial flexure strength. *Dent Mater*, 2009; 25: 188-197
9. Shah MB, Ferracane JL, Kruzic JJ. Mechanistic aspects of fatigue crack growth behavior in resin based dental restorative composites. *Dent Mater*, 2009; 25: 909-916
10. Drummond JL, Lin L, Al-Turki LA, Hurley RK. Fatigue behaviour of dental composite materials. *J Dent*, 2009; 37: 321-330
11. Moszner N, Salz U. New developments of polymeric dental composites. *Progr Polym Sci* 2001; 26: 535-578
12. Beun S, Glorieux T, Devaux J, Vreven J, Leloup G. Characterization of nanofilled compared to universal and microfilled composites. *Dent Mater* 2007; 23: 51-59
13. Moszner N, Klapdohr S. Nanotechnology for dental composites. *Int J Nanotechnol* 2004; 1: 130-516
14. Masouras K, Silikas N, Watts DC. Correlation of filler content and elastic properties of resin-composites. *Dent Mater* 2008; 24: 932-9.

15. Ikejima I, Nomoto R, McCabe JF. Shear punch strength and flexural strength of model composites with varying filler volume fraction, particle size and silanation. *Dent Mater* 2003; 19: 206-211
16. Bowen RL. Dental filling materials comprising of vinyl-silane fused silica and binder consisting of the reaction product of bispenol and glycidyl methacrylate. *US Patent* 3, 066, 112 (1962).
17. Eick JD, Kotha SP, Chappelow CC, Kilway KV, Giese GJ, Glaros AG *et al*. Properties of silorane-based dental resins and composites containing a stress-reducing monomer. *Dent Mater* 2007; 23: 1011-1017
18. Palin WM, Fleming GJ, Nathwani H, Burke FJ, Randall RC. In vitro cuspal deflection and microleakage of maxillary premolars restored with novel low-shrink dental composites. *Dent Mater* 2005; 21: 324-335
19. Weinmann W, Talacker C, Guggenberger R. Siloranes in dental composites. *Dent Mater* 2005; 21: 68–74
20. Uhl A, Mills RW, Rzanny AE, Jandt KD. Time dependence of composite shrinkage using halogen and LED light curing. *Dent Mater* 2005; 21: 278-286
21. Gerdolle DA, Mortier E, Droz D. Microleakage and polymerization shrinkage of various polymer restorative materials. *J Dent Child* 2008; 75: 125-133
22. Emami N, Sjödahl M, Söderholm KJ. How filler properties, filler fraction, sample thickness and light source affect light attenuation in particulate filled resin composites. *Dent Mater* 2005; 21:721-30
23. International Organization for Standardization. Specification of dentistry-resin-based filling materials. ISO-4049, 1988
24. Braem M, Lambrechts P, Van Doren V, Vanherle G. The impact of composite structure on its elastic response. *J Dent Res* 1986; 65: 648-653
25. Sabbagh J, Ryelandt L, Bachérius L, Biebuyck JJ, Vreven J, Lambrechts P, *et al*. Characterization of the inorganic fraction of resin composites. *J Oral Rehabil* 2004; 31: 1090-1101
26. Rueggeberg FA, Caughman WF, Curtis JW Jr, Davis HC. Factors affecting cure at depths within light-activated resin composites. *Am J Dent* 1993; 6: 91-95
27. Turssi CP, Ferracane JL, Vogel K. Filler features and their effects on wear and degree of conversion of particulate dental resin composites. *Biomaterials* 2005; 26: 4932-4937

28. Masouras K, Akhtar R, Watts DC, Silikas N. Effect of filler size and shape on local nanoindentation modulus of resin-composites. J Mater Sci Mater Med 2008; 19: 3561-3566
29. Tuteja A, Duxbury PM, Mackay ME. Multifunctional nanocomposites with reduced viscosity. *Macromolecules*, 2007; 40: 9427-9434.
30. Rüttermann S, Wandrey C, Raab WH, Janda R. Novel nano-particles as fillers for an experimental resin-based restorative material. *Acta Biomater* 2008; 4: 1846-1853
31. Xu HH, Smith DT, Jahanmir S, Romberg E, Kelly JR, Thompson VP *et al*. Indentation damage and mechanical properties of human enamel and dentin. *J Dent Res* 1998; 77: 472-480
32. Sabbagh J, Vreven J, Leloup G. Dynamic and static moduli of elasticity of resin-based materials. *Dent Mater* 2002; 18: 64-71
33. Balooch G, Marshall GW, Marshall SJ, Warren OL, Asif SA, Balooch M. Evaluation of a new modulus mapping technique to investigate microstructural features of human teeth. *J Biomech* 2004; 37: 1223-1232
34. Moszner N, Gianasmidis A, Klapdohr S , Fischer UK, Rheinberger V. Sol-gel materials 2. Light-curing dental composites based on ormocers of cross-linking alkoxysilane methacrylates and further nano-components. *Dent Mater* 2008; 24: 851-856
35. Suzuki S, Leinfelder KF, Kawai K, Tsuchitani Y. Effect of particle variation on wear rates of posterior composites. *Am J Dent* 1995; 8: 173-178
36. Cattani-Lorente M, Bouillaguet S, Godin C.H, Meyer J.M. Polymerization shrinkage of Ormocer based dental restorative composites. *Eur Cell Mater* 2001; 1: 25–26
37. Tagtekin DA, Yanikoglu FC, Bozkurt FO, Kologlu B, Sur H. Selected characteristics of an Ormocer and a conventional hybrid resin composite. *Dent Mater* 2004; 20: 487-497
38. Manhart J, Kunzelmann KH, Chen HY, Hickel R. Mechanical properties of new composite restorative materials. *J Biomed Mater Res* 2000; 53: 353-361
39. Ilie N, Hickel R. Silorane-based dental composite: behavior and abilities. *Dent Mater J* 2006; 25: 445-454

40. Price RB, Felix CA, Andreou P. Knoop hardness of ten resin composites irradiated with high-power LED and quartz-tungsten-halogen lights. *Biomaterials* 2005; 26: 2631-2641.

Chapter 6

Pulpal-temperature rise and polymerization efficiency of LED curing lights

©*Operative Dentistry, 2010,* **35-2**, 220-230

Pulpal-temperature Rise and Polymerization Efficiency of LED Curing Lights

J Leprince • J Devaux • T Mullier
J Vreven • G Leloup

6.1. Summary

The aim of this paper was to assess the effects of light characteristics and irradiation time on the Vickers microhardness (VH) of a dual-photoinitiator commercial composite and on the temperature increase in the pulp chamber (ΔT). Four recent light emitting diodes (LEDs), BluephaseG2 (BG2), Bluephase16i (B16i), G-Light (G) and Freelight2 (F2), and one control halogen light (XL3000 – X) were tested on two shades of Tetric EvoCeram (A2 and Bleach XL), whose respective commercial formulation differs by their concentration of camphorquinone and lucirin TPO. Three different irradiation times were applied, i.e. 10, 20 and 40 s, and VH was measured on the upper and lower surfaces of 2 mm thick samples. ΔT was measured using a K-type thermocouple inserted in the pulp chamber of a molar that had been prepared to obtain a 2 mm thickness of dentin. The measurements were made during polymerization of a 2 mm composite (Shade A2 or Bleach) and with an uncovered tooth. The data were analyzed with a two-way ANOVA ($p < 0.05$) test. For shade A2, all but one irradiation condition (F2 – 10 s, lower surface) generated VH values that were statistically equal to or better than the standard chosen for this study (X–40s). For Bleach shade, VH values obtained with G and BG2 – 20 and 40 s are statistically comparable to X – 40 s for both upper and lower surfaces. This is not the case either with G and BG2 – 10 s or for all procedures with other LCU, for which VH of at least one of the surfaces was significantly lower than the reference. The results also highlight the differences between the 2 photoinitiator contents whether the upper or the lower surface is considered. Regarding temperature measurements, for shade A2, B16i – 20 & 40s, BG2 – 40 s and G – 40s induced significantly higher ΔTs (3.98, 5.98, 5.21, 4.95, respectively) than X – 40 s (3.09). For Bleach shade, B16i – 20 & 40 s, F2 – 20 & 40 s, BG2 – 40 s and G – 40 s generated ΔTs significantly higher than control values (2.70, 4.05, 3.03, 4.58, 2.74, 2.44, respectively). ΔT values obtained with the uncovered tooth were generally higher than those obtained with a 2 mm layer of composite. In conclusion, this paper highlights that a perfect correspondence between light and material spectra is of prime concern, both to insure optimal polymerization and to limit heating in the pulp chamber. Some reduction in curing time is possible, but within certain limits.

6.2. Introduction

Since the introduction of photopolymerizable dental composites, various technologies have been proposed for light-curing units (LCU): Initially UV-lights were developed, then visible-light systems, e.g., quartz-tungsten halogen (QTH) lights, plasma-arc curing units, lasers, and more recently light-emitting diodes (LEDs). Among the different light curing systems available today, LEDs seem to present the best technology for several reasons: First, their narrower spectrum is better centered on the peak of maximum absorption of the main composite photoinitiator, camphorquinone (CQ), which increases irradiation efficiency.[1] Second, the low power consumption of LED LCUs enables the use of batteries; this has led to significant ergonomic improvement,[2] and to smaller and better-adapted fans or other heat dissipating devices. While the first generation LED lights did not meet with general approval because of their low power density,[2,3] new generation lights are now increasingly used by practitioners. These newer LED lights have been shown to have material properties similar to QTH lights.[4,5] Moreover, several publications have highlighted the potential of these lights to reduce irradiation time without significant loss of mechanical properties.[4,6,7]

Recently, with the emergence of tooth whitening, extra-white composites have been developed to match very light shades, which were difficult to achieve with CQ/ amines because of their yellowish aspect. For this reason, as well as to improve photoinitiation efficiency, alternative photoinitiators, such as phenylpropanedione (PPD), monoacylphosphine oxide (MAPO or Lucirin TPO) and bisacylphosphine oxide (BAPO or Irgacure 819), have been studied and some have been introduced into composites. However, the absorption spectra of these molecules are different from the CQ spectrum. The narrow spectrum of blue LED lights, initially recognized as an asset, can, therefore, become a problem because of incompatibility with these alternative photoinitiators.[8] To overcome this problem, the so-called “third generation” of LED LCUs was created, combining two different light peaks, one blue and one violet. Initial results achieved with these lights have been promising, being similar to or better than those achieved with second generation LED LCUs.[9]

Given the lack of information from manufacturers on the photoinitiating systems of commercially available composites, dentists face a difficult choice among

the diverse light curing systems. Compared to halogen LCUs, LED LCUs have two main assets (in addition to ergonomy): Reduction in tooth heating and in irradiation time. Regarding heat reduction, this asset was already present in the first generation LED lights, probably due to their lower power density. Asmussen & Peutzfeldt[10] indeed showed that temperature rise was correlated with power density. Similarly, Vandewalle *et al*.[11] observed a similar increase in pulpal temperature between an LED and a halogen LCU of the same power density. As a result, because the power densities of recent LED lights are comparable to or higher than those of QTH lights, the temperature rise in the pulp chamber can be similar or higher.[12,13] In a recent paper, Antonson *et al*.[2] proposed that the effects of heat generated by the new, high powered LED LCUs needs to be determined. In addition, as demonstrated by Schneider *et al*.,[3] temperature rise is important when evaluating the curing efficacy of new lights. This is true both from a safety point of view[2,13] and in terms of curing efficacy, as temperature increase can enhance polymer properties.[14-15] With regard to curing time, the better match between absorption/emission spectra and the higher power density of recent LED LCUs enables a reduction in curing time, sometimes down to 20 or even 10 s.[7] Shortall[4] and Yap & Soh[6] also demonstrated the potential for a second generation LED to be as effective as a halogen LCU, with a 50% reduction in curing time. However, several authors have also stressed that the ability of an increase in power density to compensate for time reduction is limited.[16-18] Peutzfeldt & Asmussen[16] notably showed that for a given energy density, when power density was increased, the degree of conversion decreased linearly, whereas flexural strength and flexural modulus showed a parabolic relationship.

This study, therefore, had two main objectives: The first was to evaluate the polymerization efficiency of 10, 20 and 40 s irradiations with 4 recent LED lights (two single peak, “second generation” LEDs, two multiple peak, “third generation” LEDs) on two variants of the same composite, Tetric Evo Ceram shade A2 and shade Bleach XL (Ivoclar Vivadent, Schaan, Liechtenstein). These materials were chosen for their different photoinitiating system, i.e., both contain camphorquinone (CQ) and Lucirin-TPO (L) but in different ratios. In T shade A2, CQ is dominant while in Bleach shade, L is present in greater concentrations.[19] A standard photoinitiation method commonly accepted for the polymerization of 2 mm composites was chosen for the comparison: Conventional halogen light for 40 s.[15,16] The second purpose of this study was to analyze the thermal effect of the different irradiation conditions on the pulp chamber.

Hence, this research aims at determining the interaction between pulpal temperature rise and composite hardness using different recent LED LCUs.

6.3. Materials and Methods

6.3.1. Spectrum characterization

Five different lights were used. A conventional halogen light was chosen as control and compared to 4 LED lights. The lights are presented in Table 1. The spectra of the five lights were determined by a mini-spectrometer (RC series C9407MA, Hamamatsu, Japan) and their irradiance was determined by 5 measurements with a Bluephase meter (Ivoclar Vivadent, Schaan, Liechtenstein). As both composite shades chosen for this study contain two photoinitiators (CQ and L) in different proportions, the absorption spectra of both pure photoinitiators were recorded using a UV-Vis-NIR spectrophotometer (Cary 500, Varian, USA).

Table 1- Tested lights

Name	Code	Manufacturer	Light type	Mode*	Expected irradiance** (mW/cm^2)	Measured irradiance (mW/cm^2)	Recommended curing time ***
BluePhase 16i	B16i	Ivoclar-Vivadent (Schaan, Liechtenstein)	LED 2nd generation	High	1600 +/- 100	1622 (+/-78)	10s
BluePhase G2	BG2	Ivoclar-Vivadent (Schaan, Liechtenstein)	LED 3rd generation	High	1200 +/- 10%	1050 (+/-14)	10s
G-Light	G	GC (Japan)	LED 3rd generation	-	1200	1166 (+/-78)	10 or 20s
Freelight 2	F2	3M-Espe (St. Paul, MN, USA)	LED 2nd generation	-	1000	644 (+/-26)	50% reduction vs conventional halogen
XL3000	X	3M-Espe (St. Paul, MN, USA)	Halogen	-	data not found	544 (+/-17)	40s

* When choice possible between Low & High power mode

** Based on information from the manufacturer

*** For 2mm micro-hybrid composite, at high power when different modes available

6.3.2. Curing efficacy

Two shades of the composite, Tetric Evo Ceram (Ivoclar-Vivadent, Schaan, Liechtenstein), A2 and Bleach XL, were chosen for this study. This choice was based on the differences in their photoinitiating mix. The samples were prepared according to the following procedure: The composite was placed in a cylindrical brass mold 3 mm in diameter and 2 mm in depth, covered by a thin Mylar film, and then light-cured from the upper surface.

Each LCU was applied to photopolymerize samples of both shades for three irradiation times (10, 20 and 40 s). Five samples were prepared for each light/time/shade combination. As microhardness is correlated with the degree of conversion[20,21] polymerization efficacy was assessed by measurements of Vickers microhardness on the upper and lower surfaces of each sample as follows: A 200 g load was applied for 30 s to the upper surface using a Durimet microhardness tester (Leitz, Wetzlar, Germany). The length of the diagonal of each indentation was measured directly using a graduated eye-lens. The Vickers Hardness Number (VHN) is obtained using the following equation: $H = 1854.4 \times P / d^2$, where H is Vickers hardness in kg/mm^2, P is the load in grams and d is the length of the diagonal in μm; note that a null VHN refers to a material too soft to record any value.

6.3.3. Temperature rise in the pulp chamber

A K-type thermocouple was used to monitor the thermal changes in the pulp chamber. The thermocouple measured a potential difference (mV), depending on the temperature difference. The potential difference was recorded and transformed, using a converter (Omega Engineering, USA), into a temperature differential (ΔT) in degrees Celsius (°C) according to the following equation: $\Delta T = a_1 (V-V_r) + a_2 (V^2-V_r^2)$, where a_1 and a_2 are constants, V is the potential difference (mV) at a given time of the measurement, V_r is the potential difference (mV) before measurement when the immersion water is at room temperature.

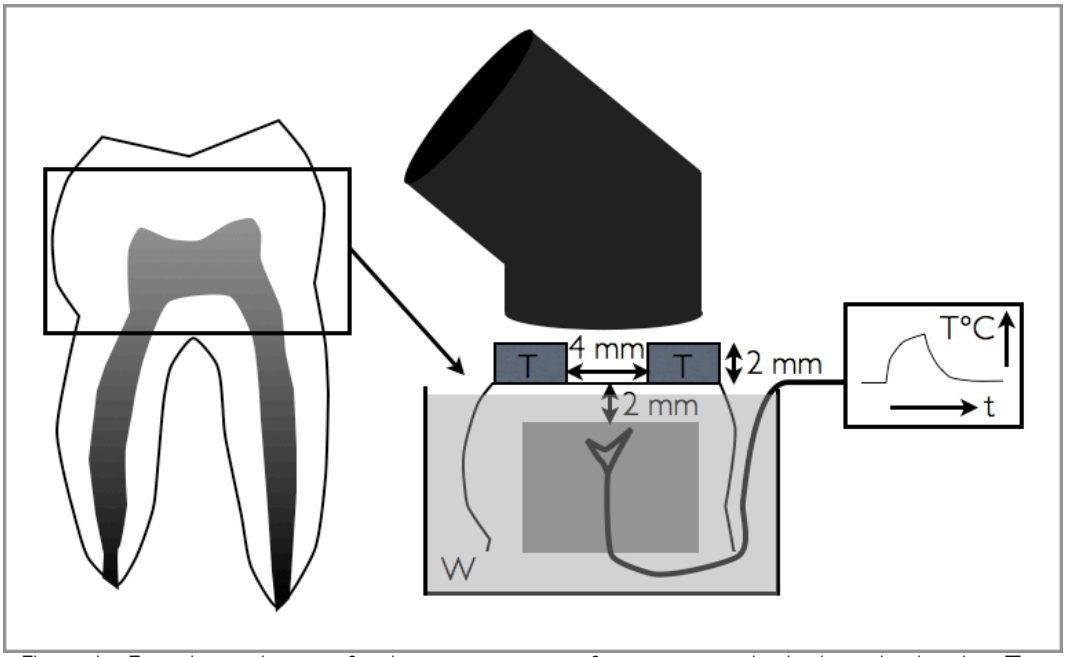

Figure 1 - Experimental set-up for the measurement of temperature rise in the pulp chamber; T = Teflon, W = Water, t = time, T°C = Temperature in degrees Celsius.

The thermocouple was inserted into the pulp chamber of an extracted molar that had been prepared according to the following procedure: After extraction, the tooth was stored in chloramine (0.1% NaCl in purified water). The major part of the root was ground away and the remains of the pulpal tissue were removed. The occlusal face of the tooth was also ground in order to keep 2 mm of dentin between the upper surface and the thermocouple (Fig. 1). During the measurements, the tooth was immersed in water at ambient temperature (23 ± 1°C) so that the pulp chamber was completely filled with water, to simulate the liquid environment of pulpal tissues. All the measurements were performed with the same tooth, to limit any effects of differences in tooth structure, thus enabling the study to concentrate on the differences among the lights. Before each measurement, a Teflon mold (2 mm-thick with a 4 mm-diameter aperture) was placed on the upper tooth surface, which had been dried using a cotton pellet. The increase in temperature during irradiation of the tooth through the aperture for 40 s with each of the 5 lights described in Table 1 was measured. These temperature measurements were performed with an empty cavity and when the cavity was filled with composite, either shade A2 or Bleach. As no adhesive system was used, the composite could easily be removed after each measurement without leaving any significant deposit on the surface. The temperature was recorded during the irradiation and the measurement was extended until ambient temperature (23 ± 1°C) had been regained. The procedure was repeated three times for each combination.

6.3.4. Statistical analysis

A two-way ANOVA ($p < 0.05$) was performed to analyze the influence of the light model and irradiation time on Vickers microhardness at the upper and lower surfaces of the sample. The same test was used to analyze the results of the increase in temperature in the pulp chamber in the three different situations: Uncovered tooth, and polymerization with 2 mm composite shade A2 and with 2 mm Bleach shade.

6.4. Results

The absorption spectra of the photoinitiators (pure CQ and L) and the emission spectra of the lights (relative intensity) are shown in Fig. 2. Based on these results, the LCUs can be divided into three groups: The first group contains the halogen light (X); the second group contains B16i and F2, which are both second generation LEDs, with

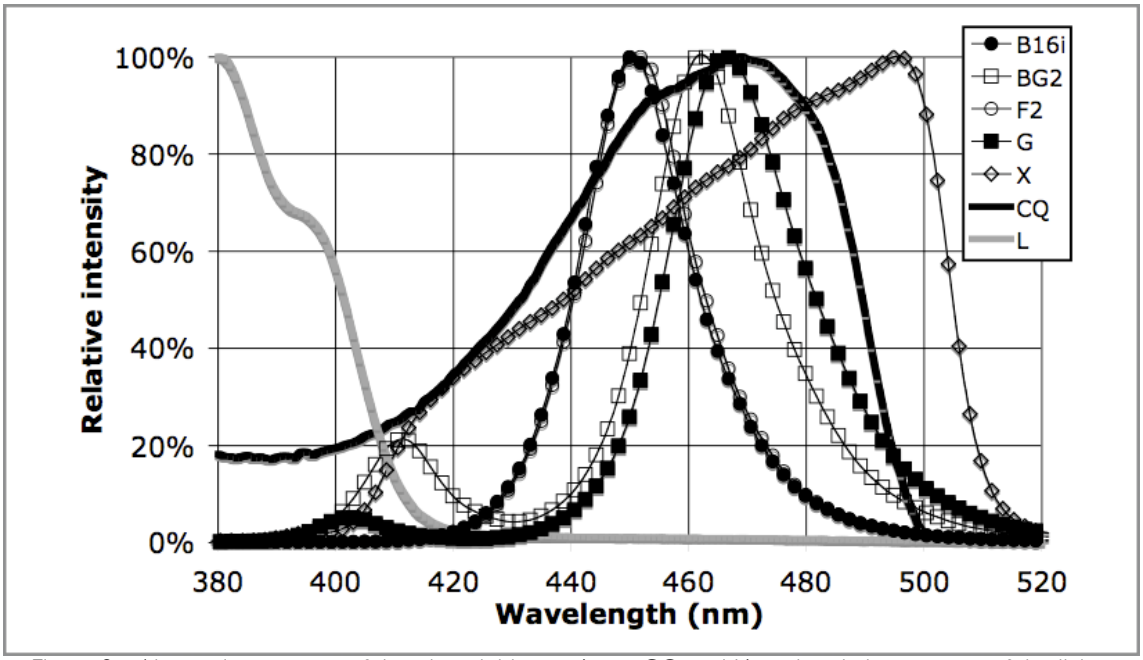

Figure 2 - Absorption spectra of the photoinitiators (pure CQ and L) and emission spectra of the light-curing units (in relative intensity of their respective maximum).

perfectly overlapping spectra, with a peak at 450 nm; the third group contains BG2 and G, which are third generation LED lights with a blue peak much better centered on the maximum absorption peak of CQ, i.e., 467 nm, and a small violet peak. The comparison between the absorption spectra of the photoinitiators and the emission spectra of the lights (Fig. 2) reveals that F2 and B16i should be completely ineffective on L and only effective on CQ. Nevertheless, their emission peak is not centred on the CQ peak of maximum absorption, contrary to G and, to a lesser extent, BG2. B, BG2 and X can excite L thanks to their emission range below 420 nm. The respective power densities measured by the Bluephase meter are shown in Table 1.

For all ANOVA tests performed, analysis of variance displayed $p < 0.001$.

For shade A2 composite, the microhardness values at the upper surface (Fig. 3a) were not very discriminant. All irradiation conditions generated VHN values statistically equal to or better than the standard chosen for this study, i.e., X – 40 s. On the lower surface, at 2 mm (Fig. 3b), the same observation was made, except for F2 – 10 s for which the VHN was statistically lower than the standard. The VHN values for BG2 – 40 s and B16i – 40 s at the upper surface were significantly higher than for the standard. At the lower surface, there were more statistical differences, indicating the importance of the irradiation time deeper in the material. For example, results for G – 10 s, G – 20 s and G – 40 s were statistically identical on the upper surface while they were very different at a depth of 2 mm.

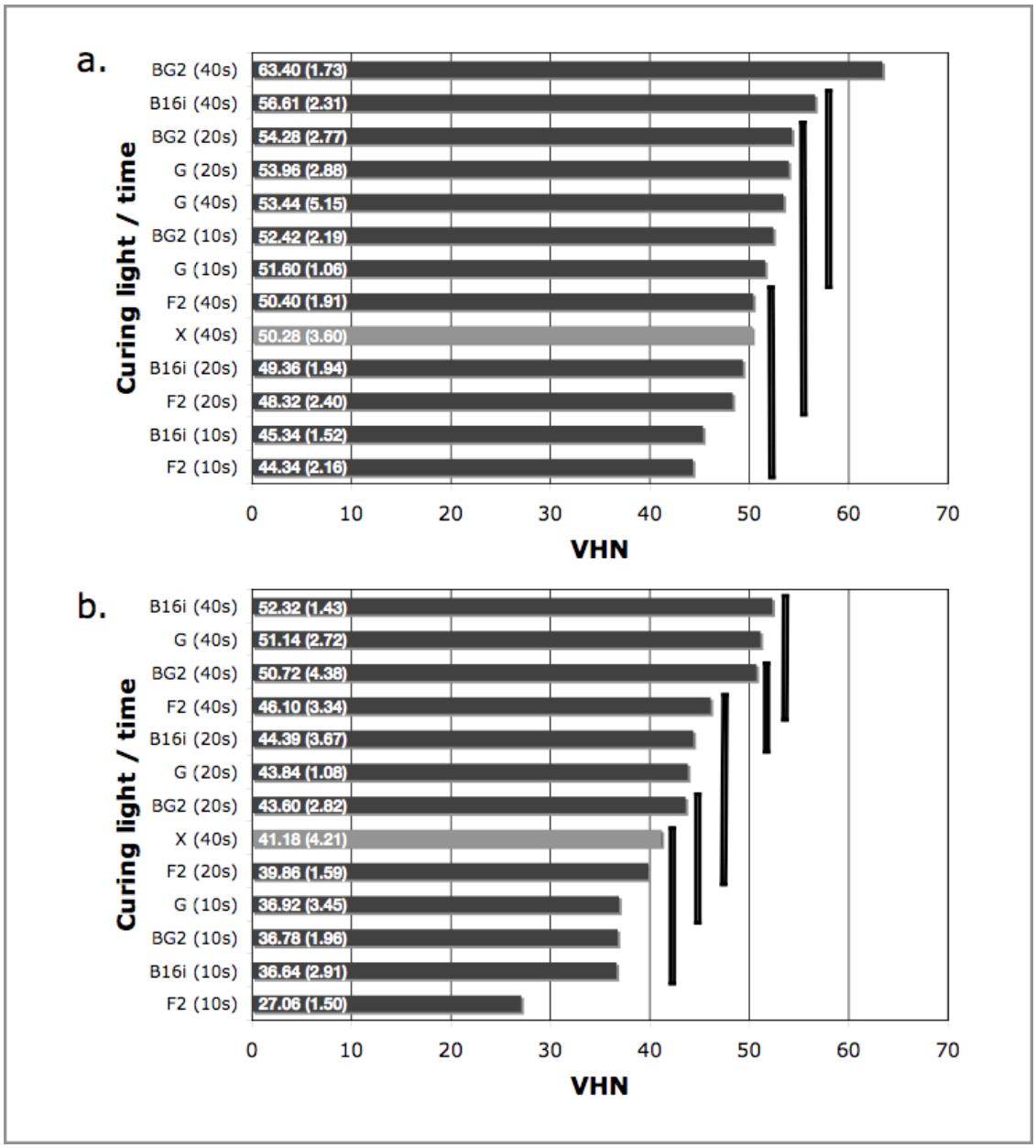

Figure 3 - Vickers microhardness values (VHN) of Tetric Evo Ceram A2 at the upper surface (a) and at 2 mm depth (b) after irradiation with each of the 5 lights for 10, 20 and 40 s. The results for each irradiation condition are ranked in descending order according to their means (n=5); means (+/- standard deviations) are written in white in each horizontal bar. The horizontal bar corresponding to the reference (XL3000, 40 s) is highlighted in light gray. Vertical bars connect materials that are not statistically different ($p<0.05$).

For Bleach shade composite, at the upper surface (Fig. 4a), VHN values for all irradiation times for G and BG2 (10, 20 and 40s) were statistically comparable to the standard, and VHN values for B16i and F2 were significantly less than the standard. At the lower surface (Fig. 4b), the irradiation time was a significant factor, as for shade A2 at this depth. VHN values for G – 10 s and BG2 – 10 s were significantly less than for the standard, as were values for F2 – 10 & 20 s.

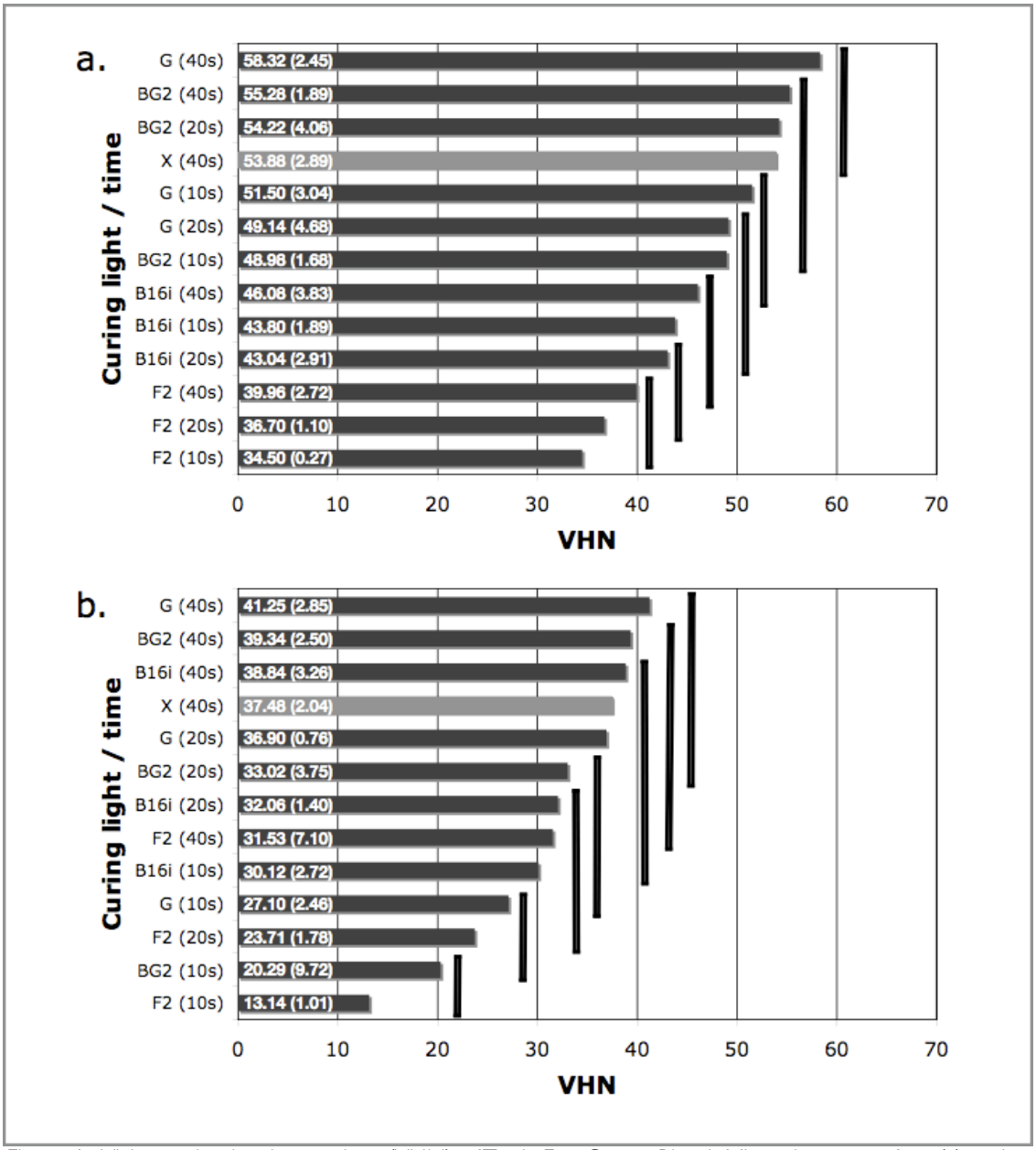

Figure 4 - Vickers microhardness values (VHN) of Tetric Evo Ceram Bleach XL at the top surface (a) and at 2 mm depth (b) after irradiation with each of the 5 lights for 10, 20 and 40 s. The results of each irradiation condition are ranked in descending order according to their means (n=5); means (+/- standard deviations) are written in white in each horizontal bar. The horizontal bar corresponding to the reference light (XL3000, 40 s) is highlighted in light gray. Vertical bars connect materials that are not statistically different ($p<0.05$).

Figure 5 shows the temperature increase in the pulp chamber (ΔT, in °C) associated with the use of each light for 10, 20 and 40 s. In the case of shade A2 (Fig. 5a), the three more powerful lights, i.e., B16i, BG2 and G, induced higher ΔTs when they were used for 40 s. These results were significantly greater than those of X – 40 s, while BG2 and G used for 20 s induced ΔTs that were statistically comparable to those of X – 40 s. For Bleach shade (Fig. 5b), the temperature changes were much lower; only B16i – 40 s and F2 – 40 s induced a ΔT greater than 4°C. These were followed in decreasing order of ΔT by the same lights for 20 s, then by G – 40 s and BG2 – 40 s.

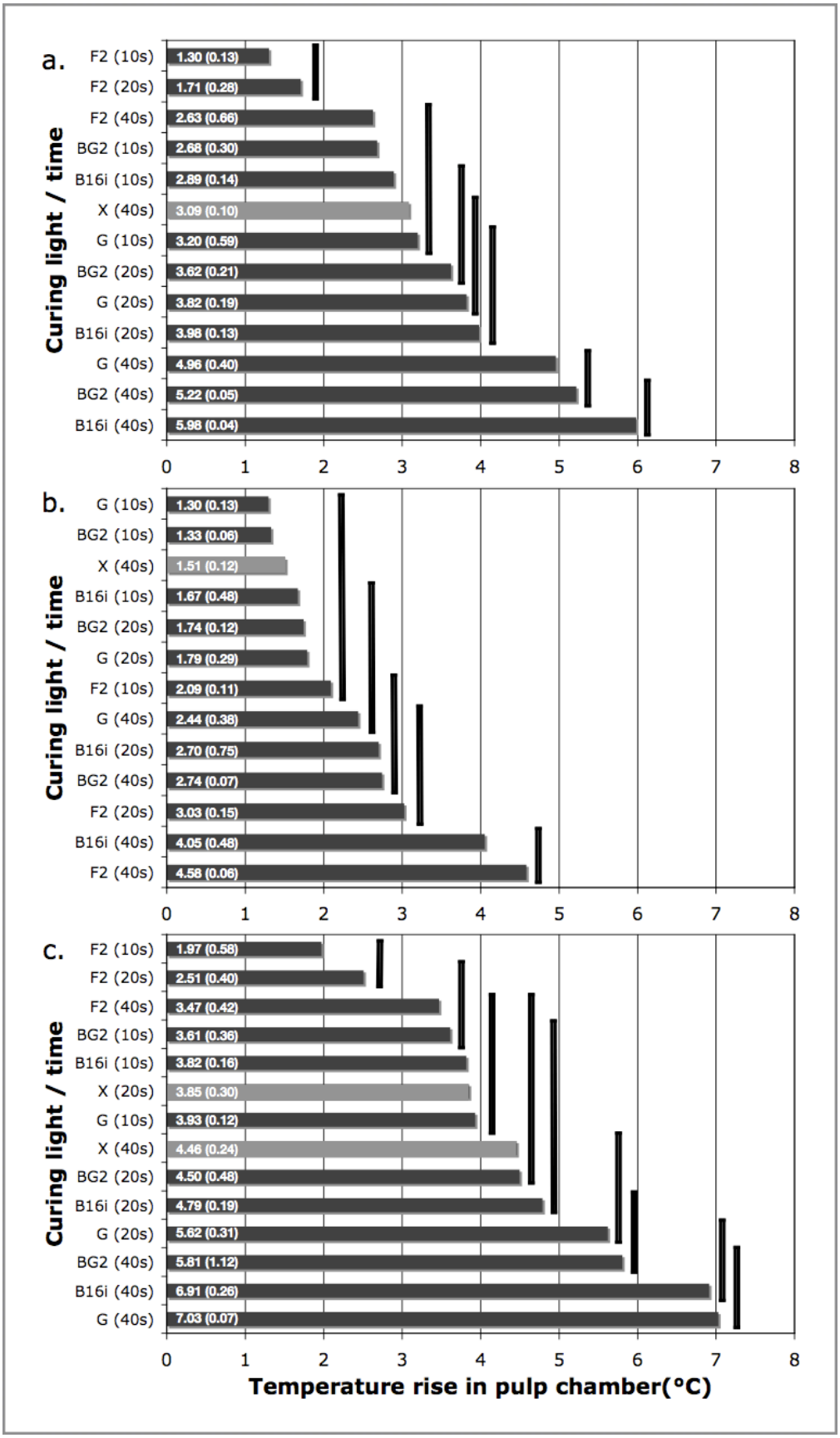

Figure 5 - Increase in pulpal temperature (°C) associated with the use of each light for 10, 20 and 40 s when the tooth was covered by 2 mm Tetric Evo Ceram A2 (a) or Bleach XL (b) during the thermal measurement or left uncovered (c). The results of each irradiation condition are ranked in ascending order according to their means (n=3); means (+/- standard deviations) are written in white in each horizontal bar. The horizontal bars corresponding to the reference light (XL3000, 20 s – time recommended for polymerization of adhesive – and 40 s – time recommended for polymerization of 2 mm composite) are highlighted in light gray. Vertical bars connect materials that are not statistically different ($p<0.05$).

For the uncovered tooth (direct irradiation of the tooth without composite in the mold) (Fig. 5c), the results were close to those seen with shade A2 in order, but about 1°C higher. Comparing Figures 5a, b and c, therefore, highlights the insulating effect of the resin composite; it also demonstrates the influence of the shade and photoinitiator content on this insulating effect as ΔT values with Bleach shade (Fig. 5b) were much lower than those with shade A2 under the same irradiation conditions.

6.5. Discussion

First, we will consider the results achieved using the shade A2 composite, which seem to validate the use of the four LED lights for irradiations of as short as 10 s (except for F2 – 10 s) as an alternative to X – 40 s, the curing protocol recognized as a reference in the literature.[15,16] Nevertheless, some of the irradiation conditions generated microhardness that was significantly greater than that of X –40 s, i.e., G – 40 s (lower surface), BG2 – 40 s and B16i – 40 s (upper/lower surface). This observation is certainly due to the higher power density of these lights in the area of maximum absorption of CQ.[3] Despite the improvement in microhardness, these irradiation conditions (high-power lights for 40 s) can only be validated after consideration of ΔT; this will be discussed below. The comparison between BG2 – 40 s and B16i – 40 s indicates the importance of having a perfect match between the light spectrum and the material spectrum. Despite the much higher power density of B16i compared to BG2, the surface hardness of BG2 – 40 s was greater. This is probably due to the better alignment of the BG2 blue peak on the CQ peak of maximum absorption.[15] In addition, the effect of BG2's additional violet peak on the small amount of L in shade A2 composite must certainly not be neglected. In other words, these results highlight the potential benefits of a combination of both photoinitiators. On the lower surface, at 2 mm, there was a greater variability in the results compared to those obtained at the upper surface. Hence, although shorter irradiation times may be sufficient to polymerize composite at the surface, irradiation time is a critical parameter for deeper polymerization. Furthermore, the positive effect of an increase in power density on the degree of conversion seems to be limited. B16i and F2 can reasonably be compared as their spectra overlap perfectly. On the surface, even though the degree of conversion for B16i – 40 s was statistically higher than that of F2 – 40 s (56.6 versus 50.4), the difference was not proportional to the huge difference in power density (644 mW/cm^2

for F2 versus 1622 mW/cm^2 for B16i), and at a depth of 2 mm there was no statistical difference between B16i – 40 s and F2 – 40s. According to Dewaele et *al.*,[17] at high levels of power density, an additional increase has limited impact on the degree of conversion. The present results confirm that there is probably an optimum power density for a given composite thickness and irradiation time; above this optimum, any excess can potentially have adverse consequences. Every photon that is absorbed by the material heats it, either directly or by the heat of polymerization. As a result, not only should the efficacy in terms of microhardness be considered but also the safety in terms of pulpal heating. This will be addressed later.

The results achieved with the Bleach shade composite will now be discussed. On the surface, the LED lights with spectra that were not effective on the main photoinitiator (L), i.e., F2 and B16i, gave statistically lower VHNs than did the standard. In contrast, BG2 and G were even more effective than the standard, regardless of the polymerization time. The high quantum yield efficiency of lucirin accounts for this observation,[1] and enabled good microhardness results despite the lower intensity of the violet peak of BG2 and G compared to the blue peak. The findings were different at the lower surface. B16i–10, 20 & 40 s and F2 – 40 s had statistically similar results to those of X – 40s, despite the lack of any significant overlap of the spectra of these two lights with lucirin. This is probably an effect of the high molar extinction coefficient of L leading to lower penetration of violet light.[22] In contrast, blue light penetrates deeper into the material due to a lower CQ concentration and molar extinction coefficient. This fact may explain the relatively better efficacy of B16i and F2 on the lower compared to the upper surface. However, these lights should remain a second choice, and lights that have a spectrum better suited to the absorption spectrum of the material, i.e., G and BG2, should be favored. With these two lights, G and BG2, an irradiation time of 20 s seems sufficient as the VHN at 20 s was statistically comparable to that at 40 s (except for G – 40 s surface where a small but significant improvement was observed). Again, ΔT must be considered, which will be discussed below.

Finally, when considering microhardness, the present results question a commonly accepted and frequently cited assumption. According to several authors,[7, 20, 23] an 80% ratio between the hardness of the upper and lower surfaces should be achieved for a satisfactory cure. However, the present results showed significant

differences among the hardness values on the upper surface. Hence, analysis of the photopolymerization efficacy based on the upper/lower ratio has little sense as both values vary. Indeed, an inappropriate curing protocol leading to low absolute conversion values could be validated by a good upper/lower ratio.[15,19] For example, for shade A2 composite, the upper/lower ratios for BG2 – 40 s and X – 40 s were 80% and 82%, respectively. However, BG2 – 40 s produced significantly better upper (63.4 versus 50.28 for X – 40 s) and lower (50.72 versus 41.18 for X – 40 s) microhardness. As the Vickers microhardness is correlated with the degree of conversion,[20,21] the conversion of samples cured with BG2 – 40 s is better than with X – 40s, despite their similar and "acceptable" upper/lower ratios.

From the microhardness results, long irradiation times are clearly of interest as they led to better microhardness on the lower surface. Nevertheless, this positive effect could be partly due to heating of the material by the light.[15] More importantly, the temperature rise in the pulp chamber followed the same trend. According to the frequently cited study of Zach & Cohen,[24] 5.5°C is the limit above which irreversible pulpal lesions can occur, although this value is controversial. More recent observations indeed contradict the results of Zach & Cohen, mostly because the latter were obtained with prolonged exposition.[25] For example, Baldissara *et al*.[26] reported that short-term exposure to thermal increases ranging from 8.9 to 14.7°C did not appear to be a major injurious factor for healthy dental pulps. In any case, it seems reasonable to keep pulpal temperature changes as small as possible. Moreover, it is very difficult to predict the temperature rise in any particular tooth due to multiple variables, including dentin thickness, preparation depth, output intensity and exposure time.[11] As ΔT is inversely correlated with the remaining dentin thickness,[27] practitioners should be aware that in the presence of a thinner dentin layer ΔT values may be higher than those presented in this work. For example, Tjan & Dunn[28] state that the temperature rise recorded at the light guide tip was reduced by between 8 and 48% with interposition of 1 mm dentin and by between 40 and 66% with 2 mm. In the present study, the remaining dentin thickness was set to a standard value of 2 mm to enable us to focus on the choice of LCU and irradiation time and highlight trends related to these variables.

In accordance with Jakubinek *et al*.,[25] the present observations indicate that safety criteria need to be determined. Similarly, Schmaltz and Arenholt-Bindslev[29] state

that data on thermal effects should be available for all marketed LCUs. As there is no consensus on the critical temperature above which pulpal damage can occur, an improvement in mechanical properties (as a result of an increase in power density and/ or time) should only be validated if the associated ΔT is reasonable. Despite the better microhardness values for shade A2 composite obtained with 40 s irradiations with the B16i, BG2 and G lights, the ΔT was significantly higher (nearly twice) than the standard (Fig. 5a). For these lights, when the irradiation time was reduced to 20 s, B16i still induced a significantly higher ΔT than the standard, while for BG2 and G there were no significant differences in ΔT compared to X – 40 s. Therefore, BG2 and G should be preferred and used for a maximum of 20 s for greater safety. However, a time of 40 s could be recommended in endodontically treated teeth. For Bleach shade (Fig. 5b), the ΔTs were much lower than for shade A2, and, therefore, less critical in terms of potential pulp damage. For BG2 and G, the LED lights that were most effective in terms of Bleach shade composite microhardness, ΔTs were lower with 20 s irradiation than with 40 s (non-significantly for BG2). As there was no/little improvement in VHN with 40 s irradiation, 20 s seems preferable. B16i and F2, the spectra of which are not adapted to L, induced the highest ΔTs, close to the 5.5°C threshold when used for 40 s; even with 40 s, the highest VHN was significantly less than that of the standard. These lights should, therefore, not be used with Bleach shade composites.

More generally, it seems that the composite plays an insulatory role, despite the exothermicity of the polymerization reaction.[13, 30] This demonstrates that the heating induced by the light has more impact on the temperature rise in the pulp chamber than the exothermicity occurring as a result of the polymerization reaction of the 2 mm composite. This also confirms that, contrary to what was expected, LEDs have the potential to overheat the pulp. As shown by Asmussen & Peutzfeldt,[10] the temperature rise increases with increasing power density. Thus, compared to shade A2 (Fig. 5a), Bleach shade (Fig. 5b) seems more effective at preventing heating of the pulp chamber. This observation can be explained by two phenomena: First, Bleach shade composite microhardness values were somewhat lower than those of shade A2 composite, suggesting a lower degree of conversion, which can explain the lower exothermicity. However, as stated earlier, the impact of this effect is probably minor. Second, Bleach shade composite is very white, and probably absorbs less light than the more yellow shades. For this reason, it may be useful to place the extra-white composite as the first

layer of the restoration. Note that the thermal values measured here concern the initial and deeper layers of a restoration. Given the insulation effect of the composite, the irradiation time could probably be safely increased for subsequent layers, but this suggestion needs to be verified. Regarding the uncovered tooth (Fig. 5c), the results can approximately be assimilated to the polymerization of the dental adhesive, as its thin nature would not significantly influence the results.[30] It is obvious that the first step of the restoration is probably the most critical for the pulp.[13, 30] Notably, the most powerful light units, B16i, G, and BG2, may represent a risk for the pulp when they are used for 40 s or even for 20 s. Hence, the irradiation time used for these lights should be adapted carefully for the adhesive layer and 10 s seems a safer choice for B16i, BG2 and, especially, for G. In contrast, F2 seems a much safer choice for polymerization of the adhesive layer, as the ΔTs of F2 – 10 s and F2 – 20 s were significantly lower than that of X – 20 s (the protocol usually advised for the adhesive layer with conventional halogen light). This finding certainly favors use of an LED LCU with a lower power density for the polymerization of the adhesive. Of course, the associated adhesion properties also need to be considered, which was not the purpose of this study.

To end up with, it must be reminded that even if dentists want to spend as little time as possible per procedure, they need to be wary of the many claims made by LCU manufacturers. The results of the present paper may help clinicians to better understand the possible adverse consequences (lack of polymerization and temperature rise in the pulp chamber) of their choice of LCU and/or curing parameters to polymerize materials with different absorption characteristics.

6.6. Conclusion

In summary, this study provides valuable information on potential problems related to the use of new LED lights to polymerize composites with different photoinitiating systems. First, we demonstrated that a perfect correspondence between light and material spectra is of prime concern, both to insure optimal polymerization (assessed by microhardness) and to limit heating in the pulp chamber. Manufacturers should, therefore, inform practitioners carefully regarding these spectra. Second, reduction in curing time is feasible as a result of a better-centered spectrum of LED and a higher power density. Nevertheless, despite the limited importance of irradiation time at the surface, time was very important at depth in order to obtain optimum

polymerization. Hence, the potential to reduce irradiation time is limited by the need to maintain VHN values as high as possible, especially at depth. In addition, time, and particularly power density, must be optimized to insure reasonable levels of pulpal heating. Notably, practitioners should remember that the effect of an increase in power density on microhardness is limited, and any excess power density can result in unjustified pulp heating in the same way as spectrum mismatch. In conclusion, the best compromise between microhardness and pulp heating must be sought, and, in this case, this appears to be achieved with G – 20 s and BG2 – 20 s. Note that these times are longer than those recommended by the manufacturers; hence, dentists should be aware that the recommended times are probably minimal times and not necessarily optimal.

6.7. Acknowledgments

J. Leprince thanks the Funds for Scientific Research (F.R.S.-FNRS) for his research fellow position. The authors are grateful to B. Francq from the statistics institute (UCL, Beglium) for his help and to J-F. Bughin for his participation in the experiments. Finally, we would also like to thank the manufacturers who supplied us with lights and composites.

6.8. References

1. Neumann MG, Schmitt CC, Ferreira GC & Correa IC (2006) The initiating radical yields and the efficiency of polymerization for various dental photoinitiators excited by different light curing units Dental Materials 22(6) 576-584
2. Antonson SA, Antonson DE, Hardigan PC (2008) Should my new curing light be an LED? Operative Dentistry 33(4) 400-407
3. Schneider LF, Consani S, Correr-Sobrinho L, Correr AB, Sinhoreti MA (2006) Halogen and LED light curing of composite: temperature increase and Knoop hardness Clinical Oral Investigation 10(1) 66-71
4. Shortall AC (2005) How light source and product shade influence cure depth for a contemporary composite Journal of Oral Rehabilitation 32(12) 906-911
5. Soh MS, Yap AU, Yu T, Shen ZX (2004) Analysis of the degree of conversion of LED and halogen lights using micro-Raman spectroscopy Operative Dentistry 29(5) 571-577

6. Yap AU, Soh MS (2005) Curing efficacy of a new generation high-power LED lamp Operative Dentistry 30(6) 758-763
7. Schattenberg A, Lichtenberg D, Stender E, Willershausen B, Ernst CP (2008) Minimal exposure time of different LED-curing devices Dental Materials 24(8) 1043-1049
8. Price RB, Felix CA (2009) Effect of delivering light in specific narrow bandwidths from 394 to 515nm on the micro-hardness of resin composites Dental Materials In Press
9. Price RB, Felix CA, Andreou P (2006) Third-generation vs a second-generation LED curing light: effect on Knoop microhardness Compendium of Continuing Education in Dentistry 27(9) 490-496
10. Asmussen E, Peutzfeldt A (2005) Temperature rise induced by some light emitting diode and quartz-tungsten-halogen curing units European Journal of Oral Sciences 113(1) 96-98.
11. Vandewalle KS, Roberts HW, Tiba A, Charlton DG (2005) Thermal emission and curing efficiency of LED and halogen curing lights Operative Dentistry 30(2) 257-264
12. Krämer N, Lohbauer U, García-Godoy F, Frankenberger R (2008) Light curing of resin-based composites in the LED era American Journal of Dentistry 21(3) 135-142
13. Millen C, Ormond M, Richardson G, Santini A, Miletic V, Kew P (2007) A study of temperature rise in the pulp chamber during composite polymerization with different light-curing units Journal of Contemporary Dental Practice 8(7) 29-37
14. Daronch M, Rueggeberg FA, De Goes MF, Giudici R (2006) Polymerization Kinetics of Pre-heated Composite Journal of Dental Research 85(1) 38-43
15. Torno V, Soares P, Martin JM, Mazur RF, Souza EM, Vieira S (2008) Effects of irradiance, wavelength, and thermal emission of different light curing units on the Knoop and Vickers hardness of a composite resin Journal of Biomedical Materials Research Part B: Applied Biomaterials 85(1) 166-171
16. Peutzfeldt A., Asmussen E (2005) Resin composite properties and energy density of light cure Journal of Dental Research 84(7) 659-662
17. Dewaele M, Asmussen E, Peutzfeldt A, Munksgaard EC, Benetti AR, Finné G, Leloup G, Devaux J (2009) Influence of curing protocol on selected properties of

light-curing polymers. I. Degree of conversion, volume contraction, elastic modulus and glass transition temperature Dental Materials In Press

18. Feng L, Carvalho R, Suh BI (2009) Insufficient cure under the condition of high irradiance and short irradiation time Dental Materials 25(3) 283-289
19. Palin WM, Senyilmaz DP, Marquis PM, Shortall AC (2008) Cure width potential for MOD resin composite molar restorations Dental Materials 24(8) 1083-1094
20. Bouschlicher MR, Rueggeberg FA, Wilson BM (2004) Correlation of bottom-to-top surface microhardness and conversion ratios for a variety of resin composite compositions Operative Dentistry 29(6) 698-704
21. Rode KM, Kawano Y, Turbino ML (2007) Evaluation of curing light distance on resin composite microhardness and polymerization Operative Dentistry 32(6) 571-578
22. Neumann MG, Miranda WG Jr, Schmitt CC, Rueggeberg FA, Correa IC (2005) Molar extinction coefficients and the photon absorption efficiency of dental photoinitiators and light curing units Journal of Dentistry 33(6) 525-532
23. Price RB, Felix CA, Andreou P (2005) Knoop hardness of ten resin composites irradiated with high-power LED and quartz-tungsten-halogen lights Biomaterials 26(15) 2631-2641.
24. Zach L, Cohen G (1965) Pulp response to externally applied heat Oral Surgery, Oral Medicine and Oral Pathology 19 515–530
25. Jakubinek MB, O'Neill C, Felix C, Price RB, White MA (2008) Temperature excursions at the pulp-dentin junction during the curing of light-activated dental restorations Dental Materials 24(11) 1468-1476
26. Baldissara P, Catapano S, Scotti R (1997) Clinical and histological evaluation of thermal injury thresholds in human teeth: a preliminary study Journal of Oral Rehabilitation 24(11) 791-801
27. Yazici AR, Muftu A, Kugel G, Perry RD (2006) Comparison of temperature changes in the pulp chamber induced by various light curing units in vitro Operative Dentistry 31(2) 261-265
28. Tjan AH, Dunn JR (1988) Temperature rise produced by various visible light generators through dentinal barriers Journal of Prosthetic Dentistry 59(4) 433-438
29. Schmaltz G & Arenholt-Bindslev D (2009) Biocompatibility of Dental Materials Springer-Verlag Berlin Heidelberg, Germany

30. Stewardson DA, Shortall AC, Harrington E, Lumley PJ (2004) Thermal changes and cure depths associated with a high intensity light activation unit Journal of Dentistry 32(8) 643-651

Chapter 7

Irradiation Modes Impact on Radical Entrapment in Photoactive Resins

Julian Leprince*, Guillaume Lamblin*, Jacques Devaux, Magali Dewaele, Michèle Mestdagh, William M Palin, Bernard Gallez, Gaëtane Leloup

Submitted to

Journal of Dental Research

*Both authors contributed equally to this work

7.1. Summary

Different irradiation protocols are proposed to polymerize dental resins and discordances remain concerning their impact on the material. To improve this knowledge, we studied entrapment of free radicals in unfilled Bis-GMA/TEGDMA (50:50 wt%) resin after light cure. The tested hypothesis was that various irradiation parameters (curing time, irradiance and radiant exposure) and different irradiation modes (continuous and pulse-delay) led to different amounts of trapped free radicals. The analysis of cured samples (n=3) by electron paramagnetic resonance (EPR) revealed that the concentration of trapped free radicals significantly differed according to the curing protocol. Comparing continuous modes with similar radiant exposure, higher concentrations of trapped free radicals were measured for longer time with lower irradiance. Concerning pulse modes, the delay had no influence on trapped radical concentration. These results give new insights into the understanding of the photopolymerization process and highlight the relevance of using EPR when studying polymerization of dimethacrylate-based materials.

7.2. Introduction

In modern dentistry, photopolymerizable resin-based composites have become the choice material for the direct restoration of damaged teeth. However, despite significant material improvements since their introduction, several drawbacks such as inadequate curing depths and deleterious effects of polymerization shrinkage stress remain. In an attempt to overcome these deficiencies various material aspects have been investigated such as inorganic filler content, resin formulation, curing light technology and photoinitiation protocols. In the latter field, despite the large number of studies analyzing the effects of various initiation modes on the properties of photoactive materials, discrepancies within the literature remain. Globally, two main goals are pursued. Firstly, there exists a demand for reduction in curing exposure to minimize chairside procedure times of multi-increment resin composite restorations. Accordingly, several researchers support the exposure reciprocity law (Emami *et al.*, 2006; Price *et al*., 2004; Sakaguchi and Ferracane, 2001; Halvorson *et al*., 2002), claiming that radiant exposure (RE, J/cm^2), the product of irradiance (I, mW/cm^2) and exposure time (t, s), is the main determining factor of the degree of conversion and mechanical properties of the photoactive material. This supposes reciprocity between I and t, and encourages a tendency among dentists and manufacturers to use or suggest a high-power illumination in order to reduce curing time. However, other studies (Asmussen and Peutzfeldt, 2005; Peutzfeldt and Asmussen 2005; Musanje and Darvell, 2003; Dewaele *et al*., 2009) have reported that although RE plays an important role, I and t independently influence polymer chain length, extent of crosslinking and mechanical properties, and as such, exposure reciprocity does not hold under all conditions. Secondly, the use of "soft-start" curing protocols was proposed to delay the onset of polymer gelation. Notably, pulse-delay modes (consisting in a short flash of light followed by a delay before the final polymerization) seem to contribute to a reduction of polymerization shrinkage stress (Chye *et al.*, 2005; Cunha *et al.*, 2008; Kanca and Suh, 2004; Soh *et al.*, 2004). Nevertheless, some authors have also highlighted lower conversion values and/or inferior mechanical properties of composites cured using those modes (Benetti *et al*., 2007; Asmussen and Peutzfeldt, 2001 and 2003; Lu *et al*., 2005; Dewaele *et al*., 2009). Although the use of alternative illumination methods may provide certain advantages, their effect on polymerization mechanisms and final polymer characteristics are poorly understood.

One interesting approach to better grasp the chemical process of photopolymerization is the observation of trapped free radical concentration. It has been previously demonstrated that vitrified dental resins contain two types of trapped free radicals ($R^{\bullet}_{Trapped}$), which are detectable by electron paramagnetic resonance (EPR), namely a "propagating" radical and an allylic radical type (Fig. 1) (Truffier-Boutry *et al.*, 2003). The study of $R^{\bullet}_{Trapped}$ is particularly relevant regarding dimethacrylate-based resins as their polymerization leads to highly crosslinked networks, where monomolecular termination, as a consequence of radical entrapment, becomes the dominant pathway (Andrzejewska, 2001). A strong relationship between autoacceleration and radical trapping was also suggested (Zhu *et al.*, 1990). This highlights the importance of considering the amount of trapped radicals when studying the impact of photoirradiation protocols, which to our knowledge, has never been investigated with clinically relevant irradiation parameters. For that reason, the aim of this paper was to test the null hypothesis that no difference in concentrations of $R^{\bullet}_{Trapped}$ existed between samples cured at similar RE but different I and t, with or without a delay.

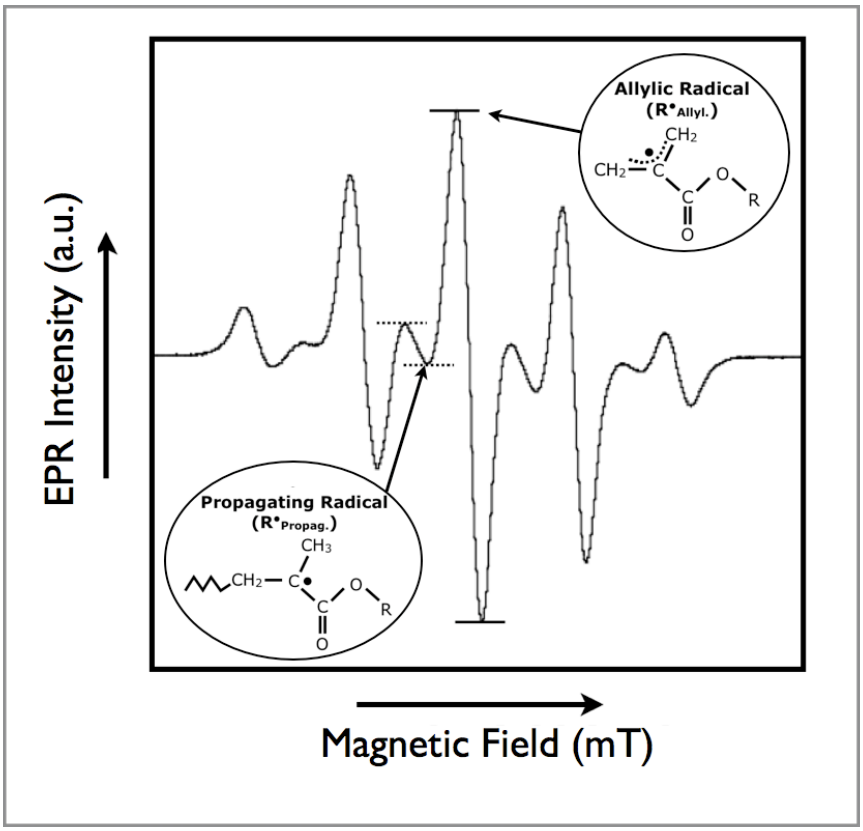

Figure 1 - 9-line EPR spectrum of experimental resin after polymerization and chemical structure of both radical species. R stands either for a pendant monomer, i.e. Bis-GMA or TEGDMA, carrying the second and unreacted methacrylated group, or for a polymer chain. The respective intensities of both radical species were assessed by the measurement of peaks indicated by arrows.

7.3. Materials and Methods

Bisphenol A glycidyl dimethacrylate (Bis-GMA) (Heraeus Kulzer, Wehrheim, Germany) and triethylene glycol dimethacrylate (TEGDMA) (Aldrich, Belgium) were used without further purification from the supplier and mixed in an equimolar concentration. A photoinitiator system comprising of 0.5 mass% camphorquinone (CQ; Aldrich, Belgium) and 0.5 mass% of N,N-dimethyl-p-aminobenzoic acid ethyl ester (DABE, Aldrich) was incorporated into the resin. The resin was placed in a rectangular brass mould (7 x 1 x 1 mm), covered with Mylar film and cured (at 23 ± 1°C) with a halogen light (Optilux 501, Demetron/Kerr Co., Orange, CA, USA) with the curing tip (8 mm exit diameter) centrally placed on the mould, in contact with the film. Two different illumination modes were used: continuous and pulse-delay (1 second cure, 1 – 2 or 3 min delay, final cure), for which t and I were adapted so that only two different REs of 6 and 12 J/cm^2 were obtained (Table 1). A rheostat was used to achieve 3 specific irradiances (150, 300 and 600 mW/cm^2) that were verified using a differential scanning calorimeter (DSC822, Mettler Toledo, Zaventem, Belgium) equipped for in situ irradiation. An aluminum crucible filled with black graphite powder was irradiated to insure complete absorption of emitted photons, while the other crucible was left empty and not irradiated. Following irradiation, specimens (n = 3) were carefully stored in a lightproof container between subsequent measurements and recovered for analysis by EPR (MiniScope MS200 with rectangular resonator TE102, Magnettech, Berlin, Germany) 5 min, 1 to 6 h, 1 day, 1, 2 and 3 months post irradiation. An alignment device was used to ensure an identical position of the sample in the EPR cavity, enabling accurate comparisons of the peak intensities. EPR parameters consisted of: center field, 3367.42 G; frequency, 9.30 – 9.55 GHz; sweep width, 198.40 G; modulation amplitude 1 G, microwave power, 0.5 mW. As peak width did not significantly vary with time, measurement of the height of some EPR peaks could be used to determine the relative concentration of $R\bullet_{Trapped}$: height of the fifth (from 334,9 to 335,5 mT) and fourth peaks (from 336,1 to 336,6 mT of the magnetic field) of the 9-line spectrum for allylic ($R\bullet_{Allyl}$) and propagating radicals ($R\bullet_{Propag}$), respectively (Fig. 1). These peaks are least influenced by the signal of the other radical types. Concentrations of $R\bullet_{Trapped}$ at each storage time were analyzed by one-way ANOVA and Tukey's test ($p = 0.05$).

7.4. Results

Figures 2a and 2b present the evolution of $R\bullet_{Trapped}$ concentrations with time for the continuous modes for $R\bullet_{Allyl}$ and $R\bullet_{Propag}$, respectively. The curves of both radical species display similar profiles (logarithmic time scale), except during approximately the first 4 h, where concentrations of $R\bullet_{Propag}$ decreased at higher rates compared with $R\bullet_{Allyl.}$, which is further highlighted in Figure 2c. As it can be observed on Figures 2a and 2b, the curves are parallel during the first 24 hours. Therefore, the results and statistical analyses for both radical types will only be displayed for 5 minutes and 24 hours storage periods (Table 1). In the same way, as pulse-mode curves showed similar profiles to continuous-mode curves, but overlapped with them, they were not displayed here for more clarity. Nevertheless, values and statistical analyses that were not reported in the manuscript are available within the Appendix. In Table 1 was also reported the mean degree of conversion of each mode (published data from Dewaele *et al.*, 2009; they were obtained with the same resin and same irradiation protocols, and are reproduced here for the reader convenience). Generally, as it can be observed in Fig. 2a, 2b and Table 1, increased concentrations of $R\bullet_{Trapped}$ were measured for continuous mode curing regimes following higher (12 J/cm^2) compared with lower RE (6 J/cm^2). However, the amount of $R\bullet_{Trapped}$ generated by 20 s x 600 mW/cm2 (12 J/cm^2) and 40 s x 150 mW/cm^2 (6 J/cm^2) were not significantly different ($p > 0.05$). Moreover, while the increase in concentration of both radicals is significant ($p < 0.05$) when using twice the exposure time (40 s x 150 mW/cm^2 to 80 s x 150 mW/cm^2 and 20s x 300 mW/cm^2 to 40 s x 300 mW/cm^2), it is not significant ($p > 0.05$) when applying twice the irradiance (40 s x 150 mW/cm^2 to 40 s x 300 mW/cm^2 and 20s x 300 mW/cm^2 to 20 s x 600 mW/cm^2). Comparing continuous modes with similar RE, higher concentrations of $R\bullet_{Trapped}$ were measured for longer exposure time with lower irradiance. There was no influence of the delay time on the concentration of $R\bullet_{Trapped}$, for either the application of a 1, 2 or 3 minute delay or when comparing pulse delay with continuous mode for the same RE (Table 1).

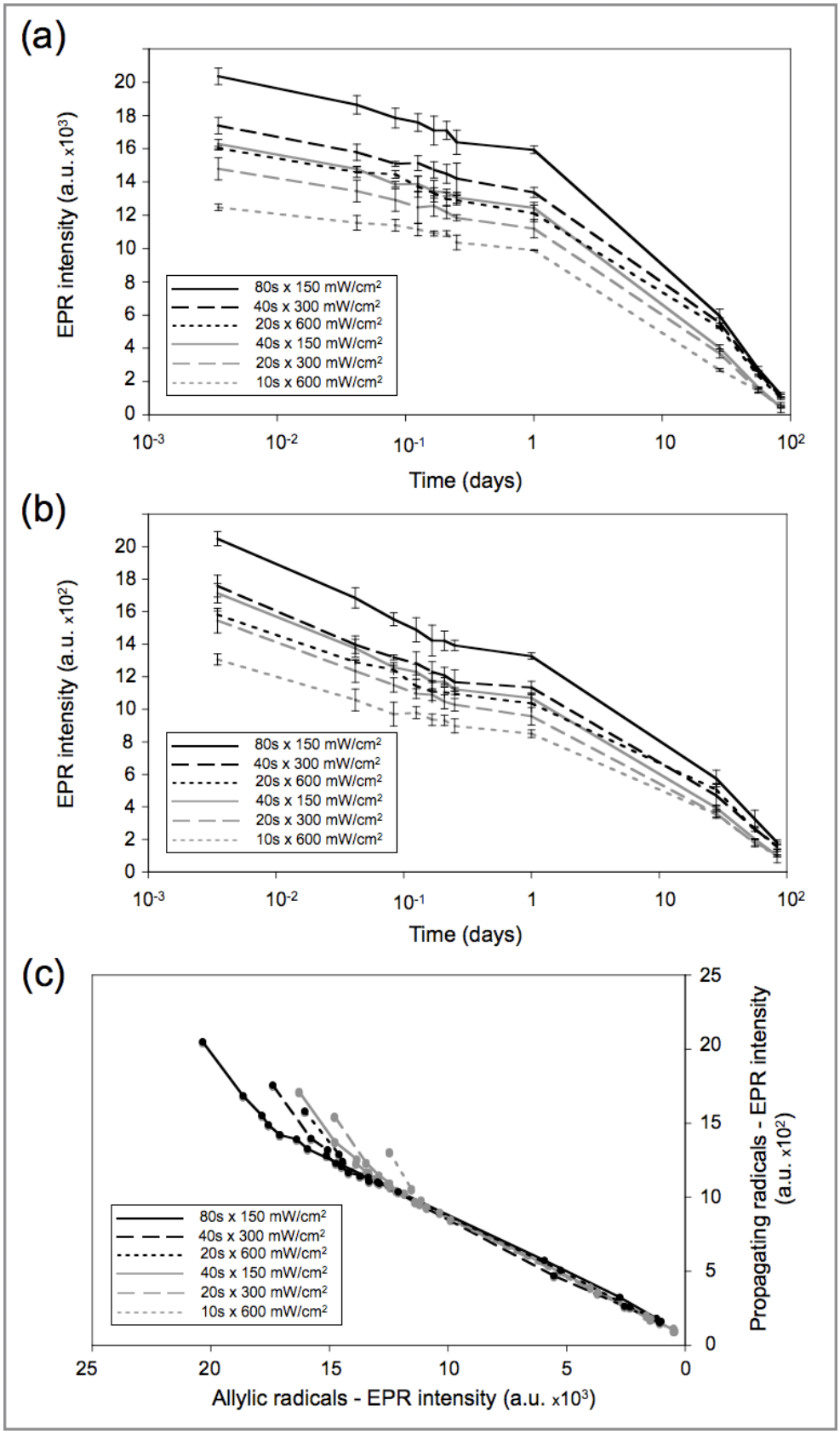

Figure 2 - Concentration (in a.u., n = 3) of allylic radical (a) and propagating radical (b) as a function of time (means +/- SD at 5 minutes, 1 to 6 hours, 1 day and 1 to 3 months – logarithmic scale) or one radical species as a function of the other (c) for continous-modes. Due to similar but overlapping profiles, pulse-mode curves were not displayed here for more clarity. Black lines represent modes of 12 J/cm^2 and grey lines modes of 6 J/cm^2. In Figure c, each point indicates the respective concentrations of both radical types at a given time.

Table 1

Modes	Radiant Exposure (J/cm²)	Trapped radicals concentration (a.u.)				DC (%; mean +/- sd)*
		Allylic Radicals		Propagating Radicals		
		5 min (mean +/- sd)	24 hours (mean +/- sd)	5 min (mean +/- sd)	24 hours (mean +/- sd)	
80s x 150 mW/cm²	12	20353 (496)^{a}	15933 (227)^{a}	2049 (44)^{a}	1327 (20)^{a}	71 (2.0)
40s x 300 mW/cm²	12	17393 (498)^{b}	13372 (302)^{b,c}	1758 (68)^{b}	1135 (37)^{b,c,d}	72 (3.3)
1s - (1min) - 39s x 300 mW/cm²	12	17456 (531)^{b}	13779 (315)^{b}	1678 (28)^{b,c}	1178 (28)^{a,b,c}	63 (1.8)
1s - (2min) - 39s x 300 mW/cm²	12	17629 (439)^{b}	14271 (106)^{b}	1753 (56)^{b}	1189 (15)^{a,b}	64 (3.2)
1s - (3min) - 39s x 300 mW/cm²	12	17402 (808)^{b}	13341 (575)^{b,c}	1730 (89)^{b,c}	1122 (32)^{b,c,d}	66 (1.8)
20s x 600 mW/cm²	12	16039 (114)^{b,c,d,e}	12106 (500)^{d,e}	1582 (22)^{b,c,d}	1037 (52)^{b,c,d,e,f,g}	69 (7.4)
1s - (1min) - 19s x 600 mW/cm²	12	16470 (225)^{b,c,d}	12317 (225)^{c,d,e}	1556 (170)^{b,c,d,e}	1035 (15)^{c,d,e,f,g}	65 (2.5)
1s - (2min) - 19s x 600 mW/cm²	12	16800 (278)^{b,c}	12567 (236)^{c,d}	1589 (59)^{b,c,d}	1089 (40)^{b,c,d,e}	65 (0.8)
1s - (3min) - 19s x 600 mW/cm²	12	15636 (76)^{c,d,e,f}	11483 (76)^{d,e,f}	1519 (148)^{b,c,d,e}	996 (110)^{d,e,f,g,h}	65 (4.2)
40s x 150 mW/cm²	6	16288 (274)^{b,c,d,e}	12440 (336)^{c,d}	1714 (59)^{b,c}	1069 (31)^{b,c,d,e,f}	69 (2.9)
20s x 300 mW/cm²	6	14792 (659)^{e,f,g}	11199 (548)^{e,f}	1546 (76)^{b,c,d,e}	957 (54)^{e,f,g,h}	68 (2.6)
1s - (1min) - 19s x 300 mW/cm²	6	13947 (894)^{g,h}	10762 (487)^{f,g,h}	1499 (59)^{c,d,e,f}	925 (50)^{f,g,h,i}	62 (1.5)
1s - (2min) - 19s x 300 mW/cm²	6	15145 (783)^{d,e,f,g}	11424 (475)^{d,e,f}	1615 (103)^{b,c}	1017 (23)^{d,e,f,g}	63 (0.4)
1s - (3min) - 19s x 300 mW/cm²	6	14373 (895)^{f,g}	10854 (524)^{f,g}	1495 (52)^{c,d,e,f}	954 (35)^{e,f,g,h}	61 (1.3)
10s x 600 mW/cm²	6	12477 (198)^{h,i}	9900 (20)^{g,h,i}	1306 (33)^{e,f,g}	850 (24)^{h,i}	65 (0.5)
1s - (1min) - 9s x 600 mW/cm²	6	11994 (170)^{i}	9565 (165)^{h,i,j}	1348 (79)^{d,e,f,g}	864 (34)^{h,i}	60 (4.0)
1s - (2min) - 9s x 600 mW/cm²	6	11218 (579)^{i}	8594 (553)^{j}	1158 (80)^{g}	792 (74)^{i}	61 (3.9)
1s - (3min) - 9s x 600 mW/cm²	6	11747 (458)^{i}	8799 (612)^{i,j}	1289 (89)^{g}	900 (93)^{g,h,i}	61 (1.1)

Similar letters connect values that are not significantly different.
*Data from Dewaele *et al.*, 2009

7.5. Discussion

The two distinct phases of radical concentration highlighting the decrease of $R\bullet_{Trapped}$ following polymerization (Fig 2a and 2b) are in accordance with previous work (Truffier-Boutry *et al.*, 2006, Leprince *et al.*, 2009). The decrease in R•Trapped from 0 to 24 h was attributed to post-cure volumetric shrinkage (Truffier-Boutry *et al.*, 2006) whereas from 24 h to 3 months the effect of oxidation by atmospheric oxygen may play a more significant role in the reduction of radical concentration (Leprince *et al.*, 2009). As two radical species are considered, the relationship between both species requires clarification. From what appears on Fig. 2c, $R\bullet_{Propag}$ concentrations decrease at higher rates than $R\bullet_{Allyl}$ during the first 4 hours. As mentioned above, during approximately the first 24 hours after light cure, volumetric shrinkage occurs. As a result, $R\bullet_{Trapped}$ move closer to each other and the probability of termination increases due to shrinkage (Truffier-Boutry *et al.*, 2006). But whilst $R\bullet_{Allyl}$ are unable to react with species other than free radicals (higher stability due to a resonance phenomenon, Fig. 1), $R\bullet_{Propag}$ exhibit sufficient reactivity to interact also with remaining double bonds. In this way, additional propagation reactions can repeat locally, slightly increasing DC (Truffier-Boutry *et al.*, 2006) and local radical mobility, leading to some bimolecular radical termination through reaction-diffusion controlled termination mechanism (Anseth *et al.*, 1995).

Regarding the comparison of free radical concentrations, the period from 5 minutes to 1 day post-cure should be considered, since radical concentration within this timeframe remains proportional between curing regimes. For continuous curing modes, the increase in $R\bullet_{Trapped}$ concentration following twice the RE, either by doubling I or t (Figures 2a and 2b, Table 1), can be explained by the creation of a higher concentration of free radicals (generated by an increase in number of photons), which are more likely to become trapped. However, for similar RE, higher concentrations of $R\bullet_{Trapped}$ were measured for longer t and lower I. This observation is in apparent contradiction with the reciprocity observed between I and t for CQ quantum yield of conversion (number of converted photoinitiator molecules per number of absorbed photons) (Chen *et al*., 2007). However, even if the same total amount of radicals are created, it does not necessarily result in the same number entrapped. This can be explained by considering both types of termination mechanism co-existing during polymerization (Lovell *et al*., 1999): while bimolecular termination probably prevails during the very initial stages of the reaction, monomolecular termination (first-order) dominates when molecular diffusion becomes limited (autoacceleration). There is probably a loss of a given amount of radicals during the early stages by bimolecular termination. This loss (or early termination) is higher for high irradiance protocols, as termination is proportional to $[R\bullet]^2$. As a result, at constant RE but higher I and shorter t, the amount of growth centers created during auto-acceleration is lower, leading to a lower final concentration of $R\bullet_{Trapped}$. In other words, the amount of $R\bullet_{Trapped}$ measured in the present work may provide an indication of the quantity of growth centers created during auto-acceleration. In light of theses results, the use of EPR to measure $R\bullet_{Trapped}$ gives valuable information on monomolecular termination, which is critical in highly crosslinked systems. Other recent work has suggested that the applicability of exposure reciprocity law depends on the other factors than irradiation parameters alone, such as Bis-GMA/TEGDMA ratio (Feng and Suh, 2007) and the efficiency of the photoinitiator (Leprince *et al*., 2009). Prospectively, the measurement of $R\bullet_{Trapped}$ will be very useful in further understanding complex photopolymerization processes and related experiments are ongoing by the authors.

For pulse-delay modes, no influence of any delay time (1, 2 or 3 minutes with no irradiation) was observed on the concentration of $R\bullet_{Trapped}$ or compared with continuous mode curing with similar RE (Table 1). However, DC values associated

with pulse-delay protocols were lower than those associated with the continuous mode of similar RE (Table 1; Dewaele *et al.*, 2009), which can be explained by differences in polymer chain growth. The initial pulse probably results in microgels with relatively linear polymer chains (few pendant double bonds available) (Poshusta *et al*., 2002; Dewaele *et al*., 2009) and where most free radicals probably terminated. During final irradiation, these microgel regions, in which unreacted double bonds are less available are certainly less reactive. Therefore, they may disturb the polymerization reaction compared with a continuous irradiation, leading to reduced DC. However, as discussed above, most of the free radicals are trapped when propagation becomes diffusion-controlled. Therefore, it might be assumed that the irradiation parameters at the time of auto-acceleration govern the final amount of trapped radicals, leading to comparable amounts of $R\bullet_{Trapped}$ with or without a delay.

In conclusion, for continuous modes, the null hypothesis must be rejected as the concentrations of $R\bullet_{Trapped}$ between samples not only depend on RE but also on I and t. Conversely, regarding pulse-delay mode, the null hypothesis cannot be rejected, as the presence of a delay does not have a significant influence on the concentrations of $R\bullet_{Trapped}$ when compared to the equivalent continuous mode of same irradiance and total irradiation time.

7.6. Acknowledgments

J. Leprince thanks the Belgian National Funds of Scientific Research (FNRS) for his fellow researcher position.

7.7. References

Andrzejewska E (2001). Photopolymerization kinetics of multifunctional monomers. Prog Polym 26:605-665.

Anseth KS, Newman SM, Bowman CN (1995). Polymeric dental composites: properties and reaction behavior of multimethacrylate dental restorations. Ad Polym Sc 122:177-217.

Asmussen E and Peutzfeldt A (2001). Influence of pulse-delay curing on softening of polymer structures. J Dent Res 80:1570-1573.

Asmussen E and Peutzfeldt A (2005). Polymerization contraction of resin composite vs. energy and power denstity of light-cure. Eur J Oral Sci 113:417-421.

Asmussen E and Peutzfeldt A (2003). Two-step curing: influence on conversion and softening of a dental polymer. Dent Mater 19:466-470.

Benetti AR, Asmussen E, Peutzfeldt A (2007). Influence of curing rate of resin composite on the bond strength to dentin. Oper Dent 32:144-148.

Chen YC, Ferracane JL, Prahl SA (2007). Quantum yield of converion of the photoinitiator camphorquinone. Dent Mater 23:655-654.

Chye CH, Yap AU, Laim YC, Soh MS (2005). Post-gel polymerization shrinkage associated with different light curing regimens. Oper Dent 30:474-480.

Cunha LG, Alonso RC, Pfeifer CS, Correr-Sobrinho L, Ferracane JL, Sinhoreti MA (2008). Contraction stress and physical properties development of a resin-based composite irradiated using modulated curing methods at two C-factor levels. Dent Mater 24:392-398.

Dewaele M, Asmussen E, Peutzfeldt A, Munksgaard EC, Benetti AR, Finné G et al. (2009). Influence of curing protocol on selected properties of light-curing polymers: degree of conversion, volume contraction, elastic modulus, and glass transition temperature. Dent Mater 25:1576-1584.

Emami N and Söderholm KJ (2003). How light irradiance and curing time affect monomer conversion in light-cured resin composites. Eur J Oral Sci 111:536-542.

Feng and Suh (2007). Exposure reciprocity law in photopolymerization of multi-functional acrylates and methacrylates. Macromol Chem Phys 208:295-306.

Halvorson RH, Erickson RL, Davidson CL (2002). Energy dependent polymerization of resin-based composite. Dent Mater 18:463-469.

Kanca J 3rd and Suh BI (1999). Pulse activation: reducing resin-based composite contraction stresses at the enamel cavosurface margins. Am J Dent 12:107-112.

Leprince J, Hadis M, Ferracane JL, Shortall AC, Leloup G, Palin WM (2009). Lucirin-TPO: Photoinitiator Reactivity and Curing Time Reduction. Abstract of ADM meeting Portland 29-30-31st october 2009

Leprince J, Lamblin G, Truffier-Boutry D, Demoustier-Champagne S, Devaux J, Mestdagh M et al. (2009). Kinetic study of free radicals trapped in dental resins stored in different environments. Acta Biomater 5:2518-2524.

Lovell LG, Newman SM, Bowman CN (1999). The effects of light intensity, temperature, and comonomer composition on the polymerization behavior of dimethacrylate dental resins. J Dent Res 78:1469-1476.

Lu H, Stansbury JW, Bowman CN (2005). Impact of curing protocol on conversion and shrinkage stress. J Dent Res 84:822-826.

Musanje L and Darvell BW (2003). Polymerization of resin composite restorative materials: exposure reciprocity. Dent Mater 19:531-541.

Peutzfeldt A and Asmussen E (2005). Resin composite properties and energy density of light cure. J Dent Res 84:659-662.

Poshusta AK, Bowman CN, Anseth KS (2002). Application of a kinetic gelation simulation to the characterization of in situ cross-linking biomaterials. J Biomater Sci Polym Ed 13:797-815.

Price RB, Felix CA, Andreou P (2004). Effects of resin composite composition and irradiation distance on the performance of curing lights. Biomaterials 25:4465-4477.

Sakaguchi RL and Ferracane JL (2001). Effect of light power density on development of elastic modulus of a model light-activated composite during polymerization. J Esthet Restor Dent 13:121-130.

Soh MS, Yap AU, Siow KS (2004). Post-gel shrinkage with different modes of LED and halogen light curing units. Oper Dent 29:317-324.

Truffier-Boutry D, Demoustier-Champagne S, Devaux J, Biebuyck JJ, Mestdagh M, Larbanois P et al. (2006). A physico-chemical explanation of the post-polymerisation shrinkage in dental resins. Dent Mater 22:405-412.

Truffier-Boutry D, Gallez XA, Demoustier-Champagne S, Devaux J, Mestdagh M, Champagne B et al. (2003). Identification of free radicals trapped in solid methacrylated resins. J Polym Sci Part A: Polym Chem 41:1691-1699.

Zhu S, Tian Y, Hamielec AE, Eaton DR (1990). Radical concentrations in free radical copolymerization of MMA/EGDMA. Polymer 31:154-159.

Chapter 8

Photoinitiator type and applicability of exposure reciprocity law in filled and unfilled photoactive resins

Julian Leprince, Mohammed Hadis, Adrian C Shortall, Jack L Ferracane, Jacques Devaux, Gaëtane Leloup, William M Palin

Submitted to

Dental Materials

This work was presented at the Academy of Dental Materials conference, 2009 (Portland, OR, USA) and winner of the Paffenbarger Award for outstanding student presentation.

8.1. Summary

OBJECTIVES: To test the influence of photoinitiator type and filler content on the validity of exposure reciprocity law.

MATERIALS AND METHODS: 50/50 mass% Bis-GMA/TEGDMA resins were prepared with equimolar concentrations of camphorquinone/DMAEMA (0.20/0.80 mass%) (CQ) or Lucirin-TPO (0.42 mass%) (L), and were used either unfilled (U) or filled (F) to 75 mass%. Specimens were cured with a halogen Swiss Master Light (EMS, Switzerland) using four different curing protocols: 400 mW/cm^2 for 45 s as reference protocol (18 J/cm^2), 1500 mW/cm^2 for 12 s (18 J/cm^2), 3000 mW/cm^2 for 6 s (18 J/cm^2) and 3 s (9 J/cm^2). Degree of conversion (DC) was measured in real time for 70 s by FT-NIRS and temperature rise using a thermocouple. Depth of cure (DOC) was determined with a penetrometer technique.

RESULTS: With respect to DC and DOC, ERL did not hold for any tested material, except for the DOC of F-CQ. At similar radiant exposure, DC was significantly higher ($p<0.05$) for all L-based materials (U-L and F-L) compared with CQ-based materials (U-CQ and F-CQ). As exposure time was reduced and irradiance increased, L-based materials exhibited higher DC whilst an opposite trend was observed for CQ-based materials ($p<0.05$). For similar curing regimes, DOC of CQ-based materials remained significantly greater than that of L-based materials. Adding fillers generally reduced DC, except at higher irradiance for CQ-based materials where a positive effect was observed ($p<0.05$).

SIGNIFIANCE: The validity of exposure reciprocity law was dependent on several factors, among which photoinitiator type and filler content were important. Lucirin-TPO is a highly reactive and efficient photoinitiator, which may allow the potential for a reduction in curing time of L-based photoactive materials in thin sections due to its reduced depth of cure.

8.2. Introduction

In restorative dentistry, there exists a significant demand for reduction in curing duration to minimize chairside procedure times of multi-increment resin composite restorations. Combined with the increasing popularity and demand for photoactive resin-based restorations as a replacement for dental amalgam, major financial implications have been suggested for dentists who chose to use high power, fast curing light sources. In order to achieve shorter exposure times (<10 s), whilst maintaining optimum material properties, the general trend among manufacturers has been to produce light curing units with increased irradiance. This is based on the assumption that the total energy of the irradiation, i.e. radiant exposure (RE, J/cm^2), is the main determining factor in degree of conversion and mechanical properties of the photoactive material. As RE is the product of irradiance (I, mW/cm^2) and irradiation time (t, s), it supposed that comparable material properties result from similar RE, no matter how RE is obtained (by different combinations of I and t). This is the principle known as the "exposure reciprocity law (ERL)". While in certain cases the law holds quite well [1-4], other studies have reported that although RE plays an important role, I and t independently influence polymer chain length, extent of crosslinking and mechanical properties, and as such, exposure reciprocity does not hold under all conditions [5-9]. A major difference among these previous citations is that some consider filled and others unfilled materials. As the experimental conditions seem critical to study ERL validity, it is relevant to include both classes of material in a single study, which to our knowledge has yet to be investigated.

Alternative photoinitiators have been integrated in commercially available materials in the last few years, mostly for aesthetic reasons, due to yellowing by camphorquinone/amine systems [10]. As some of these "alternative" photoinitiators are also interesting in terms of photopolymerization efficiency, they might also have an impact on the validity of ERL. Notably, Lucirin-TPO (L), a monoacylphosphine oxide, seems to be a promising molecule, as it presents higher molar absorptivity and curing efficiency [11, 12]. However, considering the absorption characteristics of L and the increased scattering of light of shorter wavelength, inferior curing depth of materials that replace CQ with L may be a cause for concern [13, 14]. Although recent work has highlighted the potential of Lucirin-based polymers to be cured in thick layers [15] and for use in dental adhesives [16], its application in filled resin composites has not been

fully described. To date, the curing efficiency of L in filled resin-based composite has only been studied in commercial materials [13, 14, 17], in which L is not used by itself but in combination with CQ. In the latter case, lower quantum yields were measured for polymerization initiated by a mixture of L and CQ compared to systems in which L was used alone, probably due to a transfer from the more efficient photoinitiator (L) to the less efficient one (CQ) [18]. In addition, the exact photoinitiator concentration and ratio in these materials is proprietary.

Consequently, the aim of this work was to investigate the impact of photoinitiator type on the polymerization efficiency in unfilled and filled experimental resins. Degree of conversion (DC) and depth of cure (DOC) were measured to test the null hypothesis that applicability of ERL depends neither on the photoinitiator type nor on the presence or absence of fillers.

8.3. Materials and Methods

50 / 50 mass% Bis-GMA/TEGDMA resins were prepared with two different photoinitiator (PI) systems at equimolar concentration: either camphorquinone/ dimethylaminoethyl methacrylate (shortened here as CQ) (0.20/0.80 mass%) or Lucirin-TPO (L) (0.42 mass%). The resins were tested either unfilled (U) or filled (F) with silanated barium glass fillers (0.7 μm) (Esschem Europe LTD, Seaham) and fumed silica (40 nm) (Aerosil, Evonik Industries, Germany) to 65/10 mass%, respectively. Specimens were cured with a 11 mm diameter tip halogen Swiss Master Light (EMS, Switzerland), chosen for its broad spectrum, overlapping the absorption spectrum of both photoinitiators (albeit only partially with L). Emission spectra were measured by calibrating a UV-Vis spectrometer (USB4000, Ocean Optics) using a deuterium tungsten light source (calibrated to NIST standards) with known spectral output in the UV-VIS and NIR range (Mikropack DH2000-CAL, Ocean Optics, Dunedin, USA), which allowed absolute measurements of irradiance for the light curing unit (LCU). The intensity of the LCU was controlled by stacking neutral density filters (Thorlabs, UK) which produced a 6-fold reduction in irradiance over the whole spectrum. The absorption spectra of the photoinitiators were determined in methyl methacrylate (Sigma-Aldrich, UK) using the UV-Vis spectrometer coupled to a standard cuvette holder in absorbance mode. Three different curing protocols were applied to compare the applicability of ERL and another one to assess the potential of time reduction at the

highest irradiance. 400 mW/cm^2 for 45 s was chosen as the reference protocol and compared to protocols of the same radiant exposure (18 J/cm^2): 1500 mW/cm^2 for 12 s and 3000 mW/cm^2 for 6 s. The last irradiation protocol, 3000 mW/cm^2 for 3 s, was chosen to assess the effect of half the radiant exposure on L-based materials. The irradiance values were based on the in-built radiometer of the curing-unit and verified by the spectrometer. Degree of conversion (DC) and rate of polymerization (R_p) were measured in real-time by Fourier Transform near infrared spectroscopy (FT-NIRS; Figure 1) by monitoring the height of the peak at 6164 cm^{-1}, which corresponded with the vinyl -CH2 absorbance. Curing kinetics of resins and resin composites were measured for 70 s through a 12 x 1.4 mm cylindrical white Teflon mould placed on a glass slide and covered by a thin glass cover slip (n=3) (Figure 1). Though DC is known

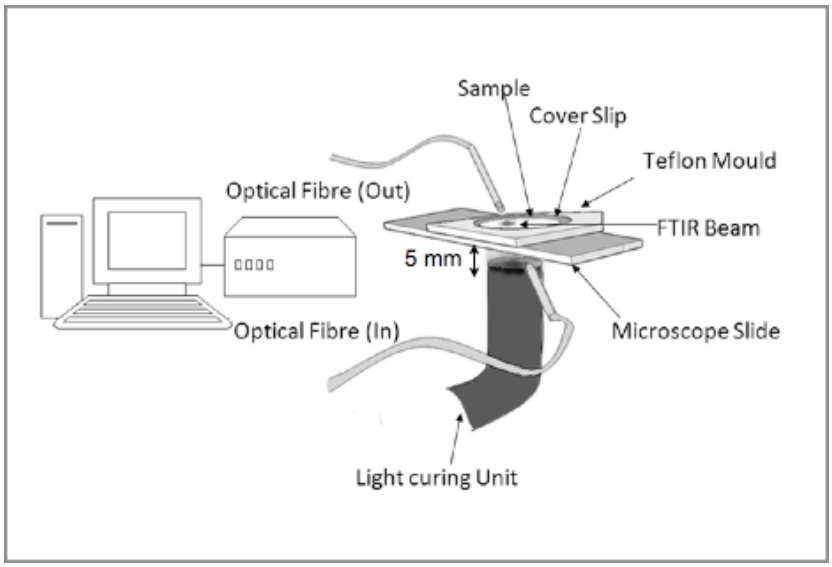

Figure 1 - Experimental setup for of real-time FT-NIRS measurements

to slightly evolve up to 24 h after irradiation, the major part of the polymerization occurs during irradiation [19]. For that reason, DC at 70 s after the start of irradiation was chosen for comparison and will be referred to as DC^{Max}. A real time measurement of the temperature rise during the polymerization was performed using a similar set up as for FTIR measurements, except that the mould was split on one side to insert a thermocouple. The latter was glued in place so that the bead of the thermocouple (1.5 mm diameter) was in contact with the outer edge of the sample. The thermocouple was calibrated against a standard mercury thermometer. The depth of cure (DOC) was measured by an penetrometer technique [20] after curing the samples in a cylindrical Teflon mould (5 mm diameter) (n=3). Statistical analyses were performed on the DC^{Max}, R_p^{Max}, DOC and T^{Max} data sets using a general linear model (GLM) three-way analysis

of variance (ANOVA) with PI (2 levels), filler inclusion (2 levels) and curing mode (4 levels) as the independent variables. Supplementary two-way ANOVA and post-hoc Tukey multiple comparison tests (p=0.05) were also performed.

8.4. Results

Figure 2 presents a comparison between the absorption spectra of both photoinitiators (CQ and L) and the emission spectra of the curing-unit at 400, 1500 and 3000 mW/cm^2. An increased power of the curing unit resulted in a greater effective irradiance at shorter wavelengths and thus the overlap with L absorption was improved. However, spectral emission was better adapted to CQ absorption, as a greater overlap of the two spectra was evident.

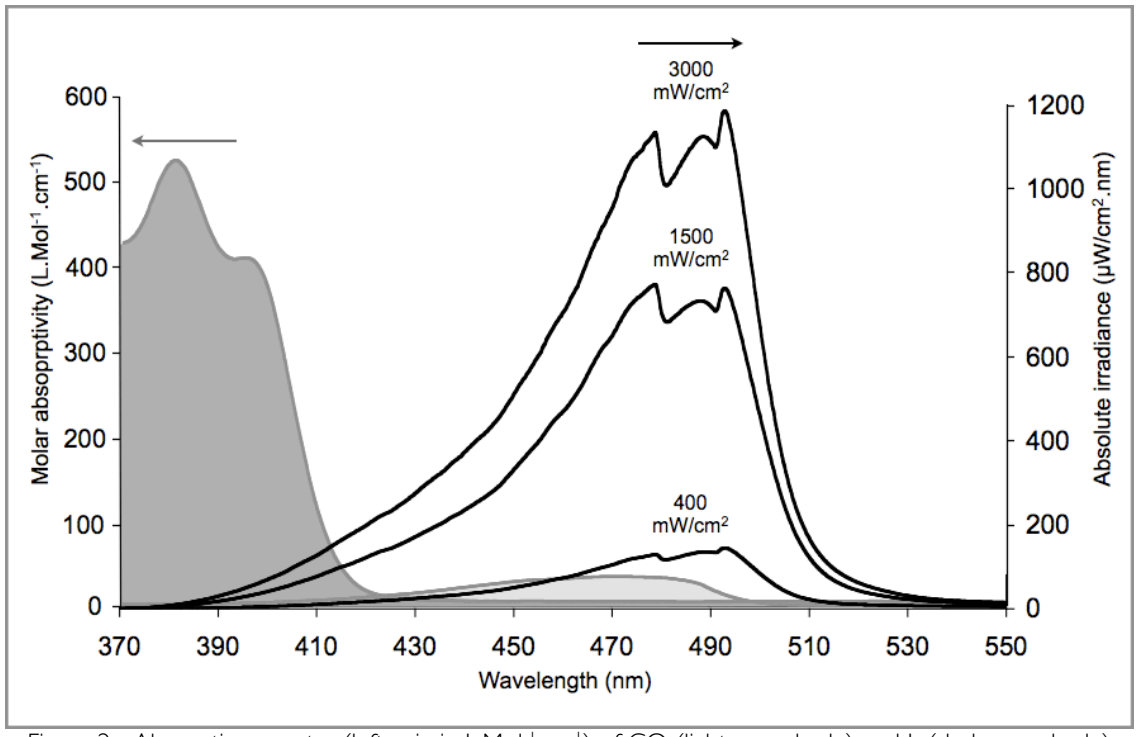

Figure 2 - Absorption spectra (left axis, in L.Mol^{-1}cm^{-1}) of CQ (light grey shade) and L (dark grey shade) compared to emission spectra of the Swiss Master Light (right axis, in µW/cm^2.nm) at different irradiances, i.e. 400, 1500 and 3000 mW/cm^2. An improvement of the overlap with L absorption can be observed with increased power of the curing unit.

The GLM of all independent variables revealed significant differences ($p<0.001$) where PI (df=1; F=5971) > filler inclusion (df=1; F=1302) > curing mode (df=3; F=809). A two-way ANOVA test of DC^{Max} results revealed significant overall differences for both PI and curing mode ($p<0.001$). Comparing irradiation modes of similar RE (18 J/cm^2), DC^{Max} was significantly higher for all resin and resin composite L-based materials compared with CQ-based materials ($p<0.05$; Figures 3a and 4a, Tables 1 and 2). For L, an increase in irradiance resulted in higher DC^{Max} regardless of

exposure duration, while a reverse trend was observed for CQ-based materials where longer exposure led to higher DC^{Max} regardless of irradiance. DC^{Max} significantly decreased in most cases with addition of fillers ($p<0.05$), except for CQ-based materials cured with the highest irradiance where filled resins exhibited a significantly increased DC^{Max} compared with the unfilled parent resin ($p<0.05$).

Table 1 – Unfilled resins

Material	Mode		Radiant Exposure (J/cm^2)	DC^{Max} (%)	R_p^{Max} (s^{-1})	T^{Max} (°C)	*DOC* (mm)
	Time (s)	Irradiance (mW/cm^2)		Mean (+/- SD)	Mean (+/- SD)	Mean (+/- SD)	Mean (+/- SD)
U CQ	45	400	18	72.1 (0.7) ^{d}	0.024 (0.000) ^{e}	33.6 (2.0) ^{b,c}	18.2 (0.2) ^{a}
	12	1500	18	65.8 (0.5) ^{e}	0.043 (0.001) ^{c,d}	29.1 (1.4) ^{c}	16.9 (0.1) ^{b}
	6	3000	18	43.9 (1.2) ^{f}	0.040 (0.001) ^{d}	19.5 (3.9) ^{d}	14.4 (0.1) ^{c}
	3	3000	9	25.7 (1.3) ^{g}	0.028 (0.001) ^{d,e}	10.6 (1.4) ^{e}	9.5 (0.1) ^{f}
U L	45	400	18	76.0 (0.1) ^{c}	0.058 (0.001) ^{c}	29.5 (1.9) ^{b,c}	9.6 (0.3) ^{f}
	12	1500	18	83.3 (0.5) ^{a,b}	0.133 (0.005) ^{b}	41.5 (3.2) ^{a}	11.8 (0.2) ^{d}
	6	3000	18	85.0 (0.3) ^{a}	0.186 (0.006) ^{a}	41.1 (1.8) ^{a}	10.4 (0.2) ^{e}
	3	3000	9	82.1 (0.2) ^{b}	0.177 (0.014) ^{a}	36.4 (3.3) ^{a,b}	4.4 (0.2) ^{g}

Similar letters within columns indicate no significant difference ($p<0.05$)

For each curing regime, all L-based materials exhibited a significantly increased R_p^{Max} ($p<0.05$) compared with CQ-based materials, except for F-L and F-CQ irradiated with the reference curing mode (400 mW/cm^2 for 45 s) ($p>0.05$) (Figures 3b and 4b, Tables 1 and 2). Regarding T^{Max} (Tables 1 and 2), values were significantly higher for U-L than for U-CQ, except for the reference curing protocol. A comparable trend was observed for filled materials, although the differences between similar curing modes were not statistically significant ($p>0.05$). Moreover, multiple regression analysis revealed that DC^{Max} and T^{Max} were highly correlated for unfilled ($R^2 = 0.95$; $p<0.0001$) and to a lesser extent for filled resins ($R^2 = 0.74$; $p<0.0001$). Contrary to the observations of DC^{Max} and R_p^{Max}, DOC was significantly higher for CQ-based compared with L-based materials (~1.5 to 3 times for unfilled and filled materials, respectively; Tables 1 and 2).

Table 2 – Filled resins

Material	Mode		Radiant Exposure (J/cm^2)	DC^{Max} (%)	R_p^{Max} (s^{-1})	T^{Max} (°C)	*DOC* (mm)
	Time (s)	Irradiance (mW/cm^2)		Mean (+/- SD)	Mean (+/- SD)	Mean (+/- SD)	Mean (+/- SD)
F CQ	45	400	18	57.6 (0.7) ^{c,d}	0.022 (<0.001) ^{e}	14 (0.3) ^{c}	10.6 (0.2) ^{a}
	12	1500	18	54.9 (0.9) ^{d}	0.043 (0.001) ^{d}	17.6 (0.5) ^{a,b,c}	10.8 (0.2) ^{a}
	6	3000	18	50.8 (0.2) ^{e}	0.056 (0.001) ^{c}	17 (1.4) ^{a,b,c}	10.1 (0.3) ^{a}
	3	3000	9	32.5 (1.0) ^{f}	0.043 (0.001) ^{d}	7.6 (0.1) ^{d}	7.3 (0.2) ^{b}
F L	45	400	18	62.7 (0.5) ^{b}	0.028 (0.001) ^{e}	14.5 (0.4) ^{b,c}	3.2 (0.2) ^{d}
	12	1500	18	65.2 (2.5) ^{a,b}	0.071 (0.01) ^{b}	18.9 (1.0) ^{a,b}	3.7 (0.1) ^{c,d}
	6	3000	18	68 (0.3) ^{a}	0.104 (0.005) ^{a}	19.9 (0.2) ^{a}	3.9 (0.3) ^{c}
	3	3000	9	59 (1.7) ^{c}	0.109 (0.002) ^{a}	13.6 (4.2) ^{c}	2.5 (0.3) ^{e}

Similar letters within columns indicate no significant difference ($p<0.05$)

Comparing modes of different RE, both DC^{Max} and DOC were significantly lower ($p<0.05$) for CQ-based materials using the lower RE (9 J/cm^2). Interestingly, in the case of L-based materials, DC^{Max} at low RE is comparable in some cases or at least close to DC^{Max} at high RE, especially for unfilled resins. However, DOC at 9 J/cm^2 RE was significantly reduced ($p<0.05$) compared to all 18 J/cm^2 REs (Tables 1 and 2).

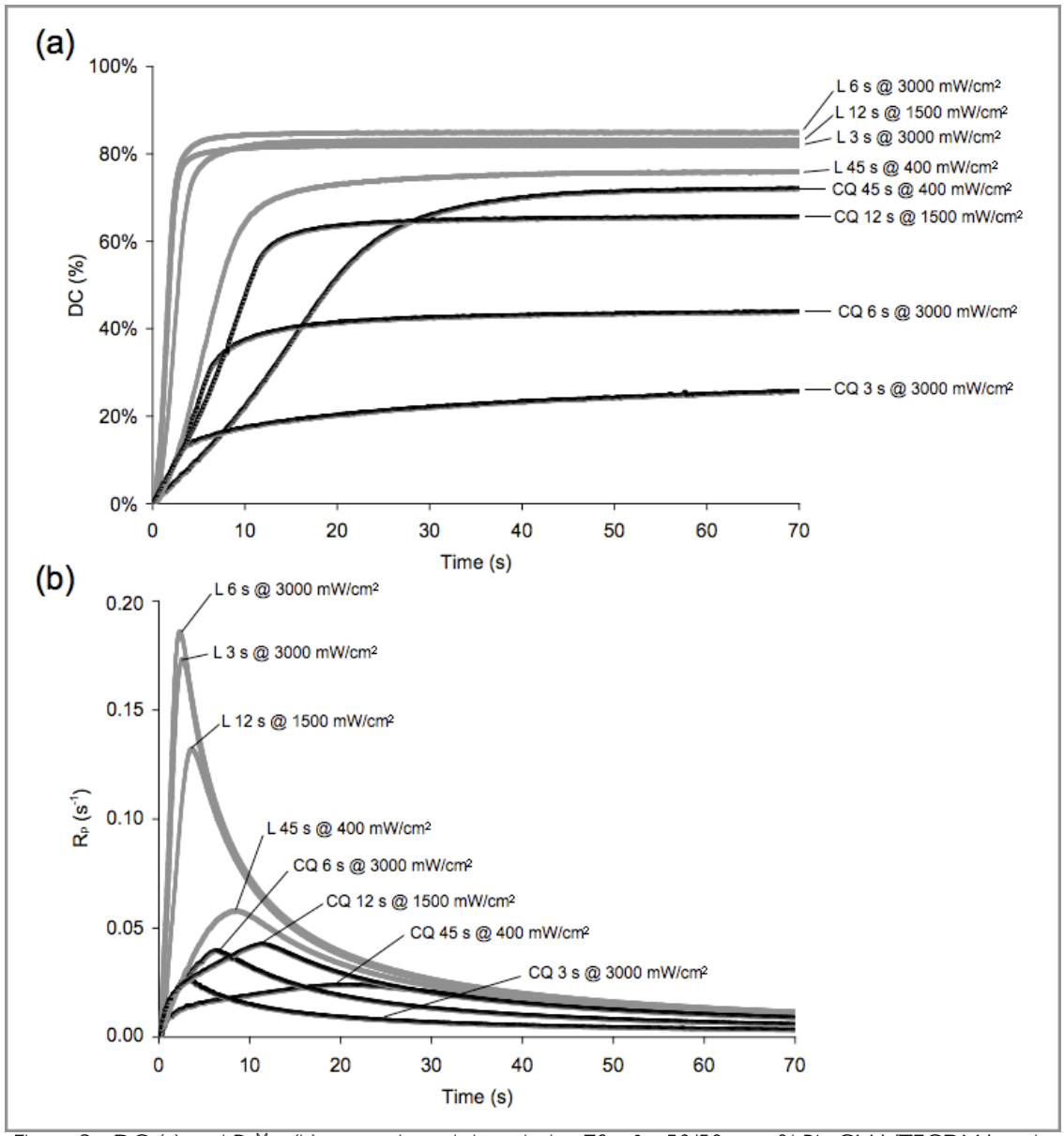

Figure 3 - DC (a) and R_p^{Max} (b) curves in real time during 70 s for 50/50 mass% Bis-GMA/TEGDMA resin. Grey and black curves correspond respectively to L-based and CQ-based resins. Irradiation modes are indicated on the charts.

8.5. Discussion

The null hypothesis was partially rejected as both PI type and filler content significantly influence material properties cured with similar radiant exposure with varying irradiance and/or exposure time, which contests the applicability of ERL. However, in certain instances comparable DC^{Max} and DOC were observed regardless of

curing protocol. Whilst reciprocity is observed for DOC of the CQ-based composite in accordance with Nomoto *et al*. [21], it is not the case for DC^{Max} of the same material tested here. The trend observed for CQ-based materials is in agreement with previous literature [6,8] supporting that for these systems, t has more impact than irradiance on the material properties. As explained in recent work on trapped free radicals [22], there is probably a loss in radical growth centers by translational diffusion and bimolecular (radical-radical) termination during the early stages of polymerization wherein system mobility is high. This loss (or early termination) is greater for high I protocols, since at low conversion termination is proportional to the squared concentration of free radicals. As a result, at constant RE with higher I (and shorter t), the amount of growth centers created during auto-acceleration is reduced and DC^{Max} is significantly decreased compared with similar RE achieved using lower I for longer t. However, while variations in DC^{Max} of CQ-based materials are obvious for unfilled systems, the differences appear more subtle in filled materials and approach a reciprocal relationship with respect to I and t. This effect may well be supported by previous findings [23] demonstrating that trapped free radical concentrations were nearly 3 times higher in the organic matrix of a filled composite than in a corresponding unfilled resin. The explanatory hypothesis proposed in that work was spatial confinement of radicals in filled resins, preventing their recombination. It could indeed be assumed that the organic fraction is located in small interstices between inorganic particles, which could restrict the diffusion of radicals to a relatively small area. But, it could also be related to an increase in local viscosity, reducing molecular mobility, thereby favoring monomolecular termination pathway. Feng and Suh [9] demonstrated that for Bis-GMA/TEGDMA ratios equal to or above a 60/40 mass%, ERL holds, while below 40/60 mass% it does not. Interestingly, Beun *et al.* [24] suggested that the large contact area between fillers and resin probably results in a significant local increase in viscosity. Surprisingly, at the highest irradiance, the filled CQ-based materials exhibited a significant increase in DC^{Max} and R_p^{Max} compared with the unfilled parent resin (50.8 and 43.9 %, 0.056 and 0.040 s-1, respectively). Since the polymerization kinetics of CQ-based materials at high irradiance are limited, inclusion of filler particulates may have affected light scattering properties through the limited specimen thickness (1.4mm) and/or provided some insulating effect which improved final conversion of the filled composite. Further work regarding the synergistic effects of filler particles on

local resin viscosity and curing kinetics is required to fully elucidate this phenomenon, which is currently being investigated by the authors.

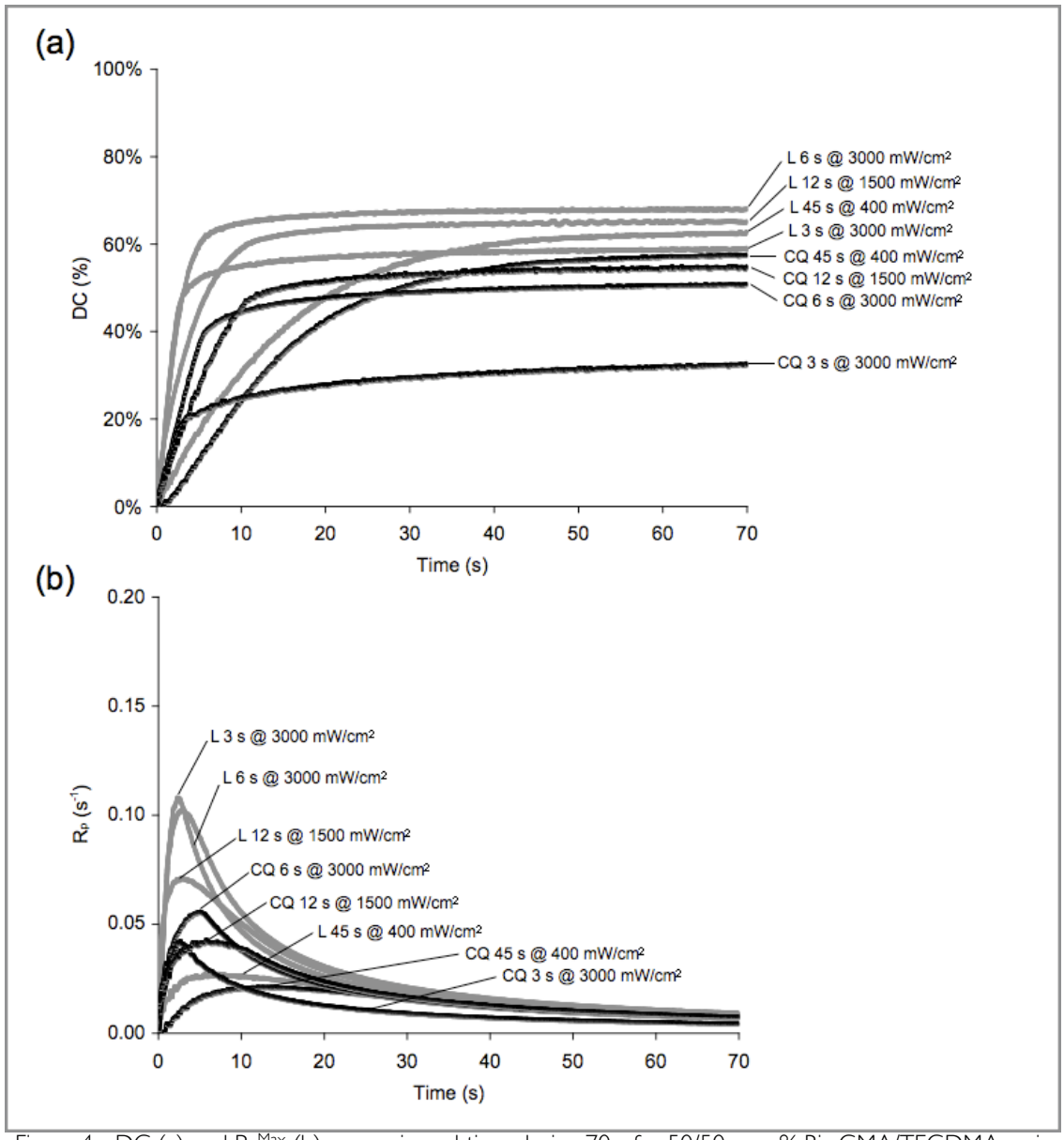

Figure 4 - DC (a) and R_p^{Max} (b) curves in real time during 70 s for 50/50 mass% Bis-GMA/TEGDMA resin filled with 75 mass% fillers. Grey and black curves correspond respectively to L-based and CQ-based resins. Irradiation modes are indicated on the charts.

By comparing CQ- with L-based materials, deviations from the simple assumption of ERL can be highlighted. The significant increase in DC^{Max} of L- compared with CQ-based materials (Figures 3a and 4a, Tables 1 and 2) can be explained by an increased generation of free radicals resulting from the vastly higher molar absorptivity (Figure 2) and quantum yield efficiency of L [11, 12] compared with CQ. Photochemical cleavage of L (a Norrish Type I photoinitiator) results in two free radical intermediates compared with one active radical in CQ/amine systems, and the absence of co-initiator for L reduces the intermediate steps required for radical production.

Nevertheless, even if it can be assumed that an increased number of free radicals led to higher R_p^{Max}, the increased efficiency of higher irradiance modes achieved by curing L-based materials with the halogen curing unit is interesting, especially in unfilled resins. First, it must be underlined that the positive impact of higher irradiance is overestimated due to a greater effective irradiance and enhanced overlap of L-absorption with increasing power of the curing unit (Figure 2). Second, the quantum yield efficiency was reported to be 5 times higher for L than for CQ with a halogen light [12]. Hence, despite some radical loss by early recombination, there is probably a much quicker build-up of the polymer network into a gel-phase, favouring radical entrapment and leading to an earlier onset of autoacceleration (Figures 3b and 4b). During autoacceleration, which is characterized by a low termination rate, L-based materials generate many more polymer growth centers. At high irradiance, this results in a significantly increased R_p^{Max} compared with CQ-systems, which can compensate time reduction and lead to high DC^{Max}. In addition, the influence of temperature must not be neglected. As high R_p^{Max} is associated with a greater and quicker reaction exotherm, it further improves DC^{Max} by increasing monomer mobility.

Despite their obvious higher curing efficiency highlighted above, L-based materials exhibit inferior curing efficiency through depth, for unfilled and even more for filled materials. Since L is a colourless photoinitiator and has been shown to exhibit efficient photobleaching properties with no absorbance of photolysis products above 360 nm [15], negligible light attenuation through unfilled L-based resin might be assumed although high exotherm and increasing UV radiation may cause some oxidation and discolouration of the polymer resin. The more likely explanation for inferior cure depth of L-based materials is related to the much higher molar absorptivity of L [11]. At similar PI concentration, L absorbs many more photons than CQ, which reduces the penetration of light through depth. In the present study, the ratio of CQ:amine was selected as an optimum combination to produce maximum DC [25] and CQ concentration represented that used in commercial composites [26], and an equimolar concentration was used for L for comparative purposes. However, given the very high polymerization efficiency of L, its concentration could probably be reduced, thereby improving DOC. As for the additional decrease of DOC in filled materials, it is probably related to an increased light scattering at the shorter wavelengths that correspond with the effective absorption of L [10]. However, the effective spectral

irradiance of the curing-unit in the absorption range of L is several times lower than that of CQ. As there is a linear correlation between irradiance and DOC [27], a higher DOC for L -based materials might be achieved using a higher intensity source emitting specifically around 400 nm.

8.6. Conclusion

In most cases, the implicit assumption of ERL was not upheld. Exposure reciprocity relies on the extent of monomolecular termination of the curing material, which is directly affected by molar absorptivity, quantum yield efficiency, material viscosity and temperature. However, while the validity of this law appears far from systematic, there is a clear interest to consider its global relevance to clinical practice and the potential of significant time reduction using modern high-irradiance curing lights. From this work, it appears that this potential clearly depends on the photoinitiator type, as L-based materials reach higher DC^{Max} than CQ-based materials at similar RE, or even with half the RE. However, the problem of low DOC of L-based materials still has to be addressed. For CQ-systems only, filler content has an impact on the efficiency of high irradiance modes, probably due to decreased local mobility of monomers. This underlines the necessity to adapt curing protocols according to the material filler content, which is of prime interest for clinicians. Research is ongoing on this topic.

8.7. Acknowledgments

This work was presented at the Academy of Dental Materials conference, 2009 (Portland, OR, USA) and winner of the Paffenbarger Award for outstanding student presentation. The authors would like to thank the Academy for their continual support for young investigators. The authors are extremely grateful to Dr Joe Oxman (Corporate Scientist, 3M Healthcare/ESPE, St Paul, MN, USA) for useful discussions regarding aspects of photoinitiator chemistry. J. Leprince thanks the Funds for Scientific Research (F.R.S.-FNRS) for his research fellow position.

8.8. References

1. Emami N and Söderholm KJ. How light irradiance and curing time affect monomer conversion in light-cured resin composites. Eur J Oral Sci, 2003; 111:536-542.
2. Halvorson RH, Erickson RL, Davidson CL. Energy dependent polymerization of resin-based composite. Dent Mater, 2002; 18:463-469.

3. Price RB, Felix CA, Andreou P. Effects of resin composite composition and irradiation distance on the performance of curing lights. Biomaterials, 2004; 25:4465-4477.
4. Sakaguchi RL and Ferracane JL. Effect of light power density on development of elastic modulus of a model light-activated composite during polymerization. J Esthet Restor Dent, 2001; 13:121-130.
5. Asmussen E and Peutzfeldt A. Polymerization contraction of resin composite vs. energy and power denstity of light-cure. Eur J Oral Sci, 2005; 113:417-421.
6. Peutzfeldt A and Asmussen E. Resin composite properties and energy density of light cure. J Dent Res, 2005; 84:659-662.
7. Musanje L and Darvell BW. Polymerization of resin composite restorative materials: exposure reciprocity. Dent Mater, 2003; 19:531-541.
8. Dewaele M, Asmussen E, Peutzfeldt A, Munksgaard EC, Benetti AR, Finné G, Leloup G, Devaux J. Influence of curing protocol on selected properties of light-curing polymers: degree of conversion, volume contraction, elastic modulus, and glass transition temperature. Dent Mater, 2009; 25:1576-1584
9. Feng L, Suh BI. Exposure reciprocity law in photopolymerization of multi-functional acrylates and methacrylates. Macromol Chem Phys, 2007; 208:295-306.
10. Price RB, Felix CA . Effect of delivering light in specific narrow bandwidths from 394 to 515nm on the micro-hardness of resin composites. Dent Mater, 2009; 25:899-908.
11. Neumann MG, Miranda WG Jr, Schmitt CC, Rueggeberg FA, Correa IC. Molar extinction coefficients and the photon absorption efficiency of dental photoinitiators and light curing units. J Dent, 2005; 33:525-532.
12. Neumann MG, Schmitt CC, Ferreira GC, Correa IC. The initiating radical yields and the efficiency of polymerization for various dental photoinitiators excited by different light curing units. Dent Mater, 2006; 22:576-584.
13. Price RB, Felix CA . Effect of delivering light in specific narrow bandwidths from 394 to 515nm on the micro-hardness of resin composites. Dent Mater, 2009; 25:899-908.

14. Leprince J, Devaux J, Mullier T, Vreven J, Leloup G. Balance between the rise in pulpal-temperature of LED curing lights and their polymerization efficiency on dual-photoinitiator composites. Accepted for publication in Oper Dent.
15. Stephenson Kenning N, Ficek BA, Hoppe CC, Scranton AB. Spatial and temporal evolution of the photoinitiation rate for thick polymer systems illuminated by polychromatic light : selection of efficient photoinitiators for LED or mercury lamps. Polymer Int, 2008; 57:1134-1140.
16. Ilie N and Hickel R. Can CQ be completely replaced by alternative initiators in dental adhesives? Dent Mater J, 2009; 27: 1-8.
17. Palin WM, Senyilmaz DP, Marquis PM, Shortall AC. Cure width potential for MOD resin composite molar restorations. Dent Mater, 2008; 24:1083-1094.
18. Neumann MG, Schmitt CC, Horn MA Jr. The effect of the mixtures of photoinitiators in polymerization efficiencies. J Appl Pol Sci, 2009; 112:129-134.
19. Truffier-Boutry D, Demoustier-Champagne S, Devaux J, Biebuyck JJ, Mestdagh M, Larbanois P, Leloup G.A physico-chemical explanation of the post-polymerization shrinkage in dental resins. Dent Mater, 2006; 22:405-412.
20. Shortall AC, Wilson HJ, Harrington E. Depth of cure of radiation-activated composite restoratives - influence of shade and opacity. J Oral Rehabil, 1995; 22:337-342.
21. Nomoto R, Uchida K, Hirasawa T. Effect of light intensity on polymerization of light-cured composite resins. Dent Mater J, 1994; 13:198-205.
22. Leprince J, Lamblin G, Devaux J, Dewaele M, Mestdagh M, Palin WM, Gallez B, Leloup G. Submitted to J Dent Res (available on demand).
23. Leprince J, Lamblin G, Truffier-Boutry D, Demoustier-Champagne S, Devaux J, Mestdagh M, Leloup G. Kinetic study of free radicals trapped in dental resins stored in different environments. Acta Biomater, 2009; 5:2518-2524.
24. Beun S, Bailly C, Dabin A, Vreven J, Devaux J, Leloup G. Rheological properties of experimental Bis-GMA/TEGDMA flowable resin composites with various macrofiller/microfiller ratio. Dent Mater, 2009; 25:198-205.
25. Yoshida K, Greener EH. Effect of photoinitiator on degree of conversion of unfilled light-cured resin. J Dent, 1994; 22: 296-99.
26. Taira M, Urabe H, Hirose T, Wakasa K, Yamaki M. Analysis of photo-initiators in visible-light-cured dental composite resins. J Dent Res, 1988; 67: 24.

27. Lindberg A, Peutzfeldt A, van Dijken JW. Curing depths of a universal hybrid and a flowable resin composite cured with quartz tungsten halogen and light-emitting diode units. Acta Odontol Scand, 2004; 62:97-101.